Lindestam Arlehamn, Cecilia Sofie (2010) *Intracellular triggering of inflammation by the extracellular bacterium Pseudomonas aeruginosa.* PhD thesis.

http://theses.gla.ac.uk/1401/

Intracellular Triggering of Inflammation by the Extracellular Bacterium *Pseudomonas aeruginosa*

A thesis submitted to the University of Glasgow for the degree of

Doctor of Philosophy

by

Cecilia Sofie LINDESTAM ARLEHAMN, M.Sc., M.Res.

Department of Immunology, Infection and Inflammation

Faculty of Biomedical and Life Sciences

University of Glasgow

2009

To Oscar

"It is about the small things, so small you can't even see them"

- Dad

Declaration

This work represents original work carried out by the author, unless otherwise stated, and has not been submitted in any form to any other University.

Cecilia Sofie Lindestam Arlehamn

November 2009

Acknowledgements

First of all I would like to thank my supervisor, Tom Evans, for your endless enthusiasm, encouragement and motivation. You are truly a great scientist and I hope we will stay in touch.

I would also like to thank the Wellcome Trust 4-year PhD-programme in Glasgow, for funding and for broadening the horizons in the scientific field. I have thoroughly enjoyed our monthly forums and yearly trips away. A special thanks to the directors of the programme Bill, Olwyn and Darren.

There are several people who has inspired and kept me sane throughout my PhD. Of course members of the Evans lab, past and present, Susan and Michelle for getting me through my first year and teaching me about the importance of tea-breaks, Alex for the cutest post-its ever and never ending sense of fun. A special thanks to my bench buddy Donna, I loved our trip to Boston and NY! In order to thank everyone else in the department I would have to write another book. Instead I would just like to thank everyone, no one mentioned and no one forgotten, past and present members of the department. Thanks for making my time here in Glasgow such an enjoyable one! Without you guys it would not be worth it. It is a great department and I feel privileged to have worked with all of you. I am certain I will stay in touch with quite a few of you, wherever we end up in the world, as I feel we have made friends for life! Don't hesitate to give us a call if anyone of you fancies a break on the Swedish south coast.

I would also like to thank my dad, for everything. You are simply the best! Also, I have to mention Oliwer, because he has been plastered all over my lab bench for the last three years. The greatest dog there will ever be. In addition, acknowledgements are due to all my friends and family back home. Thanks for visiting us here in Scotland and for everything when we have been home!

Finally and foremost Oscar, this is for you. Thanks for moving with me to Scotland, for keeping me sane, for all your support and for being you. My darling husband, I love you.

Table of contents

List of figures

Chapter 1

Chapter 2

Chapter 3

Chapter 4

Chapter 5

Chapter 6

List of tables

Chapter 1

Chapter 2

Chapter 5

Abbreviations

2-ME	2-mercaptoethanol
$AACOCF_3$	Arachidonyl trifluoromethyl ketone
ADPRT	Adenosine diphosphate (ADP)-ribosyltransferase
AIM2	Absent in melanoma 2
AM	acetoxymethyl
Amp	Ampicillin
ASC	apoptosis-associated speck-like protein containing a CARD
ATP	adenosine triphosphate
ß-gal	ß-galactosidase
BCECF	[28,78-bis-(2-carboxyethyl)-5-(and-6)-carboxyfluorescein, acetoxymethyl ester]
BIR	Baculovirus repeat
BMDM	bone-marrow derived macrophage
BSA	bovine serum albumin
cAMP	cyclic AMP
Carb	Carbenicillin
CARD	caspase recruitment domain
CBX	carbenoxolone
CFU	colony forming units
CHO	Chinese Hamster ovary
CLR	C-type lectin receptors
CPPD	Calcium pyrophosphate dihydrate
DAMP	Danger-associated molecular pattern
DAPI	4',6-diamidino-2-phenylindole
DC	Dendritic cell
DMEM	Dulbecco's modified Eagle's medium
DMSO	dimethyl sulfoxide
DNA	deoxyribonucleic acid
DOTAP	dioleoyl trimethylammonium propane
DTT	dithiothreitol
ECL	enhanced luminol-based chemiluminescent
EDTA	ethylenediaminetetraacetic acid
ELISA	enzyme-linked immunosorbent assay
FACS	fluorescence activated cell sorting

FBS	foetal bovine serum
GAP	GTPase activating protein
GDP/GTP	Guanosine 5´-di or triphosphate
GFP	green fluorescent protein
GST	Glutathione S-transferase
HBSS	Hank's buffered salt solution
HeLa	human negroid cervix epitheloid carcinoma cell line
HEK293	human embryonic kidney 293 cell line
HEPES	4-(2-hydroxyethyl)-1-piperazineethanesulfonic acid
HRP	Horseradish peroxidise
iE-DAP	γ-D-glutamyl-meso-diaminopimelic acid
IF	Immunofluorescence staining
IFN	interferon
IL	Interleukin
KO	knock-out
LAMP-1	lysosomal-ssociated membrane protein 1
LB	Luria Bertani
LDH	lactate dehydrogenase
LDS	lithium dodecyl sulphate
LPS	lipopolysaccharide
LRR	Leucine-rich repeat
LSC	laser scanning cytometry
MAFP	methyl arachidonyl fluorophosphonate
M-CSF	macrophage colony-stimulating factor
MDA-5	Melanoma differentiation-associated gene-5
MDP	muramyl dipeptide
MEM	minimal essential media
MFI	mean fluorescence intensity
MHC	major histocompatibility complex
MLD	membrane localization domain
MOI	multiplicity of infection
MSU	monosodium urate
MyD88	myeloid differentiation primary response gene 88
NACHT	domain in NAIP, CIITA, HET-E and TP1
NAD	NACHT-associated domain

NAIP	Neuronal apoptosis inhibitory protein
NB-LRR	nucleotide-binding and leucine-rich repeat protein
NF-κB	nuclear factor kappa B
NLR	NOD-like receptor
NOD	nucleotide-binding oligomerization domain
PAGE	polyacrylamide gel electrophoresis
PAMP	Pathogen-ssociated molecular pattern
PBFI	potassium-binding benzofuran isophthalate
PBS	phosphate-buffered saline
PCR	polymerase chain reaction
PEG	polyethylene glycol
PenStrep	Penicillin and Streptomycin
PFA	paraformaldehyde
PGN	peptidoglycan
PLA$_2$	Phospholipase A$_2$
PRR	pattern recognition receptor
PVDF	polyvinyliden difluoride
PYD	Pyrin domain
RICK	Receptor-interacting protein 2 (RIP2) caspase-like apoptosis-regulatory protein (CLARP) kinase
RIG-1	retinoic acid-inducible gene 1
RLR	RIG-1-like receptor
RPMI	Roswell park memorial institute
RT	room temperature
SDS	sodium dodecyl sulphate
SEM	standard error of the mean
SLO	streptolysin O
T2SS	Type II secretion system
T3SS	Type III secretion system
T4SS	Type IV secretion system
TCA	Trichloroacetic acid
Tet	Tetracycline
TIR	Toll-interleukin-1 receptor
TIRAP	TIR-containing adaptor protein
TLR	Toll-like receptor

TMB	tetramethylbenzidine
TNF	Tumour necrosis factor
TRIF	TIR-containing adaptor-inducing IFN-ß
TSA	tyramide signal amplification
TSB	trypticase soy broth
WB	Western blot
WT	wild type

Publications

- C.S. Lindestam Arlehamn, V. Petrilli, O. Gross, J. Tschopp, T.J. Evans; The role of Potassium in NLRC4 Inflammasome activation by Bacteria (submitted)

- C.S. Lindestam Arlehamn, T.J. Evans; Cytoplasmic Pilin Activates the Inflammasome (submitted)

Meeting abstracts

- C.S. Lindestam, T.J. Evans; *Pseudomonas aeruginosa* activates the NLRC4/Ipaf inflammasome via a type III secretion system dependent pathway; role of flagellin and pilin; Keystone Symposia Pattern Recognition Molecules and Immune Sensors of Pathogens, Banff, Canada, March 2009 – Poster presentation

- C.S. Lindestam, T.J. Evans; *Pseudomonas aeruginosa* Activates the NLRC4/IPAF Inflammasome via a Type III Secretion Dependent Pathway: Role of Flagellin and Pilin; T3SS meeting Bristol, UK, September 2008 – Oral Presentation

- C.S. Lindestam, T.J. Evans; Intracellular Triggering of Inflammation by the Gram-negative Bacterium *Pseudomonas aeruginosa* Requires a Functional Type III Secretion System; American Society for Microbiology (ASM) General Meeting, Boston, USA, June 2008 – Poster presentation

- C.S. Lindestam, T.J. Evans; Intracellular Triggering of Inflammation by the Gram-Negative Extracellular Bacterium *Pseudomonas aeruginosa*; Society for General Microbiology (SGM), Edinburgh, UK, March 2008 – Poster presentation

- C.S. Lindestam, T.J. Evans; Intracellular Triggering of Inflammation by the Gram-Negative Bacterium *Pseudomonas aeruginosa*; Scottish Society for Experimental Medicine (SSEM), Glasgow, UK, Autumn 2007 – Oral Presentation

- C.S. Lindestam, T.J. Evans; Intracellular Triggering of Inflammation by the Gram-Negative Bacterium *Pseudomonas aeruginosa*; SGM, Edinburgh, UK, September 2007 – Poster presentation

- C.S. Lindestam, T.J. Evans; Intracellular Triggering of Inflammation by the Gram-Negative Bacterium *Pseudomonas aeruginosa*; British Infection Society, London, UK, June 2007 – Oral Presentation

Abstract

P.aeruginosa is an extracellular, Gram-negative opportunistic pathogen. One of the most important virulence factors during infection is the type III secretion system (T3SS). This system is found exclusively in Gram-negative bacteria and it forms a conduit between the bacteria and the host cell through which effector molecules can be translocated. These effectors alter the function of the host cell to promote survival of the bacterium. Infections are detected initially by the innate immune system via germ-line encoded receptors, pathogen recognition receptors (PRRs). These receptors recognise conserved microbial patterns, known as pathogen-associated molecular patterns and molecules which signal danger, danger-associated molecular patterns. PRRs are both membrane bound, such as Toll-like receptors (TLRs), and cytosolic, such as Nod-like receptors (NLRs). Some NLRs are involved in the formation of multimeric protein complexes, the Nod-signalosome and inflammasomes. These lead to the activation of NF-κB and the activation of caspase-1 and subsequent proteolytic processing of interleukin-1ß (IL-1ß) into its mature form. Both processes contribute to the inflammatory response following infection.

In this study we sought to elucidate whether *P.aeruginosa* is able to trigger cytosolic PRRs and the mechanism of this activation. Initially we studied inflammasome activation by *P.aeruginosa*. We demonstrated that *P.aeruginosa* is able to activate the NLRC4/ASC-inflammasome complex. This was found to be dependent on a functional T3SS, but independent of any effectors passing through the system. The activation was discovered by detection of processed, and thus active caspase-1 fragments, as well as by secretion of mature IL-1ß.

The mechanism of the inflammasome activation was then investigated. We found that the NLRC4-dependent inflammasome activation is also dependent on extracellular potassium. An increase of extracellular potassium leads to a complete abrogation of inflammasome activation by *P.aeruginosa* and *Salmonella*. To further elucidate this finding, we investigated the leakiness of the pore formed by the T3SS in the host cell membrane. No flux of ions or small molecules could be detected in the host cell membrane following infection. However, host-membrane repair mechanisms were triggered, which could be detected by lysosomal-associated membrane protein (LAMP)-1-specific staining

of the plasma membrane. We hypothesize a role for membrane potential in triggering of inflammasome activation by bacteria possessing a secretion system. Potassium-efflux has previously been identified as a activator of the NLRP3 inflammasome, but no changes in intracellular potassium could be found during this study.

The activation of the NLRC4 inflammasome by the Pseudomonal strain PA103 was shown, in this study, to be independent of flagellin. Instead, the bacterial molecule responsible for inflammasome activation was shown to be pilin. Pilin is important for attachment to the host cell and the function of the T3SS. We showed that a strain lacking pilin were still able to translocate effectors through its T3SS. However, it was unable to activate the inflammasome complex. Transfection of purified pilin into cells was shown to trigger inflammasome activation. This was found to be dependent on caspase-1 but independent of NLRC4 and ASC, which is not in agreement with the results found for live bacteria. We hypothesised that the reason for this is the delivery method used, since a T3SS and infection delivers proteins and molecules differently compared to a transfection reagent.

Finally, the role for Nod1 in infection by *P.aeruginosa* was explored. We could not identify Nod1-dependent NF-κB-activation using luciferase reporter gene assays. We therefore hypothesise that Nod1 does not have a role in the innate immune response to *P.aeruginosa*.

In conclusion, we have identified NLRC4- and ASC-dependent inflammasome activation by *P.aeruginosa*. This activation was shown to be dependent on a functional T3SS and the surface protein pilin, as well as extracellular potassium. This describes a novel NLRC4-activation mechanism dependent on potassium and identifies pilin as a PRR-trigger for the first time.

1 Introduction

1.1 Introduction

The initial defence against infections is mediated by the innate immune system. Germ-line encoded receptors respond to pathogen-derived products and mount a response against the pathogen, to promote survival of the host. Pathogen recognition receptors include the well studied group of Toll-like receptors, as well as a more recent addition of Nod-like receptors (NLRs). *Pseudomonas aeruginosa* is an opportunistic pathogen and an important nosocomial pathogen. It possess several virulence factors, one of the most important being the type III secretion system (T3SS). Recent reports have implicated the bacterial T3SS not only as a virulence factor but also as a conduit for bacterial products which triggers the innate immune response.

The work presented in this thesis explores the mechanism by which the extracellular pathogen *P.aeruginosa* can activate intracellular NLRs. This chapter provides an overview to the pathogen *P.aeruginosa* and its virulence factors, as well as an introduction to the innate immune response via pathogen recognition receptors. Particular attention is paid to the NLR-proteins. The aim of this chapter is to emphasise the key role of NLRs and place in context the importance of the results presented in this thesis for the complex innate immune response.

1.2 *Pseudomonas aeruginosa*

P.aeruginosa is a Gram-negative opportunistic pathogen which belongs to the family Pseudomonadaceae. It is a free-living pathogen commonly found in soil and water but also on surfaces of plants and animals in contact with soil or water. It can survive in environments with minimal nutritional components due to its ability to metabolise a wide range of carbon sources and it is also able to survive in temperatures up to 42°C [1]. Healthy individuals can be carriers of the bacterium on their skin and in their throat and stool [2].

1.2.1 Pseudomonas aeruginosa infections

P.aeruginosa rarely causes infection in healthy tissues, but it can cause acute as well as chronic infection in almost any immuno-compromised tissue, where it exploits breaches in host defence such as skin or mucosal damage [3]. It can cause urinary tract infections, respiratory system infections, dermatitis, soft tissue infections, bacteraemia, bone and joint infections, gastrointestinal infections and a variety of systemic infections in severely immuno-compromised patients, such as burn victims, cystic fibrosis sufferers, cancer and AIDS patients, as well as ulcerative keratitis in contact-lens wearers [3]. The fatality rate in patients hospitalized with cancer, cystic fibrosis and burns is near 50 percent. In cystic fibrosis patient's infection by *P.aeruginosa* often contributes to destructive lung disease eventually leading to respiratory failure and death [4-6]. *P.aeruginosa* is a primarily nosocomial pathogen and it is responsible for 10.1 percent of all hospital-acquired infections in the USA. The natural properties of the bacterium explain its success as an opportunistic and nosocomial pathogen. It has minimal nutritional needs; it is able to grow at 37°C as well as in temperatures up to 42°C and it is resistant to high concentrations of salts and dyes, weak antiseptics and many antibiotics. It has been successfully isolated in the hospital environment from disinfectants, respiratory equipment, food, sinks, taps, toilets, showers and mops [4]. Furthermore, constant reintroduction occurs via fruits, plants, vegetables, visitors and patients. The bacterium can then spread from patient to patient via direct contact, hospital personnel or contact with contaminated reservoirs, foods or water [7].

P.aeruginosa is naturally resistant to many antibiotics greatly limiting the treating potential of infections. The resistance can be explained by the permeability barrier afforded by its Gram-negative outer membrane and its tendency to form biofilms on colonized surfaces, which results in resistance to therapeutic concentrations of antibiotics. Due to its natural habitat of soil it has developed resistance to naturally occurring antibiotics from bacilli, actinomycetes and molds. In addition *P.aeruginosa* possess several multidrug efflux pumps which also contributes to the resistance [8-12]. Finally *P.aeruginosa* is capable of horizontal gene transfer such as transduction and conjugation which enables transfer of antibiotic resistance plasmids. The

antibiotics still effective against *P.aeruginosa* include fluoroquinolones, gentamicin and imipenem, but these are not effective against all strains.

1.2.1.1   Burns

Skin is the largest organ in the human body and it is an important barrier against pathogens. This barrier is compromised after severe burns and it opens up an opportunity for *P. aeruginosa* to infect the moist tissue underlying burn wounds [3]. Infection results in destruction of healthy tissue and it can lead to sepsis. There is a burned mouse model of infection which shows only a few bacteria can lead to lethality in mice with burnt skin compared to 10^6-10^7 colony forming units (CFU) in healthy mice [13].

1.2.1.2   Cystic fibrosis

Cystic fibrosis sufferers have an imbalance in the fluid and electrolyte composition of epithelial cell secretions due to defective chloride permeability. This results in accumulation of sticky dehydrated mucus in lung airways, pancreatic ducts and in the male sex ducts [14]. The defective chloride permeability is caused by a mutation in the gene for cystic fibrosis transmembrane conductance regulator (CFTR) protein, a cyclic adenosine monophosphate (cAMP)-regulated chloride channel [3]. The main cause (90%) of death in cystic fibrosis sufferers are pulmonary disease and *P.aeruginosa* has been shown to contribute to this [15]. *P.aeruginosa* infection can lead to progressive lung damage via the aggressive inflammatory response it causes upon infection. As mentioned above, there is a great problem with antibiotic resistant *P.aeruginosa* strains and most cystic fibrosis patients eventually become infected with a strain which cannot be treated due to antibiotic resistance [16].

1.2.2 Virulence factors

P.aeruginosa has a wide array of virulence factors, which results in a multifactorial pathogenesis where normal host defences are altered or circumvented. This wide array of virulence factors contribute to the ability of the bacterium to cause such a wide variety of infections throughout the body. There are three stages of *P.aeruginosa* infection; bacterial attachment and

colonization, local invasion and finally disseminated systemic disease, but the disease process may stop at any of these three stages. *P.aeruginosa* has particular virulence factors that mediate each stage and results in the characteristic symptoms. *P.aeruginosa* has several cell-associated and secreted proteins which contribute to its virulence. Examples are elastase A, phospholipase C and the effector proteins translocated via the T3SS [17]. Some *P.aeruginosa* strains have a single polar flagellum, which contributes to the motility of the bacterium, but it is also an important virulence factor [6]. All *P. aeruginosa* strains have multiple surface pili. In following sections these virulence factors responsible for adherence to host tissue, avoidance of host immune response and multiplication of the bacterium will be discussed.

1.2.2.1 Flagella

Some *P.aeruginosa* strains produce a single polar flagellum. A flagellum is a whip like process extending from the bacterial surface. The flagellum spans the bacterial membrane and distal components are secreted through the base of the structure via a T3SS [18, 19]. The flagellum consists of these key proteins; FliC, the flagellin subunit protein and FliD, the flagellar cap protein, as well as multiple other proteins. There are over 50 genes involved in the synthesis and function of the flagella and it has been extensively studied [20]. Most environmental and nosocomical isolates of *P.aeruginosa* produce flagella. However, strains isolated from chronically infected cystic fibrosis patients have usually lost the ability to produce flagella [21].

The flagellum is an important virulence factor, but strains lacking this structure are still capable of causing infection. It was shown that antibodies and a vaccine raised against flagella are effective at protecting animals from infection [22, 23]. The importance of the flagellum as a virulence factor is partly due to its ability to bind host cells. The flagellum has been shown to bind via its FliD cap protein to neutral and acidic oligosaccharides in mucin but also to asialo GM1 (asialo-gangliotetraosylceramide receptors 1), GM1 and GD1a [24, 25]. The binding to mucin might lead to removal of the bacteria from the host by mechanical mucociliary clearance. However, during a pulmonary infection this is

reduced, as well as when mucus is trapped under a contact lens, which allows mucin binding to contribute to the survival and proliferation of the bacterium.

The host has developed a range of receptors which are capable of detecting flagellin and direct a host response against the infection; this will be described in more detail below and in chapter 5.

1.2.2.2   Pili

Pili are thin surface extensions from bacteria (Figure 1.1). All Gram-negative bacteria have type IV pili. The pilins of the type IV pili class share an N-methylated N-terminus, a conserved hydrophobic N-terminal and a C-terminal disulphide bond [26]. There are two subclasses of type IV pili, type IVa and type IVb, which differ in amino acid sequence and length [26]. *P.aeruginosa* has a pili structure belonging to the type IVa pilin class [27-29]. This class also includes pili from, for example, pathogenic *Neisseria* spp and *Moraxella bovis* [26]. Bacteria with pilin from the type IVb class includes *V.cholerae*, *Salmonella enterica* serovar Typhi, as well as both enteropathogenic and enterotoxigenic *E.coli* (EPEC and ETEC) [26].
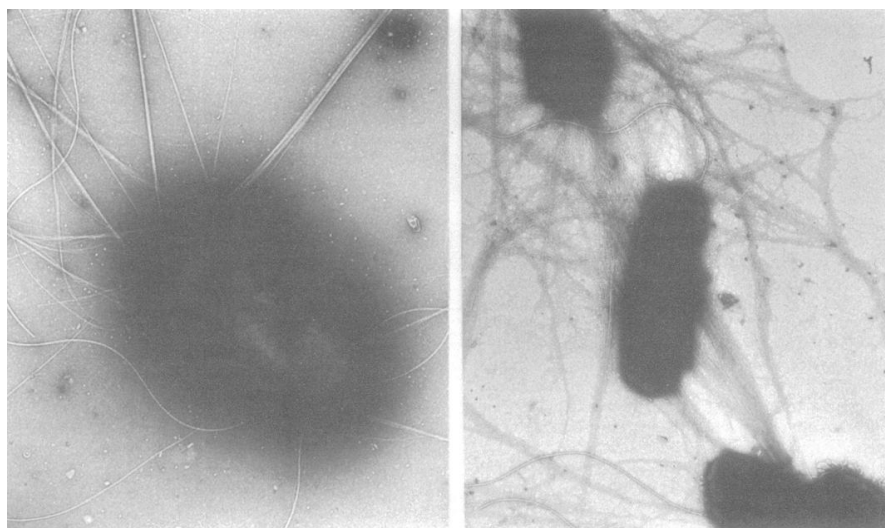
Figure 1.1; Piliated *P.aeruginosa* strain PAK

Electron micrographs of *P.aeruginosa* PAK. Left panel shows PAK WT (x 35.000) and right panel shows PAK/2PfS (x 19.920), which is a multipiliated mutant derived from PAK. Figure is adapted from [30].

Type IV pili consists of a homopolymer made of thousands of copies of the 15 kDa pilin monomer. These monomers form an extremely thin (50-80 Å) filament, which are several microns in length. The pilin monomer of *P.aeruginosa* is encoded by the *pilA* gene [31]. In addition to the *pilA* gene there are about 40 genetic loci which control pilin synthesis and pili production [32]. Pili, like flagella, are believed to act as adhesins and mediate binding to host cells, which has been demonstrated *in vitro* where pili have been shown to bind to the glycolipids asialo-GM1 and asialo-GM2 [33-35]. This, however, is disputed [36]. Pili can bind to these glycolipids through a C-terminal disulphide loop of pilin [37-39]. Initial X-ray crystallography studies suggested that the disulphide loop is buried within the pilus structure, which contradicts the possibility for this domain to be involved in host cell binding [40, 41]. However, recent studies suggest that this area is exposed in the assembled pilus filament [37, 42]. In addition, the disulphide loop is essential for pilus assembly and it is formed by two conserved C-terminal cysteines [43]. Type IV pili have been identified as the major epithelial cell adhesion protein and type IV pili mediated attachment has been implicated in efficient delivery of effector molecules via the T3SS [44-46]. The adherence of pili may be aided by production of protease enzymes, which will expose pilin receptors on the cell surface, such as specific galactose, mannose or sialic acid receptors. The attachment may also be aided by tissue injury. In addition to attachment, pili have been implicated in surface motility, microcolony and biofilm formation, cell signalling, immune evasion, DNA uptake by natural transformation and phage attachment [26].

Pili are responsible for twitching motility, a name based on microscopic observation of the bacteria [27] (Figure 1.2). Twitching motility is mediated by extension, tethering and then retraction of the pilus structure [27, 47, 48]. Retraction is mediated by disassembly of pili into pilin subunits, which are distributed throughout the inner and outer membranes and can subsequently be recycled back into new pili [48-50]. Twitching motility has been shown to be important for *in vitro* biofilm formation on abiotic surfaces. Furthermore, it is believed the twitching motility is involved in avoidance of host phagocytes. Two proteins, pilT and pilU are responsible for providing the energy needed for pilus retraction via an ATPase motor [47, 50, 51]. Mutants defective in twitching motility have reduced cytotoxicity towards various epithelial cells, as well as

reduced virulence in mouse models of acute pneumonia and corneal disease [31, 45, 52]. PilQ is a multimeric membrane protein that form gated pores in the outer membrane through which the pilus is thought to extrude [53], and homologs in bacterial type II secretion system (T2SS) have a similar role [54].
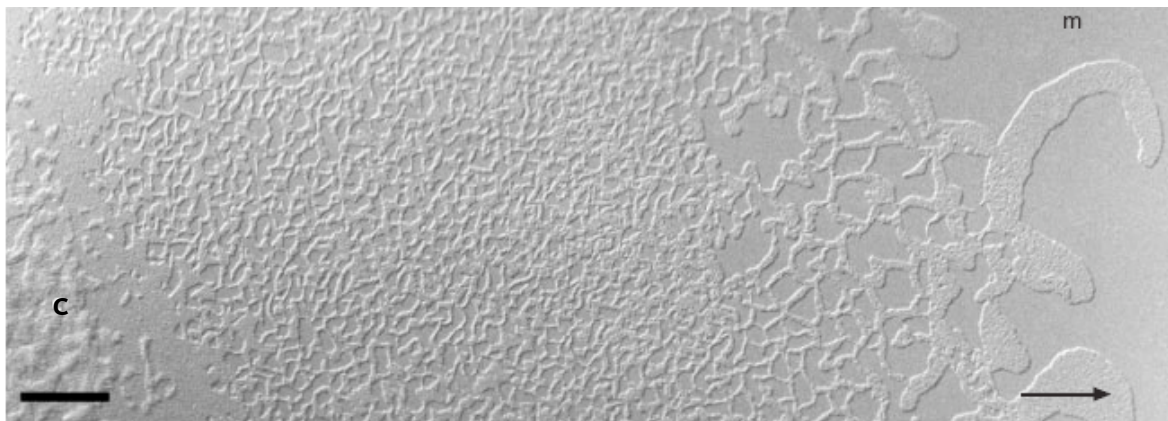
Figure 1.2; Light microscopy of zones of twitching motility

Twitching motility for PAK. Scale bar is 50 μm, c indicates the colony and m indicates the uncolonized medium. The arrow indicates the radial direction of colony expansion. Adapted from [55].

It has been shown that mutants lacking pili are less virulent than pili-expressing bacteria [31, 45]. Pili are involved in a mouse model for acute pulmonary infection as well as burn wound infection, but it is not required in the corneal scratch-injury eye model [31, 39, 56].

1.2.2.3   Lipopolysaccharide

Lipopolysaccharide (LPS) is a major component of the outer membrane of Gram-negative bacteria. This means it is an important target for the innate immune response, which will be described below.

P.aeruginosa has two isoforms of LPS, smooth and rough, which are found on most environmentally and nosocomical isolated strains and on isolates from chronically infected cystic fibrosis sufferers, respectively. LPS consists of a hydrophobic lipid A component, which anchors the molecule to the bacterial membrane and a core oligosaccharide. The smooth LPS contains a long polysaccharide O-chain (5-100 kDa) consisting of tri- or tetra-saccharide repeating units; however, only 20-30% of the LPS molecules on each bacterium

contain O-chains. The O-chains have been reported to be involved in resisting host defence by a mechanism which prevents lysis by complement [57].

1.2.2.4   Other virulence factors

P.aeruginosa has a wide range of other virulence factors which are important during infection and biofilm formation. One important virulence factor is iron acquisition. Like all living organisms *P.aeruginosa* needs iron for survival and growth. The bacteria have siderophores which have a high affinity for iron and can thus capture iron from host proteins such as transferrin and haemoglobin. *P.aeruginosa* has two siderophores called pyoverdin and pyochelin and these are secreted when the iron concentrations are low. Upon binding of iron these siderophores can bind receptors on the bacterial surface, where they are taken up, and the iron is used for various molecules. The siderophore is recirculated [58]. *P.aeruginosa* is also capable of utilising siderophores from other organisms [59]. This demonstrates an absolute requirement for iron for the survival of the bacterium and thus a requirement for siderophores in virulence.

Invasion of tissues by *P.aeruginosa* is dependent on production of extracellular enzymes and toxins, which break down physical barriers and damage host cells, as well as mediating resistance to phagocytosis and the host immune response. Examples of proteases being produced are LasA protease, protease IV, elastase and alkaline protease, which have wide substrate specificity [60, 61]. LasA protease cleaves collagen, IgG, IgA and complement and in addition to this it lyses fibronectin, disrupts the respiratory epithelium and interferes with ciliary function. In addition, elastase is capable of inhibiting monocyte chemotaxis [62]. Alkaline protease lyses fibrin and interferes with fibrin formation and together with elastase it inactivates interferon-γ (IFNγ) and tumor necrosis factor α (TNFα).

P.aeruginosa also produces exotoxin A, which is an adenosine diphosphate (ADP)-ribosyltransferase (ADPRT) [63]. Exotoxin A results in inhibited protein synthesis and cell death, which means it contributes to virulence by causing tissue damage and diminishing the activity of phagocytes [64]. In addition, *P.aeruginosa* also produces haemolysins, phospholipase C (PlcHR) and Rhamnolipid, which results in degradation of host cell phospholipids [65, 66].

Alignate, a muciod exopolysaccharide, is also produced by *P.aeruginosa*. It is a repeating polymer of mannuronic and glucuronic acid, which anchors the cells to their environment and forms the matrix for biofilms. Alginate also protects from lymphocytes, phagocytes, the ciliary action of the respiratory tract, antibodies and complement. These mucoid strains of *P.aeruginosa* are also more resistant to antibiotics [16].

Pyocyanin is a blue redox-active secondary metabolite produced by *P.aeruginosa*. It has a role in virulence by disrupting cell respiration, ciliary function, epidermal cell growth, prostacyclin release, calcium homeostasis and induction of apoptosis in neutrophils [67].

1.3 Bacterial Secretion Systems

Secretion systems are important virulence factors for bacterial species. In the case of Gram-negative bacteria, secretion requires translocation across the outer, as well as the inner membranes. In addition, a number of secreted proteins are destined to enter the host cell, thus several secretion systems include a portion which span the plasma membrane of host cells. Several secretion systems have been identified, these are classified into seven different types [68]. In Gram-negative bacteria, secreted proteins can be exported across the inner and outer membrane into the host cell in one single step via the type I, type III, type IV or type VI secretion pathways. Other proteins are first secreted into the periplasmic space via the general secretion (Sec) or two-arginine (Tat) pathways. These proteins can then be translocated across the outer membrane via the type II, type V, type I or type IV secretion system. The type VII secretion system is exclusive to the Gram-positive bacteria strains that possess a nearly impermeable cell wall, the mycomembrane [68].

The work presented in this thesis focus mainly on the T3SS of *P.aeruginosa*; however, T4SS and T2SS are also mentioned. This introduction will therefore mainly focus on the T3SS and briefly mention the T2SS and T4SS. Other secretion systems have no implications for the work in this thesis and will therefore be excluded.

1.3.1 Type III secretion system

T3SS are exclusive to Gram-negative bacteria and structurally related to the flagellum [69]. There are over twentyfive species of Gram-negative bacteria equipped with this secretion apparatus, also known as the 'injectisome'. These include *Yersinia, Salmonella, Shigella, Bordetella, Chlamydia, E.coli* and *P.aeruginosa*. The secretion system allows the bacteria to inject protein effectors into the host cell in one single step, which alters the function of the host cell and promotes survival of the bacteria. The effectors have a wide range of biochemical consequences for the host cell, with effects such as down-regulated pro-inflammatory responses, inhibited phagocytosis, induction of apoptosis and modulated intracellular trafficking. The effectors secreted by various pathogens vary in their structure and function whereas the components for the secretion system apparatus are conserved.

The T3SS of *P.aeruginosa* is closely related to that found in *Yersinia* species at both the structural and functional level. Bacterial attachment to the host cell membrane is required for delivery of proteins via the T3SS. Several surface structures of *P.aeruginosa* mediate attachment to epithelial cells [32, 34, 39, 44].

The biosynthesis and regulation of the type III secretion apparatus involve 36 genes encoded in five operons that are clustered together into the exoenzyme S regulon [70]. This regulon can then be divided into five parts, proteins for the needle complex, proteins which translocate secreted proteins, proteins that regulate the secretion process, chaperones which facilitate secretion and effector proteins [71].

The T3SS of *P.aeruginosa* is not required for infection [72] but it has been shown to enhance disease severity in models for acute pneumonia [73-76], keratitis [77], bacteraemia [78], ventilator-associated pneumonia [72] and burn-infections [79].

1.3.1.1　The needle complex

The needle complex allows proteins to pass the inner and outer membrane of the bacteria. The needle complex of *P.aeruginosa* is similar to that of *Yersinia* spp., as well as that of *Salmonella enterica* and *Shigella flexneri*. It consists of two parts; a multi-ring base and a needle-like filament (Figure 1.3). This filament has similar dimensions to that of *S.enterica*, *S.flexneri* and *Yersinia*; 60-120 nm long and 6-10 nm wide, and consists of subunits of the protein PscF (Figure 1.3) [6, 80-82]. Functional assignments can be inferred from the related *Yersinia* type III needle to the other components of the *P.aeruginosa* needle complex. PscN is believed to be an ATPase, which powers the secretion system. PscN is regulated by PscL (Figure 1.3) [83, 84]. The secretin-like protein PscC oligomerizes with the help of PscW to form a channel through the bacterial outer membrane [85, 86]. PscP is the protein responsible for the needle length through its presumed function as a molecular ruler, based on studies of YscP of *Yersinia* [87]. PscJ is predicted to be a lipoprotein component of the basal substructure of the needle complex [88]. Further studies are needed to fully understand the function of the needle complex in the secretion process [71].
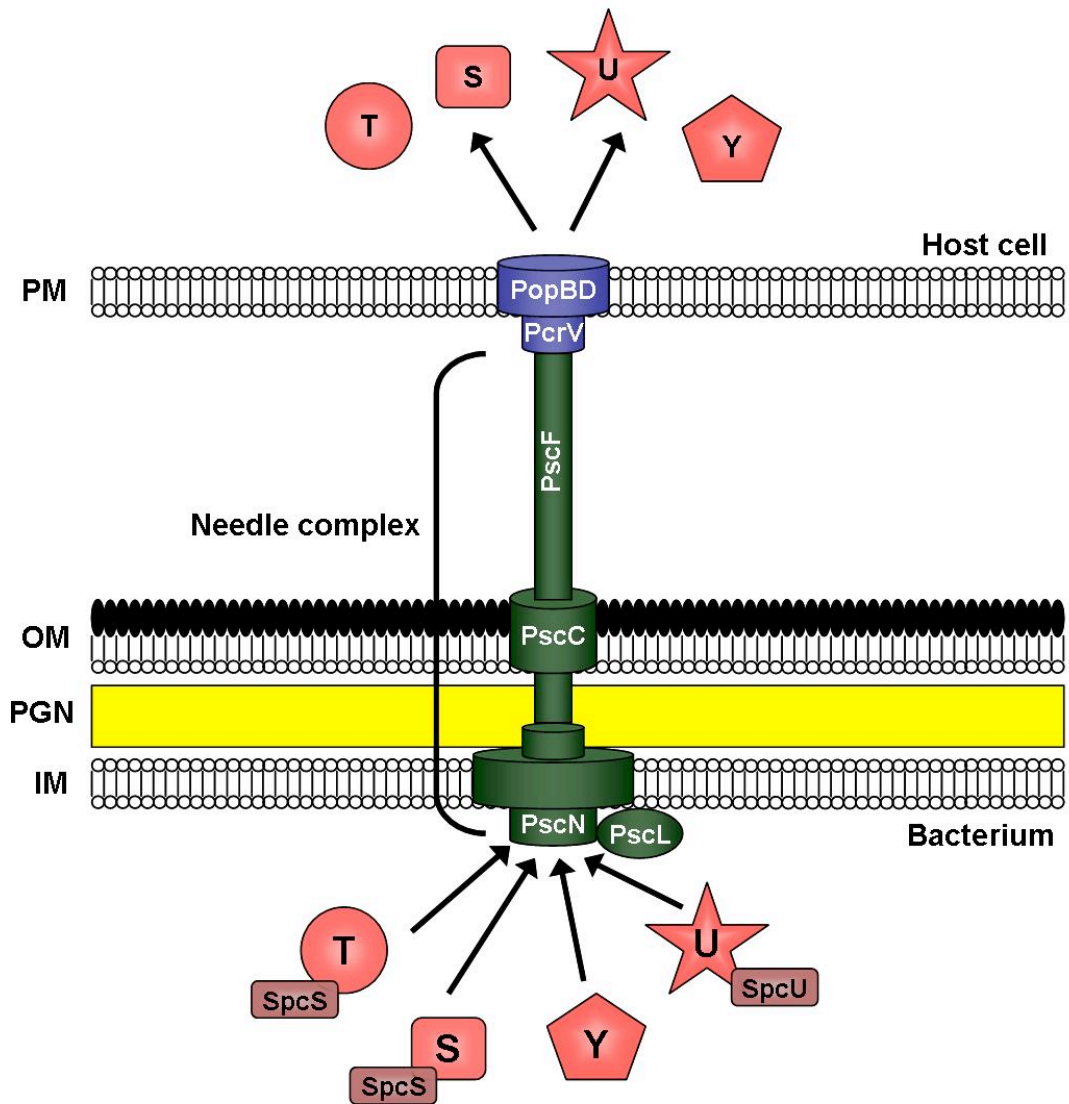
Figure 1.3; *Pseudomonas aeruginosa* **T3SS**

The T3SS has five components; the needle complex (green), translocation apparatus (blue), the effector proteins (red), chaperones (brown) and regulatory proteins (not presented in this figure). The needle complex and translocation apparatus work together to form a conduit for the effector proteins, allowing translocation into the host cell cytoplasm. PM; plasma membrane, OM; outer membrane, PGN; peptidoglycan layer, IM; inner membrane, T; ExoT, S; ExoS, Y; ExoY, U; ExoU. Figure adapted from [71].

1.3.1.2   The translocation apparatus

The effector proteins that are secreted by the needle complex are accepted by the translocation apparatus, which then delivers them across the host cell membrane (Figure 1.3). Less than 0.1% of secreted effectors escape to the extracellular milieu [89]. Translocation of the secreted effectors, Yops, in *Yersinia* into eukaryotic cells depends on the secreted translocator proteins,

LcrV, YopB and YopD [90, 91]. The translocators of *Yersinia* share high sequence similarity with *P.aeruginosa* proteins, PcrV, PopB and PopD (approximately 40% amino acid identity) (Figure 1.3) [92-94]. In addition, these proteins are conserved at the functional level. PopD and PopB are secreted by the needle complex and form a translocation pore, 2.8-6.0 nm in diameter, via interactions with each other and the host cell membrane (Figure 1.3) [92-96]. PcrV is also secreted by the T3SS needle. However, it is not part of the pore but still required for translocation (Figure 1.3) [97-99]. A *pcrV* mutant strain was unable to kill macrophages, or cause lethal infection and lung injury in an acute mouse infection model [93]. In addition, immunisation of mice with purified PcrV markedly increased survival in lung infection and burn injury models [93, 100, 101]. The LscV of *Yersinia* has been shown to form a multimeric scaffold at the tip of the T3SS needle, which facilitates assembly of the PopB-PopD translocation pore, therefore PcrV is presumed to have a similar function [98, 102]. However, PcrV might also function as a link between the needle complex to the pre-formed PopB-PopD pores [103]. Translocator mutants of *Yersinia* can be complemented with *pcrV, pcrG, pcrH, popB* and *popD* which restore function and mediate delivery of Yop effectors [99, 104]. Delivery of Yop effectors by *Yersinia* is contact-dependent and polarized; effectors are only translocated at the zone of contact between the bacterium and the eukaryotic cell [105]. In addition, the expression, secretion and delivery of Yop effectors are triggered following interaction of the bacteria with the eukaryotic cell [106]. Similarly, expression of effectors in *P.aeruginosa* is induced upon contact with epithelial cells [107, 108]. The translocation pore alone has also been shown to cause death of the host cells through pore-mediated increases in membrane permeability [75, 78, 92, 98].

1.3.1.3   Regulation of the T3SS

The T3SS is regulated both at the transcription level and at the initiation of secretion. Upon activation of the secretion process the transcription is induced, which allows expression of T3SS products at high levels following contact with the host cell [109]. The transcription of T3SS genes is controlled by ExsA, which binds to the promoter of T3SS genes (Figure 1.4B) [110]. In addition to ExsA, ExsC, ExsD and ExsE are also involved in the transcriptional regulation of the

T3SS (Figure 1.4). When ExsA is bound by ExsD secretion is prevented; under these conditions ExsC is bound to ExsE (Figure 1.4A) [111-114]. EsxE is exported through the T3SS needle complex during secretion, which allows ExsC to bind ExsD resulting in transcriptional activation of T3SS genes by ExsA (Figure 1.4B) [111, 114-116]. The result is that the production of T3SS proteins, needle complexes and effector proteins is expressed at low levels, which is then increased upon activation of secretion. Triggering of secretion is not very well described. Contact with the host cell will trigger secretion, as well as exposure to calcium-depleted medium [107].
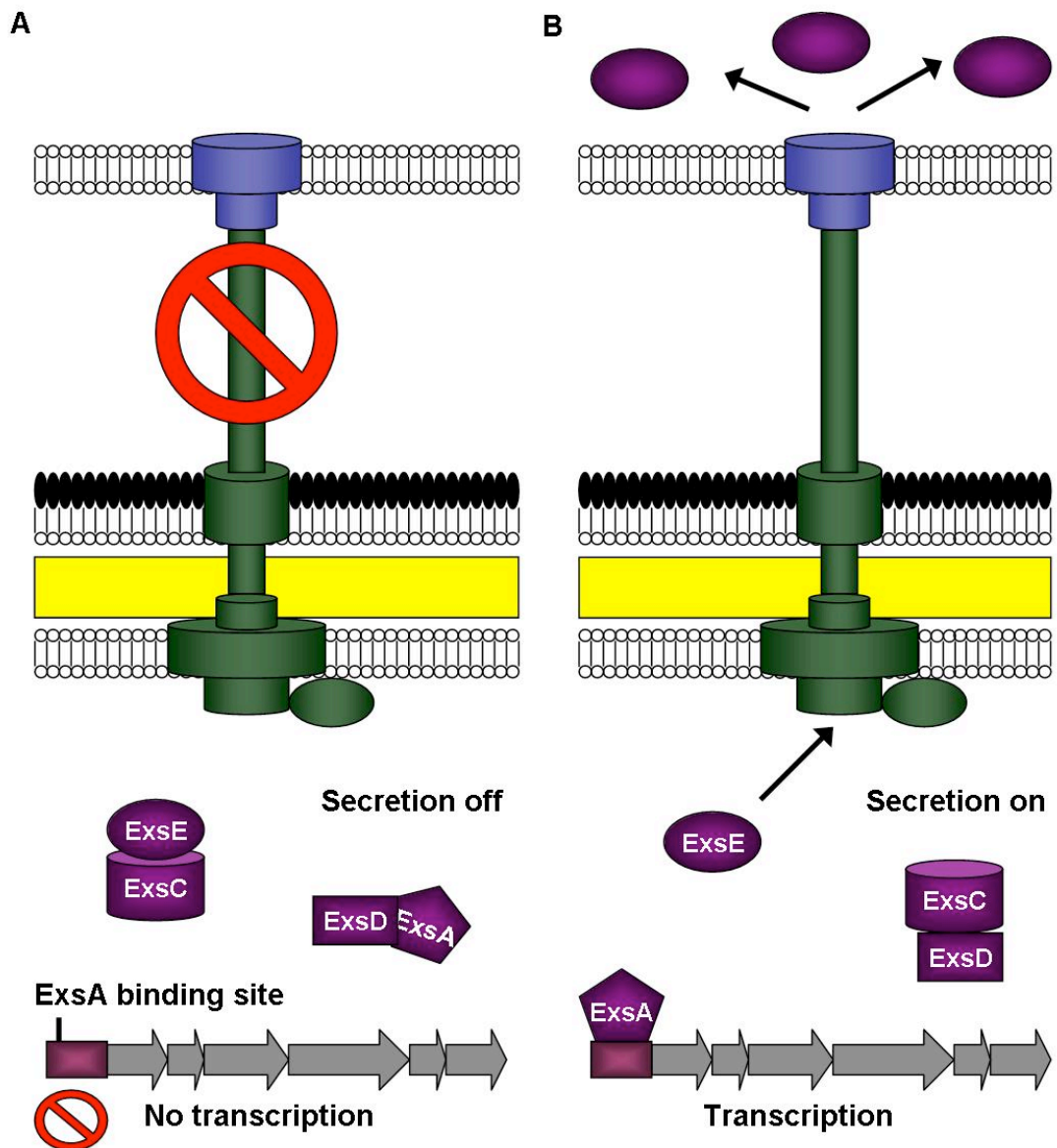
Figure 1.4; Regulation of the T3SS

T3SS transcription is linked to the effector protein secretion through the interaction of four regulatory proteins; ExsA, ExsC, ExsD and ExsE. A; When no secretion occurs ExsE is present in the bacterial cell and binds to ExsC. This allows ExsD to bind to ExsA which prevents transcription of the T3SS genes. B; Upon initiation of secretion, ExsE is secreted from the bacterial cell which allows ExsC to bind ExsD, thus freeing ExsA, the transcriptional activator, and transcription of the T3SS genes is initiated. Figure adapted from [71].

1.3.2 Effector proteins of Pseudomonas aeruginosa

P.aeruginosa is one of the Gram-negative bacteria which have a T3SS, as previously described. Four different effectors have been identified, ExoS, ExoT, ExoY and ExoU (Figure 1.3) [73, 109, 117, 118]. Not all *Pseudomonas* strains express all four effectors; instead it varies between the strains, which gives

them particular properties such as cytotoxic strains (e.g. PA103) and invasive strains (e.g. PAO1). PA103 injects ExoT and ExoU into the host cell whereas PAO1 injects ExoS, ExoT and ExoY [70, 75, 119, 120]. Strains usually possess either ExoS or ExoU but not both, the reason for which is unclear [119]. ExoS, ExoT and ExoY have clearly defined enzymatic activities, which in general results in altering of cellular cytoskeletal components. All three toxins cause cell rounding, detachment and inhibit or prevent bacterial uptake and phagocytosis (Figure 1.5). Together the effectors inhibit wound repair and the host innate immune response, which perpetuate tissue injury, and render the host susceptible to further colonization and injury by *P.aeruginosa* and other pathogens [121]. Some of the effectors have cognate chaperones to which they bind before secretion (Figure 1.3). The chaperones facilitate storage of their protein partners, as well as the delivery to the secretion apparatus [122].
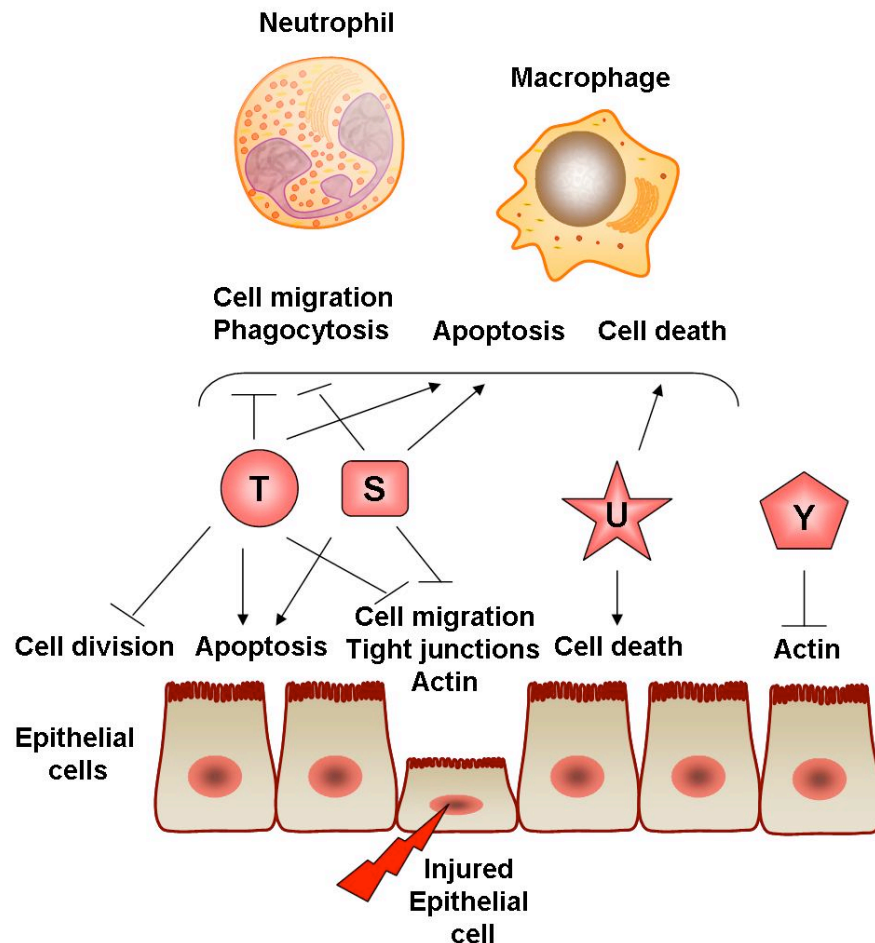
Figure 1.5; The effect of secreted *P.aeruginosa* effectors on host cells

ExoT inhibits cell division and cell migration, it can also induce cell death. ExoS induce apoptosis and inhibits cell migration, as well as disrupts tight junctions and actin in epithelial cells. Both ExoS and ExoT inhibits bacterial uptake into epithelial and phagocytic cells. ExoU cause rapid cell death and ExoY disrupts the actin cytoskeleton. Figure adapted from [121].

1.3.2.1   ExoS

ExoS is one of the best characterized effectors of *P.aeruginosa*. It is a bifunctional protein of 48 kDa, which shows GTPase-activating protein (GAP)-activity *in vitro* on the Rho-family proteins (Figure 1.6) [123]. These are small GTPases that maintain the organization of the host cell actin cytoskeleton. The active form is GTP-bound whereas the inactive form is GDP-bound. The effect of ExoS GAP-domain leads to disruption of the host cell actin cytoskeleton by switching towards the GDP-bound state [123]. The C-terminal domain of ExoS displays ADP-ribosyltransferase (ADPRT) activity that results in modification of members of the Ras family of GTP binding proteins *in vivo* (Figure 1.6) [124-

128]. The ADPRT activity correlates with cellular cytotoxicity [127], and requires a host cell cofactor, a 14-3-3 protein [129]. 14-3-3 proteins act as regulatory factors that modulate cell cycle progression, protein trafficking and apoptosis [71]. Intracellular delivery of ExoS results in an impaired phagocytic function of infected macrophages, as well as in a morphological change of the infected cells due to the disruption of the actin microfilaments (Figure 1.5) [118, 130]. In addition, ExoS inhibits DNA synthesis, vesicular trafficking and endocytosis [71, 127]. The enzymatic activity of ExoS has also been shown to induce apoptosis in macrophages and neutrophils (Figure 1.5) [131]. In addition, ExoS has been shown to be involved in the regulation of T3SS-mediated secretion through host cell membranes [132]. The chaperone of ExoS is SpcS (Figure 1.3) [133]. The extreme N-terminal of ExoS carries the information for its targeting to the T3SS apparatus (Figure 1.6) [109]. In addition, ExoS possess a binding site for the SpcS and a membrane localization domain (MLD), which is responsible for the initial transient localization of ExoS to the plasma membrane (Figure 1.6) [134, 135].

1.3.2.2 ExoT

ExoT, similar to ExoS, has an N-terminal domain that encodes GAP and a C-terminal encoded ADPRT activity (Figure 1.6) [123]. In addition, ExoT has the same chaperone, SpcS, as ExoS (Figure 1.3) [133]. The two proteins share 76% amino acid identity, and it is believed that ExoT has a similar secretion, SpcS chaperone binding and MLD domain (Figure 1.6) [136]. ExoT causes reversible disruption of the actin cytoskeleton resulting in cell rounding, cell detachment, inhibited migration and phagocytosis (Figure 1.5) [130, 137]. It also results in inhibited host cell division (Figure 1.5) [138]. The ADPRT domain of ExoT also requires binding of 14-3-3 for activation [139].

1.3.2.3 ExoU

ExoU possess a unique cytotoxic effect, both rapid and potent (Figure 1.5) [73, 74]. The *P.aeruginosa* strains which produce ExoU can destroy cellular monolayers during short infection periods [73, 74]. Production of ExoU is associated with cell death, accelerated lung injury in animals and patients, bacterial dissemination and it also has a role in the development of septic shock

[73, 140, 141]. ExoU functions as a phospholipase A_2 via its patatin-like domain (Figure 1.6) [142, 143]. It has a broad substrate specificity including hydrolysis of neutral lipids, such as diacylglycerols, triacylglycerols and phospholipids, which allows it to cause damage to internal and plasma membrane components [142, 143]. It is believed that ExoU possess a serine-aspartate catalytic dyad, which involves Ser142 and Asp344 (Figure 1.6), which is required for its function [142-144]. ExoU is delivered by the T3SS directly into the host cell cytosol, where it requires a host cell cofactor for activation [142, 143]. The copper-zinc-superoxide dismutase (SOD1) has been identified as a potential cofactor [145]. Similar to the other effectors, the secretion signal directing ExoU to the T3SS is believed to be located in the extreme N-terminus (Figure 1.6) [71]. ExoU has a chaperone called SpcU, which binds to the N-terminal of the protein (Figure 1.6) [146]. Furthermore, ExoU contains a MLD domain in its C-terminal which targets it to the plasma membrane of the host cell (Figure 1.6) [147, 148].

1.3.2.4 ExoY

ExoY is an adenylyl cyclase [117]. It contains two domains which are similar to the extracellular adenylyl cyclases of *Bordetella pertussis* (CyaA) and *Bacillus anthracis* (edema factor) [117]. These two domains act together and bind ATP (Figure 1.6). Full enzymatic activity can only be obtained in the presence of a host cell cofactor, which is not yet identified [117]. ExoY translocation results in elevated intracellular cAMP concentrations [117, 149]. The effects of ExoY on the host cell are disruption of the actin cytoskeleton, inhibition of bacterial uptake by host cells and increased endothelial permeability (Figure 1.5) [117, 150-152]. The chaperone of ExoY is yet to be identified.
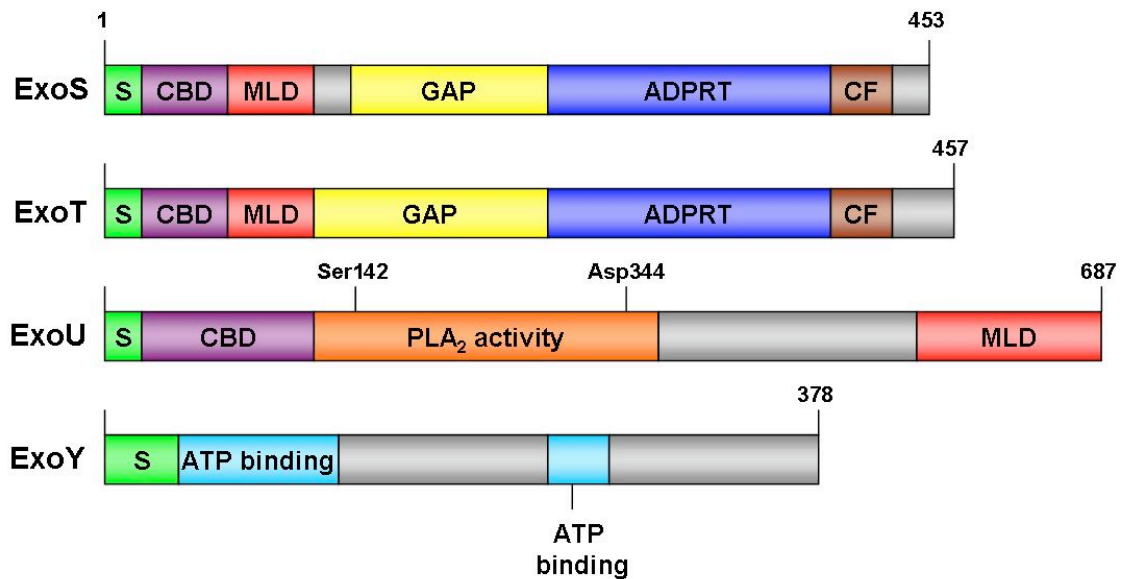
Figure 1.6; The gene structure of the effector proteins from _P.aeruginosa_

ExoS and ExoT both have GTPase activating protein (GAP) and ADP ribosyl transferase (ADPRT) activity. In addition, they both have a secretion signal domain (S), chaperone binding domain (CBD), membrane localization domain (MLD) and a cofactor binding site (CF). ExoU has a patatin-like domain necessary for its phospholipase A_2 activity (PLA_2 activity). This domain contains the Ser142 and Asp344, which are required for its activity. ExoU also contains a secretion signal domain (S), chaperone binding domain (CBD) and a membrane localization domain (MLD). ExoY is an adenylyl cyclase. It contains two domains which together bind ATP (ATP binding) and a secretion signal domain (S). Figure adapted from [71].

1.3.3 Type II secretion system

The T2SS is also known as the Sec-dependent system, since several proteins first reach the periplasm via the Sec-system and then are secreted via the T2SS. The Sec-dependent pathway is universal, but the T2SS is only found in Gram-negative proteobacteria [153, 154]. This secretion system is required for virulence of _Vibrio cholerae_, _Legionella pneumophila_ and enterotoxigenic _E.coli_. Toxins secreted via the T2SS include ADP-ribosylating toxins, such as cholera toxin and the exotoxin A from _P.aeruginosa_ [154]. The structure of the inner membrane complex and the pseudopilins, which span the periplasm, are homologs to the type IV pilus system. This suggests a common evolutionary origin [154].

1.3.4 Type IV secretion system

The T4SS can transport nucleic acids as well as proteins into plant, animal and yeast cells and other bacteria [155]. It can span both membranes of Gram-

negative bacteria or the membrane and cell envelope of Gram-positive bacteria. The type IV secretion system is classified into three subfamilies, the conjugation systems, DNA uptake and release systems and the effector translocator systems [156]. Bacterial species which possess a T4SS used for effector translocation include *Helicobacter pylori* and *Legionella pneumophila* [157, 158].

1.4 Inflammation

The word inflammation comes from the word *inflamatio*, which in Latin means to set on fire. It is a non-specific immune response to any injury such as pathogens, damaged cells or irritants. There are five cardinal signs of inflammation: redness, swelling, heat, pain and loss of function. The first four were described by Cornelius Celsus, a Roman encyclopaedist, and loss of function was added several centuries later by Rudolf Virchow. These signs can be explained by increased blood flow, elevated cellular metabolism, vasodilatation, release of soluble mediators, extravasation of fluids and cellular influx. Inflammation is normally a self-limiting process, whereby the organism tries to remove the injurious stimuli, as well as to initiate the healing process. If it becomes continuous chronic inflammation can develop [159]. Inflammation is the response of the organism to bodily injuries and it is not synonymous to infection, which is caused by an exogenous pathogen. The inflammation process requires great amount of metabolic energy and results in damage and destruction of the host tissue. It also has the potential to lead to sepsis, multiple organ failure and death. Infection or tissue injury disrupts the homeostasis of the tissue and the main goal of the inflammation is to repair the damage, clear the infection and return to homeostasis. Therefore, a rapid, accurate and self-limiting response is necessary to limit the damage caused [160].

The innate immune system mediates the first response in an inflammation process and thus plays an important role by secreting cytokines, chemokines and inducing the expression of adhesion and costimulatory molecules [159, 161]. The acute inflammation is characterized by infiltration of innate immune response cells such as neutrophils and macrophages [159]. Acute inflammation is a short-term process, which usually appears in a few minutes or hours and ceases once the injurious stimulus has been removed. The acute inflammation is

characterized by the five cardinal signs described above. During a chronic inflammation there are also influx of T lymphocytes and plasma cells [159]. The T lymphocytes and plasma cells are part of the adaptive immune response. This is triggered following an antigenic challenge to the organism. The adaptive immune response has a high degree of specificity and also the property of memory.

1.5 Innate immune system

Immunity is defined as a state of protection from infectious disease. The innate immune system provides the first line of defence in an immune response against danger and is usually sufficient to clear the infection. This response includes a range of processes which are not specific to a particular pathogen; as a result, it is able to recognize a wide range of pathogens such as viruses, bacteria and fungi. Important features of the innate immune system are barriers, such as anatomic (skin), physiologic, phagocytic and inflammatory, as well as the synthesis of antimicrobial products and phagocytosis by macrophages and neutrophils. Physical and anatomic barriers such as skin and mucosal surfaces, prevent entry of pathogens into the host and provide the first line of defence against infections. Skin has an acidic pH (between 3-5) which inhibits the growth of most microorganisms. Breaches of the integrity of the skin, such as wounds, provide a route of entry for pathogens. Mucosal surfaces can be found in the conjunctivae, alimentary, respiratory and urogenital tracts. Saliva, tears and mucous secretions prevent microorganisms from entering via these routes. Physiologic barriers include temperature, pH and a variety of soluble and cell associated molecules. High temperature can prevent growth of pathogens as well as low pH. Examples of soluble molecules are: lysozyme, which digests peptidoglycan in bacterial cell walls; interferon, which results in an antiviral response; and complement, which is able to damage the walls of pathogens or facilitating their clearance.

The innate immune system can recognize and respond to danger signals and non-self, which are a limited number of highly conserved structures of microorganisms, known as pathogen-associated molecular patterns (PAMPs), and cell products associated with a breach in host defence also known as danger-

associated molecular patterns (DAMPs) [159, 162, 163]. This is a fundamental feature of the host defence against bacterial infections. If the pathogens were able to change their PAMPs they would escape the immune response. However, the immune system has evolved to recognize structures that are essential for the survival of the microbe and are therefore less prone to modifications. PAMPs can be sugars, flagellin, peptidoglycan and lipopolysaccharide (LPS), while examples of DAMPs are mammalian dsDNA and uric acid crystals [161, 164]. DAMPs are often released during infections, as a result of tissue damage and cell lysis [161]. The wide variety of pathogens, PAMPs and DAMPs can be recognized by a limited number of germline-encoded receptors called pattern-recognition receptors (PRRs) [165]. It is not clear whether these are actual receptors, so a more accurate term for them would therefore be pattern recognition molecules (PRMs) [159]. These PRRs do therefore not only recognize invading pathogens but also the damage caused by them. PRRs are expressed by several cell types such as macrophages, monocytes, dendritic cells (DCs), neutrophils and epithelial cells [161]. PRRs include soluble receptors; pentaxins, membrane-bound receptors: Toll-like receptors, TLRs [166] and C-type lectin receptors, CLRs [167], as well as cytosolic receptors: Nod-like receptors, NLRs [161], RIG-like helicases, RLRs [168] and DNA sensors [169-171] (Figure 1.7).
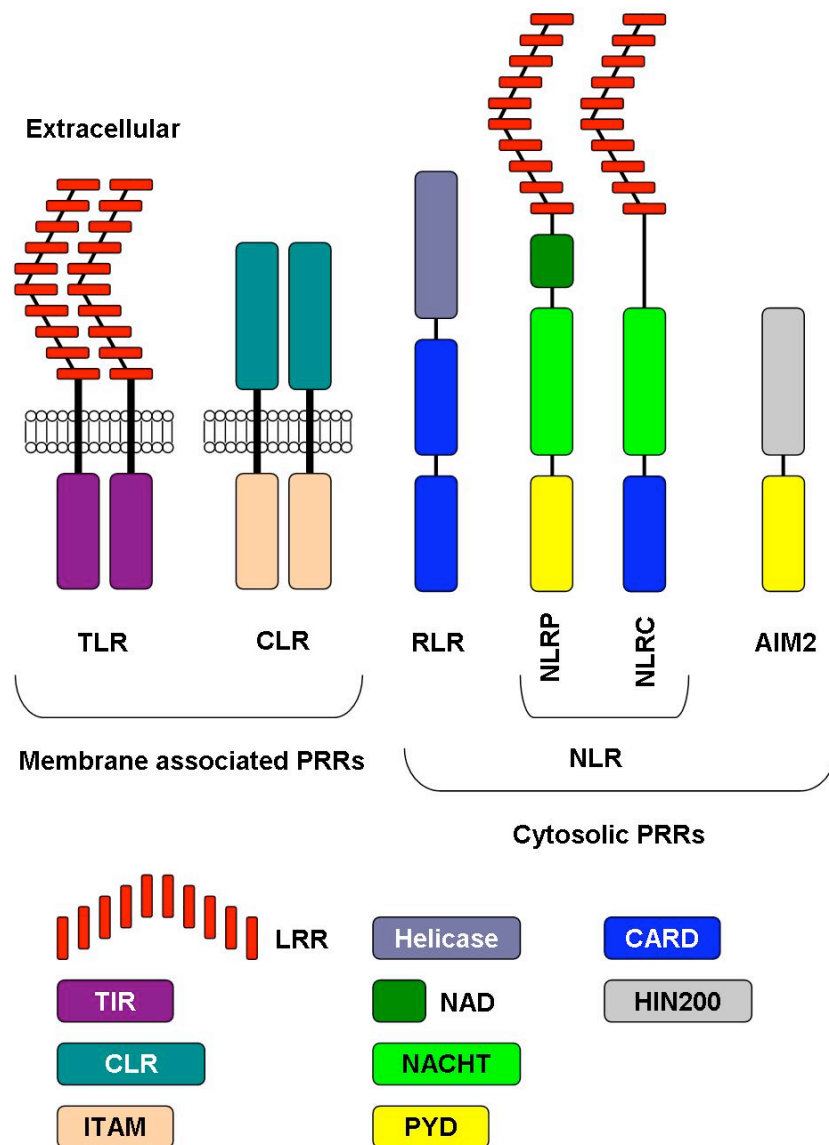
Figure 1.7; Comparison of basic structure of different PRRs

Schematic representation of PRRs. Abbreviations; TLR; Toll-like receptor, CLR; C-type lectin receptor, RLR, RIG-1-like receptor; NLR. NOD-like receptor, NLRP and NLRC; major subfamilies in the NLR-protein family, AIM2; absent in melanoma 2 (DNA sensor), LRR; leucine-rich repeats, TIR; Toll-interleukin-1 receptor interacting domain, ITAM; immunoreceptor tyrosine-based activation motif, NAD; NACHT associated domain, NACHT; nucleotide binding and oligomerization domain, PYD; pyrin domain, CARD; caspase recruitment domain and HIN200; HIN200 domain. Figure is adapted from [172].

1.5.1 Toll-like receptors (TLRs)

Toll-like receptors (TLRs) were first discovered as homologues of *Drosophila* Toll [173]. *Drosophila* Toll was shown to be involved in antifungal immune responses [174]. TLRs are expressed by several cell types such as mononuclear, endothelial and epithelial cells. These are type I transmembrane proteins, which contain

extracellular leucine-rich repeat domains (LRR). These LRR domains functions as the pathogen sensor (Figure 1.7). The LRR transmit signals through the cytoplasmic Toll-interleukin (IL)-1 receptor (TIR) domain (Figure 1.7) [166, 175]. The TIR-domain functions as a platform for downstream signalling, which involves recruitment and interactions with TIR-domain containing adaptor proteins (Table 1.1), for example, myeloid differentiation primary response gene 88 (MyD88) and TIR domain-containing adaptor inducing IFN-ß (TRIF) [176]. The signalling event triggered is dependent on the associated adaptor protein, but they ultimately lead to activation of transcription factors nuclear factor kappa B (NF-κB), activator protein (AP)-1 and interferon-regulatory factor (IRF)-3 [161]. Generally, the MyD88-pathway controls inflammatory responses, while TRIF mainly mediate type I IFN responses [177]. Activation of TLRs leads to the production of antimicrobial peptides, inflammatory cytokines and chemokines, TNFα, costimulatory and adhesion molecules and upregulation of major histocompatibility complexes (MHCs).

TLRs can recognize and/or sense the presence of LPS, lipoproteins, flagellin and RNA from viruses or bacteria, directly or indirectly via homo- or hetero-dimers. To date, 10 human and 13 mouse TLRs have been identified and these are either surface expressed (TLR1, 2, 4, 5, 6 and 10) or endosome localised (TLR3, 7, 8 and 9) [166] (Table 1.1). Surface expressed TLRs recognize bacterial and fungal cell wall components, as well as viral proteins. In contrast, endosomal TLRs recognize nucleic acids; such as viral DNA/RNA (Table 1.1) [178-180]. Direct binding of dsRNA and lipopeptides to TLR3 and TLR1/TLR2 has been shown [181]. In contrast LPS is sensed indirectly by TLR4, which involves MD-2 [182]. TLRs were discovered as a class of membrane receptors that sense extracellular microbes and trigger antipathogen signalling cascades. One pathogen triggers several TLRs, which leads to the most appropriate response against one particular pathogen. Following studies of TLR signalling pathways and TLR-deficient mice it was shown that TLRs were not alone as innate immune receptors.

Table 1.1; Mouse TLRs with PAMPs and adaptors

Localization	TLRs	PAMPs	Adaptors
Surface expressed	TLR1/2	Triacyl lipopeptides (Bacteria and mycobacteria)	MyD88, TIRAP
	TLR2	Hemagglutinin protein (Measles virus), Glycosylphosphophatidyl-Inositol mucin (Trypanosoma), Phopholipomannan (*Candida albicans*), Lipoarabinomannan (Mycobacteria), Porins (*Neisseria*)	MyD88, TIRAP
	TLR4	LPS (Gram-negative bacteria), Mannan (*Candida albicans*), Glycoinositolphospholipids (Trypanosoma), Envelope proteins (RSV, MMTV)	MyD88, TIRAP, TRAM, TRIF
	TLR5	Flagellin (flagellated bacteria)	MyD88
	TLR6/2	Zymosan (*Saccharomyces cerevisiae*), Lipoteichoic acid (*Streptococcus*), Diacyl lipopeptides (Mycoplasma)	MyD88, TIRAP
	TLR11	Uropathogenic bacteria, Profilin like molecule (*Toxoplasma gondii*)	MyD88
Endosome expressed	TLR3	poly I:C, dsRNA (Reovirus), ssRNA (WNV),	TRIF
	TLR7	ssRNA viruses (Influenza virus, VSV), RNA (bacteria)	MyD88
	TLR9	dsDNA virus (HSV, MCMV), CpG-DNA motifs (bacteria and viruses), Hemozoin (Plasmodium)	MyD88

The PAMPs for mouse TLR8, TLR12 and TLR13 have not yet been identified. Abbreviations; MyD88; myeloid differentiation primary response gene 88, TIRAP; TIR-containing adaptor protein, TRAM; TRIF-related adaptor molecule, TRIF; TIR-containing adaptor-inducing IFN-β, RSV;

Respiratory Syncytical Virus, MMTV; Mouse Mammary Tumour Virus, WNV; West Nile Virus, VSV; Vesicular Stomatitis Virus, HSV; Herpes Simplex Virus, MCMV; Mouse Cytomegalovirus. Table adapted from [180, 183].

1.5.2 RIG-I-like receptors (RLRs)

RLRs are soluble proteins that survey the cytoplasm for intracellular invaders. The RLRs that have been identified so far are involved in antiviral responses by recognizing viral RNA. Helicases identified include the RNA helicases RIG-1 (retinoic acid-inducible gene I) and MDA-5 (melanoma differentiation-associated gene-5) [184-186]. RIG-1 and MDA-5 have two N-terminal CARD domains, a central helicase domain and a C-terminal regulatory domain [186]. RIG-1 has been shown to sense hepatitis C virus, Sendai virus, influenza virus, vesicular stomatitis virus, Newcastle disease virus, rabies virus and Japanese encephalitis virus, while MDA-5 senses picornaviruses and poly I:C (poly-cytidylic acid) [187, 188]. Furthermore, RIG-1 is triggered by short dsRNAs, whereas MDA-5 is triggered by long dsRNAs [189]. In addition Dengue virus triggers both RIG-1 and MDA-5 [189]. The viral RNA is distinguished from cellular RNA by a 5´-triphosphate modification [190]. Viral nucleic acids are also recognized within the endosomes by TLR7 and TLR9, mainly in plasmacytoid DCs. Other cell types recognize viral RNA via RLRs in the cytoplasm [184, 186]. Activation of these receptors results in NF-κB and IRF3/7 activation which leads to transcription of type I IFN, which in turn leads to antiviral immunity and triggering of adaptive immunity [168].

1.5.3 C-type lectin receptors (CLRs)

CLRs are important in antifungal immunity [191]. The CLR family of proteins is a large family where all proteins possess a C-type lectin-like domain (CTLD). Out of the 17 groups of this family, the mannose receptor (MR), Dectin-1 and -2, dendritic cell-specific ICAM-3-grabbing non-integrin (DC-SIGN) and the collectins have been shown to be involved in antifungal immunity [191]. These receptors result in fungal binding, uptake and killing, as well as contributing to the immune response.

The MR can be both membrane-bound and soluble, with the majority located within the endocytic pathway. MR recognizes carbohydrates, such as mannose, fucose and N-acetyl glucosamine from bacteria and viruses. In addition, MR is involved in recognition of fungi, which contain mannose-based structures on their cell walls [192, 193]. In response to fungi, MR activation leads to NF-κB activation and secretion of IL-12, IL-8, IL-1ß and IL-6 [191, 193].

Dectin-1 recognizes ß-1,3-glucans and mediates signalling through its cytoplasmic ITAM-like motif [167]. This results in activation of the respiratory burst, activation and regulation of phospholipase A_2 (PLA_2) and cyclooxygenase 2 (COX2), endocytosis and phagocytosis and TNF, macrophage inflammatory protein 2 (MIP-2), IL-2, IL-10, IL-6 and IL-23 production [167]. The production of proinflammatory cytokines requires collaborative signalling from TLRs [167]. Dectin-2, on the other hand, has been shown to recognize mannose structures and fucose [194]. Upon activation it induces TNF and IL-1R antagonist, but the role of this receptor in antifungal immunity is still unclear [195].

The collectins are an example of secreted multimeric complexes [191]. Several collectins have been implicated in antifungal immunity, such as mannose-binding lectin (MBL) and surfactant protein A and D (SP-A, SP-D) [191]. Collectins lead to activation of complement, which promotes opsonic fungal recognition, triggering of microbial agglutination, as well as modulation of phagocytosis, cytokine production and respiratory burst [191].

1.5.4 NOD-like receptors (NLRs)

NLRs (NOD (Nucleotide oligomerization domain)-like receptors) have been identified as intracellular microbial sensors [161]. They are a large family of proteins with 23 members in humans and 34 in mice so far identified [172]. They contain LRRs and resemble plant disease-resistance genes. Plants have a wide range of intracellular pathogen detectors; these were the first receptors that revealed the importance of intracellular pathogen detection [196]. The first NLR to be identified was Nod1 (nucleotide-binding oligomerization domain 1), as a homologue to a *C.elegans* protein (CED-4) responsible for regulating apoptosis [197]. Several different names have been used for the same NLRs in different

publications, but recently a standard nomenclature was described for these proteins [198]. This nomenclature will be used in this thesis.

NLRs are multidomain proteins consisting of C-terminal LRRs, a central nucleotide domain (called NACHT, domain in NAIP, CIITA, HET-E and TP1, or NBD, nucleotide binding domain) and N-terminal effector domain (Figure 1.8). The LRRs have been implicated in ligand sensing and autoregulation of NLRs and TLRs, as mentioned above. The mechanism by which the LRRs sense their ligands is still unknown, as no direct binding has been identified. Therefore it is believed that the sensing via NLR-LRRs is indirect, which has also been described for some TLRs. The LRR contain 20-30 amino acids rich in Leucine, which form a horseshoe-shaped molecule via its tandem repeats of a ß-strand and α-helix [199]. The NACHT domain is present in all NLRs and is similar to a motif (NB-ARC) in the apoptotic mediator APAF-1 [161]. Binding of cytochrome c to APAF-1 results in oligomerization of APAF-1 via its NB-ARC domain, which initiates apoptosis. Similarly it has been shown that oligomerization of the NACHT domain is important for activation of the NLR protein. This results in the formation of active multimeric protein complexes, such as inflammasomes and NOD signalosomes [200, 201]. The N-terminal effector domain of NLRs divides them into different subfamilies (Figure 1.8). These effector domains mediate signal transduction to downstream targets, such as inflammatory caspases for the inflammasomes and NF-κB activation for the NOD signalosomes. Most NLRs have a death-fold domain in their N-terminal, such as a caspase recruitment domain (CARD) or pyrin domain (PYD). These death-fold domains were described for proapoptotic signalling pathways and include, in addition to CARD and PYD, the death domain (DD) and the death effector domain (DED) [202]. Death-domains can form homologous dimers or trimers, which allows receptors to bind to adaptors and effector proteins. This allows CARD- or PYD-containing NLRs to recruit other CARD or PYD containing proteins to the signalling platforms.
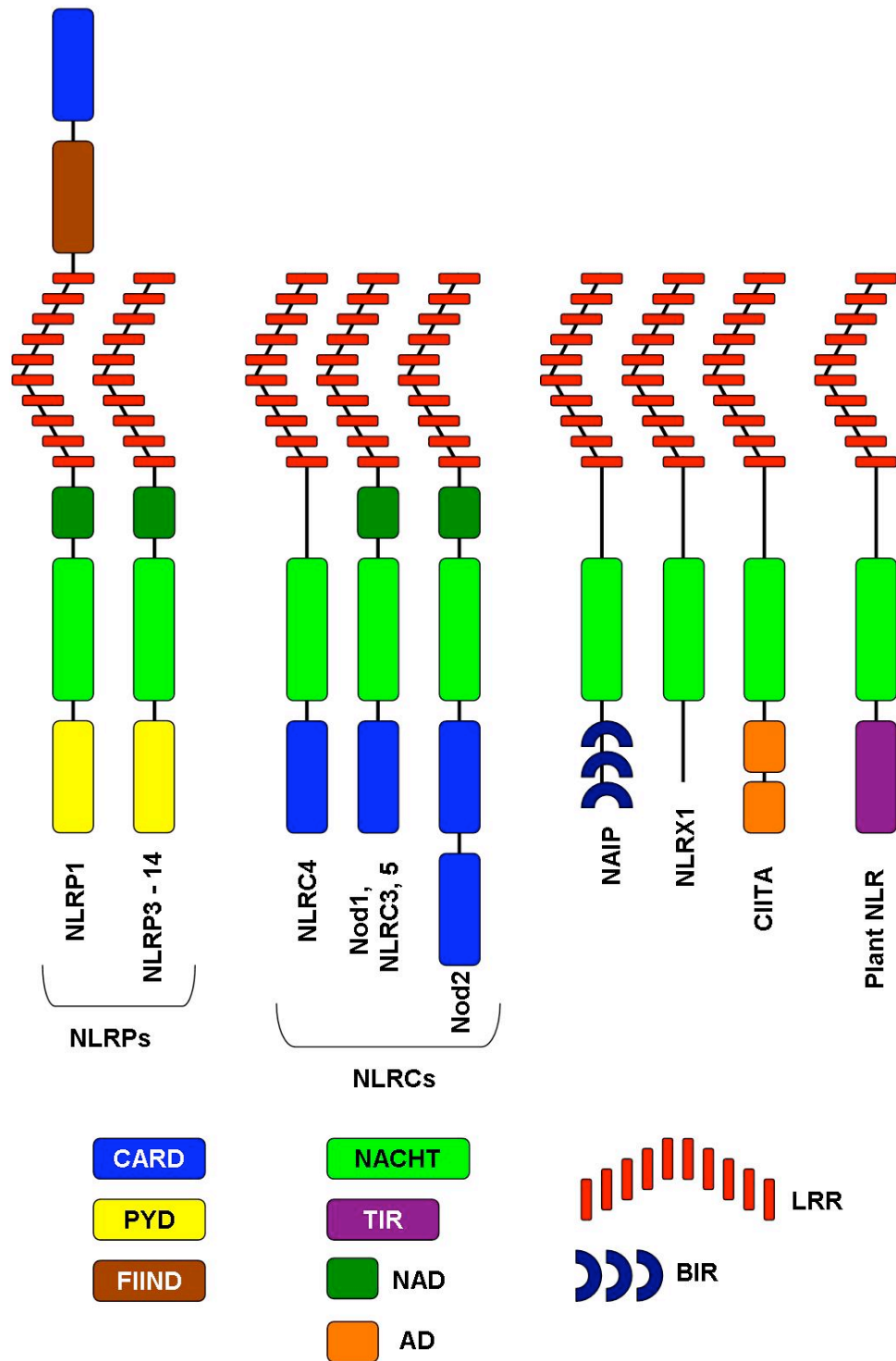
Figure 1.8; Domain organization of NLRs

NLRs have three distinct domains, a C-terminal leucine-rich repeats, involved in ligand sensing, a central NACHT domain, involved in oligomerization and an N-terminal effector domain, which is a CARD, PYD or BIR depending on NLR subfamily. Some NLRs have a NAD domain at the C-terminal side of NACHT. NLRs are divided into five subfamilies, NLRPs, NLRCs and NAIP, NLRX1 and CIITA. A comparison with plant NLR-like gene is also shown. Abbreviations; CARD, caspase recruitment domain, PYD, pyrin domain, FIIND, function to find, NACHT, domain conserved in NAIP, CIITA, HET-E and TP1, NAD, NACHT associated domain and BIR, baculovirus IAP repeat, NAIP, NLR family apoptosis inhibitory protein, AD, activation domain, CIITA, class II transcription activator. Figure adapted from [161, 198].

There are five different NLR subfamilies, characterized by a specific molecular structure (Table 1.2) [198, 203, 204]. The largest subfamily is NLRP, which has 14 genes in the human genome [204]. NLRP1, NLRP2 and NLRP3 have been identified as proteins present in the inflammasome complexes. Proteins in the NLRP subfamily contain an N-terminal PYD. In contrast, another NLR subfamily called NLRC contains an N-terminal CARD-domain. This subfamily includes Nod1, Nod2, NLRC3, NLRC4 and NLRC5 [198, 203, 205]. The remaining subfamilies are called NLRA, NLRB and NLRX and only contain one identified NLR protein in each family; CIITA, NAIP and NLRX1 respectively [198]. NLRC4 and NAIP are also involved in the formation of inflammasome complexes, together or separately. CIITA is involved in the transcriptional regulation of MHC II [206]. The function of NLRX1 is not fully understood; it is recruited to the outer membrane of mitochondria and might function as a negative regulator of antiviral response or promoting the production of reactive oxygen species [207-209]. Nod3 and Nod4 have no described function yet.

Table 1.2; NLRs

NLR subfamily	Nomenclature		Names and aliases	Structure
	Human	**Mouse**		
NLRA	CIITA	CIITA	MHC2TA, C2TA, NLRA	(CARD)-AD-NACHT-NAD-LRR
NLRB	NAIP	NAIP a-g	BIRC1, NAIP1-7, Birc1 a-g, NLRB1, CLR5.1	BIR-BIR-BIR-NACHT-LRR
NLRC	Nod1	Nod1	CARD4, CLR7.1, NLRC1	CARD-NACHT-NAD-LRR
	Nod2	Nod2	CARD15, CD, BLAU, IBD1, PSORAS1, CLR16.3, NLRC2	CARD-CARD-NACHT-NAD-LRR
	NLRC3	NLRC3	Nod3, CLR16.2	CARD-NACHT-NAD-LRR
	NLRC4	NLRC4	IPAF, CARD12, CLAN, CLR2.1	CARD-NACHT-LRR
	NLRC5	NLRC5	Nod4, NOD27, CLR16.1	CARD-NACHT-LRR
NLRPs	NLRP1		NALP1, DEFCAP, NAC, CARD7	PYD-NACHT-NAD-LRR-FIIND-CARD
		NLRP1a		NACHT-NAD-LRR-FIIND-CARD
	NLRP2	NLRP2	NALP2, Pypaf2, NBS1, PAN1	PYD-NACHT-NAD-LRR

NLRP3	NLRP3	NALP3, Cryopyrin, Pypaf1, CIAS1	PYD-NACHT-NAD-LRR
NLRP4	NLRP4 a-g	NALP4, Pypaf4, PAN2, RNH2	PYD-NACHT-NAD-LRR
NLRP5		NALP5, Pypaf8, Mater, PAN11	PYD-NACHT-NAD-LRR
	NLRP5		NACHT-NAD-LRR
NLRP6	NLRP6	NALP6, Pypaf5, PAN3	PYD-NACHT-NAD-LRR
NLRP7		NALP7, Pypaf3, NOD12	PYD-NACHT-NAD-LRR
NLRP8		NALP8, PAN4, NOD16	PYD-NACHT-NAD-LRR
NLRP9	NLRP9 a-c	NALP9, NOD6	PYD-NACHT-NAD-LRR
NLRP10	NLRP10	NALP10, PAN5, NOD8, Pynod	PYD-NACHT-NAD
NLRP11		NALP11, Pypaf6, NOD17	PYD-NACHT-NAD-LRR
NLRP12	NLRP12	NALP12, Pypaf7, Monarch1, RNO2, PAN6	PYD-NACHT-NAD-LRR
NLRP13		NALP13, NOD14	PYD-NACHT-NAD-LRR

	NLRP14	NLRP14	NALP14, NOD5	PYD-NACHT-NAD-LRR
NLRX	NLRX1	NLRX1	Nod5, NOD9, CLR11.3	X-NACHT-LRR

Table adapted from [161, 198].

NLRs are mainly expressed in cells and tissues that have a role in immunity. Epithelial cells form the first barrier against infection, as mentioned above, and several NLRs are expressed by these cells such as Nod1, Nod2, NLRP3 and NAIP [210-212]. NLRP3 is also expressed by immune cells and osteoblasts [213]. In contrast, NLRP1 is widely expressed. NAIP and NLRC4 are expressed in macrophages and brain, spleen, liver and lung [214, 215]. The expression of NLRs such as Nod1, Nod2 and NLRP3 are increased by TLR stimulation [216].

1.5.4.1 Nod1 and Nod2

Nod1 was the first NLR protein identified, as mentioned above [197, 217]. Upon activation of Nod1 and Nod2 the receptor-interacting protein 2 (RIP2) caspase-like apoptosis-regulator protein (CLARP) kinase (RICK) is recruited via CARD-CARD interactions. This leads to activation of NF-κB [218]. Both proteins detect peptidoglycan derived muropeptides, Nod2 detects muramyl dipeptides (MDP) and Nod1 detects meso-diaminopimelic acid (meso-DAP) [219, 220]. Nod1 and Nod2 are crucial for the innate immune response in epithelial cells. They control infection via the gastro-intestinal route, for example by *H.pylori* and *Listeria monocytogenes* [221, 222]. Nod1 and Nod2 will be discussed in more detail in chapter 6.

Mutations, mainly in the LRR-region, of the Nod2 gene are associated with Crohn's disease (inflammatory bowel disease) [223]. The disease is believed to develop as a consequence of loss of tolerance toward commensal bacteria or allowing proliferation of pathogenic bacteria in the gut. In addition, a gain-of-function mutation in the Nod2 gene results in Blau syndrome (autoinflammatory disorder resulting in skin rashes and joint inflammation) [224]. Nod2 has also been shown to be involved in the MDP- and NLRP3-dependent inflammasome activation [225, 226].

1.5.4.2   Inflammasome complexes

Some of the NLR proteins have been shown to form large protein complexes in the cytosol, called inflammasomes. These complexes link the sensing of microbial products and metabolic stress to the proteolytic activation of the pro-inflammatory cytokines IL-1ß and IL-18 [227]. The name inflammasome comes from the word inflammation, which reflects the function of the complex, and "some", which is from the Greek word soma (body). The name also reflects similarities with the apoptosome, which triggers apoptosis [228].

So far, four inflammasome complexes have been identified; the NLRP1, NLRP3, NLRC4 and AIM2 inflammasome. In addition, several NLRP proteins might be involved as scaffolding proteins of the inflammasome complexes [229]. The three inflammasome complexes, NLRP1, NLRP3 and NLRC4 described are prototypes. Evidence suggests that other NLRs are also involved in the complex formation or modulation of their activity, for example, NAIP or Nod2. The mechanism of this is not yet identified. Furthermore, it has been suggested that multiple NLR proteins form heterocomplex inflammasomes [230, 231]. Therefore the complexity and diversity of inflammasomes might be greater than previously anticipated [232]. The adaptor protein ASC (apoptosis-associated speck-like protein containing a CARD) contains an N-terminal PYD and a C-terminal CARD. It is essential for inflammasome formation and it is believed to be recruited to NLRP proteins via PYD-PYD interactions [227, 233, 234]. The CARD of ASC can then interact with the CARD of caspase-1. ASC is also involved in the NLRC4 inflammasome complex via an unknown mechanism, since NLRC4 is able to recruit caspase-1 directly via CARD-CARD interactions [215]. In addition, it has recently been shown that ASC is redistributed to the cytosol from the nucleus upon infection, suggesting an additional role for ASC in inflammasome regulation [235].

The inflammasome complexes respond to a wide variety of signals both DAMPs and PAMPs (Figure 1.9). The NLRP3 inflammasome is triggered following disruption of cellular integrity and potassium efflux [227, 236-238]. The NLRP3 inflammasome is triggered by a wide variety of stimuli such as danger signals, bacterial toxins and viral DNA, as well as MDP [161]. Known mediators that

activate the NLRP3 inflammasome will be described in more detail in chapter 4. In contrast to NLRP3, NLRC4 has been shown to respond to bacterial derived products delivered via secretion systems. The NLRC4 inflammasome will be discussed in more detail in chapter 5. The NLRP1 inflammasome has been shown to be activated following exposure to anthrax lethal toxin and MDP [200, 239]. Anthrax is caused by *Bacillus anthracis* through the action of its secreted toxins. One of these toxins is anthrax lethal toxin. It has been shown that a polymorphism in the NLRP1 gene results in impaired caspase-1 activation [239]. In the commonly used mouse strain C57BL/6, NLRP1 is inactive [239]. The role of NLRP1 in the pathology of anthrax is still unknown. In order to activate the NLRP1 inflammasome the toxin requires binding, uptake and endosome acidification to mediate translocation of the lethal factor (subunit of anthrax lethal toxin) into the host cell. Furthermore, it has been shown that catalytically active lethal factor activates caspase-1 by a mechanism involving proteasome activity and potassium efflux [240-242]. AIM2 (absent in melanoma 2) was recently identified as the key sensor for cytoplasmic dsDNA [169-171]. AIM2 is a member of the PYHIN (pyrin and HIN domain-containing protein) family. Double-stranded DNA triggers AIM2 oligomerization, which results in AIM2 inflammasome formation together with ASC and caspase-1 [170].

The inflammasome complexes sense both DAMPs and PAMPs, as previously mentioned. The resulting outcome of activation, independent of stimulus, is activation of inflammatory caspases, mainly caspase-1. The NACHT domain in the NLR-proteins of the inflammasome complex oligomerize upon activation. Binding of ATP/dATP by both NLRC4 and NLRP3 is necessary for oligomerization [243].This leads to proteolytic processing of pro-caspase-1 to its active form, caspase-1. This protease then processes pro-IL-1ß and IL-18, which contribute to the inflammatory response, discussed below. Secretion of mature IL-1ß requires two separate signals (Figure 1.9). Upon activation of TLRs, transcription of the IL-1ß gene is induced, which results in the accumulation of pro-IL-1ß. This pro-form is then processed following activation of the inflammasome complex and caspase-1 (Figure 1.9). The mature form of IL-1ß is then secreted from the cell. In addition to maturation of IL-1ß and IL-18, inflammasome activation can lead to cell death. This cell death is called pyroptosis from "pyro" meaning fire, which indicate the release of proinflammatory mediators, and "ptosis" meaning

falling, which is commonly used to describe cell death (Figure 1.9) [244]. Pyroptosis is dependent on caspase-1 activation and is associated with a high inflammatory activation state. Pyroptosis has been described for *S.flexneri* since cell death caused by this pathogen is dependent on caspase-1 but independent of caspase-3 [245, 246]. Pyroptosis has also been reported for macrophages infected with *Y.pseudotubercolosis* [247], *S.typhimurium* [248], *P.aeruginosa* [249], *F.tularensis* [250], *L.pneumophila* [251] and *L.monocytogenes* [252]. The requirements differ between caspase-1-dependent IL-1ß and IL-18 secretion compared to pyroptosis. *Salmonella* induced pyroptosis is dependent on NLRC4, whereas both NLRC4 and ASC is required for cytokine production [234]. Similar results have been observed for both *P.aeruginosa* and *S.flexneri* [249, 253, 254]. Pyroptosis was shown to be triggered in the pyroptosome, which is dependent on ASC but NLRP-independent [255]. However, this was challenged by the fact that pyroptosis caused by *B.anthracis* is NLRP1-dependent [240].
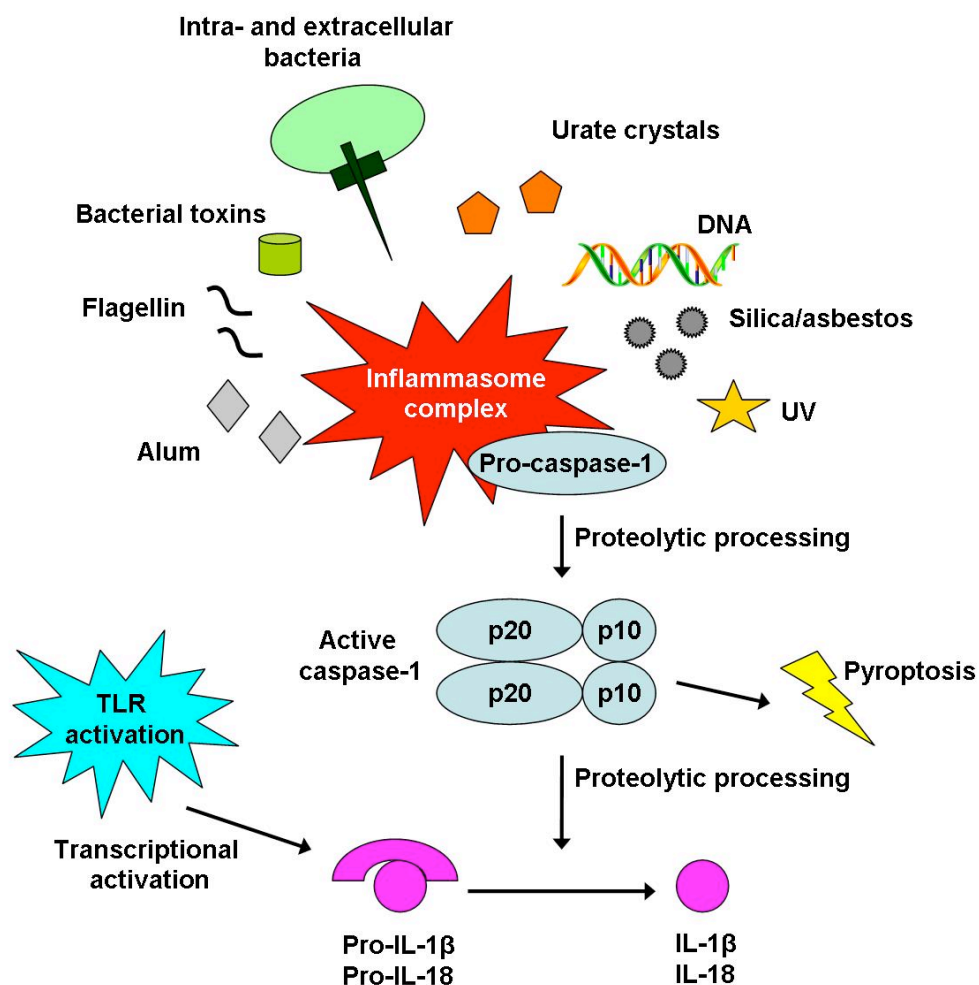
Figure 1.9; Caspase-1 activation and processing of IL-1β and IL-18

Upon activation of the inflammasome complex by a wide range of stimuli pro-caspase-1 is proteolytic processed and active caspase-1 is formed via the formation of p10/p20 heterodimer. Active caspase-1 leads processing of pro-IL-1β and pro-IL-18, and it can lead to inflammatory cell death; pyroptosis. TLR activation is required for the transcriptional activation and accumulation of pro-IL-1β and pro-IL-18. Figure is adapted from [256].

Inflammasome activation is believed to be a regulated process via synergism, feedback loops and checkpoints. NF-κB is involved in the down-modulation of the inflammatory response, which includes inflammasome activation [257]. Two major forms of inflammasome regulators have been identified; one group has a CARD domain and the other contains a PYD domain. The group containing a PYD domain is believed to interfere with interactions between NLRP proteins and ASC [258]. These proteins include Pyrin, Pyrin-only proteins; POP1 and POP2, as well as viral PYDs. These short proteins mainly contain a PYD domain [258]. The mouse genome does not contain any of the POPs, but upon disruption of Pyrin in mice there is enhanced caspase-1 activation [259]. Pyrin has been shown to

interact with ASC via PYD-PYD interactions, which possibly blocks the recruitment of ASC to the inflammasome complex [259]. The regulators containing a CARD domain include iceberg, inhibitory CARD (INCA), CARD-only protein (COP) and caspase-12 [260]. It is believed that these proteins prevent recruitment of ASC or caspase-1 via CARD-CARD interactions. Caspase-12 is the only one of these proteins that is present in the mouse genome. Caspase-12-deficiency results in enhanced bacterial clearance and production of IL-1ß and IL-18 [261]. In addition, the plant orthologs of the proteins SGT1 and HSP90 have been shown to regulate and interact with plant NB-LRR proteins. They are therefore presumed to have a similar effect in mammals since NLRC4 and NLRP3 have been shown to bind these proteins [262, 263].

Mutations of genes involved in inflammasome complex formation have been linked to hereditary periodic fevers (HPFs) [264]. These heritable disorders cause recurrent episodes of fever and severe inflammation. Gain-of-function mutations in the NLRP3 gene, resulting in a hyperactive inflammasome, can result in familial cold autoinflammatory syndrome (FCAS), Muckle-Wells syndrome (MWS) and chronic infantile cutaneous neurological articular syndrome (CINCA, also known as neonatal-onset multisystem inflammatory disease (NOMID)) [265, 266]. Macrophages from patients with mutations in the NLRP3 gene have increased secretion of IL-1ß [265, 267]. A HPF called familial Mediterranean fever (FMF) is caused by mutations in the gene of the inflammasome regulator Pyrin [267]. Chronic exposure to inflammasome activating agents such as monosodium urate (MSU), calcium pyrophosphate dihydrate (CPPD) and dust particles, asbestos and silica can result in aberrant NLRP3 inflammasome activation [268]. This results in the autoinflammatory diseases gout, pseudogout, silicosis and asbestosis [268].

Several inflammasome activators also have adjuvant properties; these include MDP, MSU and alum [269-271]. Adjuvants enhance the immune response to an antigen. Both MSU and alum are dependent on NLRP3, ASC and caspase-1 for their adjuvant properties [272-274].

1.5.4.3 Caspases

Caspases are produced as inactive zymogens; upon activation they undergo proteolytic processing which results in a catalytically active protease [275].

Caspases are involved in apoptosis where they cleave substrates. There are executioner caspases (caspase-3, -6 and -7 in mammals), which are activated by initiator caspases (caspase-8, -10, -2 or -9). The initiator caspases have an N-terminal death-fold domain (similar to NLR-proteins), which is required for the activation of the C-terminal catalytic region. Different initiator caspases are activated via different molecular platforms, for example, caspase-9 is activated by the apoptosome [161].

Activation of the inflammasome complexes results in the activation of inflammatory caspases [201, 276]. These include caspase-1 and -12 (human and murine), caspase-11 (murine) and caspase-4 and -5 (caspase-1 related human) [260]. The N-terminal domain of inflammatory caspases is a CARD-domain adjacent to a catalytic residue cysteine. The inflammatory caspase, caspase-1, processes cytokines such as IL-1ß [277], IL-18 and possibly IL-33, hence the name inflammatory as these cytokines are crucial in the inflammatory response. The involvement of caspase-1 in proteolytic processing of IL-33 is still unclear [278, 279]. The cytokines can be processed by caspase-1 following proteolytic processing of the pro-caspase-1 which occurs upon inflammasome activation. Pro-caspase-1 is processed into a p10 and p20 fragment. Active caspase-1 consists of a heterodimer of these fragments (Figure 1.9). Other roles for caspase-1, such as regulation of unconventional protein secretion and proteolysis of glycolysis enzymes, have also been identified, which might result in the description of new inflammasome functions in the future [280-283]. Caspase-1 was the first caspase to be identified in mammals, by the discovery that cell lysis in hypotonic buffer can lead to the processing of pro-IL-1ß [284], but the activation pathway via inflammasome complexes were only recently identified [227]. Caspase-1 activation has been associated with human caspase-5 and murine caspase-11, but the substrates of these caspases have not been identified. The CARD-domain of NLRP1 has been shown to recruit caspase-5, which suggests a role in the NLRP1 inflammasome complex. Caspase-4 and caspase-12 are activated upon endoplasmic reticulum (ER) stress but the role of this activation is not described [276]. Caspase-12 has also been shown to inhibit inflammasome activation by interfering with caspase-1 activation [261].

1.5.4.4   Interleukin-1β

IL-1ß is a member of the IL-1 family of ligands, which include, for example, IL-1α, IL-1 receptor antagonist (IL-1Ra), IL-18 and IL-33 [285]. IL-1ß is related to IL-18 and IL-33 and all of these cytokines result in the initiation of a MyD88-dependent signalling pathway, similar to the pathway initiated by TLR signalling. Inflammasome activation therefore leads to the activation of a TLR-like receptor such as IL-1R and IL-18R. The data presented in this thesis will focus on IL-1ß secretion resulting from inflammasome activation, therefore this cytokine will be described in more detail.

IL-1ß, a proinflammatory cytokine, is one of the most important mediators of inflammation [159, 286]. It is produced mainly by blood monocytes but also by macrophages, dendritic cells and a variety of other cells in the body [159]. IL-1ß production results in fever [285], hypotension, and the release of adrenocorticotrophic hormone and the production of other cytokines such as IL-6 [159]. Other effects on the central nervous system except fever include; induction of slow-wave sleep, anorexia and inflammatory pain hypersensitivity [285]. These effects are mediated via the ability of IL-1ß to induce cyclooxygenase type 2 (COX-2), type 2 phospholipase A and inducible nitric oxide synthase (iNOS) [285]. IL-1ß is also able to increase the expression of adhesion molecules. All these effects of IL-1ß result in infiltration of inflammatory and immunocompetent cells from the circulation into tissues, via the extravascular space.

As described above, maturation of IL-1ß require two signals; translation is initiated following TLR activation and proteolytic processing is mediated by active caspase-1 following inflammasome activation. The molecular mechanisms regulating the transcription of pro-IL-1ß are not fully understood, but reports have shown a role for both NF-κB and mitogen-activated protein (MAP) kinase [287, 288]. Pro-IL-1ß amounts are usually low within the cell, therefore transcriptional activation is required in order to secrete IL-1ß. Several pathways have been described for the secretion of mature IL-1ß [289]. These include; exocytosis of secretory lysosomes [290-292], shedding of plasma membrane microvesicles [293], export through the plasma membrane using specific

membrane transporters [294], multivesicular bodies containing exosomes [295] or release upon cell lysis [296, 297]. IL-1ß is generally released before a significant release of lactate dehydrogenase (LDH) can be observed [294]. The secretion of IL-1ß has also been shown to be dependent on an increase in intracellular calcium and phospholipase C [292]. The diversity of IL-1ß secretion pathways might be due to different methods used during the investigation of this subject, or there is a possibility that IL-1ß is secreted via more than one exclusive pathway [289]. In addition to proteolytic processing by caspase-1, pro-IL-1ß can be processed by neutrophil proteinase-3, elastase, matrix metalloprotease 9 and granzyme A in the extracellular space [257, 285, 298].

IL-1ß is believed to be the major mediator of inflammation in the periodic fever syndromes caused by mutations in the NLRP3 gene. It has been shown that treatment of these patients with an inhibitor of IL-1 (IL-1Ra) improves their symptoms [299, 300]. IL-1Ra has also been shown to help patients with rheumatoid arthritis [285].

The IL-1 receptor family encodes 10 members, from which IL-1R 1-3 respond to IL-1ß [285]. IL-1R1 has a cytoplasmic TIR-domain, similar to TLRs. Upon binding of IL-1ß to IL-1R1, MyD88 is recruited and signalling via IRAK and TRAF lead to degradation of IκB and activation of NF-κB. In addition, mitogen-activated protein kinase (MAPK) and JNK is also activated. The IL-1R2 is a decoy receptor, which binds IL-1ß but does not signal [285].

1.5.5 Plant immunity

The ability to detect and respond to an infection is important in all living organisms, even plants. Plants have both PAMP-triggered immunity and effector-triggered immunity [301]. Pathogens have developed means to suppress the PAMP-triggered immunity, which then triggers effector immunity. The effector-triggered immunity mainly detects, directly or indirectly, pathogen-driven modifications, stress or danger signals in the infected host cell [302]. This immunity is mediated by single genetic loci that control the resistance to specific plant pathogens [303]. These genes are called resistance (R) genes, and sequencing has revealed a similar structure to NLR-proteins with C-terminal LRRs, a central nucleotide-binding domain, related to NB-ARC, and an N-

terminal effector domain [304, 305]. The N-terminal effector domain can be either a TIR domain or a coiled-coil domain [306]. The proteins encoded by the R genes, nucleotide binding leucine-rich repeat (NB-LRR) proteins, are intracellular and recognize avirulence factors, which are pathogenic bacterial effector proteins [304]. Direct binding between NB-LRR protein and the corresponding avirulence factor has rarely been described [301]. Instead, NB-LRR proteins indirectly detect the activity of pathogenic effectors, via the modifications the virulence proteins inflict on host target proteins [301]. The avirulence factors gain access to the intracellular environment by T3SS. The resulting response is a form of programmed cell death [305]. Plants express several R-genes, which imply that a specific R-gene recognize a specific avirulence gene [307].

NLR-proteins and plant R-genes are structurally similar but no evidence for common evolutionary origin can be found. These innate immune sensors are a result of convergent evolution [308].

1.5.6 Collaboration between innate immune receptors

There are several examples of collaboration between innate immune receptors. Receptors may transduce intracellular signals within a phagocyte that interact with each other to define the net transcriptional and cellular response. Another possibility is that not all cells express the same repertoire of receptors, thus the set of receptors that recognise a specific microbe may also define the type(s) of cells that become activated. Collaboration between receptors defines whether a phagocyte becomes activated or not and the amounts and types of cytokines and chemokines produced, as well as shaping of the downstream adaptive immune response. Upon infection it is likely that a Gram-negative bacterium is recognized both by TLR4 (LPS) and TLR5 (flagellin), providing that the pathogen is flagellated. Collaboration has been shown for TLR4 and TLR7 *in vitro* [309]. More cytokines are produced upon stimulation of TLR3 or TLR4 together with TLR7, TLR8 or TLR9 than with either receptor alone [310]. It has been shown that coactivation of TLRs have this effect when one receptor relies on MyD88-dependent signalling and the other one is independent of MyD88, such as TLR2/TLR4 [311]. TLR5, NLRC4 and NAIP5 all respond to flagellin, although the

parts of flagellin required are not the same for these receptors [312]. Due to the different location of TLR5 and the NLR-proteins it is possible that the immune detection of flagellin is mediated via cooperation between these proteins in a synergistic or concurrent manner [231]. Secretion of mature IL-1ß requires activation of both TLRs and NLRs, as mentioned above. In addition, other PRRs, other than TLRs, trigger NF-κB activation and might therefore be involved in the translation initiation of pro-IL-1ß [172]. The CLR-receptor dectin-1 also requires collaborative signalling from TLRs for the production of proinflammatory cytokines [167], and a collaboration between Dectin-1 and NLRP3 in the response to *Candida albicans* has recently been described [313]. Furthermore, it has been recently shown that NF-κB activation by TLRs, as well as cytokine receptors such as the TNF-receptor, not only controls IL-1ß gene transcription, but also initiates NLRP3 transcription [314, 315]. This provides evidence for an additional control of inflammasome expression, Nod1 and Nod2 have been shown to synergize with TLR4 and TLR3, which results in enhanced production of TNF-α, IL-1ß, IL-6, IL-8, IL-10, IL-12p40 and IL-12p70 as well as dendritic cell maturation (CD40, CD80 and CD86) [316-318]. Current experimental models fail to explain how and whether more than two receptors collaborate [310]. Collaboration potentially provides advantages for the host by providing a robust response, since several receptors are harder to evade. It also provides compensation for potential genetic weaknesses as a more accurate and potent response can be triggered [310].

1.5.7 Link between PRRs and adaptive immunity

TLRs have been shown to control adaptive immune responses by control of antigen uptake, antigen selection for presentation in DCs, control of DC maturation and cytokine production as well as control of survival of activated T-cells [319]. Inflammasome activation is important in linking innate immunity to adaptive immunity. This is demonstrated by the adjuvant activities by MSU and alum, which triggers an influx of neutrophils and in the presence of antigen an efficient Th2-dependent immune response [164, 272-274]. In addition, silicosis triggered by silica dust is dependent on NLRP3 and results in a Th2 response [320]. The IL-1ß, IL-18 and IL-33 cytokines are known to trigger various aspects of Th2 immune responses [321, 322]. It has also been shown that signalling

through Dectin-1 can trigger Th17-cell responses [323]. Furthermore, a role for T-cells in dampening the innate immune response was recently described. The T-cells suppress activation of NLRP1 and NLRP3 via cell-cell contact [324]. This suggests a novel role of T-cells in suppressing a potentially damaging inflammatory response.

1.6 Aims

NLR proteins have been studied extensively after their discovery. They have been shown to be important innate immune sensors of PAMPs and DAMPs. We hypothesised that the Gram-negative extracellular bacterium *P.aeruginosa* can activate intracellular inflammation responses via its T3SS. The aim of this study was to investigate whether NLR-proteins, such as Nod1 and inflammasome complexes could be activated by *P.aeruginosa*. This would be studied by investigating cellular responses dependent of activation of these proteins, for example NF-κB activation, caspase-1 processing and IL-1β secretion. Furthermore, the aim was to investigate the mechanism of activation and role of bacterial mediators. Finally, the role of the T3SS in triggering of membrane repair mechanisms would be investigated.

2 Materials and Methods

2.1 Tissue culture

2.1.1 Cell lines

2.1.1.1 HeLa, CHO and HEK293 cells

Human Negroid cervix epitheloid carcinoma cells (HeLa), Chinese Hamster Ovary (CHO) cells and Human Embryonic Kidney 293 cells (HEK293) [325] were grown routinely in Dulbecco's Modified Eagle's Medium (DMEM with 4500 mg/l D-glucose and sodium pyruvate) supplemented with 2 mM L-glutamine, 10% foetal bovine serum (FBS, Sigma), 100 μg/ml Streptomycin and 100 U/ml Penicillin. To maintain the culture, cells were split at approximately 80% confluence (1 in 5 dilution). Briefly, cells were washed twice with sterile PBS or Hank's buffered salt solution (HBSS). One ml Trypsin (0.05%) with EDTA was added or enough to cover the cells. The flask was incubated for 5 min at 37°C until cells had completely detached. Complete media was added to stop the Trypsin and appropriate dilution was added to a new flask.

Prior to infection cells were grown 12 h in DMEM supplemented as above, but without Penicillin and Streptomycin.

2.1.1.2 RAW264.7 cells

RAW264.7 cells are a murine macrophage cell line from blood. Cells were grown as described for HeLa cells except for the treatment with Trypsin; instead the RAW264.7 cells were scraped off with a cell scraper (Greiner BioOne), and the appropriate dilution was added to a new flask.

Twelve hours before infection, cells were seeded in complete DMEM without Penicillin and Streptomycin.

2.1.1.3 L929 cells

L929 cells are a murine cell line which produces M-CSF in culture. They were derived from normal murine subcutaneous areolar and adipose tissue. Cells were obtained from Prof A Mowat, Glasgow. The L929s were cultured in order to

obtain M-CSF for culturing of BMDM. They were cultured in RPMI 1640 supplemented with 10% FBS, 100 µg/ml Streptomycin, 100 U/ml Penicillin and 2 mM L-glutamine. When cells were around 80% confluent they were scraped off and resuspended in fresh media. When culturing to obtain M-CSF, cells were split into large (T150) TC-flasks and cultured for 3 days following full confluency. Supernatant was taken off, sterile filtered and then stored at -20°C until used for culturing of BMDM. Each batch was tested for the ability to obtain F4/80$^+$ cells from bone marrow progenitors, typically results were between 90-95% F4/80$^+$ (Figure 2.1).
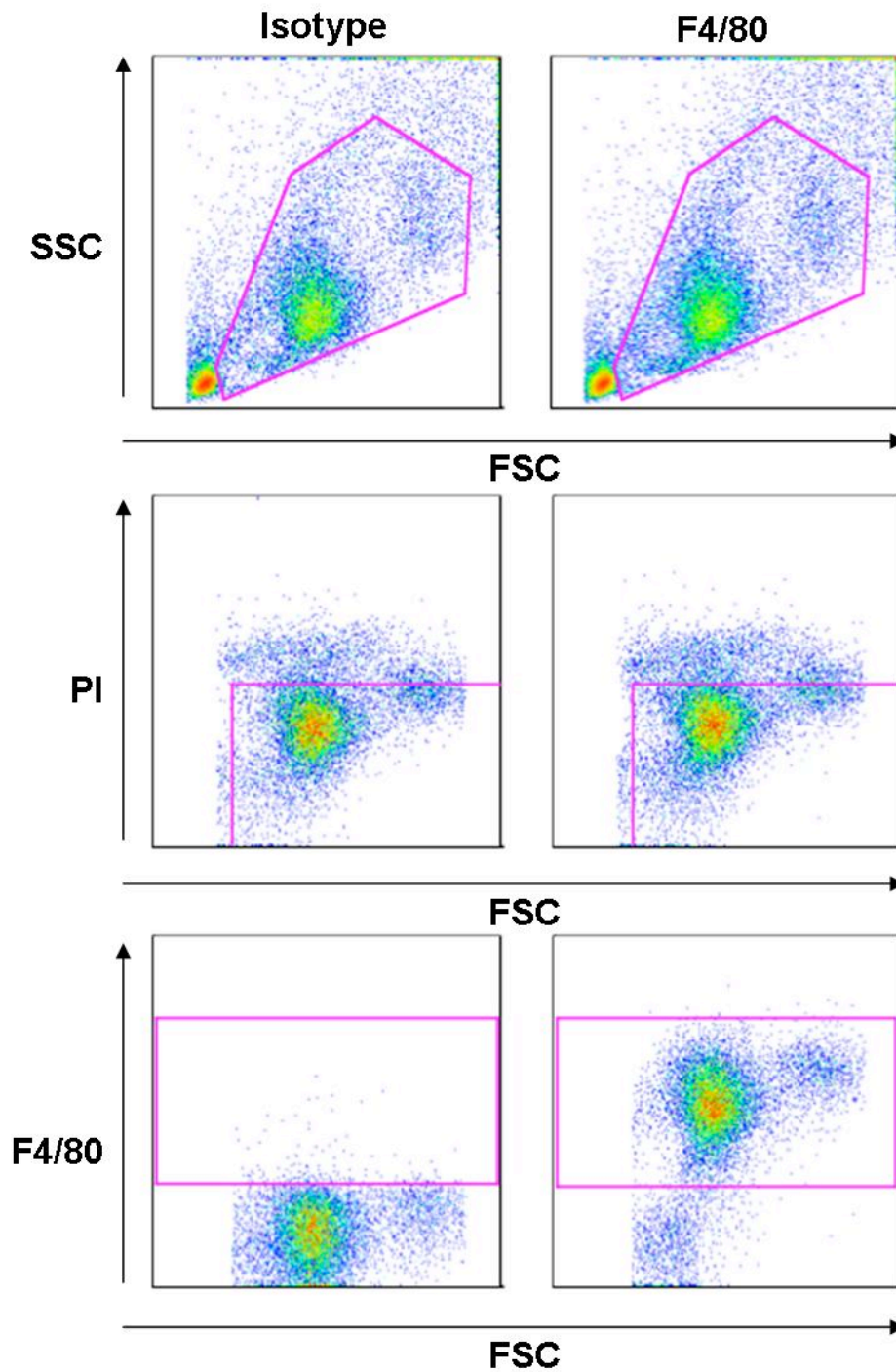
Figure 2.1; F4/80 staining of BMDMs

BMDM analysed for F4/80 after propagation in L929 conditioned media. F4/80 staining (right column) compared to isotype staining (left column). BMDM were gated based on forward and side scatter (top panels, 60.7% for isotype, 59% for F4/80), these events were then gated based on PI staining (middle panel, PI negative are alive cells, 83,2% isotype, 82,2% F4/80). Alive cells were gated based on F4/80 staining (bottom panels, 1,54% isotype, 91,2% F4/80).

2.1.1.4   PT-67 retroviral packaging lines

The PT-67 cell line was obtained from Dr. A.M. Michie, Glasgow. This packaging cell line is based on NIH-3T3 cells expressing the 10A1 viral envelope. Viruses packed from PT-67s can enter cells via the amphotropic retrovirus receptor or via the GALV receptor [326]. These cells were maintained in DMEM (4500 mg/l glucose and with L-glutamine, Lonza, Basel, Switzerland) supplemented with 10% FBS (Sigma), 100 U/ml penicillin, 100 µg/ml Streptomycin, 2 mM L-glutamine, 1 mM sodium pyruvate, 10 mM HEPES, 50 µM ß-mercaptoethanol (2-ME) and 10 µg/ml gentamicin (Sigma). Cells were split when they reached approximately 80% confluency. Cells were covered with Trypsin (0.05%) with EDTA and left until cells had completely detached. Media was added to stop the effect of the Trypsin and cells were centrifuged at 400 x g for 6 min at 4°C. The pellet was resuspended in complete media and added at an appropriate dilution to a new culture flask.

2.1.1.5   GP+E.86 retroviral packaging lines

The GP+E.86 cell line was obtained from Dr. A.M. Michie, Glasgow. GP+E.86 are a _gag_-_pol_ and _env_ retroviral packaging line which was used for retroviral gene transfer. These cells were generated by co-transfection of the plasmid containing the _gag_ and _pol_ genes derived from Moloney murine leukaemia virus (MMLV) and the plasmid containing the _env_ gene derived from the helper virus into NIH-3T3 cells [327, 328]. These cells were cultured in the same media as the PT-67s and maintained using the same method.

2.1.1.6   Generation of retroviral packaging lines

Retroviral vectors can be used to introduce a nonviral gene into mitotic cells _in vivo_ and _in vitro_. This requires active cell division [329]. Stable proviral integration in the target chromosomal DNA can be mediated by retrovirus-mediated gene transfer. Most cells including primary cells express viral receptors on the surface. The retroviral vector used (pMigR1) lack genes encoding virion structural proteins (_pol, env_), which disable the retrovirus from replicating by itself, but still retaining the efficiency of infection. Infectious viral particles can

be produced using this retroviral vector and a retrovirus-packaging cell line. These cells express gag, pol and env, which are necessary for encapsidation, infection, reverse transcription and integration into the genome of infected cells. Two packaging cell lines with different tropism, ecotropic and amphotropic, are used to obtain a high viral titer. When *env* is overexpressed the cognate receptor is bound and blocked, which means cells cannot be infected by viruses of the same tropism. One cell line is transiently transfected with the retroviral vector and the viruses produced are used to obtain a second stable virus producing cell line. The viruses produced by this cell line can then be used to infect other cells.

The gene of interest was subcloned into the retroviral vector pMigR1, as described below in section 2.3.1.1. At day one of the experiment, 1×10^5 PT-67 retroviral packaging cells were seeded per well into a 6-well plate in complete medium. The retroviral vectors were transfected into the PT-67 on day two, using Lipofectamine 2000 (Invitrogen) as per manufacturer's instructions. Briefly, vectors (1 µg per sample) were diluted into 200 µl Opti-MEM I Reduced-Serum medium (Invitrogen), simultaneously 8 µl Lipofectamine 2000 was diluted into 200 µl Opti-MEM. After 5 min at room temperature the vector mix was added to the Lipofectamine to allow for complex formation, which proceeded over 15 min. The complex mixture was added to the PT-67s, which were washed and new media was added, final total volume was 2 ml/well. After 24 h, media was complemented with 0.5 ml complete media, after further 24 h, supernatant containing the viral particles was filter-sterilised using a 0.2 µm filter membrane (Minisart, Sartorius) attached to a 5 ml syringe (BD Biosciences). This ensured no carry over of PT-67 cells into the next part of the experiment. 1×10^5 GP+E.86 retroviral packaging cells per tube were added to FACS tubes (BD Biosciences) and resuspended in supernatants from the PT-67s supplemented with 6 µg/ml polybrene (Sigma). The GP+E.86s were spin-infected by centrifugation at 620 x g on a Jouan CR322 centrifuge for 45 min at room temperature (RT). Cells were resuspended in complete media supplemented with 4 µg/ml polybrene and supernatant from the PT-67s and placed in culture for 48 h. After 24 h, cells were further supplemented with complete media and 4 µg/ml polybrene.

Retrovirally transduced GP+E.86 packaging cells were trypsinised and resuspended in sterile PBS, passed through Nitex mesh (Cadish) and sorted on

the basis of GFP-expression using a FACSAria cell sorter (BD Biosciences) and FACSDiva software (BD Biosciences). After 2-3 weeks the GP+E.86s were resorted to a purity of >98 % GFP⁺, thus establishing stable retroviral packaging cell lines. These cells were maintained as described for the GP+E.86s.

2.1.2 Primary cell preparations

2.1.2.1   Bone-marrow derived macrophages

Mice were sacrificed by cervical dislocation and femurs and tibias were dissected out, obtained from Prof A Mowat, Glasgow. Cells were isolated as previously described [330]. Briefly, femurs and tibias were flushed with media using a 21G needle to obtain bone marrow mononuclear phagocytic precursor cells. To remove tissue and debris the cell suspension was passed through a Nitex mesh. Culture media used was RPMI 1640 supplemented with 20% heat inactivated FBS, 100 µg/ml Streptomycin, 100 U/ml Penicillin, 2 mM L-glutamine, 2.5 µg/ml Fungizone (amphotericin B) and 100 µM/ml Sodium pyruvate. Bone marrow mononuclear phagocytic precursor cells were seeded into untreated 9 cm petri dishes (Sterilin) at a concentration of $3x10^6$ cells/plate. Complete media was further supplemented with M-CSF. M-CSF was obtained from 10 ng/ml recombinant murine M-CSF (Peprotech) or supernatant of L929 cells. Cells were cultured 3 days, after which media and M-CSF were added and cells were grown for further 3-4 days. Matured macrophages were scraped off and seeded into TC-dishes before experiments.

2.2   Methods

2.2.1 Bacterial cultures

Bacterial cultures were grown routinely in Luria-Bertani (LB) media (Invitrogen) containing the appropriate antibiotics depending on bacterial strain (Table 2.4). A single colony or 50 µl of a glycerol stock was added into 10 ml of LB and grown overnight at 37°C at 225 rpm. The next morning, the overnight culture was diluted 1 in 30 in LB and allowed to grow for another 90 min or until OD600 was between 0.4 and 0.6. The bacteria were then centrifuged at 3000 x g for 10 min

at 4°C, the pellet was washed twice in sterile PBS and then resuspended in the same media as the cells being infected to a concentration of approximately 1 x 10^6 cfu/µl, = (OD600 / 0.4) x 1.8 ml. Cells were then infected at indicated multiplicity of infection (MOI) and time.

2.2.2 Microscope studies

All microscope studies were done using a Zeiss Axiovert S100 microscope and OpenLab software (Improvision).

2.2.2.1   LAMP-1 staining

Cells were seeded into 2-well glass chamber slides with cover (Nunc), 5 x 10^5 cells/well, one day prior to treatment or infection. On the day of experiment cells were infected or treated as indicated. Cells were then washed in icecold PBS (3x), followed by incubation in the primary antibody, anti-human LAMP-1 (BD Biosciences) or mouse IgG1 isotype control 2 µg/ml in PBS with 10% goat serum (Sigma) for 60 min at 4°C. Following three washes cells were then fixed in 1% paraformaldehyde (PFA) in PBS for 30 min at 4°C. After another wash, cells were stained using the tyramide amplification kit (TSA kit #2 with HRP-goat anti-mouse IgG and Alexa Fluor 488 tyramide, Invitrogen) according to manufacturer's instructions. Briefly slides were incubated with 20 ng/µl anti-mouse IgG-HRP (diluted 1 in 100) in PBS/10% goat serum for 25 min at 4°C. Slides were then washed in icecold PBS (3x) and incubated in AF488 tyramide diluted 1 in 100 in amplification diluent with 0.0015% H_2O_2 for 10 min at RT. Following washes in PBS, slides were mounted in Vectashield containing DAPI (Vector labs) and then imaged. The amount of LAMP-1 specific staining was quantified by Dr. A. Morton, University of Glasgow, using a Laser scanning cytometer (LSC).

LSC can be used to quantify specific immunofluorescence staining on cells which are located on a microscopic slide. The LSC has the sensitivity of flow cytometry and allows gating of relevant cells on the slides. The threshold value is used to identify the cells and their nuclei; in this study DAPI was used to stain the cell nucleus. The intregration value is set according to the cell surface, which in this study was stained for LAMP-1 and the peripheral contour is set between the

threshold and the intregration value which can be used to quantify intracellular staining and subcellular localisation of markers [331]. This was not used in this thesis.

2.2.2.2   Lucifer Yellow exclusion assay

The method was adapted from Neyt et al. [332]. Cells (5×10^5 per chamber) were seeded onto 2-well glass chamber slides with cover (Nunc, NY) a day before the experiment. Cell culture media used was complete media without Penicillin and Streptomycin appropriate for each cell type. Cells were washed in prewarmed (37°C) complete media with 30 mM dextran 6000 (Sigma). The dextran 6000 acts as an osmoprotectant and prevents cells from flattening [332]. Cells were then infected or treated accordingly in 1 ml complete media with 30 mM dextran per well. After infection or treatment, slides were placed on ice and cells were washed for 10 min in PBS with 30 mM dextran. Following the wash, 0.625 mg/ml Lucifer Yellow CH lithium salt (Invitrogen) in complete media with 30 mM dextran was added and incubated on ice for 60 min. Cells were washed seven times with ice-cold PBS with 30 mM dextran and then fixed with 2% paraformaldehyde dissolved in PBS with 30 mM dextran for 20 min on ice. Following this, cells were washed twice in ice-cold PBS / 30 mM dextran. After washing, chambers were removed from the slides and 2 drops of Vectashield with DAPI (Vectorlabs) was added per slide. Coverslips were mounted and edges sealed with clear nail varnish.

2.2.2.3   Potassium imaging

The potassium indicator potassium-binding benzofuran isophthalate (PBFI) is used for fluorometric determination of potassium concentrations (Invitrogen). When potassium binds to the dye the ratio of energy absorbed at 340/380 nm changes, but the emission wavelength of 500 nm remains constant. The excitation wavelength of 340 nm is sensitive to potassium whereas 380 nm is very near the isobestic point. Increasing amounts of potassium results in increasing fluorescence intensity, which can be plotted as mean fluorescence intensity (MFI) against time. The acetoxymethyl (AM) ester of PBFI AM allows the dye to be loaded into cells as it makes the dye cell-permeant by resulting in an

uncharged molecule. Once the dye has entered the cell the ester is cleaved off by nonspecific esterases resulting in a charged molecule, which diffuses from the cell at a much slower rate compared to the uncharged molecule.

BMDM were seeded onto chamber slides, 5 x 10^5 cells/well (Nunc), in complete RPMI without Phenol red (Invitrogen). Cells were allowed to settle and the media was changed to RPMI with 5% FBS and 25 mM HEPES, cells were loaded with 2 µM PBFI AM cell permeant (Invitrogen), together with Pluronic F-127 (a non-ionic detergent polyol used to facilitate cell loading of large dye molecules, Invitrogen) for 60 min at RT, as per manufacturer's instructions. After one wash in media, cells were outlined and imaged using time lapse and tracing on a 37°C heated stage with the ratio between 340 and 380 nm being plotted. After an initial period of imaging, cells were infected or treated as indicated; this was done without disrupting the stage or time lapse imaging.

2.2.2.4 Calcium imaging

Fluo-4 is a calcium indicator analogous to Fluo-3 (Invitrogen). It is excited at 488 nm and the emission wavelength is 516 nm. Upon binding of calcium the intensity is significantly increased with no shift in the fluorescence spectra.

Cells were imaged in Phenol Red free complete media appropriate for each cell line. Cells were loaded with 3 µM fluo-4 AM (Invitrogen) for 60 min at 37°C. Cells were then washed with media for 30 min at 37°C. Cells were outlined and calcium changes were measured, using time lapse and tracing on a 37°C heated stage.

2.2.2.5 Zinc imaging

Fluo-Zin 3 is a zinc sensitive fluorescent indicator, which upon binding of zinc has increased fluorescence intensity (Invitrogen). It has an excitation wavelength of 496 nm and emission wavelength of 516 nm.

BMDM were seeded at a concentration of 5 x 10^5 cells/well in complete RPMI without PenStrep in chamber slides (Nunc). Media was then changed to RPMI without Phenol Red supplemented with 25 mM HEPES. Cells were loaded with 2

µM FluoZin3 AM (Invitrogen) together with Pluronic F-127 for 45 min at RT. After loading, cells were washed three times in media and then imaged. Just before imaging 5 µg/ml propidium iodide (PI, Sigma) and 20 µM Zinc sulphate (ZnSO$_4$, Sigma) was added. Cells were outlined and imaged using time lapse and tracing on a 37°C heated stage. Cells were infected without disturbing stage or time lapse. Finally 20 µM Pyrithione (Sigma) was added, again without disturbing stage or time lapse.

2.2.2.6 Ethidium bromide uptake assay

The method was adapted from [333]. BMDM were seeded at 5 x 10^5 cells/well onto chamber slides in complete RPMI. Before imaging media was changed to standard physiological extracellular solution [333] (147 mM NaCl, 10 mM HEPES, 13 mM glucose, 2 mM CaCl$_2$, 1 mM MgCl$_2$ and 2 mM KCl). Cells were preincubated with 500 µM pannexin-1 or control peptide for 15 min at 37°C, following the addition of 20 µM ethidium bromide. Cells were traced in brightfield and then imaged 2 min before the addition of 5 mM ATP on a 37°C heated stage. The result was followed 20 to 30 min with imaging every 10 s. Ethidium bromide fluorescence was measured at 543 nm excitation and 590 nm emission. Mean fluorescence intensity were obtained by measuring ethidium bromide fluorescence for isolated (non touching) cells, which was then averaged.

2.2.3 Spectrofluorimeter methods

2.2.3.1 BCECF release assay

BCECF [28,78-bis-(2-carboxyethyl)-5-(and-6)-carboxyfluorescein, acetoxymethyl ester], can be used to measure changes to the cytosolic pH. It is classified as a small intracellular marker molecule with a molecular weight of 623 Da. Similar to other esters, BCECF is cell-permeable and only becomes fluorescent after cleavage inside the cell by esterases. It can be used to investigate pore-formation in the host cell membrane. Cells are loaded with the dye which becomes fluorescent, this fluorescent species can then be detected in the extracellular media only if a pore is formed in the plasma membrane.

The BCECF release assay was adapted from Neyt et al. [332] which was based on the principle described by Bhakdi et al. [334]. Cells were seeded into a 6-well plate (1 x 10^6 cells/well) one day before experiments in media without antibiotics. Cells were washed twice with pre-warmed HBSS (37°C) and incubated with 5 μM BCECF-AM (Invitrogen) for 20 min at 37°C. Cells were then washed twice in DMEM without Phenol red. After infection, at indicated times, section 4.2.4.3, supernatants were collected and centrifuged for 10 min at 16100 x g. The supernatant was immediately measured using a spectrofluorimeter with an excitation wavelength at 490 nm and emission at 535 nm and with measurement for 5 s. Cells treated with 1% Triton X-100 for 10 min at 37°C were used as a positive control. Percentage of BCECF release was calculated according to % BCECF release = (sample - uninfected) / (Triton X-100 - uninfected) x 100.

2.2.3.2   β-hexosaminidase assay

The method was adapted from [335, 336]. Cells were seeded into a 6-well plate, 1 x 10^6 cells/well, in media appropriate for each cell type but without PenStrep, one day before experiment. On the day of experiment, cells were washed twice in 37°C PBS and 1 ml of media was added into each well. Cells were then treated or infected as indicated in section 4.2.5.2. Supernatants were collected and centrifuged at 13400 x g for 10 min at 4°C. Samples were then diluted 1 in 100 in HBSS (Invitrogen) and mixed as follows; 200 μl sample with pre-warmed (37°C) 200 μl 2.6 mM substrate (4-methylumbelliferyl *N*-acetyl-ßD-Glucosaminide dihydrate; Sigma) in 330 mM citrate / phosphate buffer pH 4.8 and 200 μl dH$_2$O. The mixture was incubated at 37°C for 10 min and reactions were terminated by the addition of 600 μl 0.1 M glycine pH 10 and 2 M Na$_2$CO$_3$. The formation of reaction product (4-methylumbelliferone) was measured using a spectrofluorimeter (LS 55 Luminescence Spectrometer, Perkin Elmer) with a single cell reader and excitation at 358 nm, emission at 448 nm and 5 s read time. % total was calculated using sample / Triton X-100 x 100 and % β-hexaminidase release was calculated from (sample – uninfected sample) / (Triton X-100 – uninfected) x 100.

2.2.4 Western blotting

Cells were infected, or stimulated as indicated. Then, the supernatant was kept for ELISA and LDH assays. The cell samples were washed in PBS and lysed in lysis buffer (50 mM Tris-HCl (pH 7.4), 150 mM NaCl, 5 mM EDTA, 1% (v/v) Triton X-100 supplemented with a EDTA-free protease inhibitor cocktail (Complete Mini EDTA-free; Roche) [249]). After lysis for 15 min at RT, cells were scraped off and stored at -70°C before Western blot analysis.

Cell lysates were resolved using SE 260 Mini-vertical Unit (GE Healthcare) with NuPAGE Novex pre-cast 4-12% Bis-Tris gels and NuPAGE buffers and reagents (Invitrogen). Lysates were diluted in LDS sample buffer (Invitrogen) supplemented with 100 mM DTT (Sigma). Samples were heated at 70°C for 10 min before being loaded onto the gel. Samples were resolved using the NuPAGE MES SDS running buffer at 100 V for 90 min or until loading dye reached the bottom of the gel. As a protein size marker, the prestained marker SeeBlue Plus 2 standard (Invitrogen) was used. Polyvinyliden difluoride (PVDF) membrane Hybond-P (GE Healthcare) was activated by immersing it in methanol. The resolved proteins were transferred from the gel onto the PVDF membrane using Hoefer TE 22 tank transfer unit (GE Healthcare) and NuPAGE transfer buffer (Invitrogen) supplemented with 20% methanol at 30 V for 2 h.

Following transfer, PVDF membranes were blocked in PBS/0.1% (v/v) Tween-20 with 5% non-fat milk (Marvel powdered milk) for at least an hour at RT on an orbital shaker (AROS 160 Thermolyne). All antibodies were diluted in PBS/0.1 % Tween with 5% milk and all steps were carried out on an orbital shaker. Membranes were then incubated with the appropriate primary detection antibody (Table 2.3), for 1 h at RT or overnight at 4°C. The membranes were washed (3 x for at least 10 min) with PBS/Tween and the appropriate secondary biotinylated antibody was added at 1.5 µg/ml for 1 h at RT (Table 2.3). Following three washes, streptavidin HRP ELISA grade (Invitrogen) was added for 30 min at RT. After another three washes, protein bands were visualised using ECL Plus Western blotting detection reagent (GE Healthcare) as per manufacturer's instructions. Membranes were incubated in the detection reagent for 5 min before exposure to Kodak X-Ray film.

When membranes needed to be reprobed with a new primary antibody, they were stripped in stripping buffer (100 mM 2-mercaptoethanol, 2% (w/v) SDS and 62.5 mM Tris-HCl pH 6.7, all from Sigma) at 50°C for 30 min. Membranes were then washed (3 x 10 min) in PBS/Tween following a block in 5% milk / PBS / Tween. Reprobe of membranes were performed as described above.

2.2.5 Lactate dehydrogenase (LDH) assay

Cells were incubated in media lacking Phenol red. Lactate dehydrogenase release determinations were performed using the CytoTox 96 cytotoxicity assay kit (Promega). The amount of LDH in the supernatant is coupled to the enzymatic conversion of tetrazolium salt (INT) into a red formazan product:

NAD^+ + lactate -> pyruvate + NADH (reaction mediated by LDH)

NADH + INT -> NAD^+ + formazan (reaction mediated by Diaphorase)

After infection supernatants were collected and centrifuged at 16100 x g for 5 min at 4°C. Supernatants were transferred to a new tube and 100 µl of sample was added to a 96-well plate. In addition, all samples were diluted 1 in 10 in Phenol red free media. The substrate mix (50 µl) was then added and the plate was incubated in the dark at RT for 30 min. The reaction was terminated by the addition of 50 µl stop solution and the absorbance at 490 nm was recorded using a Tecan sunrise plate reader and the Magellan software. Background values were subtracted from the sample readings. As a positive control for total cell-associated LDH, cells were lysed with 1% Triton X-100 at 37°C for 20 min. The % cell death was determined according to % cytotoxicity = (experimental LDH release / maximum LDH release) x 100.

2.2.6 Protein precipitation

When supernatants were analysed for protein expression, proteins were first precipitated before being resolved by SDS-PAGE.

TCA precipitation was performed as follows; 5 volumes of 10% (w/v) TCA in acetone were added per 1 volume of protein solution. After 30 min incubation at

-20°C, samples were centrifuged at 13200 x g at 4°C for 15 min. The pellet was washed with ice cold acetone and centrifuged again at 13200 x g for 5 min at 4°C. The pellet formed was dried and resuspended in LDS sample buffer. Proteins were resolved as described for Western blotting in section 2.2.4.

Chloroform precipitation was performed in a similar manner. Protocol was provided by Dr. O. Gross, University of Lausanne. The supernatant was mixed with an equal volume of methanol and 1/3 volume of chloroform. Samples were then vortexed and centrifuged at 13200 x g for 5 min at RT. The supernatant was removed, except for the protein interface on top of the chloroform. The proteins were washed with methanol and following vortexing the samples were centrifuged again at 13200 x g for 5 min at RT. The pellet was dried at 37°C for 15 min and then resuspended in LDS sample buffer, as described for Western blotting in section 2.2.4.

2.2.7 Enzyme-Linked immunosorbent assay (ELISA)

ELISA for IL-1β was performed according to manufacturer's instructions (BD Biosciences). Briefly Immunolon 4HBX flat bottom 96-well plates (Thermo) were coated with capture antibody diluted in PBS overnight at RT. Plates were washed with PBS / 0.025% Tween 20 and blocked in PBS / 1% BSA. After three washes, samples (100 µl/well) and standards were added with a top standard of 1000 pg/ml serially diluted 1:2 10 times. After 2 h incubation at RT and three washes, detection antibody was added and incubated at RT for 2 h. Following three washes, streptavidin was added for 20 min at RT and after a final wash step, Tetramethylbenzidine (TMB) substrate was added for 20 min at RT. Development was stopped by the addition of TMB stop solution and plates were read at 405 nm with correction set at 630 nm on a Tecan sunrise plate reader using the Magellan software. The release of pro-IL-1β from dead cells was controlled for by analysing Triton X-100 treated wells for mature IL-1β, since the ELISA kit is less sensitive to pro-IL-1β, as previously described [337]. Mature IL-1β = total IL-1β signal – pro-IL-1β lysis x percent release of LDH.

2.2.8 Flame photometry

Flame photometry can be used to determine the concentration of metal ions such as sodium, potassium, lithium and calcium. It is an atomic emission method where quantitative analysis is performed by measuring the flame emission of solutions containing the metal salts. There is little interference as the emission lines from the gas-phase atoms in the flame are very narrow and characteristic for each atom. The sample is first aspirated into the flame, which due to its heat evaporates the solvent and atomizes the metal. During this a valence electron is excited to an upper state and as the electron returns to the ground state light is emitted, at characteristic wavelengths. Each metal is selected for by different optical filters. Samples with unknown concentrations are then compared to that of standard solutions, which allows quantitative analysis of the metal in the sample. The standard solutions used cover the range of concentrations expected of the samples [338].

The method is limited to easily ionized metals, alkali and alkali earth metals, due to the low temperature of the natural gas and air flame. The low temperature renders the method sensitive to interference and lack of stability of the flame and aspiration. These are affected by rates and purity of fuel and oxidant flow, aspiration rates, solution viscosity and concomitants in the sample. Due to this it is important to measure the emission of the standards and samples under conditions which are as close to identical as possible [338].

BMDMs were seeded at 1×10^6 cells per well in a 6-well plate (Corning) in complete media without antibiotics. Cells were allowed to settle and were then infected or stimulated for indicated time points. Cells were washed twice in Tris-buffered saline pH 7.4 and then lysed in 10% nitric acid. Samples were centrifuged at 13100 x g for 5 min at 4°C and then diluted 1 in 4 in dH_2O. Intracellular K^+ content were measured using a Sherwood MA10C Flame Photometer and compared with standards ranging between 1 mg/l to 8 mg/l.

2.2.9 Polymerase chain reactions (PCR)

PCRs were performed on a Techne gene cycler by T.J. Evans. Reaction volume was 50 µl in a thin walled PCR tube. The Taq polymerase, Expand High Fidelity

PCR System (Roche) was used and dNTPs were bought from Sigma. For primers used see Table 2.2.

2.2.10   Agarose gel electrophoresis

PCR products, plasmid preparations and restriction enzyme digests were resolved using agarose gel electrophoresis and a Horizon 58 Gibco Horizontal gel electrophoresis apparatus. 1% agarose (Invitrogen) were dissolved in Tris / Borate / EDTA (TBE) buffer and 50 µg/ml ethidium bromide was added. Gels were viewed and photographed using Gel Logic 200 imaging system (KODAK).

2.2.11   NF-κB luciferase reporter gene assay

Prior to transfection, HEK293 cells were seeded onto a collagen coated 12-well tissue culture plate. The plate was coated with 0.25 mg/ml collagen type I from Rat tail (BD Biosciences) by diluting it in HBSS. After addition to the plate the solution was aspirated and the plate allowed to airdry. The plates were kept at 4°C and washed before use. HEK293 cells were transfected with 0.4 µg/ml reporter plasmid for NF-KB (pNF-KB-Luc Stratagene) and 0.5 µg/ml control ß-gal plasmid (Galacto-Star ß-Galactosidase Reporter Gene assay system, Applied Biosystems). Where indicated cells were cotransfected with a DN-NOD1 (ΔCARD) construct or a human NOD1 construct, kindly supplied by Richard L Ferrero (Monash University, Melbourne, Australia) at indicated concentrations. Transfections were carried out using Lipofectamine 2000 (Invitrogen) according to manufacturer's instructions. Briefly, DNA and transfection reagent were mixed with OPTI-MEM (Invitrogen) separately, left for five minutes before mixing. The DNA-reagent solution was left for 20 minutes before addition to the cells. Transfections were left at 37°C 5 hours before the media was replaced with fresh complete DMEM, and then left overnight before cells were infected or treated.

On the day of infections bacteria was grown to mid log-phase, as described in section 2.2.1., and then washed twice with phosphate buffered saline (PBS). The pellet was resuspended in DMEM to a concentration of 1×10^{6} bacteria/µl. Cells were then infected using indicated multiplicity of infections (MOI). After

infections cells were washed once in HBSS and media was replaced with DMEM supplemented with 10% FCS, 2 mM L-glu and 50 µg/ml Gentamicin. Cells were also treated, where indicated, with peptidoglycan (PGN) or lipopolysaccharide (LPS, Sigma) and were incubated at 37°C overnight.

Luciferase assay was carried out in duplicate for each well according to manufacturer's instructions (Stratagene). Briefly, cells were washed once with PBS and then 500 µl lysis buffer was added to each well. Lysis was allowed to continue for 15 minutes. Lysates was scraped with cell scrapers and transferred to Eppendorf tubes. Lysates were then centrifuged in a bench top centrifuge at 16000 x g 2 minutes at RT. Just before measuring luciferase activity, 5 µl lysate was added to 100 µl luciferase substrate. Luciferase activity was measured in a luminometer (Lumat LB 9507, Berthold Technologies) over a 10 s period.

Luciferase catalyzes the following chemiluminescent oxidation-reduction reaction:

Luciferin + ATP + O_2 -> Oxyluciferin + light (560 nm) + AMP + PPi + CO_2

The amount of light is a measure of the amount of luciferase present, which correlates with the amount of NF-κB.

After measurement, 300 µl Galacto Star (Applied Biosystems) substrate was added to each sample according to manufacturer's instructions. Briefly, after addition, samples were left for 45 minutes before measurement in a luminometer. Results were calculated using Excel software and Graph Pad Prism 4 software (GraphPad Software Inc). Calculations were; luciferase activity / ß-gal activity, fold NF-κB differences were then calculated from ratio (luc / ß-gal) / mean of control sample.

2.2.12   DOTAP transfection

BMDM were seeded, 2.5×10^5 cells per well, into 24-well plates (Corning) in complete media with 2 µg/ml LPS. After three hours at 37°C in a humidified incubator, cells were washed and media was replaced with 300 µl RPMI without Phenol Red (Invitrogen) supplemented with 2 mM L-glutamine and 2 µg/ml LPS.

Proteins were diluted in media to a final volume of 50 µl and 2 µg DOTAP (dioleoyl trimethylammonium propane) liposomal transfection reagent (Roche) was added to appropriate tubes. After 15 min incubation at RT the transfection mixture was added to the cells and plates were swirled to allow for even distribution. Plates were incubated at 37°C for 3.5 h or as indicated. Following this incubation cell lysates were prepared as described in section 2.2.4 and supernatants were kept and analyzed for LDH release and IL-1ß secretion.

2.2.13   Lipofectamine 2000 transfection

Transfections with Lipofectamine 2000 (Invitrogen) were carried out according to manufacturer's instructions. Briefly DNA and Lipofectamine 2000 were diluted in Opti-MEM I Reduced serum media (Invitrogen) and left at RT for 5 min. Following the incubation the DNA mixture was added into the Lipofectamine mixture and complexes were allowed to form during 15 min at RT. Complexes were then added to the cells and plates were swirled to allow even distribution of mixture. Plates were incubated in a humidified incubator at 37°C until analysis.

2.2.14   Gentamicin protection assay

This assay was preformed as described by Travassos et al. [17, 339]. BMDM were seeded at $5x10^5$ cells per well into a 12-well plate (Corning) in complete media without Penicillin and Streptomycin. After infection (90 min) cells were washed twice in sterile PBS and complete media supplemented with 100 µg/ml Gentamicin (Sigma) was added. The Gentamicin containing media was kept on the cells for 90 min, in order to kill off any extracellular bacteria. Cells were then washed twice in sterile PBS and then lysed in 250 µl 0.1% SDS / 1% Triton X-100 / PBS. The lysates and initial inoculums were diluted and plated onto agar plates. The agar plates were incubated at 37°C overnight and the following morning the colonies were counted. Percent invasion was calculated using # CFU after / # CFU added x 100 and # CFU after was calculated using # CFU on the plate x total volume x dilution factor.

2.2.15   Transformation of electrocompetent E.coli (EC100)

TransforMax EC100 electrocompetent *E.coli* (Epicentre Biotechnologies) were transformed according to manufacturer's instructions. Briefly, electroporation cuvettes GenePulser Cuvettes 0.2 cm (BioRad) were chilled on ice and 50 μl electrocompetent cells were defrosted on ice. Plasmids were added and mixed gently with the bacteria, immediately following this, cells were transferred to an electroporation cuvette and pulsed on a Gene Pulser X cell system (BioRad) using a preset program for *E.coli* (2500 V, 25 μF, 200 Ω, 4 s time constant). Pulsed bacteria were then added to RT 950 μl super optimal broth with catabolite repression (SOC) medium (Invitrogen) and placed in a shaking incubator (225 rpm) at 37°C for 1 hour to allow expression of antibiotic resistance marker. Bacteria (250 μl) were then plated onto appropriate LB-Agar plates (Luria Bertani medium with 1% w/v agar) with antibiotic selection and allowed to grow at 37°C overnight.

2.2.16   Plasmid purification, restriction enzyme digests and ligations

Plasmids were purified using QIAprep spin mini prep kit (Qiagen), HiSpeed plasmid maxi kit (Qiagen) or PureLink HiPure Plasmid filter maxiprep kit (Invitrogen) all according to manufacturer's instructions. Ligations were preformed using Rapid DNA Ligation kit (Roche) according to manufacturer's instructions.

2.2.17   Transformation of P.aeruginosa

Tranformation of *P.aeruginosa* was performed according to the protocol described by Choi et.al [340]. *P.aeruginosa* strains were grown overnight in a 10 ml LB medium culture at 37°C, from this culture 3 ml was pelleted at 16100 x g and then washed twice in 300 mM sucrose. Bacteria were resuspended in 100 μl 300 mM sucrose and 1 μg/ml plasmid. Transformation mixture was transferred to a prechilled electroporation cuvette Gene Pulser cuvette 0.2 cm (BioRad) and pulsed on a Gene Pulser X cell system (BioRad) using a preset protocol for *P.aeruginosa* (2500 V, 25 μF, 200 Ω, 4 ms). Cells were allowed to recover and to

express antibiotic resistance markers in 1 ml LB at 37°C 225 rpm for 1.5 hours. Following this, transformed bacteria were plated onto LB/agar plates with appropriate antibiotic selection and left overnight at 37°C.

2.2.18   Pilin purification

The pilin purification method used was based on a modified flagellin purification method and a method described by Smedley et al. [341]. Bacterial strains were grown in Trypticase Soy Broth (TSB) at 60 rpm and 37°C overnight. The overnight culture was pelleted at 8000 rpm for 13 min at 4°C in a Beckman Coulter Avanti J-26 XP centrifuge. The pellet was resuspended in 25 ml PBS and vortexed hard, which was followed by rough stirring using a magnetic stirrer for 30 min at RT with intermediate vortexing. Bacterial suspension was then centrifuged at 16000 rpm in a Beckman Coulter Avanti J-26 XP centrifuge at 4°C for 30 min. The supernatant was kept and NaCl concentration was increased to 0.5 M by the addition of 0.36 M NaCl, polyethylene glycol PEG 3000 was added to a final concentration of 3% v/v. The solution was kept at 4°C for at least 18 hours. This was followed by pelleting of the precipitated proteins at 9500 rpm (10917 x g) at 4° for 20 min. The proteins were dissolved in 1 ml water and analysed using SDS PAGE, as described for Western Blotting, and BioRad protein assay. After resolving the proteins on a NuPage 4-12% Bis-Tris gel, the results were visualised using Instant Blue one step protein staining, a colloidal Coomassie blue staining solution (Expedeon) according to manufacturer's instructions. Briefly, the gel was placed in 20 ml of staining solution for 1 hour and then washed in water for at least an hour. The gel was then dried using the Dry-Ease Mini gel drying system (Invitrogen) according to manufacturer's instructions. Briefly, the cellophane sheets were soaked in the gel drying solution for 2 min, the gel was placed between them and allowed to air dry in the vertical cassette system.

The BioRad protein assay was performed according to manufacturer's instructions. BSA was used as standard with a high standard of 20 µg/ml. Samples were diluted and 100 µl of each sample or standard was added to each well following an addition of 100 µl Coomassie Brilliant Blue G-250 Dye. The plate was read on Tecan Sunrise ELISA plate reader at 595 nm and protein concentration was calculated based on the standard curve.

2.2.19 Flagellin purification

Bacterial strains were grown in TSB at 225 rpm and 37°C overnight. The culture was pelleted at 8000 rpm for 10 min at 4°C and resuspended in PBS by vortexing for 3 min. The washed bacteria were then pelleted at 11000 rpm for 15 min at 4°C. The NaCl concentration in the supernatant was then increased from 0.14 M in PBS to 0.5 M and PEG was added to a final concentration of 1%. The proteins were allowed to precipitate at 4°C for 18h.

Following precipitation, the proteins were centrifuged at 9500 rpm for 20 min at 4°C. The pellet was resuspended in 10% ammonium sulphate ($(NH_4)_2SO_4$) and chilled for 2 h at 4°C, which was followed by centrifugation at 7000 x g for 20 min at 4°C. The pellet was then resuspended in dH_2O and dialysed against PBS at 4°C overnight using Slide-A-Lyzer dialysis cassettes (Pierce) according to manufacturer's instructions. The proteins were finally extracted from the dialysis cassette and analysed using SDS-PAGE and Instant Blue staining, as well as BioRad protein assay.

2.2.20 Peptidoglycan purification

Bacteria were grown overnight at 37°C and then cooled on ice before being pelleted at 12000 x g for 15 min at 4°C. Pellet was resuspended in boiling 4% SDS for 20 min including vortexing to ensure resuspension. The mixture was then pelleted at 12000 x g for 8 min at RT and the boiling in 4% SDS and centrifugation was repeated. The pellet was washed 5 times in 60°C dH_2O and centrifuged as above. After the wash steps, the pellet was resuspended in 50 mM Tris pH 7.0 and 1 mg/ml α-amylase (Sigma) was added, this was allowed to digest for 1 h at 37°C. Following the digest 2 mg/ml Pronase (Sigma) was added and incubated for 1 h at 60°C. The enzymes were inactivated at 95°C for 10 min and digested material was pelleted at 16000 x g for 8 min at 4°C and washed once in dH_2O. The pellet was resuspended in sodium phosphate buffer pH 6.0 with 1 mM $MgCl_2$ and 125 U mutanolysin (Sigma) and incubated overnight at 37°C. Insoluble material was removed by centrifugation at 16000 x g at 4°C for 15 min. Muramyl peptides in the supernatant were then freeze dried using a Christ Freeze-drier according to instructions. Material obtained were quantified by weighing and resuspended in dH_2O.

2.2.21   Twitch and swimming assays

Twitch agar plates were made up according to Huang et al. [342], 0.5% yeast extract, 100 mM potassium phosphate buffer pH 7.0, 1% agar and 5% tryptone. Colonies from an agar plate were picked with a p200 pipette tip and stabbed through the agar of a twitch agar plate. Plates were left at RT for 2 days and then analyzed for twitch zones.

2.2.22   Recombinant pilin

PA103 pilin was amplified using PCR and cloned into the pET41c vector, which results in PA103 pilin fused with a Glutathione S-transferase (GST) protein, containing a His-tag. The vector was transformed into chemically competent Rosetta cells according to manufacturer's instructions. The competent cells were thawed on ice and 1 µl of plasmid DNA was added. This was incubated on ice for 30 min, which was followed by heat shock at 42°C for 30 s and then transfer to ice. Bacteria were allowed to recover in 80 µl SOC medium at 37°C for 30 min. The entire transformation mixture was then added to 10 ml of LB with 50 µg/ml Kanamycin and were allowed to grow overnight at 37°C with 225 rpm shaking. The following day 2.5 ml of culture was added to 250 ml of LB with 50 µg/ml Kanamycin and allowed to grow at 30°C and 225 rpm until OD_{600} reached 0.5. The expression of pilin-GST was then induced by the addition of 1 mM isopropyl ß-D-1-thiogalactopyranoside (IPTG) and this was allowed to proceed for 3 h at 30°C and 225 rpm. Samples to check induction were taken at time points 0, 1, 2 and 3 h.

The bacterial culture was centrifuged for 10 min at 7500 rpm and 4°C in a Beckman Coulter Avanti J-26 XP centrifuge. The bacterial pellet was resuspended in 10 ml ice-cold PBS by vortexing and then centrifuged at 8739 x g and 4°C for 10 min. The pellet was stored at -20°C overnight.

A cleared bacterial lysate was prepared using the Ni-NTA His-Bind resin (Novagen). The bacterial pellet was thawed on ice for 15 min followed by resuspension by vortexing in 5 ml 1x NiNTA bind buffer with Roche protease inhibitors added. When the pellet was completely resuspened, 0.5 mg/ml lysozyme was added and lysates were incubated at 30°C for 10 min. The lysates

were chilled on ice and the viscosity was reduced by sonication with 10 s bursts at 80% power for a total of 1.5 min with cooling on ice between bursts. The lysate was then centrifuged at 8500 rpm and 4°C for 20 min, after which supernatant was carefully removed and kept on ice.

Recombinant pilin was purified using 1 ml Ni-NTA agarose slurry which was allowed to settle to 0.5 ml. The agarose was mixed with 4 ml of 1 x bind buffer and then the agarose was allowed to settle again. Supernatant was removed and the cleared lysate was added to the agarose, which was allowed to mix at 4°C using a rotating wheel for 1 h. The mixed slurry was then poured into a mini-column (Sigma) and allowed to settle; all remaining steps were performed at 4°C. The settled resin was washed with total of 8 ml 1 x Ni-NTA His Bind wash buffer, which was added in aliquots and allowed to drip through. The pilin-GST with a His-tag was then eluted in four fractions by adding 4 x 0.5 ml of 1 x Ni-NTA elution buffer. The protein concentrations were determined using the BioRad protein assay as described for pilin purification in section 2.2.18. Samples were stored in at 4°C until further purification was performed.

The GST protein with a His-tag was cleaved off from the eluted fusion protein using Tag-off high activity recombinant enterokinase (rEK, Novagen). The protocol was optimised by Alexandrea MacPherson and she found the 1 in 50 ratio i.e. 1 U rEK for 50 µg of protein to work best. 1 mg of His-tagged pilin was digested with 20 U rEK in 1 x rEK cleavage/capture buffer at RT for 16 h. Following cleavage the rEK was captured with 1 ml EKapture agarose. The EKapture agarose was centrifuged at 1000 x g for 5 min, washed once in 1 x rEK cleavage/capture buffer and then centrifuged again at 1000 x g for 5 min. The agarose was then resuspended in 1 x rEK cleavage/capture buffer and the protein rEK mixture was added and incubated at RT for 5 min, which was followed by centrifugation at 1000 x g for 5 min. The supernatant containing pilin and GST-His-tagged proteins was kept and a sample was taken for SDS-Page analysis.

The recombinant pilin was further purified using 1 ml Ni-NTA agarose, which was allowed to settle and the supernatant was removed. The elution buffer contains 250 mM imidazole whereas the wash buffer contains 20 mM, the protein mixture was therefore diluted to a final concentration of 20 mM imidazole. The protein

mixture was then mixed with the settled Ni-NTA agarose and allowed to mix using the rotating wheel at 4°C for 60 min. Finally, the slurry protein mixture were centrifuged at 1000 x g for 5 min and the supernatant with pure recombinant pilin was stored at -20°C in aliquots.

The purified recombinant pilin and samples prepared during the purification was analysed using the BioRad protein assay, as previously described, and SDS-Page analysis followed by staining in Instant Blue solution.

2.2.23   *Retroviral transduction*

Retroviral transduction was preformed as previously described [312, 327]. Briefly, BMDM were seeded at 7×10^5 cells per well in a 6-well plate in complete medium. Plates were centrifuged at 400 x g for 5 min and media was replaced with filtered supernatant from retroviral packaging line GP+E.86s containing 6 µg/ml polybrene. Plates were then centrifuged again at 2500 rpm at 21°C for 2h, followed by incubation at 37°C for 1 h. After an additional centrifugation at 2500 rpm for 5 min, media was replaced with complete media supplemented with 4 µg/ml polybrene. Plates were incubated at 37°C in a humified incubator for indicated time points.

Before FACS analysis, cells were scraped off and resuspended in complete media in FACS tubes (BD Biosciences). Following centrifugation at 400 x g for 5 min, cells were resuspended in FACS buffer (PBS with 1% FCS and 2 mM EDTA) and analysed using a BD FACS Calibur and the Cell Quest software (BD Biosciences). Prior to analysis, 4 µl 7-AAD (BD Biosciences) was added to each sample to exclude dead cells.

2.2.24   *Statistical analysis*

Statistical evaluations were carried out using the GraphPad Prism 4 software and an unpaired two-tailed Student's t-test with a confidence interval of 95 %. The results are showed as mean and standard error of the mean (SEM). Statistical significance was defined as $p < 0.05$ (*), $p < 0.01$ (**) and $p < 0.001$ (***).

2.3   Materials

2.3.1 Plasmids

Table 2.1; Plasmids used in this study

Construct	Resistance	Origin	Ref
p-NF-κB-Luc	Amp	Stratagene	
p-β-gal	Amp		
pCDNA3	Amp	R.L. Ferrero	[222, 343]
pCDNA3 ΔCARD Nod1	Amp	R.L. Ferrero	[217, 222]
pCDNA3 hNod1	Amp	D.J. Philpott	[222, 343]
pucp20	Amp/Carb	H. Schweizer	
pucp20 PA103 pilA	Amp/Carb	This study	
pucp20 PAO1 pilA	Amp/Carb	This study	
pucp20 ExoY	Amp/Carb	F.S Stirling	
MigR1	Amp	A.M. Michie	[344]
MigR1 PA103 pilin	Amp	This study	
MigR1 PA103 pilin C134A	Amp	This study	
MigR1 PA103 pilin T133*	Amp	This study	

2.3.1.1 Construction of plasmids

Restriction enzymes used were from Promega, all were used according to manufacturer's instructions in suitable buffers (provided with enzyme).

PA103 pilin was amplified using the upstream and downstream PA103 pilin primers (Table 2.2) from the genome of PA103 (accession number M14850). The resulting product was cloned into pucp20 between EcoR1 and BamH1.

PAO1 pilin was amplified using the forward and reverse PAO1 pilin primers (Table 2.2) from PAO1 (accession number M11323). The resulting product was cloned into pucp20 between EcoR1 and PstI. Both pucp20 pilin constructs, PA103 and PAO1, were verified by sequencing.

PA103 pilin was amplified using forward and reverse PA103 pilin primers for the MigR1 construct (Table 2.2), same accession number as previous for PA103. The product was cloned into the MigR1 vector between BglII and EcoR1. The retroviral sequence was checked using the sequencing primers for MigR1 (Table 2.2).

2.3.2 Primers, siRNAs and peptides

Table 2.2; Primers, siRNA and peptides used in this study

Construct	Sequence (5´-3´)	Origin	Ref
SYT7 siRNA	CATCATCACCGTCAGCCTTAG	Ambion	[345]
Silencer negative control #1 siRNA	not provided	Ambion	
hNod1 siRNA 1	ACAACTTGCTGAAGAATGACT	D.J. Philpott	[222]
Control hNod1 siRNA	GCAAGCTGACCCTGAAGTTCA	D.J. Philpott	[222]
SYT7 hairpin siRNA pSilencer 4.1 CMV (sense)	GATCCTCATCACCGTCAGCCTTAGTTCAA GAGACTAAGGCTGACGGTGATGATG	Ambion	[345]
SYT7 hairpin siRNA pSilencer 4.1 CMV (antisense)	AGCTTCATCATCACCGTCAGCCTTAGTCT CTTGAACTAAGGCTGACGGTGATGAG	Ambion	[345]
PA103 pilin forward MigR1 construct	CTGAGATCTGCTTGTTGAGGTTCAGGCG TTAG	T.J. Evans	
PA103 pilin reverse MigR1 construct	TCAGAATTCTGCTCTACCGACTGAGCTAA TCCG	T.J. Evans	
MSCV - sequencing primer for MigR1	CCCTTGAACCTCCTCGTTCGACC	T.J. Evans	
IRES - sequencing primer for MigR1	CCTCACATTGCCAAAAGACG	T.J. Evans	

Upstream PA103 pilin for pucp20 construct	TCA<u>GAATTC</u>CCAGCTTGTTCTGCACCAGG	T.J. Evans	
Downstream PA103 pilin for pucp20 construct	CGC<u>GGATCC</u>CAAAAACAGCTATTAAGGCTCATT	T.J. Evans	
Forward PAO1 pilin for pucp20 construct	TCA<u>GAATTC</u>CGAGTAGATTGGCTTGGACGAG	T.J. Evans	
Reverse PAO1 pilin for pucp20 construct	CAT<u>CTGCAG</u>AACCCCCGACCTTCTCATTACG	T.J. Evans	
Pannexin peptide	H-WRQAAFVDSY-NH2	Euro-gentec	[346]
Control peptide	H-SGILRNDSTVPDQF-NH2	Euro-gentec	[346]

Underlined parts of primer sequences indicate RE-sites.

2.3.3 Antibodies

Table 2.3; Antibodies used in this study

Description	Reactive species	Clone	Format	Isotype	Use	Manufacturer
Rabbit polyclonal Caspase-1 p10	Mouse Rat	M-20	Affinity purified		WB	Santa Cruz Biotechnology
Rabbit polyclonal Synaptotagmin 7	Rat Mouse Hamster Human		Lyophilized serum		WB	Synaptic Systems
Mouse monoclonal anti-FliC (Flagellin)	FliC protein	FLIC-1	Affinity purified	Mouse IgG1 κ	WB	Bio Legend
Rabbit polyclonal CARD4 (Nod1)	Human Mouse Monkey		Whole antiserum	IgG	WB	Abcam
Rabbit polyclonal Nod1	Human Mouse Rat Monkey		Affinity purified		WB	Cell signalling Technology
Mouse monoclonal CD107a (LAMP-1)	Human	H4A3	Affinity purified	Mouse IgG1 κ	IF	BD Biosciences
Mouse IgG Kappa					IF	Serotec

myeloma

Purified rat CD16/CD32 (Mouse FC block)	Mouse	2.4G2	Affinity purified	Rat IgG2b κ	FACS	BD Biosciences
Alexa Fluor 488 goat IgG	Mouse				IF	Molecular Probes
Mouse monoclonal beta Actin	Multiple	AC-15	Ascites	Mouse IgG1	WB	Abcam
Biotinylated goat IgG	Rabbit		Affinity purified		WB	Vector labs
Biotinylated rabbit IgG	Rat		Affinity purified		WB	Vector labs
Biotinylated horse IgG	Mouse		Affinity purified		WB	Vector labs

WB; western blotting, IF; immunofluorescence staining; FACS; used for flow cytometry straining

2.3.4 Bacterial strains

Table 2.4; Bacterial strains used in this study

Strain	Description	Resistance	Origin	Ref
PA103 WT	*P.aeruginosa* strain PA103 wild type which lacks flagellin		Long term in the lab	[347]
PA103 pilA⁻	*P.aeruginosa* strain PA103 lacking pilin, functional T3SS and translocated toxins	Gent	B. I. Kazmierczak	[348]
PA103 ΔUΔT	*P.aeruginosa* strain PA103 lacking translocated toxins (exoU and exoT) with a functional T3SS	Tet	D.W. Frank	[150]
PA103 ΔUΔT pilA⁻	*P.aeruginosa* strain PA103 lacking pilin and translocated toxins (exoU and exoT) with a functional T3SS	Tet Gent	This study	
PA103 ΔpcrV	*P.aeruginosa* strain PA103 lacking the pore-forming protein of the T3SS (pcrV), which makes it unfunctional	Tet	D.W. Frank	[93]
PA103 ΔUΔT:exoU	*P.aeruginosa* strain PA103 lacking translocated toxins (exoU and exoT) with a functional T3SS, complemented with a functional exoU toxin	Tet Carb	F.R. Stirling	

PA103 ΔUΔT:exoU S142A	*P.aeruginosa* strain PA103 lacking translocated toxins (exoU and exoT) with a functional T3SS, complemented with a non-functional exoU toxin	Tet Carb	F.R. Stirling	[143]
PAO1 WT	*P.aeruginosa* strain PAO1 wild type with flagellin		J. Mekalanos, A. Rietsch	[78]
PAO1 ΔSTY	*P.aeruginosa* strain PAO1 lacking translocated toxins (exoS, exoT and exoY) with a functional T3SS		J. Mekalanos, A. Rietsch	[78]
PAO1 ΔpopB	*P.aeruginosa* strain PAO1 lacking popB which makes the T3SS unfunctional		J. Mekalanos, A. Rietsch	[78]
PAO1 pilA⁻	*P.aeruginosa* strain PAO1 lacking pilin, functional T3SS and translocated toxins		B. I. Kazmierczak	[348]
PAO1 FliC⁻	*P.aeruginosa* strain PAO1 lacking flagellin, functional T3SS and translocated toxins	Tet	B. I. Kazmierczak	[348]
PAO1 FliC⁻ pilA⁻	*P.aeruginosa* strain PAO1 lacking flagellin and pilin, functional T3SS and translocated toxins	Tet	B. I. Kazmierczak	[348]
PAO1 FliC⁻ pilA⁻:PA103	*P.aeruginosa* strain PAO1 lacking flagellin and pilin, recomplemented with pilin	Tet	This study	

pilA pucp20	from PA103	Carb	
PAO1 FliC⁻ pilA⁻:PAO1 pilA pucp20	*P.aeruginosa* strain PAO1 lacking flagellin and pilin, recomplemented with pilin from PAO1	Tet Carb	This study
PAO1 FliC⁻ pilA⁻:pucp20	*P.aeruginosa* strain PAO1 lacking flagellin and pilin, recomplemented with the empty plasmid pucp20	Tet Carb	This study
PAOC : PAO1 FliC	*P.aeruginosa* strain PAOC wild type complemented with PAO1 flagellin		R. Ramphal [349]
Salmonella	*Salmonella enterica* Typhimurium strain SL1344		M. Roberts

2.3.5 Reagents

Table 2.5; Reagents used during this study

Reagent	Use	Manufacturer
RNase-free DNase Set	DNaseI treatment of pilin preparations	Qiagen
Glybenclamide / Glyburide	Inhibition of ATP-dependent potassium channels	Sigma
Methyl Arachidonyl Fluorophosphonate (MAFP)	Inhibition of ExoU-dependent cytotoxicity	Calbiochem
Ionomycin calcium salt	Permeabilisation of cells for Lucifer Yellow assay and calcium imaging	Sigma
Streptolysin O from *Streptococcus pyogenes*	Permeabilisation of cells for Lucifer yellow assay	Sigma
Proteinase K (Fungal)	Proteinase K treatment of pilin preparation	Invitrogen
LPS from *E.coli* O127:B8 purified by ion-exchange chromatography	Priming of BMDM 2 µg/ml for 3 h. Stimulation of HEK293 cells	Sigma
LPS from *E.coli* O127:B8 purified by phenol extraction	Stimulation of HEK293 cells, a source of PGN	Sigma
ATP	Activation of inflammasomes after LPS priming. 5 mM for 20 min	Sigma

Flagellin recombinant *E.coli* from *Salmonella muenchen*	Flagellin-dependent inflammasome activation	Calbiochem
Pluronic F-127	Dispersion of acetoxymethyl (AM) esters of fluorescent ion indicators	Invitrogen
Carbenoxolone (CBX)	Blocking reagent of the P2X7R and thus pannexin-1 channel.	Sigma

2.3.6 Buffers used for potassium-dependence studies

A range of buffers were used when the potassium-dependent inflammasome activation was studied, described in chapter 4. These were adapted from known extracellular buffers and previous publications.

High and low potassium buffer contained 147 mM NaCl, 10 mM HEPES, 13 mM glucose, 2 mM $CaCl_2$, 1 mM $MgCl_2$ and 2 or 130 mM KCl. Hank's buffer [280] were supplemented with 1 x MEM vitamin solution, 2 mM L-glutamine, 1 x MEM amino acids solution and 100 μM/ml sodium pyruvate (all from Invitrogen), in order to keep the buffer as close to normal media as possible, high K^+-buffer had 140 mM KCl and 5 mM NaCl. Isotonic buffers were supplemented Hank's buffers with varied concentrations of KCl and NaCl. The combined total of KCl and NaCl were always 145 mM i.e. 5 mM KCl with 140 mM NaCl, 45 mM KCl with 100 mM NaCl, 90 mM KCl with 55 mM NaCl and 120 mM KCl with 25 mM NaCl. Finally, complete media (RPMI), which normally contains 5 mM KCl was also used. This was supplemented with 130 mM KCl, for high KCl concentration.

3 Inflammasome activation by *Pseudomonas aeruginosa*

3.1 Introduction

3.1.1 Inflammasome activation by Gram-negative bacteria

The inflammasome complexes involved in the detection of Gram-negative bacteria are NLRC4 and NAIP5. It has been shown that both *Salmonella typhimurium* and *Shigella flexneri* activate the NLRC4 inflammasome, an activation which is dependent on ASC [234, 350]. In contrast, *Legionella pneumophila* requires NLRC4 and NAIP5 for activation of the inflammasome but this is ASC-independent [251, 351, 352]. However, a recent study challenged these findings and found a role for ASC in inflammasome activation by *L.pneumophila* independent of NLRC4 [353]. Furthermore, it was shown, subsequently to results presented in this chapter, that inflammasome activation by *P.aeruginosa* is dependent on NLRC4 and ASC [249, 253, 354]. *Francisella tularensis* infection results in activation of the inflammasome [250]. This activation is dependent on ASC but not NLRC4 or NLRP3 [250, 355]. *F.tularensis* activates a type I IFN response upon entry into the cells, which has been shown to be required for inflammasome activation by this bacteria [356]. This was also shown for *L.monocytogenes* but not for the inflammasome activation by ATP or *S.typhimurium* [356].

So far, activation of the NLRC4 inflammasome has been shown to be dependent on a functional bacterial secretion system, such as a T3SS or a T4SS. Inflammasome activating proteins can pass through these secretion systems, for example flagellin [248, 337, 354]. However, there must be other factors passing through the T3SS or T4SS, as *S.flexneri* is able to activate the NLRC4 inflammasome despite the fact that it lacks flagellin [254]. Similar results were obtained with a strain of *P.aeruginosa* which lacks flagellin [249].

3.1.2 Role of NAIP5 in inflammasome activation

The A/J mouse strain has a mutation in the gene for the NLR protein NAIP5 (also known as NLRB5). This mutation results in susceptibility to *L.pneumophila* infection [357, 358]. Thus, NAIP5 restricts infection by *L.pneumophila* [251, 351, 357]. This is true both for mouse and human cells [212, 251, 351, 357]. Further

studies in NAIP5 KO mice confirmed the role for NAIP5 in resistance to *L.pneumophila* [312]. This study also demonstrated that NAIP5 together with NLRC4 and ASC is required for the inflammasome activation in response to flagellin from *L.pneumophila* [312]. The *Naip5* mutated allele in the A/J mice is partially functional and as a result the use of KO mice is more relevant in NAIP5 investigations [312]. Furthermore, a role of NAIP5 could not be detected in the inflammasome activation by *P.aeruginosa*, *S.typhimurium* and *L.monocytogenes* [354].

We hypothesised that *P. aeruginosa* could activate the inflammasome and that this might occur through molecules introduced via its T3SS. The results reported here show that *P.aeruginosa* is able to activate the inflammasome in a T3SS-dependent manner, but independent on any effectors being translocated. This is described for the PA103 and PAO1 strains. In addition, inflammasome activation by PA103 and PAO1 is dependent on NLRC4, ASC and caspase-1. The differences observed are not due to differences in internalization.

3.2 Results

3.2.1 Pseudomonas aeruginosa activates the inflammasome in a T3SS-dependent manner

Several bacteria have been shown to activate inflammasome complexes, as previously discussed. In order to investigate whether *P.aeruginosa* is able to activate the inflammasome, BMDM were infected with PA103 ΔUΔT and PA103 ΔpcrV. ATP is a known activator of the NLRP3 inflammasome and this was used as a positive control. LPS-primed BMDM were treated with ATP, which resulted in IL-1ß secretion (Figure 3.1). PA103 ΔUΔT were also able to induce secretion of IL-1ß from the cells (Figure 3.1), significantly more than PA103 ΔpcrV. These results indicate that the inflammasome activation by *P.aeruginosa* requires a functional T3SS.
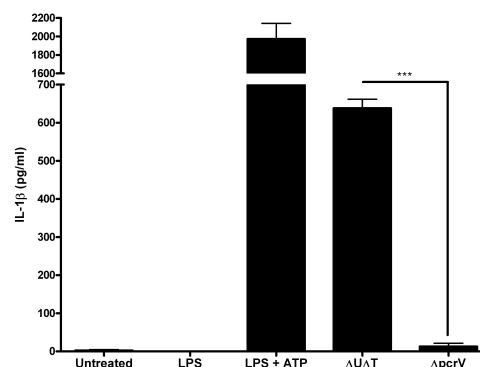
Figure 3.1; PA103 activates the inflammasome in a T3SS-dependent manner

BMDM were infected with PA103 ΔUΔT or PA103 ΔpcrV at a MOI of 100 for 90 min in the absence of LPS priming, or BMDM were primed with LPS for 3 h followed by treatment with ATP for 20 min as a control. Secreted IL-1β released immediately following incubation is measured by ELISA. Columns are means of triplicates and error bars are SEM. *** indicates a significant difference, where p<0.001, unpaired Student's t-test. Results are representative of at least 6 experiments.

Secretion of mature IL-1ß requires processing of pro-IL-1ß by active caspase-1. Upon activation of the inflammasome pro-caspase-1 is processed into p10 and p20 fragments, which form an active heterodimer capable of processing pro-IL-1ß. Caspase-1 processing was investigated using immunoblotting in cell lysates from BMDM infected with PA103 ΔUΔT or PA103 ΔpcrV or cells primed with LPS and then treated with ATP. Pro-caspase-1 could be detected in all samples (Figure 3.2), whereas the active form of caspase-1 (p10) could only be detected

in the samples where IL-1β secretion was observed, ATP treated and PA103 ΔUΔT infected cells (Figure 3.2).
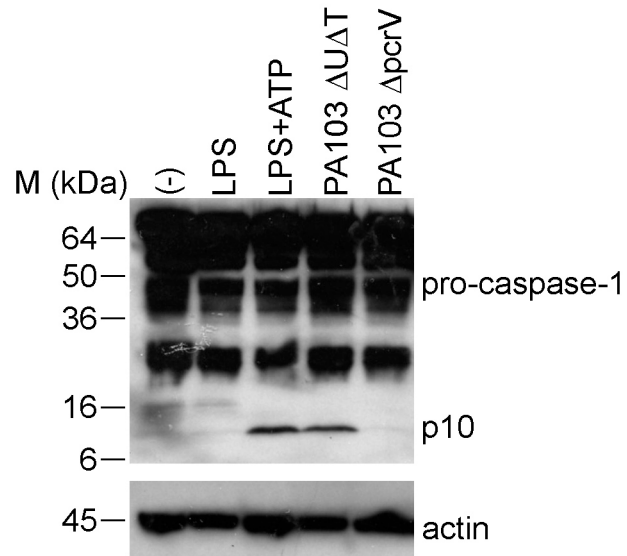
Figure 3.2; Inflammasome activation by PA103 is dependent on a functional T3SS.

Cell lysates from Figure 3.1 were analysed for caspase-1 processing by immunoblot with caspase-1 antibody. The 45 kDa pro-caspase-1 and processed form, p10, is shown, as well as a reprobe with actin (lower panel) showing even loading of the gel. Results are representative of at least 6 experiments.

PA103 ΔUΔT lacks all its T3SS effectors and thus have an empty T3SS with no effectors being translocated during infection. In order to investigate whether translocated effectors would have an effect on the inflammasome activation by *P.aeruginosa*, PA103 ΔUΔT was compared to a strain which translocates a non-functional effector PA103 ΔUΔT:ExoUS142A. BMDM were infected with these strains and PA103 ΔpcrV was used as a control. There was no significant difference in the IL-1ß secretion from PA103 ΔUΔT compared to PA103 ΔUΔT:ExoUS142A (Figure 3.3A). These two strains also resulted in comparable cytotoxicity of the cells (Figure 3.3B). The percent cytotoxicity was below 10% for all samples, which indicate that the IL-1ß secretion seen is not due to increased cell death in these samples. Thus, there is no effect on the inflammasome activation by *P.aeruginosa* when effectors are translocated through the T3SS.
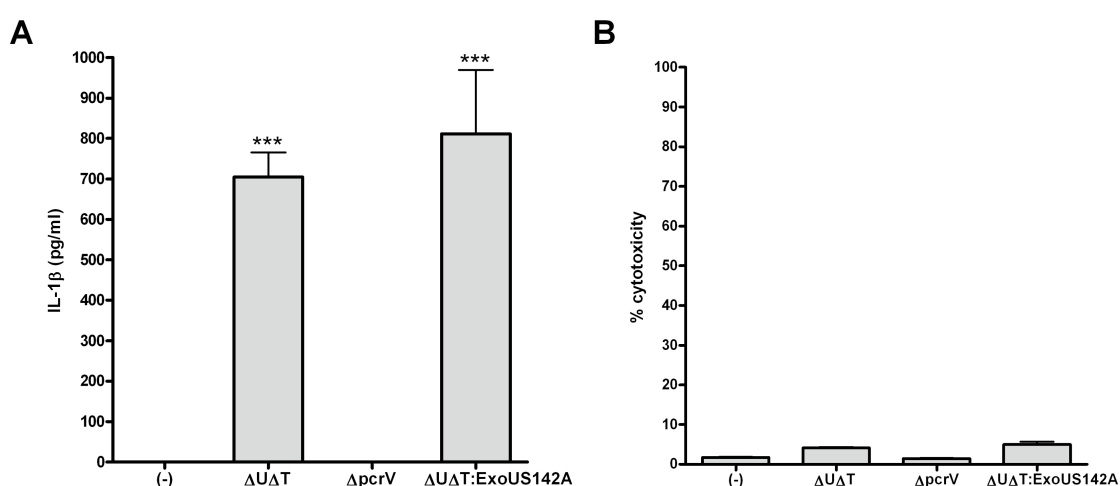
Figure 3.3; PA103 activates the inflammasome independent of translocated effectors.

BMDM were infected with PA103 strains at a MOI of 20 for 90 min. A, Secreted IL-1β released during infection is measured by ELISA. B, Supernatants were analysed for cytotoxicity caused by measurement of LDH release. Columns are means of triplicates and error bars are SEM, where *** is $p < 0.001$, untreated cells with infected samples, unpaired Student's t-test. Results are representative of at least 3 experiments.

Following infection with PA103 ΔUΔT and PA103 ΔpcrV of BMDM, IL-1ß secretion can be detected after 90 min of infection at a MOI of 20 (Figure 3.4A). PA103 ΔpcrV does not result in IL-1ß secretion even after 180 min of infection (Figure 3.4A), as expected since this strain lacks a functional T3SS. The cytotoxicity caused by PA103 ΔUΔT increases with increasing infection time, whereas the cytotoxicity by PA103 ΔpcrV remains low and constant (Figure 3.4B).
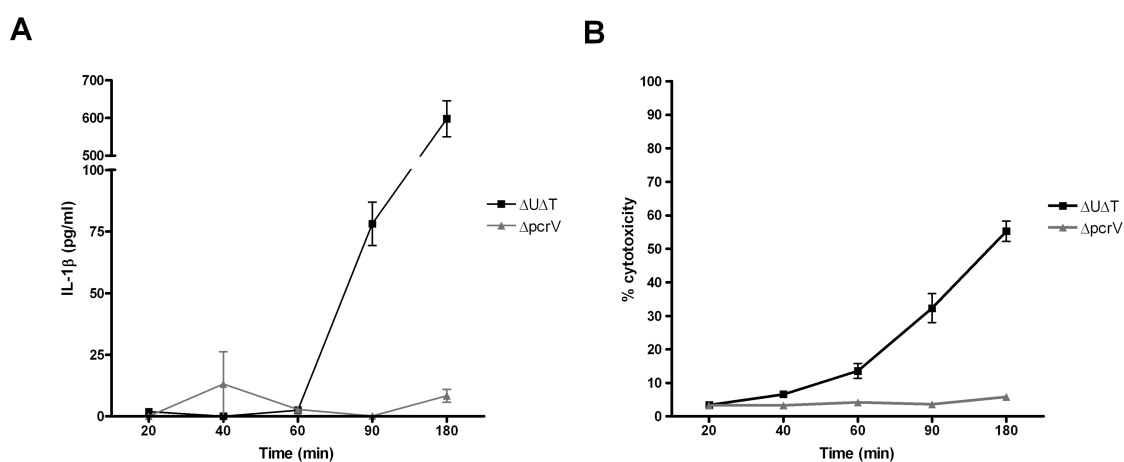
Figure 3.4; Inflammasome activation by PA103 can be detected after 90 min of infection.

BMDM were infected with PA103 ΔUΔT and PA103 ΔpcrV at a MOI of 20 for indicated time periods. A, IL-1β secretion was measured by ELISA from supernatants. B, Percent cytotoxicity were analysed in supernatants by measurement of LDH release. Means of triplicates are plotted and error bars are SEM.

The amount of IL-1ẞ secretion caused by PA103 ΔUΔT is dependent on MOI. BMDM were infected with PA103 ΔUΔT and PA103 ΔpcrV at varied MOIs for 90 min. Increasing MOIs results in increasing amounts of IL-1ẞ secretion following infection with PA103 ΔUΔT (Figure 3.5A). PA103 ΔpcrV does not result in IL-1ẞ secretion at any MOI investigated (Figure 3.5A). Furthermore, increasing MOIs also result in increasing amount of cytotoxicity caused by PA103 ΔUΔT (Figure 3.5B).
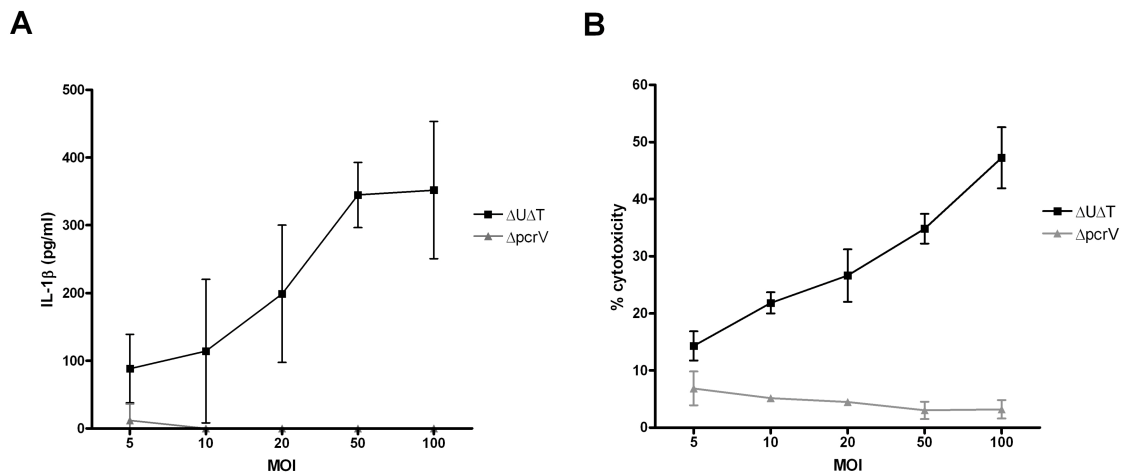
Figure 3.5; Higher MOI results in more inflammasome activation by PA103.

BMDM were infected with PA103 ΔUΔT and PA103 ΔpcrV at indicated MOIs for 90 min. A, IL-1β secretion was analysed by ELISA in supernatants. B, Percent cytotoxicity were analysed by measurement of LDH release in supernatants. Means of triplicates are plotted and error bars are SEM.

Active caspase-1 (p10) can be detected following infection with PA103 ΔUΔT at all MOIs tested (Figure 3.6). In general, levels of p10 increased with MOI over 10 although levels at MOIs of 20 and 50 were less than the amount seen at 10 (Figure 3.6). No caspase-1 activation could be detected following infection with PA103 ΔpcrV as expected (Figure 3.6). The amount of pro-caspase-1 was similar in all samples (Figure 3.6, lower panel).
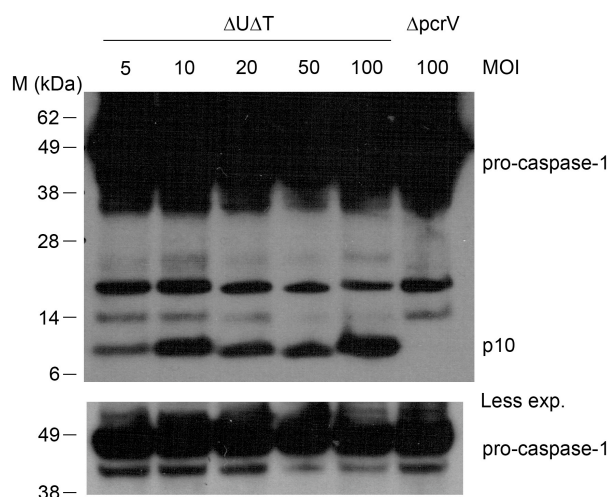
Figure 3.6; More caspase-1 is activated at higher MOIs by PA103.

Cell lysates from Figure 3.5 were immunoblotted with caspase-1 antibody. Top panel shows processed caspase-1 (p10) and pro-caspase-1 (45 kDa). Lower panel shows pro-caspase-1 following a shorter exposure.

PA103 activates the inflammasome in a T3SS-dependent manner. In order to investigate whether other strains of *P.aeruginosa* also activate the inflammasome in a similar manner, the PAO1 strain was tested. BMDM were infected with various strains of PAO1; PAO1 WT, which has a functional T3SS as well as effectors passing through the system; PAO1 ΔSTY, has a functional T3SS but no translocated effectors (equivalent to PA103 ΔUΔT); and PAO1 ΔpopB; which has a non-functional T3SS resulting from the deletion of the essential T3SS protein popB. PAO1 also activated the inflammasome in a T3SS-dependent manner which is independent of any effectors passing through the T3SS (Figure 3.7). IL-1β secretion was detected following infection with PAO1 WT and ΔSTY, and levels were not changed when there are effectors being translocated (Figure 3.7). These strains resulted in significantly more IL-1β secretion compared to PAO1 ΔpopB, similar to the results seen with PA103 ΔUΔT and PA103 ΔpcrV.
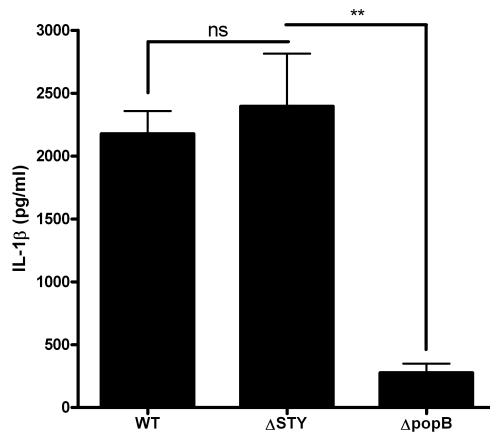
Figure 3.7; PAO1 activates the inflammasome in a T3SS-dependent manner, independent of translocated effectors.

BMDM were infected with PAO1 strains as indicated for 90 min at a MOI of 100. Supernatants were analysed for IL-1β secretion using ELISA. Columns show means of triplicates and error bars are SEM. ** indicate significant difference where $p<0.01$, ns is non significant difference, $p>0.05$, unpaired Student's t-test.

Following infection with the different PAO1 strains, active caspase-1 (p10) was detected in samples infected with PAO1 WT or PAO1 ΔSTY, but not after infection with PAO1 ΔpopB (Figure 3.8). These results show that PA103, as well as PAO1 activate the inflammasome in a T3SS-dependent but effector-independent manner.
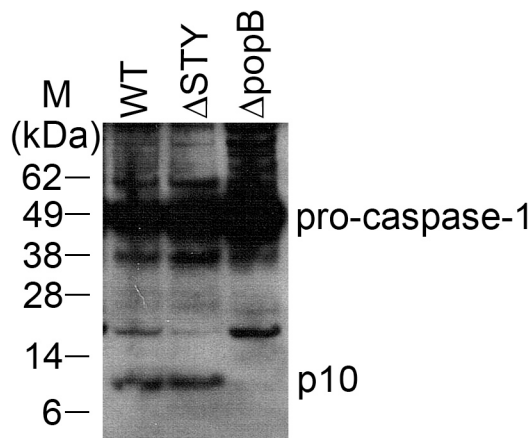
Figure 3.8; Inflammasome activation by PAO1 is dependent on a functional T3SS.

Cell lysates from Figure 3.7 were immunoblotted with caspase-1 antibody. Pro-caspase-1 and processed p10 of activated caspase-1 is shown.

3.2.2 Inflammasome activation by Pseudomonas aeruginosa strain PA103 and PAO1 is dependent on NLRC4 and ASC

The NLRC4 inflammasome has previously been described to respond to bacterial products secreted via a functional secretion system. The inflammasome component dependence during infection with *P.aeruginosa* was investigated using BMDM from mice with specific homozygous deletion of genes encoding inflammasome components. These were kindly provided by Prof Jürg Tschopp from University of Lausanne, Switzerland. The BMDM from KO mice were primed with LPS and then infected with PA103 ΔUΔT or treated with ATP. No IL-1ß or cytotoxicity could be detected from LPS-primed cells alone, as expected (Figure 3.9A and B). Cells treated with ATP were dependent on NLRP3, ASC and caspase-1, but not NLRC4 (Figure 3.9A), which has been described previously [238]. ATP treatment did not result in significantly higher cytotoxicity compared to LPS-primed cells (Figure 3.9B). Inflammasome activation by PA103 ΔUΔT was dependent on NLRC4, ASC and caspase-1, but not NLRP3 (Figure 3.9A). The cytotoxicity caused during infection with PA103 ΔUΔT was less than 15% for all samples; however, the cell death corresponded to the IL-1ß secretion seen.
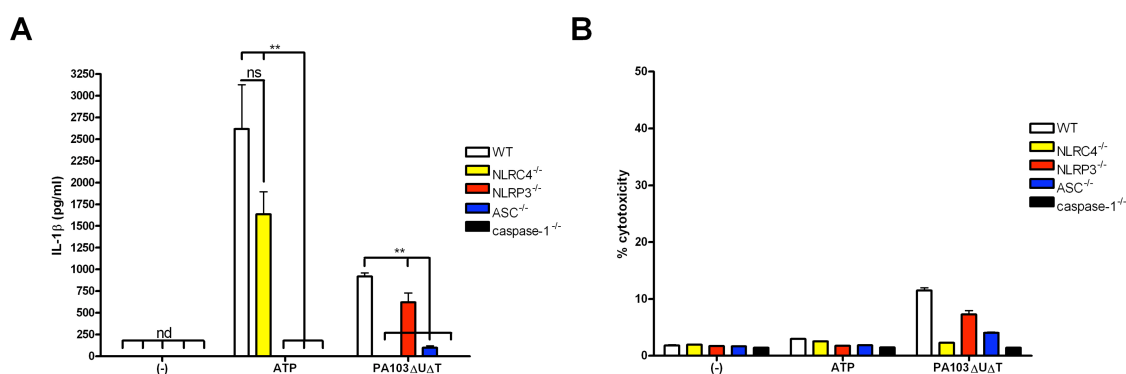
Figure 3.9; Inflammasome activation by PA103 ΔUΔT is dependent on NLRC4, ASC and caspase-1.

BMDM with specific homozygous deletions of genes encoding inflammasome components were primed with LPS for 3h and then infected with PA103 ΔUΔT at a MOI of 30 for 90 min or treated with ATP for 20 min. Columns are means of triplicates and error bars are SEM. A, Supernatants were analysed for IL-1β secretion using ELISA. Nd; non detected. ** indicates a significant difference analysed by unpaired Student's t test (** p<0.01, ns; non significant difference p>0.05). B, Percent cytotoxicity were analysed by measurement of LDH release in supernatants.

The inflammasome dependence following infection with PAO1 ΔSTY was also investigated. LPS-primed BMDM were infected with PAO1 ΔSTY. ATP treatment and LPS-primed cells alone are shown as reference; these are described in Figure 3.9. Inflammasome activation by PAO1 ΔSTY was also dependent on NLRC4, ASC and caspase-1 (Figure 3.10A), which is similar to PA103 ΔUΔT. Infection with PAO1 ΔSTY results in very high cytotoxicity, dependent on NLRC4 and caspase-1, but not ASC (Figure 3.10B).
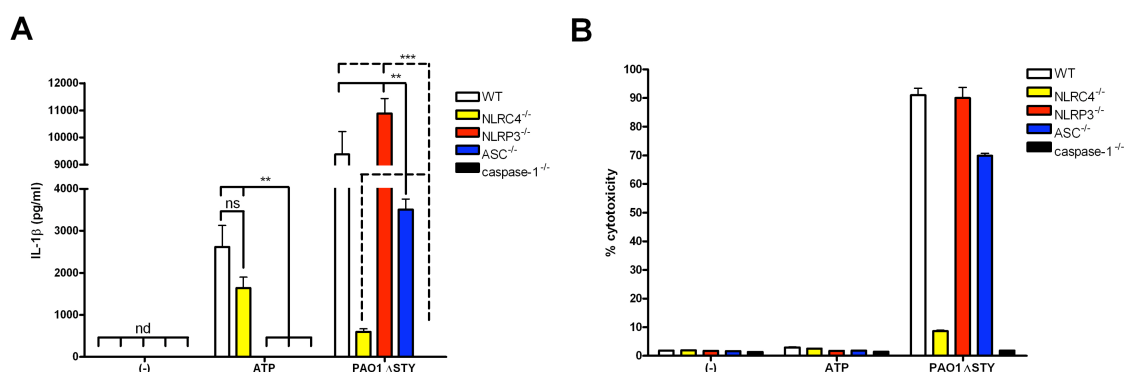
Figure 3.10; Inflammasome activation by PAO1 ΔSTY is dependent on NLRC4, ASC and caspase-1.

BMDM with specific homozygous deletions of genes encoding inflammasome components were primed with LPS for 3h and then infected with PAO1 ΔSTY at a MOI of 30 for 90 min or treated with ATP for 20 min. Columns are means of triplicates and error bars are SEM. A, Supernatants were analysed for IL-1β secretion using ELISA. Nd; non detected. ** and *** indicates a significant difference analysed by unpaired Student's t test (*** $p<0.001$, ** $p<0.01$, ns; non significant difference $p>0.05$). B, Percent cytotoxicity were analysed by measurement of LDH release in supernatants.

The inflammasome KO cell lysates were analysed for caspase-1 activation following infection with PA103 ΔUΔT and PAO1 ΔSTY, as well as following treatment with ATP. The caspase-1 activation corresponds to the IL-1β secretion observed. ATP treated cells are dependent on NLRP3, ASC and caspase-1 for caspase-1 activation (Figure 3.11). PA103 ΔUΔT and PAO1 ΔSTY are dependent on NLRC4, ASC and caspase-1 (Figure 3.11).
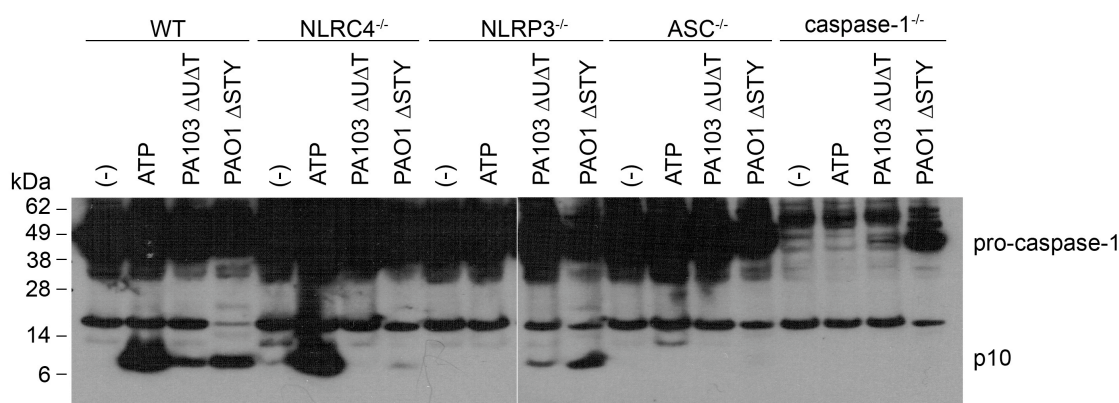
Figure 3.11; Inflammasome activation by *P.aeruginosa* is dependent on NLRC4, ASC and caspase-1.

Cell lysates from Figure 3.9 and 3.10 were immunoblotted with caspase-1 antibody. Pro-caspase-1 (45 kDa) and processed caspase-1, p10, are shown.

The inflammasome dependence was also investigated at a higher MOI (100 compared to 30 during previous experiments) following infection with PA103 ΔUΔT and PAO1 WT. KO BMDM were primed with LPS and treated with ATP or left unprimed and infected with PA103 ΔUΔT and PAO1 WT. As previously seen, ATP dependent inflammasome activation is dependent on NLRP3 and ASC and it does not result in significant cytotoxicity (Figure 3.12A and B). Furthermore, PA103 ΔUΔT remains dependent on NLRC4 and ASC for its inflammasome activation at this MOI (Figure 3.12A). The cytotoxicity caused by PA103 ΔUΔT is not significantly different compared to cells alone in WT, NLRC4 and ASC. However, the cytotoxicity is very high in the NLRP3 KO, suggesting a protective effect of NLRP3 for cell death at this higher MOI (Figure 3.12B). PAO1 WT showed some differences at this higher MOI compared to the lower value used before. There was now some dependence on NLRP3, although as before most of the response seems to be dependent on NLRC4 and ASC (Figure 3.12A). This strain seems to be just dependent on NLRC4 for the cytotoxicity seen at this MOI (Figure 3.12B).
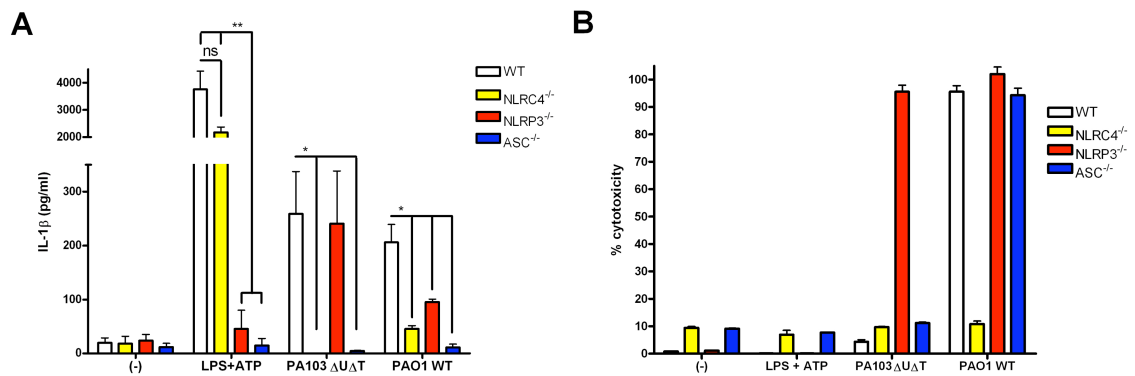
Figure 3.12; Inflammasome activation by *P.aeruginosa* is dependent on NLRC4 and ASC.

BMDM with specific homozygous deletions of genes encoding inflammasome components were primed with LPS for 3h and then treated with ATP for 20 min, or left unprimed and were infected with PA103 ΔUΔT or PAO1 WT at a MOI of 100 for 90 min. Columns are means of triplicates and error bars are SEM. A, Supernatants were analysed for IL-1β secretion using ELISA. * and ** indicates a significant difference analysed by unpaired Student's t test (* p<0.05, ** p<0.01, ns; non significant difference; p>0.05). B, Percent cytotoxicity were analysed by measurement of LDH release in supernatants.

3.2.3 NAIP5 is not critical for the response to Pseudomonas aeruginosa infection

Inflammasome activation by *Legionella pneumophila* has previously been shown to be dependent on NAIP5 [312]. The A/J mouse strain has a mutation in the *Naip5* gene [357]. In order to investigate the role of NAIP5 in inflammasome activation by *P.aeruginosa* BMDM were obtained from A/J mice, as well as C57/BL6, the strain normally used for inflammasome studies in BMDM. BMDM from these mice were primed with LPS and then infected with PA103 ΔUΔT, *Salmonella* SL1344 or PAO1 WT. No effect could be seen on IL-1β secretion following infection with these bacteria in the A/J strain compared to the C57/BL6 (Figure 3.13A). However, upon a repeat of the experiment at a slightly higher MOI, there was an effect on IL-1β secretion from PA103 ΔUΔT and PAO1 WT infected cells. Significantly less IL-1β was secreted from A/J cells compared to C57/BL6 (Figure 3.13C). The *Salmonella* infected samples remained the same between the two mice strains (Figure 3.13C). These results suggest that NAIP5 may have a role in inflammasome activation by *Pseudomonas* but definitive proof will require the use of *Naip5* knockout animals. These cells were also analysed for percent cytotoxicity caused following infection. In both experiments the cytotoxicity was significantly less in the A/J cells compared to

C57/BL6 for all infected samples (Figure 3.13B and D). This indicates an effect of NAIP5 on cytotoxicity seen following inflammasome activation by Gram-negative bacteria.
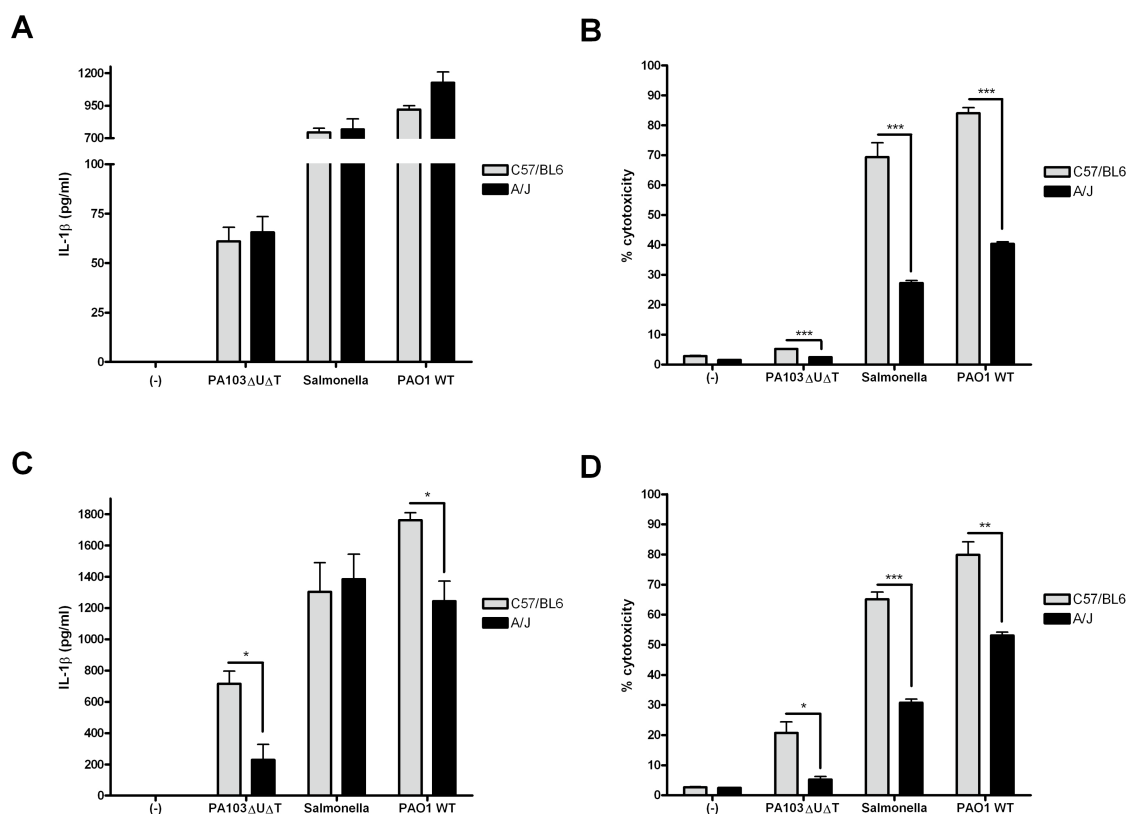
Figure 3.13; NAIP5 is not critical for the response to infection with Gram-negative bacteria.

BMDM from C57/BL6 and A/J mice were primed with LPS for 3h and then infected with indicated strains at a MOI of 20 (A and B) and 30 (C and D) for 90 min. Columns are means of triplicates and error bars are SEM. Two separate experiments are shown (A, B and C, D). A and C, Secretion of IL-1β were analysed in supernatants using ELISA. B and D, Percent cytotoxicity were analysed by measurement of LDH release. *, ** and *** indicates a significant difference between the two different mouse strains. Unpaired Student's t test where * is $p < 0.05$, ** is $p < 0.01$ and *** is $p < 0.001$.

Caspase-1 activation was also investigated in these cells, comparing cell lysates from A/J mice to C57/BL6 infected at a MOI of 30 (Figure 3.14). As observed with the levels of secreted IL-1β, there was little difference between the mouse strains in the degree of activation of caspase-1 following *P.aeruginosa* infection (Figure 3.14).
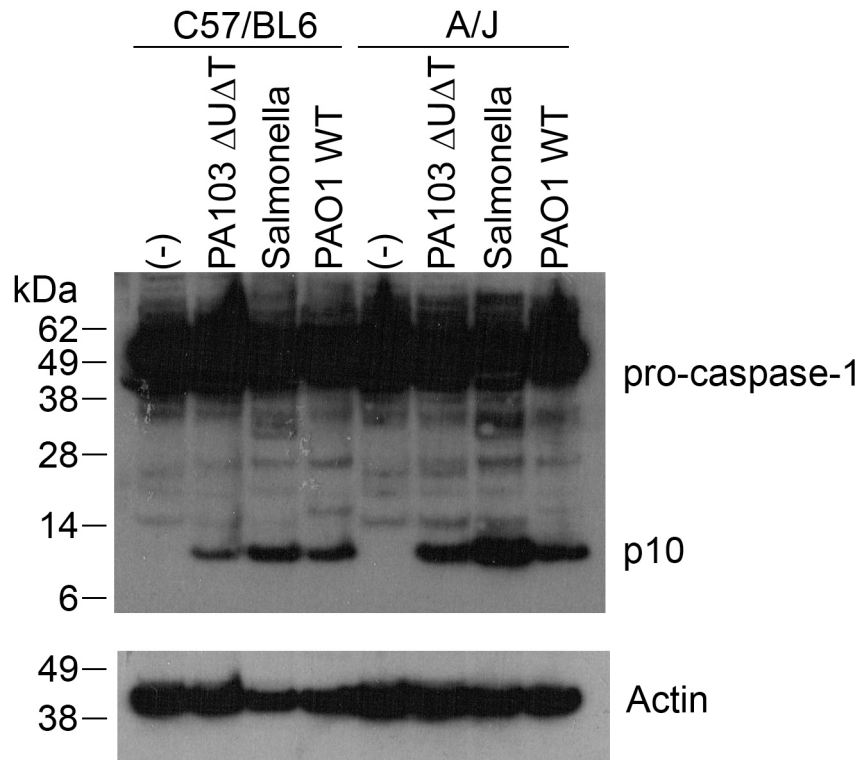
Figure 3.14; NAIP5 is not critical for the inflammasome activation by Gram negative bacteria.

Cell lysates from Figure 3.13A were immunoblotted with caspase-1 antibody. Top panel shows pro-caspase-1 (45 kDa) and processed caspase-1 (p10). Lower panel shows reprobe with actin antibody, to show even loading of the gel.

3.2.4 Internalisation does not account for differences in inflammasome activation

P.aeruginosa is an extracellular pathogen. However, small amounts of bacteria are internalised, and these might affect the degree of inflammasome activation. Following infection, extracellular bacteria were killed with Gentamicin and the intracellular microbes were counted following culture and compared to the initial inoculums. Following infection with PA103 ΔUΔT and PA103 ΔpcrV, less than 1.5% of bacteria are internalised (Figure 3.15A). Furthermore, as expected, no bacteria could be detected in cells alone treated with Gentamicin (Figure 3.15A). In addition significantly more PA103 ΔpcrV were internalised compared to PA103 ΔUΔT (Figure 3.15A), which is a strain that has no effect on inflammasome activation. PAO1 ΔSTY is also not significantly internalised during infection of BMDM, with less than 1.5% of bacteria internalised (Figure 3.15B).

Finally, the internalisation in a fibroblast cell line (HEK293T cells) was investigated. Less than 0.5% of bacteria were internalised during infection of these cells (Figure 3.15C). Thus, differences in the degree of *P.aeruginosa* internalisation between the strains cannot account for the differences observed in inflammasome activation.
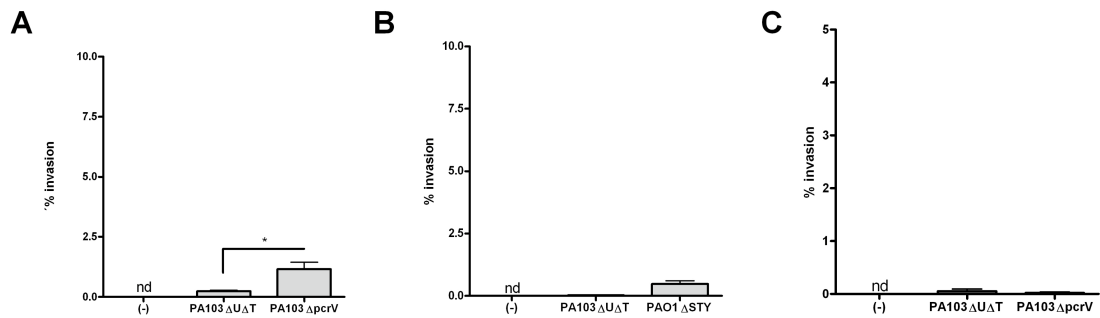
Figure 3.15; *P.aeruginosa* **is not significantly internalised upon infection.**

Various cell types were infected with indicated *P.aeruginosa* strains for 90 min. Gentamicin was then added for 60 min to kill extracellular bacteria. Cells were then lysed and intracellular bacteria were counted following culture, which was compared to initial inoculum. Results are means of triplicates and error bars are SEM. Nd; non detected, * indicates significant difference between the strains, unpaired Student's t test where * is p<0.05. A, BMDM infected at a MOI of 100. B, BMDM infected at a MOI of 50. C, HEK293T cells infected at a MOI of 100.

3.3 Discussion

There have been several reports about bacterial strains which trigger inflammasome activation. Gram-negative bacteria such as *Salmonella typhimurium*, *Shigella flexneri*, *Legionella pneumophila*, *Francisella tularensis* and *Pseudomonas aeruginosa* have all been reported to activate the inflammasome [234, 249-251, 253, 350-352, 354, 355]. In this study it was first investigated whether *P.aeruginosa* can activate the inflammasome. It was found that PA103 activates the inflammasome in a process which is dependent on a functional T3SS. After we had performed these experiments, this was also described by Franchi et al., Miao et al., and Sutterwala et al. [249, 253, 354]. The study by Sutterwala et al. investigates the same strain of *P.aeruginosa* (PA103). The inflammasome activation by PA103 is independent of any effectors being translocated through the T3SS. This is also seen in the study by Sutterwala et al. and Franchi et al. [249, 253]. Importantly, PA103 lacks flagellin and thus inflammasome activation by this strain is independent of flagellin, discussed further in chapter 5.

The cytotoxicity resulting from infection with PA103 ΔUΔT is dependent on MOI and infection time, as expected. At a higher MOI the bacterial burden is increased for the cell which leads to increased cell stress. Furthermore, inflammasome activation and processing of pro-caspase-1 to active caspase-1 can result in pyroptosis [359]. Increased bacterial burden can therefore be assumed to lead to increased activation of the inflammasome and thus increased pyroptosis, as well as IL-1β secretion. An increased infection time will have the same effect.

The inflammasome activation by PAO1 is also dependent on a functional T3SS and independent of translocated effectors. The study by Miao et al. also found that PAO1 activates the inflammasome in a process which is dependent on a functional T3SS [354].

During this study both LPS-primed and unprimed BMDM have been used for the investigation whether *P.aeruginosa* can activate the inflammasome. The amount of IL-1β released following LPS-priming compared to unprimed cells is higher due

to increased time for the pro-IL-1ß to accumulate. To secrete mature IL-1ß two signals are needed. Firstly, a signal which stimulates pro-IL-1ß transcription and translation is required, usually mediated by TLR signalling. The second signal needed is activation of a NLR-protein in an inflammasome complex leading to active caspase-1 and processing of pro-IL-1ß to mature IL-1ß [260, 360], as described in section 1.5.4.2. *P.aeruginosa* can activate the inflammasome complex in BMDM, a process which does not require LPS-priming of the cells. *P.aeruginosa* is a Gram-negative bacterium, and thus has LPS in its outer membrane. The LPS on *P.aeruginosa* will act on TLR4 [361, 362] and induce transcription of pro-IL-1ß, thus LPS-priming of the BMDM occurs during infection. During an infection *in vivo* the cells will not have encountered LPS prior to the bacterium and they will thus not be primed prior to infection. The unprimed cells therefore portray the most accurate response believed to happen *in vivo* using an *in vitro* model. Interestingly, it was found that inflammasome activation by *Salmonella typhimurium* require LPS-priming of the BMDM in order to be able to detect IL-1ß secretion. *Salmonella* is an intracellular pathogen, which might influence the LPS-priming on the cellular surface. *P.aeruginosa* on the other hand is an extracellular pathogen and continuous priming therefore occurs.

The dependence on various inflammasome components by *P.aeruginosa* was tested using BMDM from KO mice. Inflammasome activation following ATP treatment was found to be dependent on NLRP3, ASC and caspase-1, which has been reported previously [164, 297, 355, 363, 364]. The inflammasome activation by PA103 ΔUΔT and PAO1 ΔSTY was shown in this study to be dependent on NLRC4, ASC and caspase-1. Subsequently to these results, this was also published [249, 253, 354]. This ties in well with other Gram-negative bacteria which have also been shown to be dependent on NLRC4 and ASC, such as *S.typhimurium* and *S.flexneri* [234, 350]. At higher MOIs the dependence for PA103 ΔUΔT was still on NLRC4 and ASC, but an increased cell death was observed in the absence of NLRP3. This suggests that NLRP3 may protect against cell death in this model, which has previously been described by Sutterwala et al. [364].

Interestingly, during infection at a higher MOI with PAO1 WT, the inflammasome activation seems to be dependent on NLRC4 and ASC, as expected, but also to a lesser degree on NLRP3. PAO1 WT has flagellin, a functional T3SS, as well as

effectors being translocated. This might influence the inflammasome dependence. Further studies are needed to evaluate these results. In addition, the cell death following infection with PAO1 WT is dependent on NLRC4, which indicates that the cell death is mediated via NLRC4 activation and subsequently leads to pyroptosis. This effect might be dependent on inflammasome activation mediated by the flagellin protein, a process which will be discussed further in chapter 5.

NAIP5 have been extensively investigated in the inflammasome activation by *L.pneumophila* [212, 251, 312, 351, 357, 358, 365]. It was shown that NAIP5 is required for the inflammasome activation by *L.pneumophila* [312] and that it is involved in restriction of infection by *L.pneumophila* [251, 351, 357]. NAIP5 KO mice were only recently constructed [312] and previous studies were done in the A/J mouse strain. This strain has a mutation in the gene encoding *Naip5*. BMDM from this strain were used in this study, to investigate whether NAIP5 has a role in inflammasome activation by *P.aeruginosa*. No effect could be seen on inflammasome activation, such as IL-1β secretion and caspase-1 activation. This has previously been described by Miao et al. for PAO1 [354]. Interestingly, there was an effect on cytotoxicity observed following infection in A/J cells compared to C57/BL6 cells. Following infection of BMDMs from A/J mice, less cytotoxicity were observed in samples infected with *P.aeruginosa* or *S.typhimurium* compared to the C57/BL6 BMDMs. The reason for this difference is not clear. It might reflect varied sensitivity to infection between the different mouse strains and further studies are needed to draw any conclusions. Furthermore, the involvement of NAIP5 during inflammasome activation by various Gram-negative bacteria should be confirmed in the NAIP5 KO mouse. The mutation in the A/J strain is partially functional and for more definite answers the KO should be used [312].

P.aeruginosa is an extracellular pathogen [366]. The percent invasion was investigated in this study. The inflammasome complexes are located in the cytosol and if a significant amount of bacteria were internalised upon infection this might have an effect on inflammasome activation, rather than being mediated by extracellular bacteria. However, the results presented in this chapter demonstrate that the internalisation of *P.aeruginosa* does not account for the inflammasome activation seen. Only a fraction of inoculated bacteria are

internalised. In addition, more of the T3SS mutant strain, PA103 ΔpcrV, is internalised and yet this strain does not activate the inflammasome.

In conclusion, the results presented in this chapter demonstrate that the extracellular bacterium *P.aeruginosa* activates the NLRC4 inflammasome. This process is dependent on a functional T3SS but independent of translocated effectors. It is also dependent on ASC and caspase-1. Furthermore, no effect of NAIP5 could be attributed to the inflammasome activation by *P.aeruginosa*. Further studies are needed using NAIP5 KO mice rather than the mutated A/J mouse strain to confirm or contradict these results. Finally, it was shown in this chapter that PA103 ΔUΔT can activate the NLRC4 inflammasome independent of flagellin. Other bacterial inflammasome activators must therefore exist. This will be discussed in the following chapters of this thesis.

4 Potassium-dependent inflammasome activation by *Pseudomonas aeruginosa* and leaky pore formation by the T3SS

4.1 Introduction

4.1.1 Potassium-dependent inflammasome activation

Potassium-dependent IL-1ß release was first described by Walev et al. [367]. This study described release of IL-1ß from cells which had been depleted of potassium using agents such as α-toxin and the ionophores nigericin and valinomycin. The IL-1ß release was shown to be inhibited when the extracellular potassium was increased.

The NLRP3 inflammasome has been shown to spontaneously assemble after disruption of cellular integrity. This assembly is inhibited in extracellular potassium concentrations higher than 70 mM, which is the concentration of potassium found in the cytosol of healthy cells [227, 237, 238]. These results imply that the NLRP3 inflammasome can sense drops in intracellular potassium concentration. It has been shown that danger signals and stimuli that activate the NLRP3 inflammasome also lead to triggering of potassium efflux, which further strengthens the hypothesis that the NLRP3 sense drops in intracellular potassium concentration (Figure 4.1) [236, 238]. In addition, it has been shown that high potassium levels prevent oligomerization of ASC [255]. Multiple inflammasome activators have been shown to trigger potassium efflux and/or reactive oxygen species (ROS), as well as frustrated phagocytosis that eventually leads to activation of the NLRP3 inflammasome, examples are bacterial toxins, such as Aerolysin (*A.hydrophila*), Maitotoxin (Dinoflagellates), α-toxin (*S.aureus*) and Listerolysin (LLO, *L.monocytogenes*), and danger signals, such as monosodium urate (MSU), calcium pyrophosphate dehydrate crystals (CPPD), Alum, Asbestos and silica, ATP and UV [164, 236, 238, 255, 272-274, 280, 355, 364, 368-371] (Figure 4.1).
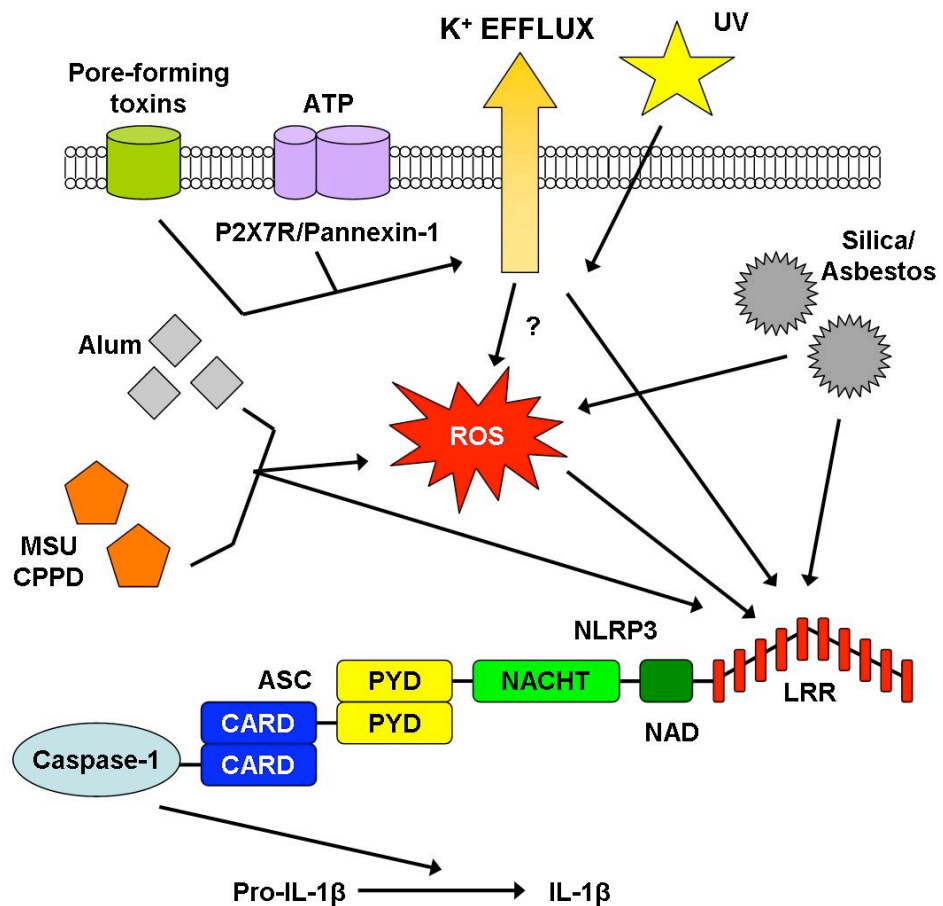
Figure 4.1; NLRP3 inflammasome activation

Multiple inflammasome activators trigger potassium efflux and reactive oxygen species (ROS), which leads to activation of the NLRP3 inflammasome. Abbreviations; MSU; monosodium urate, CPPD; calcium pyrophosphate dihydrate, UV; ultraviolet light. Figure adapted from [161, 372].

Extracellular ATP acts as a danger signal to the immune system and it was shown early to mediate IL-1β release [296, 373]. Extracellular ATP triggers efflux of intracellular potassium, as well as IL-1β secretion, which led to the assumption that IL-1β is released in response to intracellular potassium depletion [373]. The role for ATP as a danger signal is still unclear since high levels of ATP (2 to 5 mM) are required to activate the NLRP3 inflammasome *in vitro*. The physiological importance of this inflammasome activation is still to be confirmed *in vivo*. In healthy tissues there is a very low extracellular concentration of ATP, whereas the intracellular concentration is high [374]. The intracellular ATP is rapidly released when cell damage occurs [374], but it has been shown that extracellular ATP *in vivo* is rapidly hydrolysed by ectonucleotidases [375]. In

contrast however, there is emerging evidence of ATP as a modulator of inflammation [376]. Upon cellular damage or stress ATP is released into the extracellular space. It has been shown that the NLRP3 inflammasome can bind ATP or dATP, as well as having a function as an ATPase [243]. This was shown using purified full-length protein [243]. The binding is mediated within the nucleotide binding region (NACHT) and mutation within this region disrupts binding [243]. Furthermore, NLRP3 requires ATP binding to mediate inflammatory signalling [243]. These studies do not distinguish whether nucleotide binding by NLRP3 controls signal transduction, or whether it is required for proper folding or stabilisation of a signalling component protein. In comparison, binding of dATP by Apaf-1 is a critical step in apoptosome formation [377].

4.1.2 Role of pannexin-1 in inflammasome activation

Plasma membrane receptors for extracellular nucleotides are called P2 receptors, which are classified into two different families; P2Y, coupled to G-proteins, and P2X, cation-selective channels [378]. ATP can bind the purinoreceptor P2X7R, which was identified using P2X7-specific inhibitors and P2X7$^{-/-}$ mice, respectively [379, 380]. Upon activation of the P2X7R, a typical ion channel is opened within milliseconds, which mediates passage of small cations. Sustained activation (2-10 s) of the P2X7R results in the formation of a reversible plasma membrane pore permeable to hydrophilic solutes with a molecular mass up to 900 Da [378, 381]. This activation leads to activation of the NLRP3 inflammasome (Figure 4.2) [164, 297, 355, 363, 364]. The P2X7-dependent inflammasome activation is dependent on potassium efflux [382]. The pore formed upon P2X7R activation is open as long as ATP is bound to the receptor due to its nondesensitising nature (Figure 4.2) [378]. This pore is nonselective and permeable to dyes, such as ethidium bromide and YoPro1, which can be used to assay passage through the pore [346, 378, 381]. Prolonged ATP stimulation (over 30 min) leads to irreversibly injured cells which are committed to death [383].

Pannexin-1 was identified as the P2X7R-activated large pore (Figure 4.2) [346, 383]. Pannexin-1 is a member of the pannexin protein family, which are proteins

expressed on the plasma membrane [374]. In addition to its function as a specific ATP-release channel, pannexin-1 can form functional gap junctions [384]. This has only been demonstrated *in vitro* and there is no evidence to date suggesting that this occurs *in vivo*. Within the plasma membrane of isolated cells, pannexin-1 is capable of forming a hemichannel [346, 384]. This is because in isolated cells only half of the gap junction channel is assembled, which allows release of cytoplasmic content into the extracellular space [385]. The function as an ATP-release channel, which has been suggested to allow ATP to enter into the cell, leads to amplified P2X7-mediated inflammasome activation, which has been observed *in vitro* [386]. Furthermore, the P2X7R and pannexin-1 are up-regulated in response to LPS and other inflammatory stimuli [346, 378].

Pannexin-1 is an ion-channel and thus it might be responsible for the change in intracellular potassium concentration seen after ATP binding to the P2X7R. It was shown by Pelegrin et al. [333] that inhibition of pannexin-1 blocks inflammasome activation and thus IL-1β secretion. These published results were performed on noncytolytic pathways. This inhibition had no effect on the ATP-stimulated potassium efflux, indicating that the large P2X7R pore is not the main conduit for ATP-stimulated potassium-efflux, but also that potassium efflux alone can not drive inflammasome activation (Figure 4.2) [333]. However, when potassium efflux was blocked in these experiments, so was the inflammasome activation and IL-1β secretion. This indicates that in the sequence leading to inflammasome activation, potassium efflux is upstream of pannexin-1 involvement, and also that potassium efflux is necessary for activation of pannexin-1 [333]. There is no evidence of any binding of pannexin-1 to inflammasome components. The functional significance of potassium efflux in inflammasome activation is unknown, but data suggests that it might facilitate or even precipitate this process.
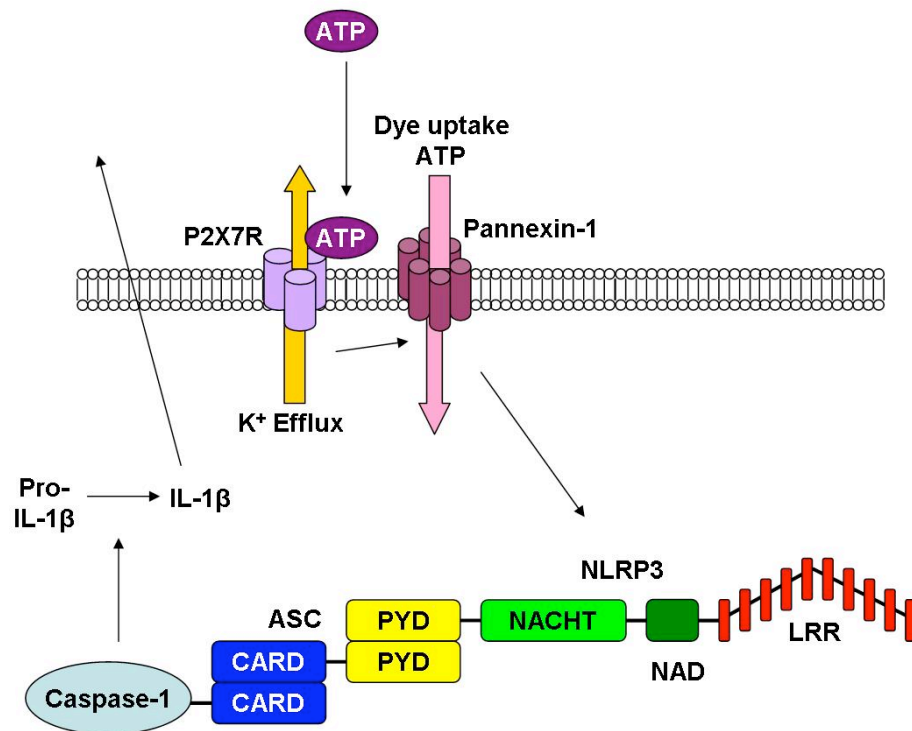
Figure 4.2; Pannexin-1 dependent inflammasome activation

High extracellular ATP activates the ion-channel properties of P2X7R. ATP binding to P2X7R results in activation of pannexin-1. The activation of pannexin-1 might result in ATP uptake through the pore. In addition, pannexin-1 is involved in the initial rapid dye uptake as a result of P2X7R activation. The dye-uptake is downstream of potassium efflux and upstream of inflammasome activation. Figure adapted from [333, 387].

Pelegrin et al. has shown that there are two distinct outcomes following P2X7R activation and pannexin-1 inhibition regarding dye uptake, a rapid initial phase and a slower pannexin-1-independent phase. Other activators of the NLRP3 inflammasome were not affected when it came to dye uptake inhibition by pannexin-1, such as maitotoxin. Furthermore, nigericin, which has been shown to activate the NLRP3 inflammasome, did not activate the P2X7R and no dye uptake could be detected. The inflammasome activation by maitotoxin and nigericin could be inhibited by the pannexin-1 peptide, indicating that a mechanism that is not dependent on pannexin-1 functioning as a hemichannel must be responsible for the effects seen [333].

Pannexin-1 has also been shown to have a role in inflammasome activation by MDP [388]. The study described a NLRP3-dependent inflammasome activation by MDP which was also dependent on ATP and pannexin-1. This was shown to be

independent of Nod2. The induction of pro-IL-1ß by MDP was shown to be dependent on Nod2. This suggests that the MDP primes the cells similar to LPS, and following ATP treatment, the pro-IL-1ß is processed by the caspase-1, which is activated in a NLRP3-dependent fashion by the ATP. MDP was first identified as an inflammasome activator by Martinon et al. [389].

4.1.3 Inflammasome activation by Salmonella

Salmonella typhimurium activates the NLRC4 inflammasome, which was shown to be dependent on ASC [234, 350, 355]. In addition it is dependent on a functional T3SS, as well as flagellin [337, 365, 390]. However, at high MOIs the inflammasome activation by *Salmonella* is not dependent on flagellin [337]. NLRC4$^{-/-}$ mice infected orally with *Salmonella* did not have enhanced susceptibility to infection, whereas caspase-1 deficient mice did [350]. This reflects a possibility of additional undefined pathways that lead to *Salmonella* induced caspase-1 activation which is not dependent on NLRC4. Inflammasome activation by *Salmonella* has also been shown to be independent of potassium efflux, at certain extracellular potassium concentrations [236, 238].

4.1.4 T3SS and pore formation upon contact with the host cell

Upon contact with the host cell the T3SS of Gram-negative bacteria forms a pore in the host cell membrane, as previously discussed in section 3.1.2. Håkansson et al. observed that *Yersinia* has a contact dependent lytic activity upon contact with the host cell with its T3SS [90]. This suggested that the T3SS involves some kind of pore in the host cell membrane which is involved in translocation [90]. However, the lytic activity was higher when the strain lacked effectors passing through the T3SS, suggesting that the pore is normally filled with effectors [90]. The lytic activity was inhibited by osmoprotectants of a given size and lead to the conclusion that the pore formed is between 1.2 nm and 3.5 nm [90]. It has previously been shown for *Yersinia* that the T3SS can allow passage of molecules smaller than 623 Da, and that the injectisome thus does not form a tight association with the host cell [332]. This was shown for a mutant strain of *Yersinia* lacking effectors passing through the T3SS. When effectors were passing through the T3SS, no dye uptake or release could be detected [332]. In addition,

it has been shown for *Salmonella* that the T3SS of the Salmonella pathogenicity Island (SPI)-1 promote calcium influx [391]. This was further confirmed by Roy et al. who found that the permeabilization by the SPI-1 T3SS is dependent on a functional T3SS but not on any effectors [392]. This study used entry of ethidium bromide into the host cell as a measurement of the permeabilisation ability of the T3SS [392]. Bacterial pore-forming toxins, such as Streptolysin O (SLO), can be used to deliver molecules or proteins into living cells [393]. This property was used as a positive control when investigating pore-formation by the T3SS [332]

4.1.5 Membrane repair via lysosomal exocytosis and involvement of Synaptotagmin VII

Upon plasma membrane disruption it is vital for the cell to rapidly reseal or repair the damage [394]. This was first described by Chambers et al. [395] and Heilbrunn et al. [396] in the early 1960s. Rapid repair is mediated by endomembrane via activation of cytoskeletal and membrane fusion proteins [397-399]. The endomembrane is delivered in a calcium-dependent manner to the plasma membrane by exocytosis [397-399]. Failure to reseal or repair its membrane has fatal consequences for the cell, which results in disease for the host, examples being muscular dystrophy and diseases releated to keratin mutations (Epidermolysa bullosa simplex, EBS) [394]. Cell wounding occurs *in vivo* under normal physiological conditions during, for example, skeletal and cardiac muscle contraction [394]. However, several adaptations exist in mammalian bodies and cells to prevent membrane disruptions [394]. Examples of adaptations are architectural design of organs, highly elastic connective tissue, expression of keratin and the dystrophin-glycoprotein complex, as well as dynamic responses [394]. There are two possible models proposed for calcium-triggered repair of membranes: reduction of membrane tension and patch formation. Both methods require internal membrane and exocytosis. The reduction of membrane tension promotes resealing [400]. The patch formation involves larger disruptions of the plasma membrane, where a homotypic fusion response results in repair [399, 401, 402]. Following disruption, calcium enters the cell which triggers vesicle-vesicle homotypic fusion resulting in a large patch vesicle, which fuses with the membrane and repairs the damage [398, 401, 403]. There are several calcium-sensitive exocytic compartments involved in

membrane repair, such as cortical granules [397, 399], yolk granules [396, 397, 399, 401, 402], endosomal compartments [398, 400], lysosomes [404-409] and enlargosomes [407, 410-412].

Following treatment with a calcium ionophor, calcium-dependent membrane proximal lysosomal exocytosis is triggered [405]. Membrane proximal lysosomes are already associated with the plasma membrane prior to calcium stimulation [405]. Lysosomal exocytosis results in relocation of lysosomal associated membrane protein 1 (LAMP-1) to the cellular surface, as well as release of lysosomal content into the extracellular space, for example the enzyme ß-hexosaminidase (Figure 4.3) [335, 336, 408, 409, 413].

Synaptotagmins are calcium binding proteins, first identified in synaptic junctions, involved in calcium triggered exocytosis [414]. The cytoplasmic domains of synaptotagmins consist of tandem C2-domains, which are calcium-binding motifs [415]. These proteins were originally known as p65 but were subsequently renamed to synaptotagmins [416]. Over thirteen isoforms of synaptotagmins have been identified [417]. Synaptotagmins span the vesicle membrane once, with a short intravesicular domain and large cytoplasmic domain composed of two C2 domains [418, 419]. Synaptotagmins undergo calcium-dependent oligomerization upon calcium binding [420]. The majority of synaptotagmins are primarily expressed in brain, but isoforms such as Syt VII are more widely expressed [421-423]. Synaptotagmin VII have been shown to regulate lysosomal exocytosis (Figure 4.3) [406], as well as being involved as plasma membrane calcium sensors for secretion from cells [424]. Moreover, it has been shown to be involved in phagolysosome fusion, which is also a calcium-dependent process [392, 425-427]. The identification of Syt VII explained the occurrence of lysosomal exocytosis as a membrane repair event, as Syt VII is located, but not exclusively, on the membrane of lysosomes (Figure 4.3) [406, 408, 424, 428]. Syt VII is translocated to the plasma membrane following calcium-dependent lysosomal exocytosis (Figure 4.3) [408]. Syt VII KO mice were shown to have impaired membrane repair but accelerated lysosomal exocytosis [429, 430]. This was also shown using a gene silencing approach where Syt VII was shown to be indispensable for exocytosis [431]. One of the C2 domains in Syt VII, the C2B region was shown to be essential for exocytosis [406]. However, when the C2B domain is blocked it has no effect on lysosomal exocytosis, which

implies that lysosomes are not exclusively used in membrane repair [432]. This is further strengthened by the fact that vacuolin-1 could block lysosomal exocytosis without affecting membrane resealing [335, 413, 433]. One explaination to these results could be the involvement of enlargosomes, an organelle which have been identified to be involved in calcium-dependent membrane repair [335, 410].
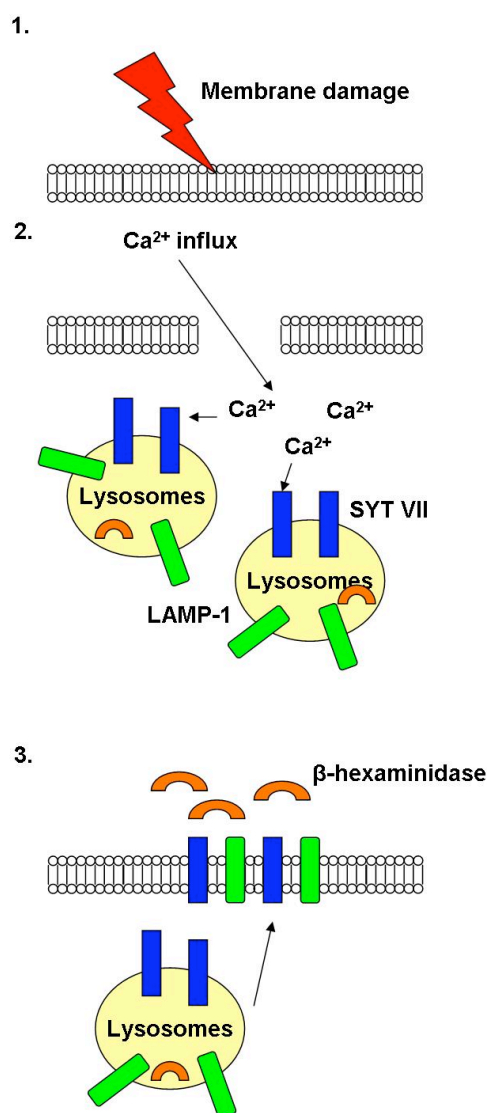
Figure 4.3; Mechanism of lysosomal exocytosis

Upon membrane damage (1.) the plasma membrane is disrupted. This results in calcium influx (2.) and binding of calcium to Syt VII, located on lysosomes. Upon binding lysosomal exocytosis is triggered (3.) and Syt VII and LAMP-1 can be found on the cellular surface as well as β-hexosaminidase in the extracellular medium.

Syt VII has also been shown to be involved in the controlling of intracellular bacterial infections [392]. It was shown that Syt VII is required for phagolysosomal fusion, which inhibits intracellular growth of pathogenic

bacteria. Furthermore, the study by Roy et al. investigated the effect of a T3SS from intracellular pathogenic bacteria, which was shown to trigger membrane permeabilization and lysosomal exocytosis [392]. These results were also confirmed for *Yersinia*, which induced lysosomal exocytosis in a T3SS-dependent manner and had enhanced intracellular survival in Syt VII KO [392].

Another method to repair membrane injury has been described by Idone et al. [434]. This study illustrates a role for calcium-dependent endocytosis following mechanical injury, as well as injury from microbial toxins and pore-forming proteins. It is suggested that endocytosis is capable of removing the lesions from the plasma membrane.

The work described in this chapter investigates whether inflammasome activation by *P.aeruginosa* is dependent on potassium efflux, and whether the pore formed by the T3SS upon contact with the host cell forms a tight association with the host cell membrane, or if it allows passage of extracellular and intracellular molecules. Finally, the role of Syt VII was explored following infection with *P.aeruginosa*. The results reveal that the inflammasome activation by *P.aeruginosa*, as well as *Salmonella*, originally used as a positive control, is dependent on extracellular potassium, which has not previously been described. Furthermore, the results show that upon association with the host cell, the T3SS from *P.aeruginosa* does not allow passage of molecules from within the cell or extracellular molecules. The final section of this chapter demonstrates that membrane repair is triggered upon contact with a T3SS, but the involvement of Syt VII is still unknown.

4.2 Results

4.2.1 Potassium-dependent inflammasome activation by Pseudomonas aeruginosa

4.2.1.1 Potassium-dependent inflammasome activation by PA103

As described in previous sections, potassium efflux is important for the activation of the NLRP3 inflammasome. In response to LPS-priming, followed by ATP treatment, the inflammasome activation is NLRP3 dependent, as well as potassium efflux dependent.

In order to investigate whether the inflammasome activation by *P.aeruginosa* PA103 is dependent on potassium efflux, we infected BMDM in buffers containing low (2 mM KCl) or high (130 mM KCl) potassium concentrations (Figure 4.4). As a positive control BMDM were primed with LPS and then treated with ATP, as previously described [333, 346]. Unprimed BMDM were infected with PA103 ΔUΔT and PA103 ΔpcrV at a MOI of 100 for 90 min in high and low potassium buffers. As expected, LPS with ATP were dependent on potassium efflux for inflammasome activation and thus IL-1β release (Figure 4.4A). Inflammasome activation following infection with PA103 ΔUΔT was also dependent on potassium efflux, as the IL-1β release was completely abrogated in the presence of high extracellular potassium (Figure 4.4A), similar to LPS with ATP. PA103 ΔpcrV was used as a negative control and increasing the extracellular potassium concentration had no effect on IL-1β release from this strain.

Hank's buffer has previously been used during investigation of potassium-dependent inflammasome activation [280]. Rather than just increasing the potassium concentration as in previous studies, the sodium chloride concentration was adjusted to produce an isotonic buffer, which is less harmful to cells. The buffer was further supplemented with vitamins, amino acids and sodium pyruvate in order to make the buffer as close to normal cell culture media as possible. When BMDM were infected with PA103 ΔUΔT at a MOI of 20, in this supplemented Hank's buffer with high or low potassium, the inflammasome activation was still potassium-dependent (Figure 4.4B). Furthermore, the

potassium-dependence was not altered with increasing infection times, from 90 min up to 180 min. Although there was an increase in IL-1β release following the longer infection time, this was true both in low and high potassium concentrations. The percent cytotoxicity was below 10% and remained constant for all time points (results not shown).
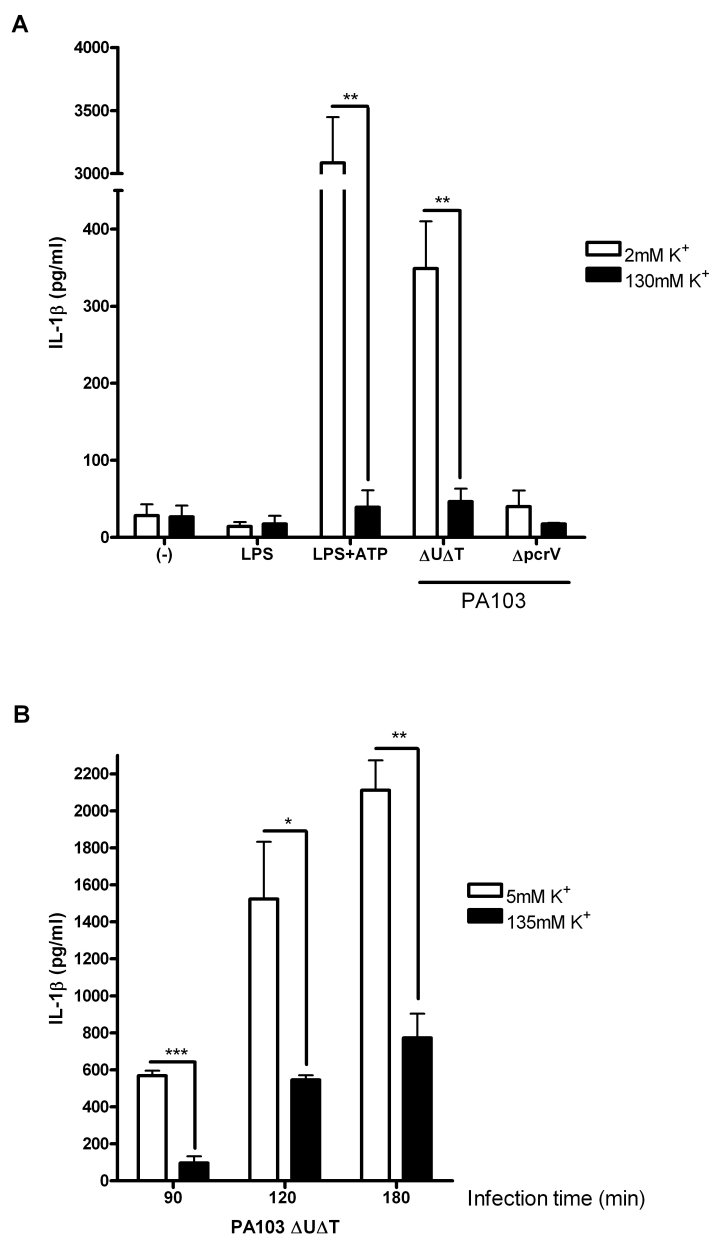
Figure 4.4; The inflammasome activation by PA103 is dependent on potassium efflux and a functional T3SS.

A; BMDM were treated with LPS followed by ATP or infected with PA103 ΔUΔT and PA103 ΔpcrV at a MOI of 100 for 90 min in high and low potassium buffer. B; BMDM were infected with PA103 ΔUΔT at indicated infection times at a MOI of 20 in supplemented Hank's buffers with 5 or 135 mM KCl. IL-1β secretion was measured by ELISA. Columns are means of triplicates and error bars are SEM. Asterixes indicate significant difference where * is p<0.05, ** is p<0.01 and *** is p<0.001, unpaired Student's t-test.

The inflammasome activation by PA103 is dependent on potassium efflux and a functional T3SS. To determine whether MOI had any effects on the potassium dependence, BMDM were infected with PA103 ΔUΔT at different MOIs for 60 min in supplemented Hank's buffer with high or low potassium concentration. PA103 ΔUΔT activates the inflammasome in a potassium-dependent manner independent of MOI (Figure 4.5). There was a trend of increased IL-1ß release dependent on MOI. Additionally, more caspase-1 was activated as a result of higher MOI (Figure 4.5B). This is probably due to a higher bacterial burden with increasing MOIs and as a result more inflammasome complexes and thus caspase-1 are activated. Finally, percent cytotoxicity was measured. There was no correlation between MOI and increasing cell death. Instead, the cell death remained constant and below 15% for all samples (Figure 4.5C). Thus, PA103 is dependent on potassium efflux for activation of the inflammasome rather than an indirect effect caused by dying cells.
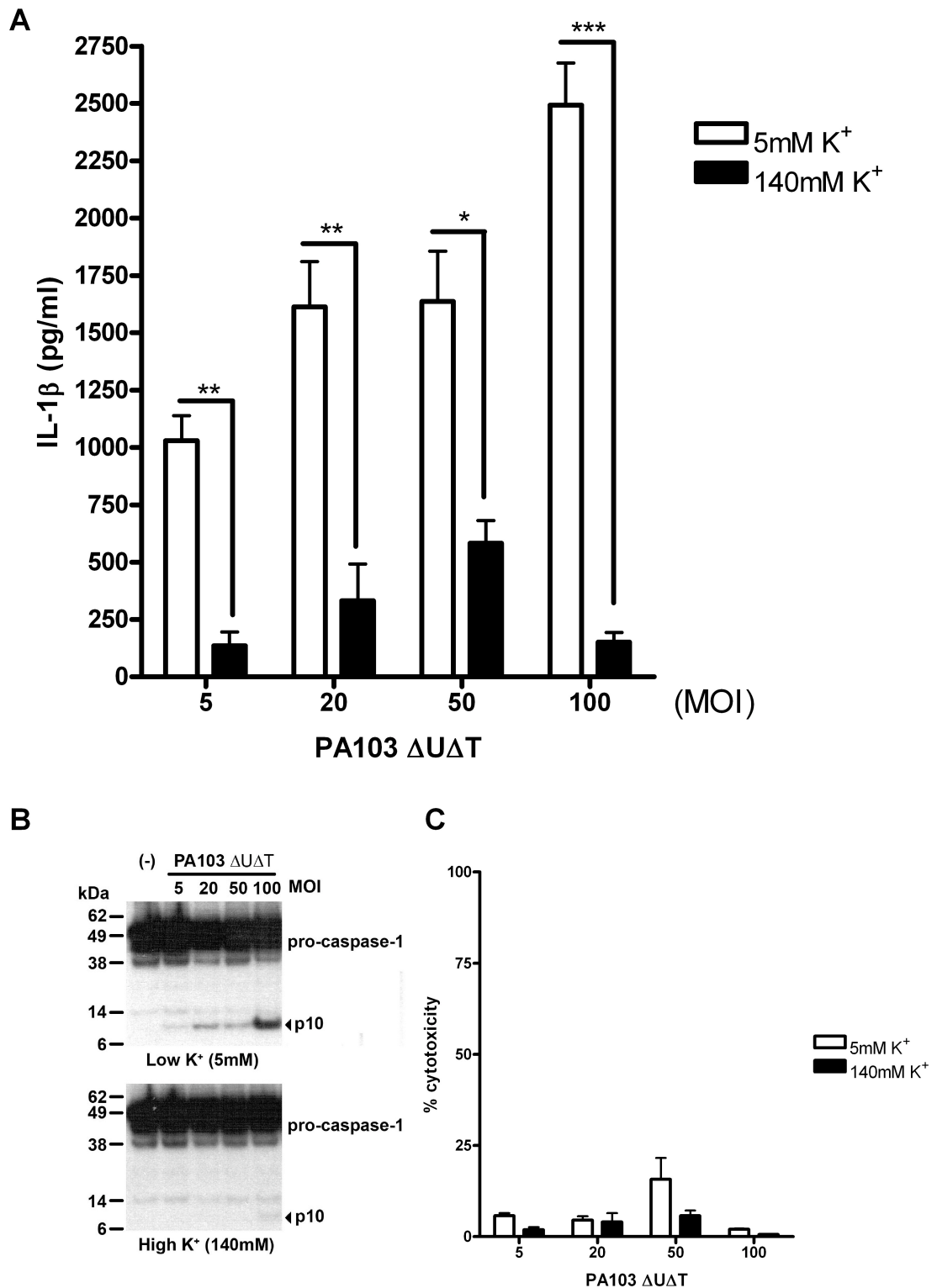
Figure 4.5; Potassium-dependent inflammasome activation by PA103 is independent of MOI.

A; LPS-primed BMDM were infected with PA103 ΔUΔT at indicated MOIs for 60 min in supplemented Hank's buffers with high or low K$^+$-conc. IL-1β secretion was measured by ELISA. B; Cell lysates from A were immunoblotted with caspase-1 antibody. C; Percent cytotoxicity in supernatants were measured using LDH release. Columns are means of triplicates and error bars are SEM. Asterixes indicate significant difference where * is $p<0.05$, ** is $p<0.01$ and *** is $p<0.001$, unpaired Student's t-test.

The amount of IL-1ß release has previously been shown to be dependent on extracellular potassium concentration and the length of LPS priming of the cells [367]. BMDM were therefore infected with PA103 ΔUΔT at a MOI of 30 for 90 min in buffers with varied potassium concentration. The higher the potassium concentration during infection, less IL-1ß was secreted (Figure 4.6A). This correlates with less activation of caspase-1 in the presence of higher potassium concentrations (Figure 4.6B).

A
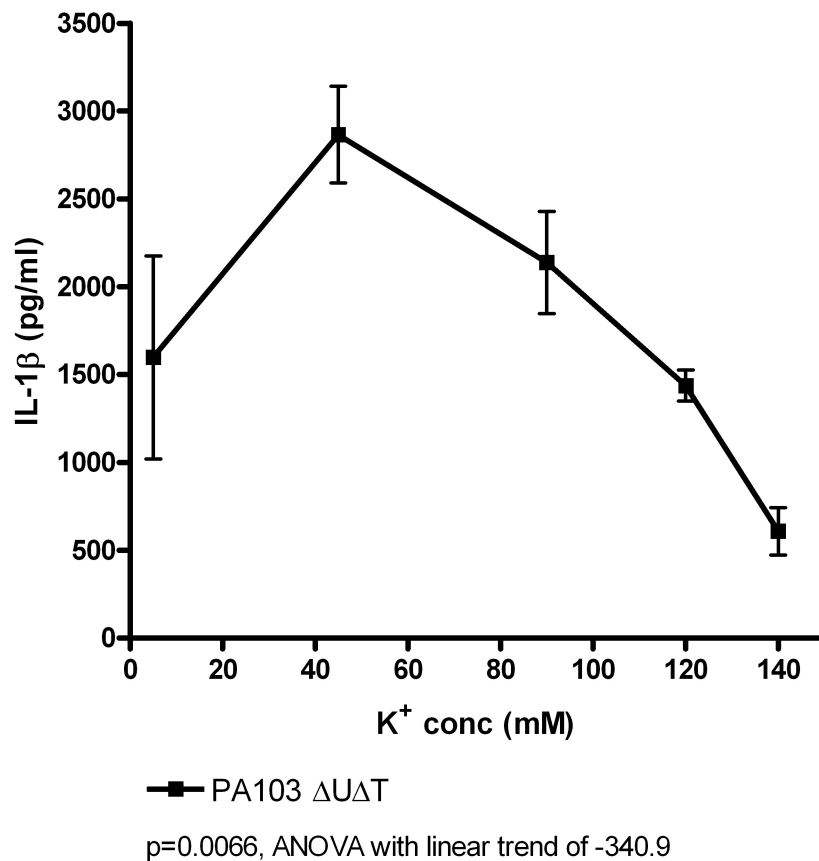
B
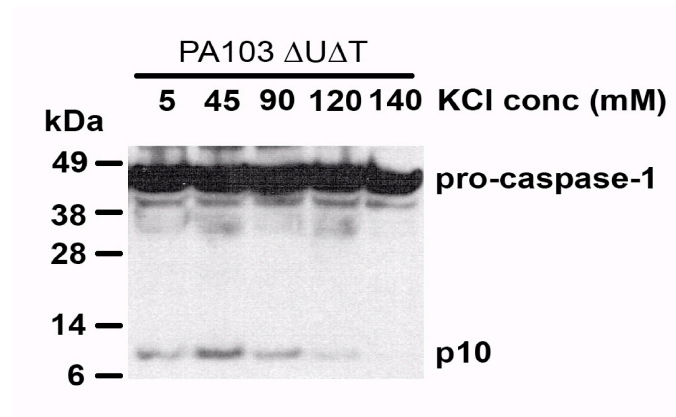
Figure 4.6; The potassium-dependent inflammasome activation by PA103 is dose-dependent.

A; BMDM were infected with PA103 ΔUΔT at a MOI of 30 for 90 min in isotonic buffers with indicated K^+-conc. IL-1β secretion was measured by ELISA. Means of triplicates are plotted and error bars are SEM. Significant difference of variation in IL-1β secretion is analysed by one-way ANOVA significant linear trend for decrease in IL-1β with increasing extracellular potassium $p<0.01$. B; Cell lysates from A were immunoblotted with caspase-1 antibody.

Changing the extracellular potassium concentration might influence other aspects of the cell than just inflammasome activation, such as membrane

potential, signalling etc. Glybenclamide is an inhibitor of ATP-dependent potassium channels, which are one of the main potassium channels in cells [435]. In order to test the effect of Glybenclamide on inflammasome activation by PA103, BMDM were treated with 100 μM Glybenclamide 30 min before infection. Treatment with Glybenclamide inhibits IL-1ß release following infection with PA103 ΔUΔT (Figure 4.7A), but does not affect cell death (Figure 4.7B). The inhibition of inflammasome activation following Glybenclamide treatment is not as dramatic as after infection in high potassium extracellular media. This indicates that there is more than one potential potassium channel involved and the effect of Glybenclamide might be limited by the activity of other channels.

A   **B**
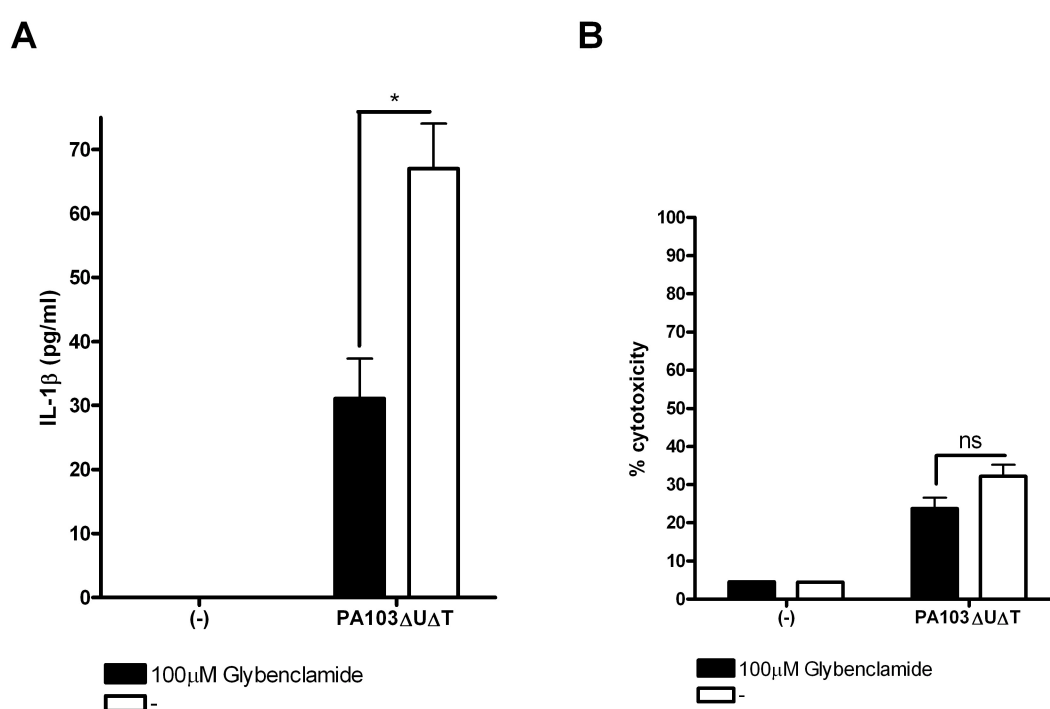
Figure 4.7; Inflammasome activation by PA103 can be inhibited using Glybenclamide.

A; BMDM were treated with Glybenclamide 30 min before infection with PA103 ΔUΔT at a MOI of 30 for 90 min in complete media without antibiotics. IL-1β secretion was measured by ELISA. B; Percent cytotoxicity were measured by LDH release in supernatants from A. Columns are means of triplicates and error bars are SEM. * indicate significant difference $p<0.05$, ns is non-significant difference $p>0.05$, unpaired Student's t-test.

Glybenclamide treatment had no detectable effect on caspase-1 cleavage (Figure 4.8). As mentioned above; the effect of Glybenclamide might be masked by activating other potassium channels. Considering this possibility it is likely that a small effect on caspase-1 cleavage might not be detected on the Western

blot. Other potassium channel inhibitors need to be used to rule out upregulation of activity.
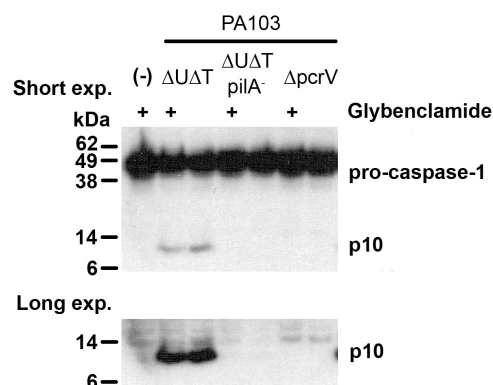
Figure 4.8; There is no noticeable difference in caspase-1 activation following Glybenclamide treatment.

Cell lysates from Figure 4.7 were immunoblotted with caspase-1 antibody.

4.2.1.2 Potassium-dependent inflammasome activation by *PAO1*

PAO1 is a flagellated strain of *P.aeruginosa*, as previously described. Flagellin has been linked to activation of the NLRC4 inflammasome. In order to determine if PAO1 is dependent on potassium efflux for inflammasome activation the experiments performed for PA103 were repeated using PAO1. The inflammasome is activated in a T3SS- and potassium-dependent manner by PAO1, similar to PA103 (Figure 4.9). There is some residual activation in the presence of high extracellular potassium, but it can be concluded that the activation is highly dependent on potassium efflux. The residual activity might be due to the differences seen with this strain compared to PA103. PAO1 does have flagellin, which might be involved in a potassium-independent inflammasome activation.
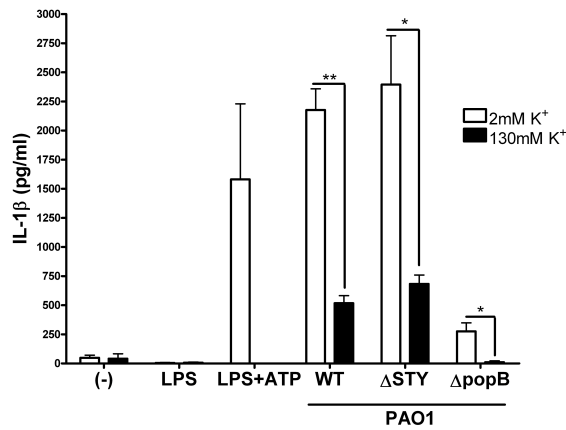
Figure 4.9; The inflammasome activation by PAO1 is dependent on potassium and a functional T3SS.

BMDM were primed with LPS followed by stimulation with ATP or infected with PAO1 strains at a MOI of 100 for 90 min in high and low potassium buffer. IL-1β secretion was measured by ELISA. Columns are means of triplicates and error bars are SEM. * and ** indicate significant difference where * is $p<0.05$ and ** is $p<0.01$, unpaired Student's t-test.

In order to investigate whether flagellin is involved in the residual activity seen in high potassium concentration, BMDM were infected with PAO1 WT, PAO1 FliC⁻ and PAOC:PAO1 FliC. There was no effect on potassium dependence following infection with either of these strains (Figure 4.10A). However, there was an effect in the amount of IL-1ß secreted from cells infected in low potassium between the different strains used (Figure 4.10A). PAO1 FliC⁻ results in less IL-1ß than PAO1 WT or the recomplemented strain PAOC:PAO1 FliC. This indicates an effect of flagellin on inflammasome activation, which has been previously shown for *Salmonella* [337], *Legionella* [351] and *Pseudomonas* [253, 354]. Furthermore, there was significantly more IL-1ß secreted from the BMDMs infected with PAOC:PAO1 FliC than PAO1 WT (Figure 4.10A). This might be a result of the recomplementation of this strain with flagellin. The expression levels of the complemented protein may vary in the complemented strain compared to the WT strain.

The cytotoxicity of these PAO1 strains was not affected in the presence of high extracellular potassium (Figure 4.10B). In addition, there was no effect of flagellin on cell death, as all the strains result in similar amount of cell death following 90 min infection (Figure 4.10B).
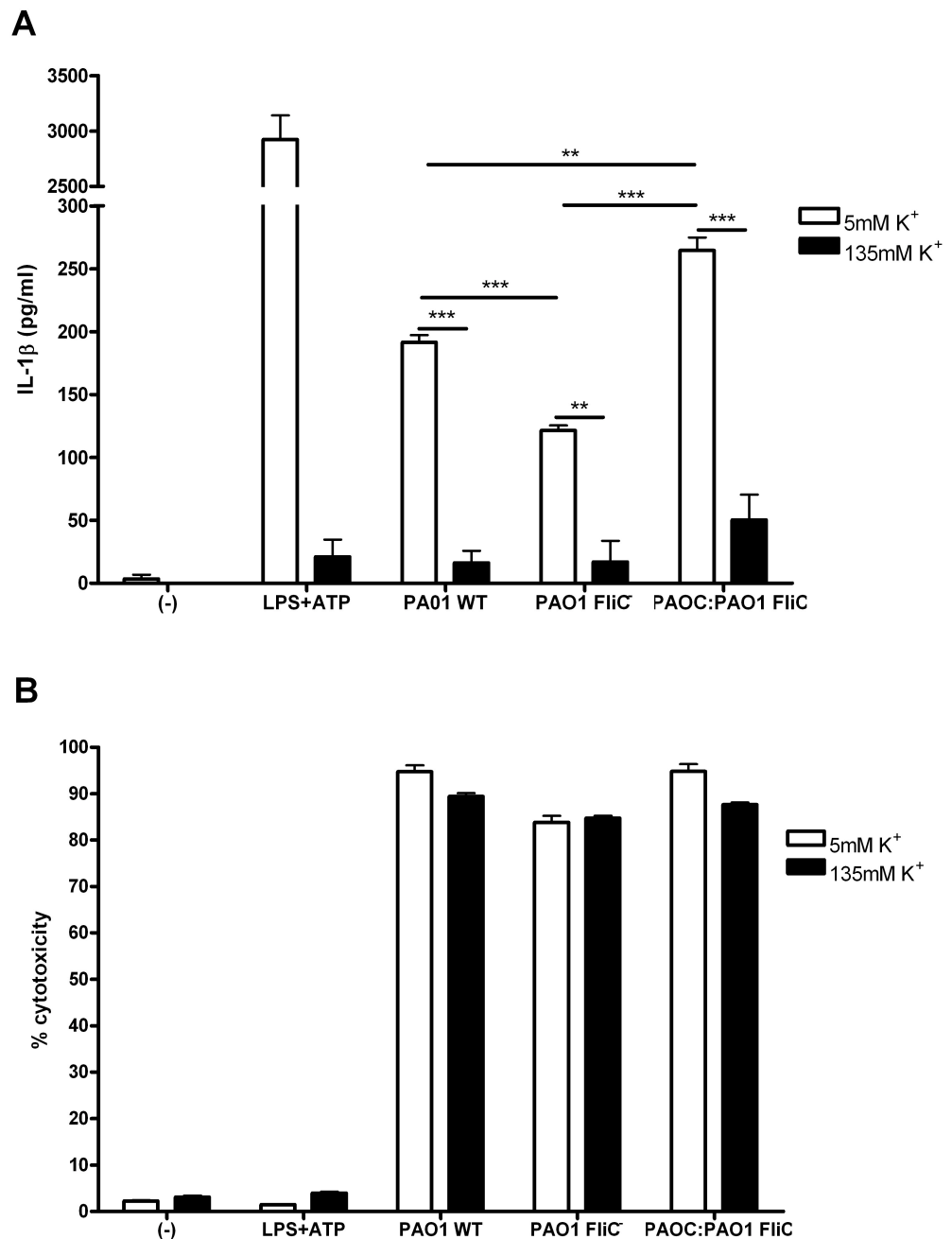
Figure 4.10; PAO1 activates the inflammasome in a potassium-dependent manner independent of flagellin.

A; BMDM were primed with LPS and stimulated with ATP or infected with indicated PAO1 strains at a MOI of 50 for 90 min in complete media supplemented with KCl. IL-1β secretion was measured by ELISA. B; Percent cytotoxicity were measured by LDH release in supernatants from A. Columns are means of triplicates and error bars are SEM. ** and *** indicate significant difference where ** is $p < 0.01$ and *** is $p < 0.001$, unpaired Student's t-test.

Similar to PA103 ΔUΔT, the inflammasome activation by PAO1 ΔSTY can be partially inhibited by treatment with Glybenclamide (Figure 4.11A). As previously described, this has no effect on the cytotoxicity caused by the bacteria (Figure 4.11B). Moreover, in contrast to PA103 ΔUΔT the treatment with

Glybenclamide results in less caspase-1 activation compared to untreated cells
(Figure 4.11C).
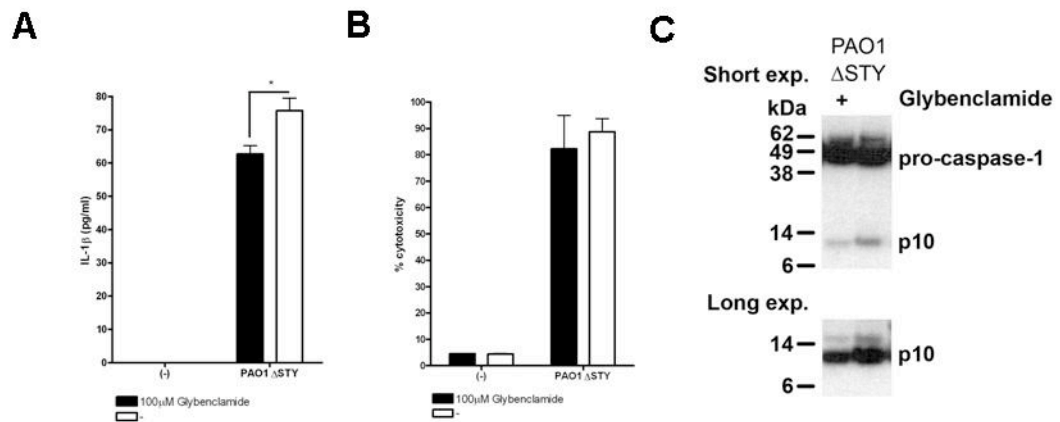
Figure 4.11; Inflammasome activation by PAO1 can be inhibited by Glybenclamide.

A; BMDM were treated with Glybenclamide 30 min before infection with PAO1 ΔSTY at a MOI of
30 for 90 min in complete media. IL-1β secretion was measured by ELISA. B; Percent cytotoxicity
were measured by LDH release in supernatants from A. Columns are means of triplicates and error
bars are SEM. * indicate significant difference where * is $p<0.05$, unpaired Student's t-test. C; Cell
lysates were immunoblotted with caspase-1 antibody.

4.2.1.3 Role of pannexin-1 in inflammasome activation by *PA103*

Pannexin-1 inhibitory peptide has been shown to block IL-1ß secretion from
BMDM, as well as blocking ethidium bromide uptake [346]. The peptide is
believed to block the P2X7R pore pannexin-1.

The method described by Pelegin et al. was used for dye uptake studies [346].
BMDM were preincubated with the peptides together with ATP and then imaged
using time-lapse microscopy, i.e. ATP alone, or with control peptide, or
pannexin-1 blocking peptide. Following treatment with pannexin-1 peptide the
uptake of ethidium bromide was blocked in BMDM (Figure 4.12). This is shown by
a slower uptake rate as well as less increase in mean fluorescence intensity
(MFI). In comparison ATP treatment results in dye uptake comparable to the
results seen after treatment with the control peptide (Figure 4.12).
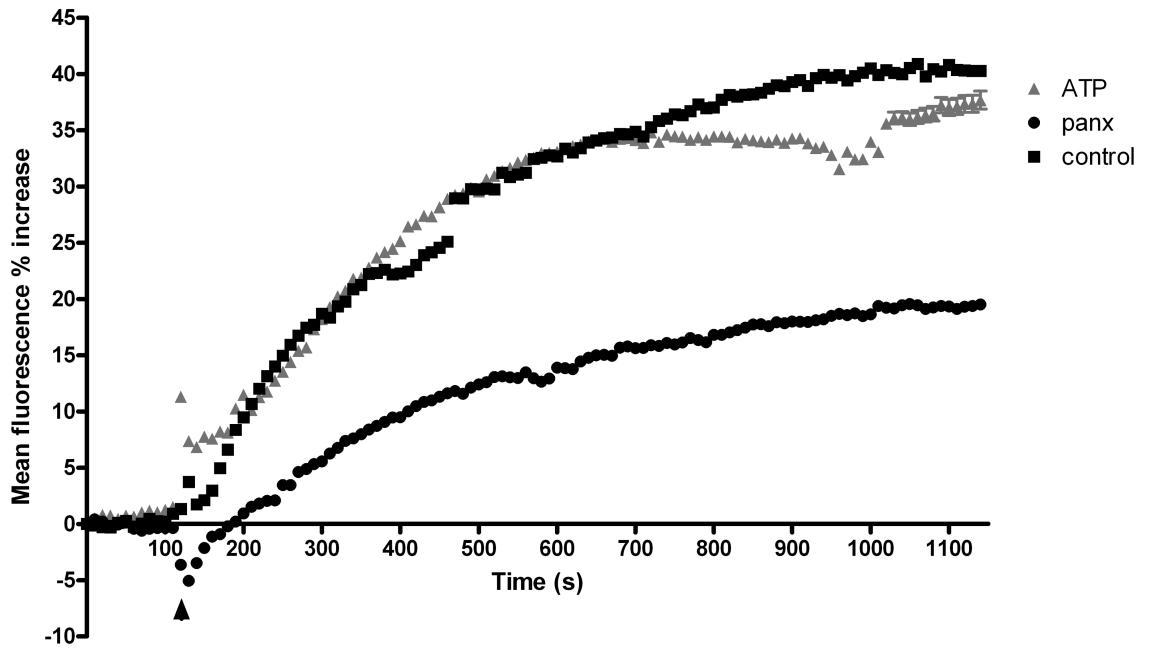
Figure 4.12; Pannexin blocks uptake of ethidium bromide in BMDM.

BMDM were treated with peptide before treatment with ATP when cells were followed using time lapse fluorescence microscopy. The ethidium bromide uptake was measured. Arrow indicates addition of ATP. Means of 20 individually measured cells are plotted and error bars are SEM. Results are representative of three individual experiments.

The effects of peptide preincubation on IL-1β secretion were investigated on LPS-primed BMDM, as previously described [346]. LPS-primed BMDM were preincubated with pannexin-1 peptide, control peptide or carbenoxolone (CBX) at a variety of concentrations. The peptides were used at 500, 250, 100 and 50 μM, whereas carbenoxolone were used at 100, 50, 20 and 5 μM. Carbenoxolone is a nonspecific gap-junction and hemichannel blocking drug derived from licorice [333, 383]. Following preincubation, cells were treated with ATP and the IL-1β release was measured using ELISA. There was no effect of the peptide treatment or carbenoxolone treatment on IL-1β secretion compared to ATP treatment alone (Figure 4.13).
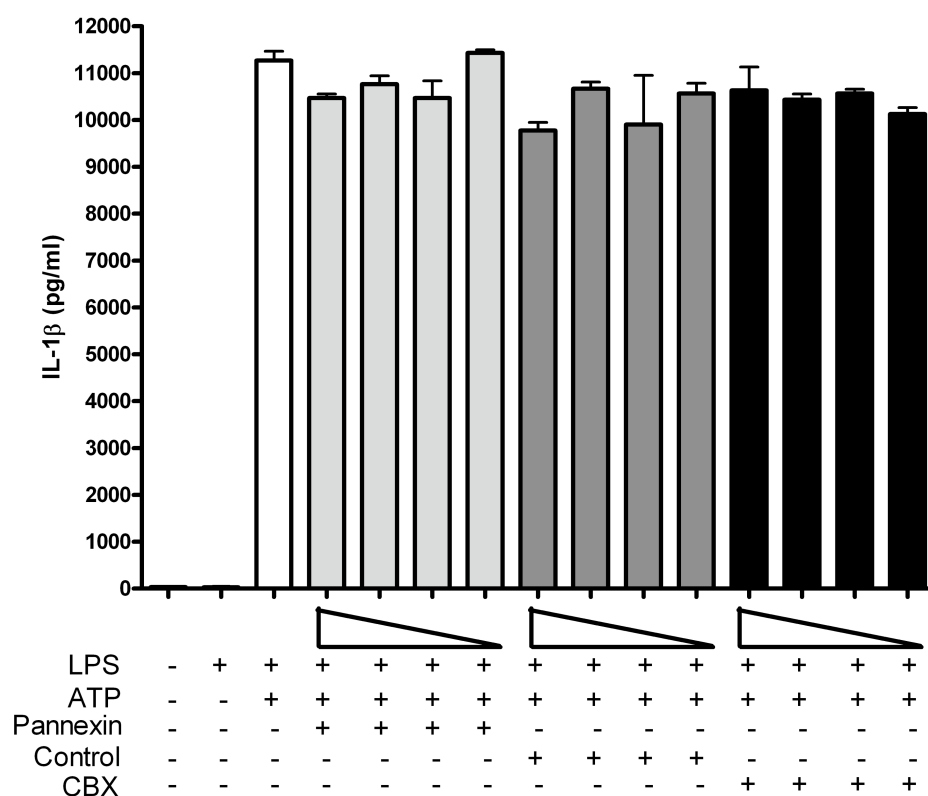
Figure 4.13; Pannexin-1 peptide cannot block secretion of IL-1β from BMDM.

LPS-primed BMDM were treated with peptides or CBX at varied conc. (Peptides 500, 250, 100 and 50 μM, CBX 100, 50, 20, 5 μM) for 30 min following treatment with ATP. IL-1β secretion was measured by ELISA. Columns are means of triplicates and error bars are SEM.

The effects of pannexin-1 treatment on IL-1β secretion triggered by infection were investigated. BMDM were preincubated with peptides and then infected. The effects on IL-1β secretion were investigated with ELISA. As previously described (Figure 4.13), there was no effect of the peptides on IL-1β secretion from LPS-primed BMDM treated with ATP (Figure 4.14). The preincubation with peptides resulted in less IL-1β secretion from PA103 ΔUΔT infected BMDM, compared to untreated infected BMDM (Figure 4.14). This effect was not specific for pannexin-1, as the control peptide resulted in less IL-1β secretion compared to untreated cells and there was no difference between the two different peptides (Figure 4.14). The peptides have no effect on infection by PA103 ΔpcrV, as expected since this strain lacks a functional T3SS and can not induce inflammasome activation (Figure 4.14). Together these results suggest that the pannexin-1 channel is not involved in the inflammasome activation by ATP or PA103 ΔUΔT.
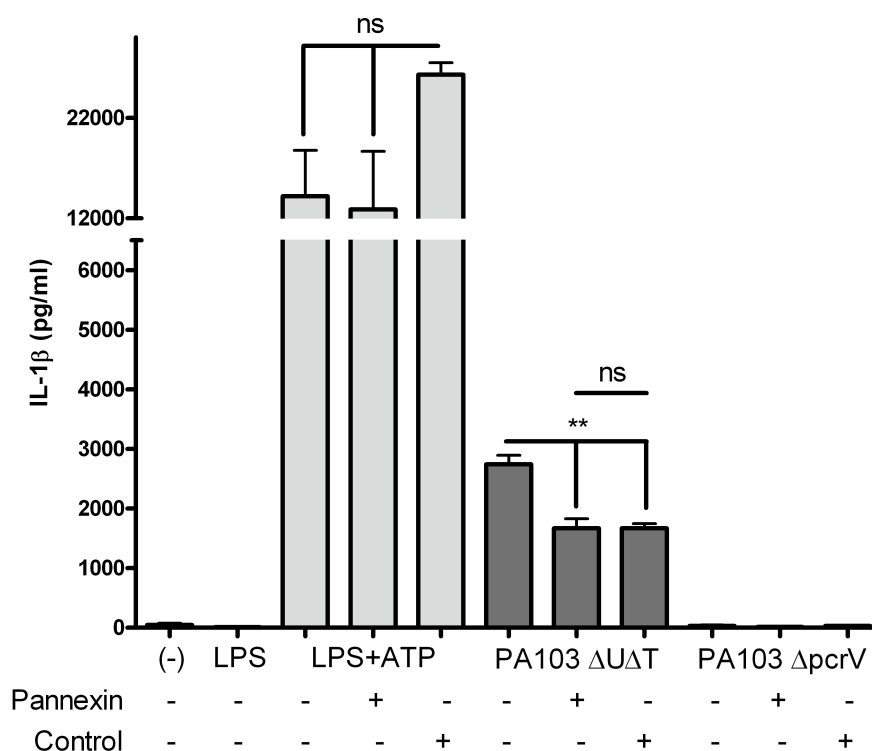
Figure 4.14; There is no effect of pannexin-1 peptide treatment on IL-1β release following infection.

LPS-primed BMDM were treated with peptides followed by ATP treatment or infection. IL-1β secretion was measured by ELISA. Columns are means of triplicates and error bars are SEM. ** indicate significant difference where p<0.01, ns is non-significant difference, unpaired Student's t-test.

4.2.2 Potassium-dependent inflammasome activation by Salmonella

Salmonella SL1344 has previously been shown to activate the inflammasome in a potassium-independent manner, as described above in section 4.1.3. The reason for using Salmonella in this study was originally as a positive control. However, under all conditions used, it was found that inflammasome activation by *Salmonella* was dependent on the extracellular potassium concentration. This will be discussed further at the end of this chapter.

Following infection with SL1344 of LPS-primed BMDM in media supplemented with 130 mM KCl, there was clear potassium-dependent inflammasome activation (Figure 4.15A). This potassium-dependent IL-1β secretion cannot be explained by increased cell death upon infection in high extracellular potassium.

The cytotoxicity is significantly less in low potassium, but below 10% in all samples, however, this does not seem to have an effect on IL-1ß secretion (Figure 4.15B).
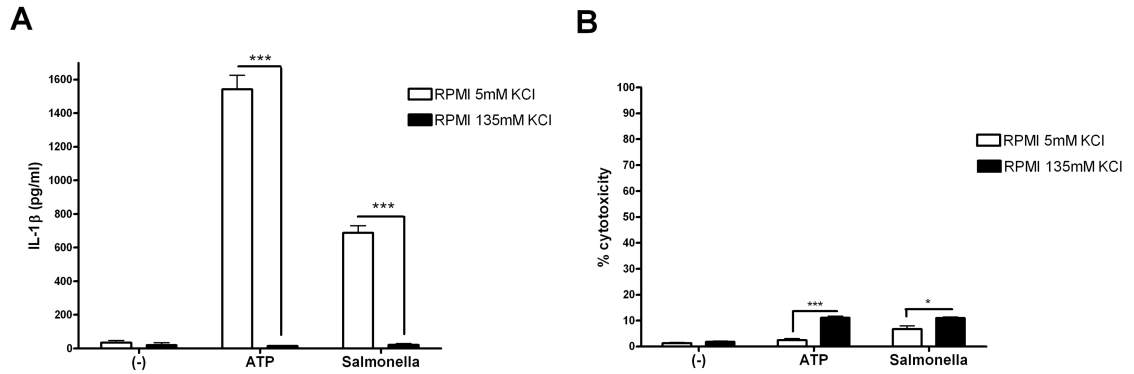
Figure 4.15; *Salmonella* **activates the inflammasome in a potassium-dependent manner.**

A; LPS-primed BMDM were treated with ATP or infected with *Salmonella* SL1344 at a MOI of 20 for 90 min in media. IL-1β secretion was measured by ELISA. B; Percent cytotoxicity were measured by LDH release in supernatants from A. Columns are means of triplicates and error bars are SEM. * and *** indicate significant difference where * is p<0.05 and *** is p<0.001, unpaired Student's t-test.

Previous reports have treated the BMDM with Gentamicin following an initial period of infection with *Salmonella*, in order to limit extracellular bacterial growth. In order to test whether this had an effect on the potassium dependent inflammasome activation seen, BMDM were infected with *Salmonella* at a MOI of 20 for 60 min. This was followed by Gentamicin treatment for 30, 60 and 120 min. The limiting of extracellular bacterial growth by Gentamicin had no effect on potassium-dependent inflammasome activation by *Salmonella* (Figure 4.16). More IL-1ß is secreted the longer infection time, but this is true for both low and high extracellular potassium and is thus not a specific effect dependent on extracellular medium (Figure 4.16).
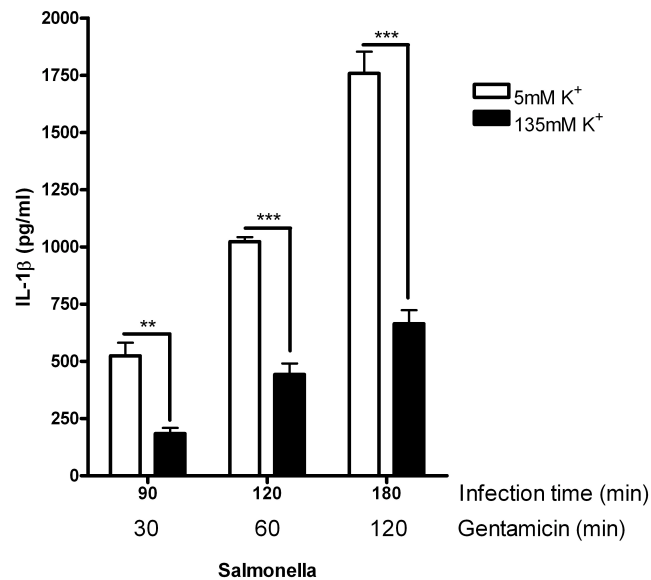
Figure 4.16; *Salmonella* **activates the inflammasome in a potassium-dependent manner independent of Gentamicin treatment.**

BMDM were primed with LPS and infected with *Salmonella* at a MOI of 20 for 60 min in supplemented Hank's buffers, followed by Gentamicin treatment to kill extracellular bacteria for indicated time points. IL-1β secretion was measured by ELISA. Columns are means of triplicates and error bars are SEM. ** and *** indicate significant difference where ** is $p<0.01$ and *** is $p<0.001$, unpaired Student's t-test.

As previously described for PA103 in section 4.2.1.1, the potassium-dependent inflammasome activation is not dependent on MOI. To test whether the same hypothesis holds true for *Salmonella*, BMDM were infected in supplemented Hank's buffer for 60 min at various MOIs. Independent of MOI, the IL-1ß secretion seen is dependent on potassium efflux (Figure 4.17A). No caspase-1 activation can be detected by Western blot in the cell lysates from the infected cells in the presence of high extracellular potassium (Figure 4.17B). The cytotoxicity is below 15% for all samples and there is no correlation between higher cytotoxicity results in increased IL-1ß release, as previously shown (Figure 4.15B, results not shown).

A

B
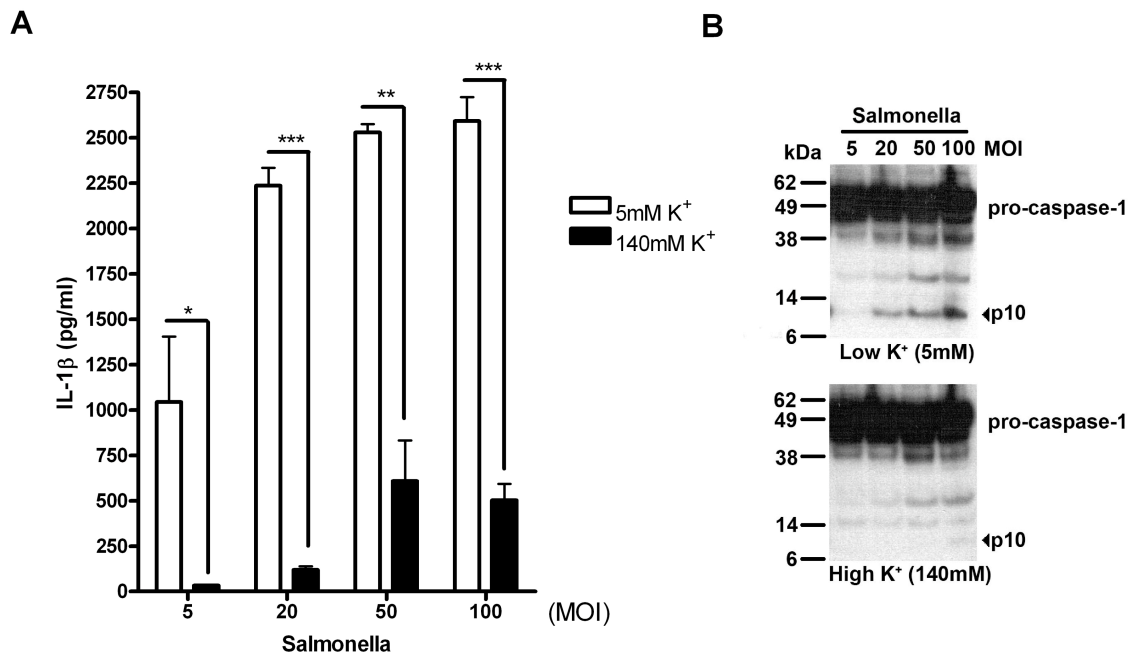
Figure 4.17; Potassium-dependent inflammasome activation by *Salmonella* is independent of MOI.

A; BMDM were primed with LPS and then infected with *Salmonella* at indicated MOIs for 60 min in supplemented Hank's buffer. IL-1β secretion was measured by ELISA. Columns are means of triplicates and error bars are SEM. Asterixes indicate significant difference where * is $p<0.05$, ** is $p<0.01$ and *** is $p<0.001$, unpaired Student's t-test. B; Cell lysates from A were immunoblotted with caspase-1 antibody.

Similar to inflammasome activation by PA103, the amount of IL-1β secretion following *Salmonella* infection is dependent on extracellular potassium concentration. BMDM were infected with *Salmonella* in isotonic buffers with varied concentrations of KCl. There is less IL-1β secreted in higher concentrations of potassium (Figure 4.18A). This is due to less caspase-1 activation in higher concentrations of potassium as shown by Western blot of cell lysates (Figure 4.18B).

A

p<0.001, one-way ANOVA with a linear trend of -566.3
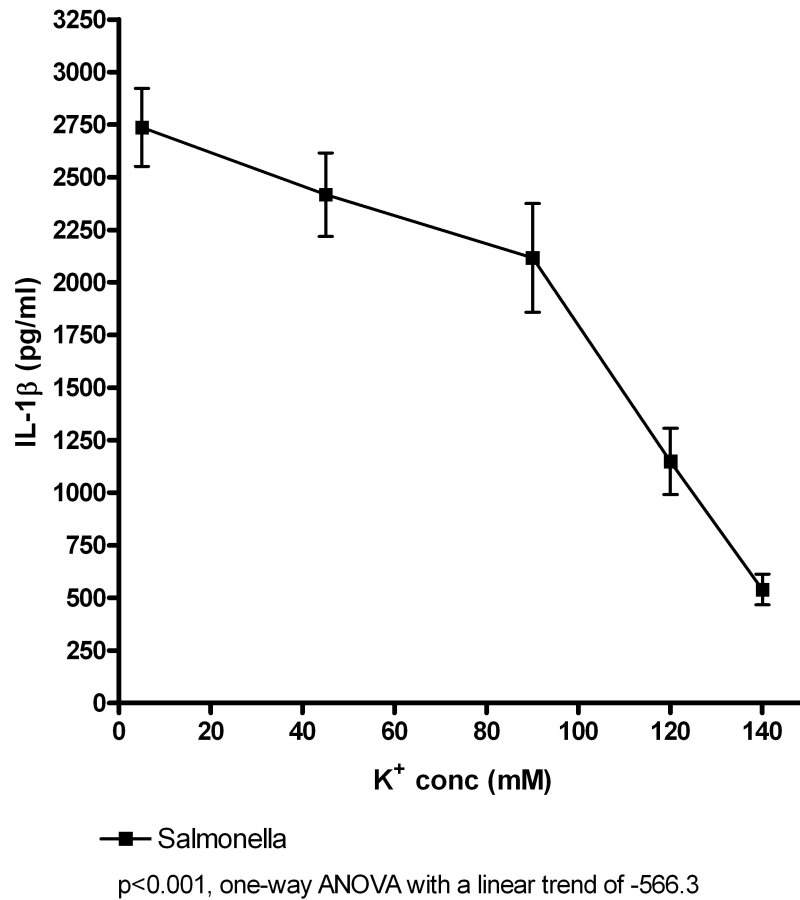
B
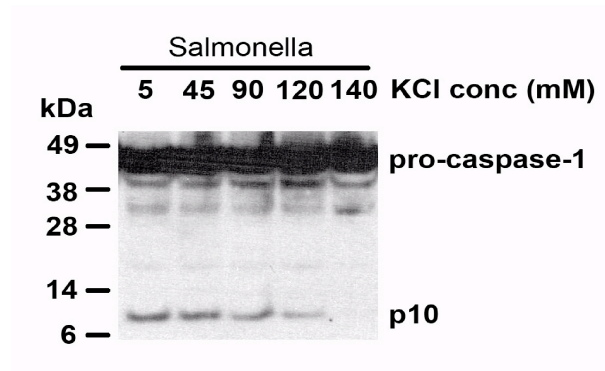
Figure 4.18; Potassium-dependent inflammasome activation by *Salmonella* is dose-dependent.

A; LPS-primed BMDM were infected with *Salmonella* at a MOI of 30 for 90 min in isotonic buffers with indicated KCl conc. IL-1β secretion was measured by ELISA. Means of triplicates are plotted and error bars are SEM. Significant difference of variation in IL-1β secretion is analysed by one-way ANOVA significant linear trend for decrease in IL-1β with increasing extracellular potassium p<0.001. B; Cell lysates from A were immunoblotted with caspase-1 antibody.

The inflammasome activation and thus IL-1ß secretion by both PA103 and PAO1 can be inhibited by glybenclamide as shown in section 4.2.1.1 and 4.2.1.2. *Salmonella* induced IL-1ß secretion is significantly inhibited in glybenclamide treated cells (Figure 4.19A). This further strengthens the hypothesis concerning potassium-dependent inflammasome activation by *Salmonella*. There is no difference in cell death between glybenclamide treated and untreated cells following infection, as expected (Figure 4.19B). Surprisingly no difference could be seen in caspase-1 activation following glybenclamide treatment (Figure 4.19C). The lack of difference in caspase-1 activation is possibly due to very low levels in lysates, which therefore mask any difference. Also, the cytotoxicity in this experiment is relatively high and as a result less caspase-1 would be available.
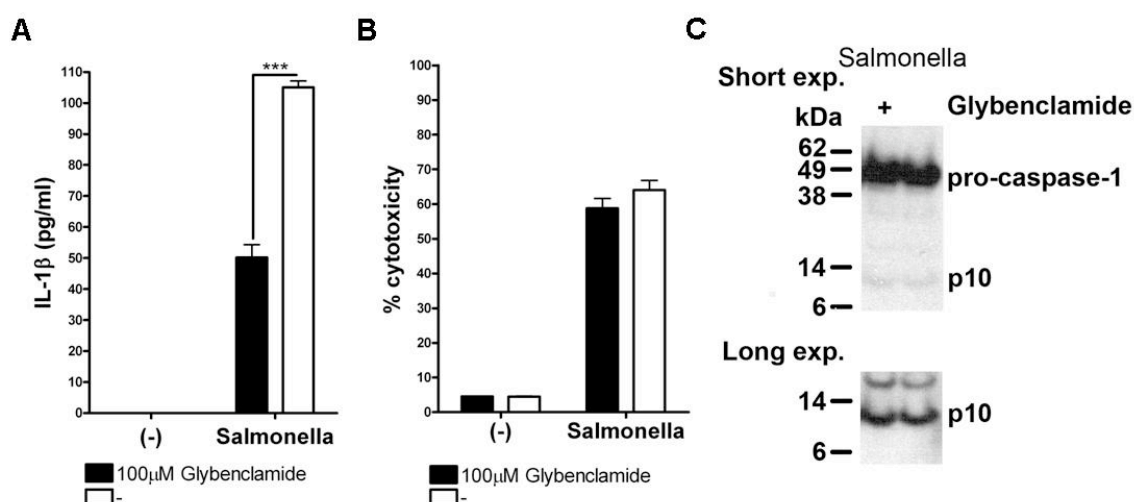
Figure 4.19; Inflammasome activation by *Salmonella* can be inhibited by Glybenclamide.

A; BMDM were treated with Glybenclamide 30 min before infection with *Salmonella* at a MOI of 30 for 90 min in complete media. IL-1β secretion was measured by ELISA. B; Percent cytotoxicity were measured by LDH release in supernatants from A. Columns are means of triplicates and error bars are SEM. *** indicate significant difference where $p < 0.001$, unpaired Student's t-test. C; Cell lysates were immunoblotted with caspase-1 antibody.

4.2.3 Measurement of intracellular potassium concentration

Intracellular potassium concentration can be measured using flame photometry, a method commonly used by inorganic chemists to measure metal ion concentrations in solutions. Following infection with *Salmonella*, PA103 ΔUΔT and PAO1 or treatment with ATP, BMDM lysates were analysed using a flame

photometer. After treatment with ATP, the intracellular potassium concentration is significantly decreased (Figure 4.20), as expected. Infection with PA103 ΔUΔT and *Salmonella* however, does not result in significant changes in intracellular potassium concentration (Figure 4.20A). Surprisingly, infection with PAO1 results in rapid loss of intracellular potassium, as after 30 min the concentration is significantly less compared to infection with PA103 ΔUΔT (Figure 4.20B). The effect is never as profound as seen after ATP treatment.

A

B
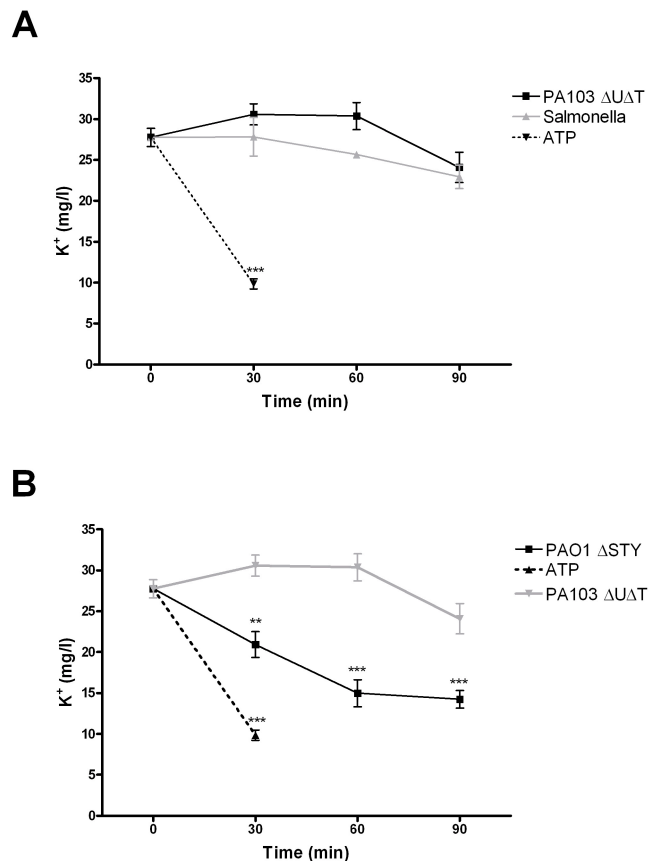
Figure 4.20; Only infection with PAO1 results in changes in intracellular potassium concentration.

A; BMDM were infected with PA103 ΔUΔT and *Salmonella* at a MOI of 30, or treated with ATP for indicated time points in complete media. Intracellular potassium concentration were analysed in cell lysates using flame photometry. B; BMDM were infected with PAO1 ΔSTY at a MOI of 30. Means of triplicates are plotted and error bars are SEM. ** and *** indicate significant difference from untreated cells (t=0) where ** is $p<0.01$ and *** is $p<0.001$, unpaired Student's t-test.

Intracellular potassium concentration was also measured using the fluorescent potassium indicator PBFI. BMDM were traced on the microscope and imaged during infection. The changes in mean fluorescence intensity were plotted against time. No change in intracellular potassium concentration could be

detected following infection with either PA103 ΔUΔT or PA103 ΔpcrV (Figure 4.21). There is a general decline in potassium concentration for the infected samples, however there is no differences between PA103 ΔUΔT and PA103 ΔpcrV (Figure 4.21). This indicates a general effect on the dye due to long incubation times, rather than an effect of the T3SS.
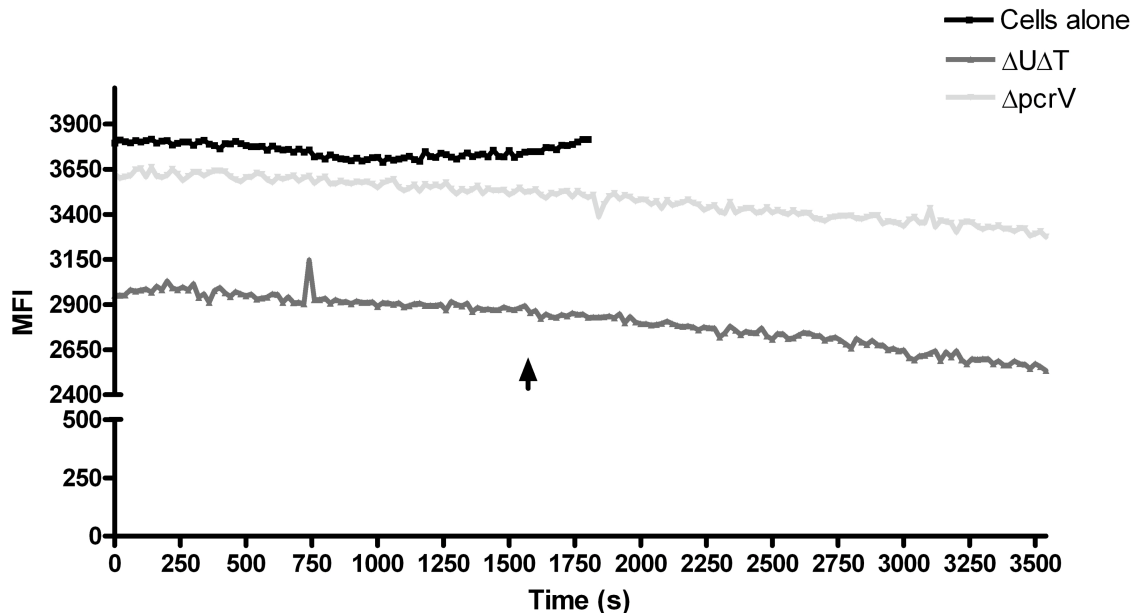
Figure 4.21; There is no change in intracellular potassium concentration following infection.

Changes in intracellular potassium concentration in BMDM during infection at a MOI of 10 were measured using PFBI and time lapse imaging. Arrow denotes addition of bacteria. Representative traces from 3 separate experiments with at least ten isolated cells for each condition is plotted.

4.2.4 The T3SS of Pseudomonas aeruginosa does not form a leaky pore upon contact with the host cell

4.2.4.1 Investigation of dye-exclusion following infection

Dye exclusion experiments have previously been shown to indicate whether a bacterial T3SS upon contact with a host cell forms a tight pore, or if dyes can leak into the host cell from the extracellular environment [332]. If a pore is formed in the plasma membrane Lucifer yellow is able to enter the cell during incubation in media containing this dye. This can then be visualised on a fluorescent microscope. This method was used to see whether the T3SS of *P.aeruginosa* forms a leaky pore upon contact with the host cell. Ionomycin, a

calcium ionophore produced by *Streptomyces conglobatus* was used as a positive control. After ionomycin treatment Lucifer Yellow can enter the cells through the pores formed as indicated by FITC-positive cells (Figure 4.22). Following infection with PA103 ΔpcrV and also for cells alone, no FITC signal can be detected in cells, as expected due to lack of functional T3SS, or lack of infection (Figure 4.22). The PA103 ΔUΔT with a functional T3SS does not result in dye entry into the cells following infection (Figure 4.22). As an additional positive control, the PA103 ΔUΔT:exoU was used. Upon infection with this strain, Lucifer Yellow can enter the cells due to the cytotoxic effect of the ExoU effector (Figure 4.22).
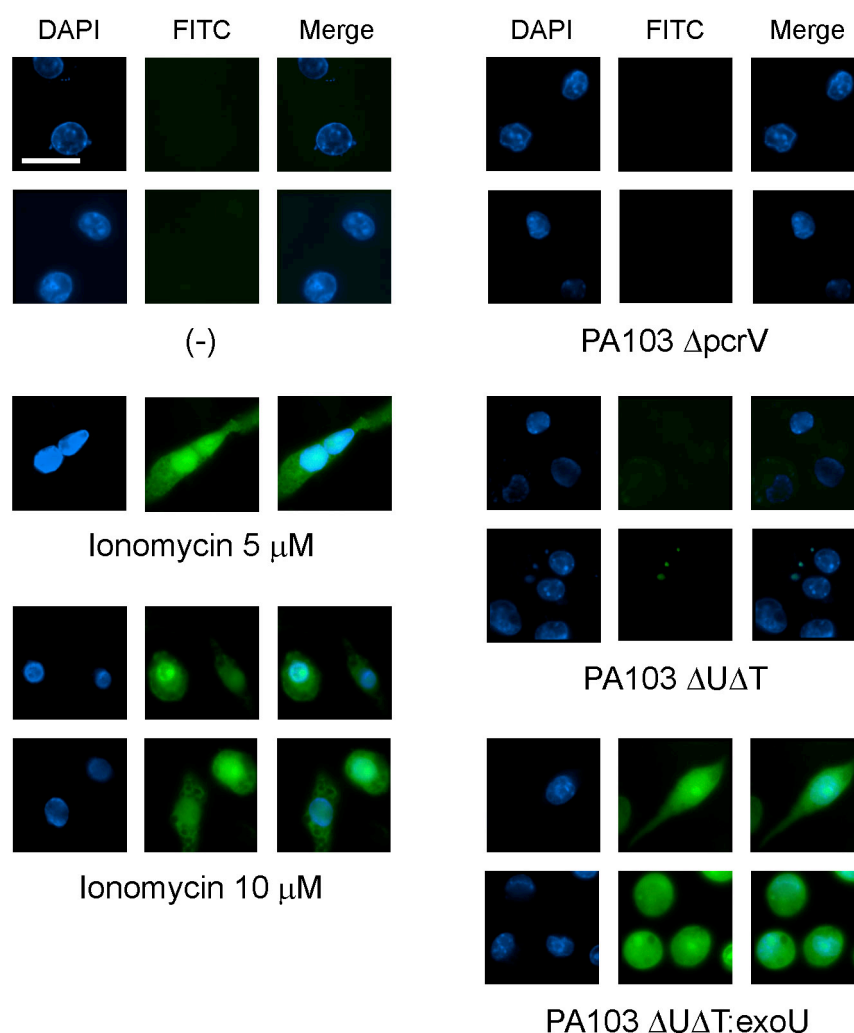
Figure 4.22; There is not a leaky pore formed by the T3SS in the host cell during infection.

RAW 264.7 cells were infected with indicated PA103 strains at a MOI of 300 for 60 min or treated with ionomycin for 10 min at indicated conc. Dye exclusion was investigated using Lucifer yellow and fluorescence microscope. Images are representative of results from three separate experiments.

Streptolysin O (SLO) is a cytolytic toxin produced by group A, C and G streptococci. It binds to membrane cholesterol where, following polymerisation, it forms transmembrane channels. SLO has previously been used to permeabilise the plasma membrane of the host cell, in order to introduce molecules or proteins [393]. Following treatment with SLO, Lucifer Yellow can enter the cells, as indicated by FITC-positive staining (Figure 4.23). As a comparison, infection with PA103 ΔUΔT and PA103 ΔpcrV does not result in FITC-positive cells (Figure 4.23). These results indicate that the T3SS of *P.aeruginosa* does not form a leaky pore upon contact with the host cell.
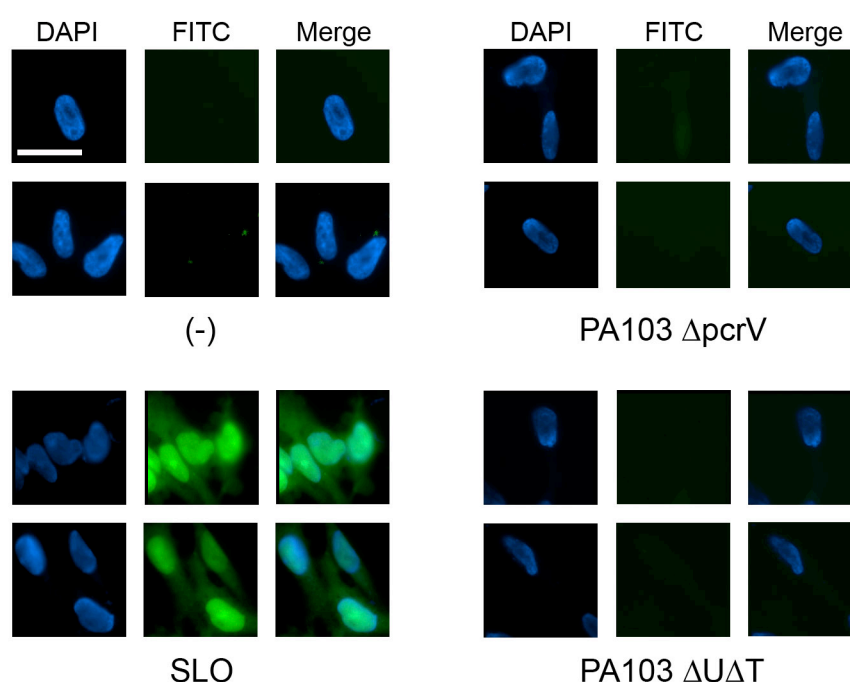
Figure 4.23; SLO mediates dye uptake into the cells but a functional T3SS does not.

HeLa cells were infected with indicated PA103 strains at a MOI of 200 for 90 min or treated with SLO for 30 min. Dye exclusion was investigated using Lucifer yellow and fluorescence microscope. Images are representative of three separate experiments.

4.2.4.2 Investigation of ion-permeability through the pore formed by the T3SS

Lucifer Yellow has a molecular size of 457 Da, and as described in section 4.2.4.1 it cannot enter the host cell following infection with PA103 ΔUΔT and thus a functional T3SS. Ions are smaller than Lucifer Yellow and in order to address this, calcium entry into host cells following infection was studied using Fluo 4-AM, a fluorescent calcium indicator. Cells were traced and the MFI were

plotted against time. After treatment with ionomycin, calcium enters the cell and there is an increase in MFI (Figure 4.24). After a peak in intensity the Fluo-4 signal is lost, indicated by decrease in MFI, as the cell dies (Figure 4.24). No changes in calcium can be seen during infection with either PA103 ΔUΔT or PA103 ΔpcrV (Figure 4.24).
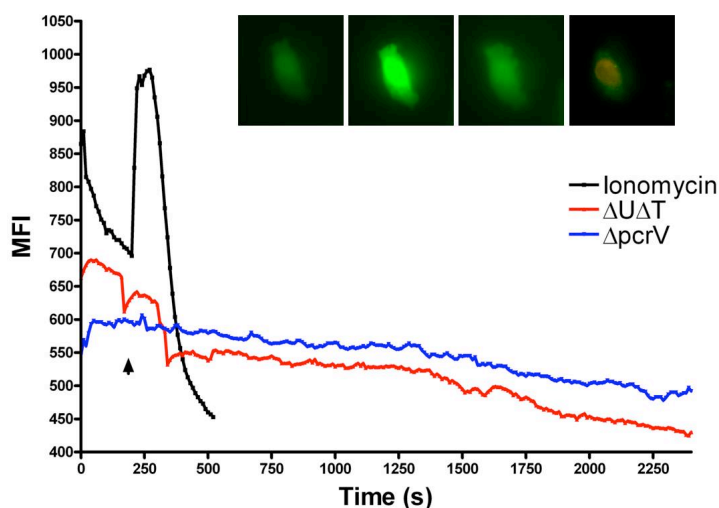
Figure 4.24; There is no calcium influx during infection with PA103.

Calcium influx were measured using Fluo 4-AM in HeLa cells during infection with indicated PA103 strains at a MOI of 150 for indicated time or treated with ionomycin. Arrow indicates addition of bacteria or ionomycin. Inset shows changes in calcium concentration following treatment with ionomycin at time points 100, 260, 330 and 500 (s). Representative traces for at least three separate experiments with at least ten isolated cells measured for each condition are plotted.

Calcium is an important ion for membrane potential and signalling within cells. To rule out the possibility that calcium is maintained following infection via intracellular stores and thus does not produce a change in MFI, passage of zinc ions was used instead. The intracellular concentration of zinc is extremely low in most cell types, which makes this method ideal to investigate whether the T3SS forms a leaky pore upon contact with the host cell. With zinc in the extracellular media and the Fluo-Zin 3 dye loaded into the cells the increase in fluorescence upon binding of the ion to the dye is easily detected. There is no change in MFI following infection by PA103 ΔUΔT or PA103 ΔpcrV (Figure 4.25). After addition of the zinc ionophore, pyrithione there is an increase in MFI due to Zn^{2+}-influx into the cell (Figure 4.25). Infection with PA103 ΔUΔT:exoU results in Zn^{2+}-influx, as a result of the strains cytotoxic properties (Figure 4.25), similar to the effects observed for the dye exclusion experiments described in section 4.2.4.1.
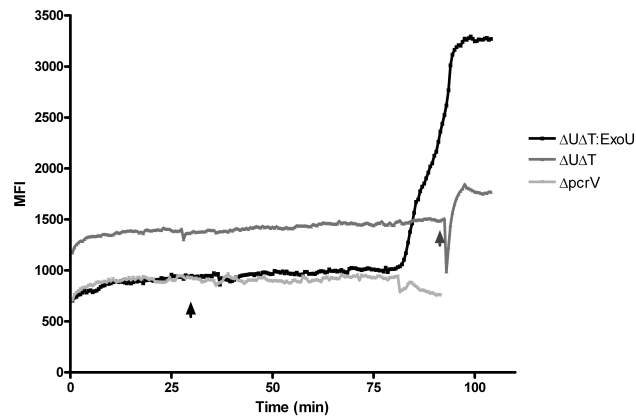
Figure 4.25; There is no Zn^{2+}-influx during infection with PA103.

Zinc influx was measured using Fluo Zin-3 in BMDM during infection with indicated PA103 strains at a MOI of 20 for indicated time. Black arrow indicates addition of bacteria and grey arrow indicates treatment with pyrithione. Representative traces for at least three separate experiments with at least ten isolated cells measured for each condition are plotted.

4.2.4.3 Investigation of BCECF release upon contact with a functional T3SS

BCECF, a pH-sensitive small intracellular marker molecule has a molecular weight of 623 Da. It was previously described that BCECF was released from cells infected with a strain of *Yersinia* which lacks any effectors passing through the T3SS [332]. This strain is similar to PA103 ΔUΔT. Furthermore, it was shown that this release of the loaded dye was inhibited when the T3SS had any effectors passing through [332]. In order to investigate whether infection with PA103 ΔUΔT results in release of BCECF from loaded cells, the method described by Neyt et al. was repeated. Cells (HeLa) were originally loaded in Margo's solution; this proved unsuccessful as uninfected samples released more BCECF than infected samples. This can be explained by a centrifugation step to collect samples at 250 x g, as described [332]. Following further investigation this centrifugation step was discovered to be too slow and bacteria were left in the sample, which interferes with the measurement. After optimization of the method, cells were loaded with BCECF in HBSS, followed by infection in Phenol red free complete culture medium and samples were collected after a centrifugation step at 16100 x g.

SLO was used as a positive control for BCECF release. Increasing concentrations of SLO results in increasing amount of released BCECF (Figure 4.26A). In contrast

to SLO (400U/ml), which results in 100% lysis of cells, infection with PA103 ΔUΔT or PA103 ΔpcrV does not result in release of BCECF (Figure 4.26B). This is true for all cell types tested, HeLa (Figure 4.26B), CHO and RAW264.7 (results not shown). Furthermore, PA103 ΔUΔT:exoU results in lysis of the cells as a result of the ExoU toxin, and ionomycin treatment cause BCECF release due to cell death (Figure 4.26B).
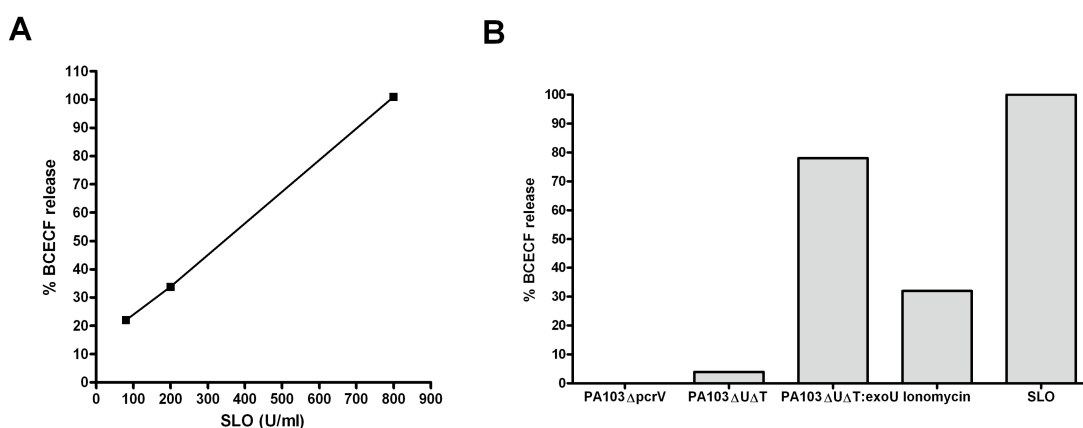
Figure 4.26; BCECF can not pass through the pore formed by the T3SS.

A; HeLa cells were loaded with BCECF and then treated with SLO at indicated concentrations for 30 min at 37°C. Supernatants were collected and analysed for BCECF release. B; HeLa cells were loaded with BCECF and then infected with PA103 strains at a MOI of 300 for 2h or treated with ionomycin or SLO. Supernatants were collected and analysed for BCECF release.

4.2.5 The T3SS trigger membrane repair upon contact with the host cell

It has previously been shown that upon contact with a T3SS, membrane repair and lysosomal exocytosis is triggered [392]. This was shown for *Yersinia* and it is not known whether *P.aeruginosa* has the same effect. *Yersinia* and *Pseudomonas* have homologous T3SS which indicate that they might behave in the same way.

4.2.5.1 LAMP-1 relocates to the cellular surface following contact with a T3SS

Lysosomal exocytosis and thus membrane repair can be detected by relocation of LAMP-1 to the cellular surface. LAMP-1 relocates to the cellular surface after ionomycin treatment (for 10 min at 10μM) by LAMP-1 specific fluorescent

staining of the cellular surface (Figure 4.27). HeLa cells are treated with ionomycin, fixed and then stained with LAMP-1 specific antibody.
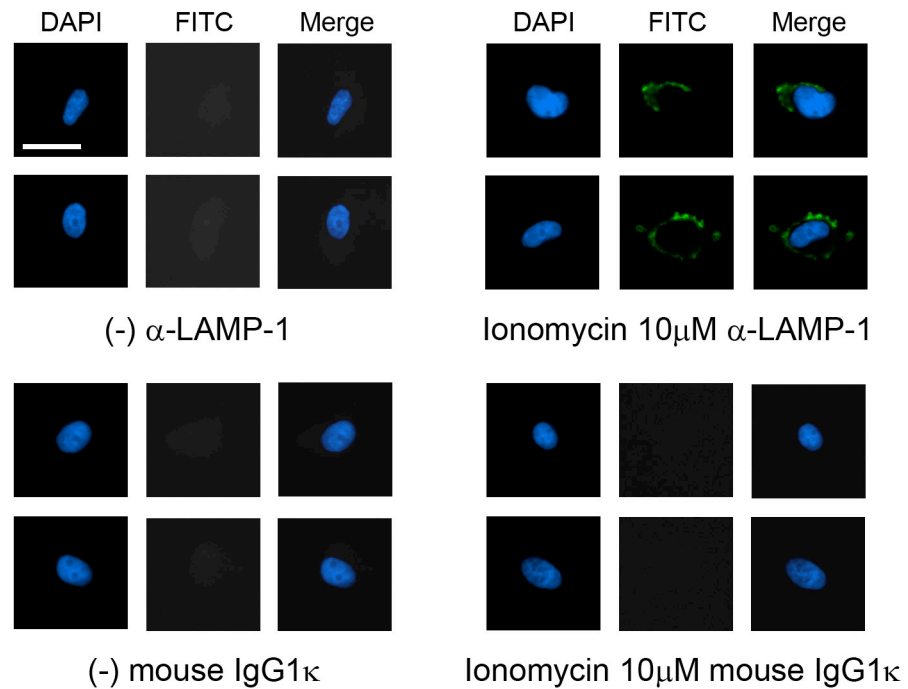
Figure 4.27; Ionomycin treatment results in relocation of LAMP-1 to the cellular surface.
HeLa cells were treated with ionomycin for 10 min and then immunofluorescently stained with LAMP-1 antibody or mouse IgG1κ as a control, followed by imaging on a fluorescence microscope. Scale bar is 50 μm. Images are representative of three separate experiments.

Ionomycin can be used as a positive control for lysosomal exocytosis (Figure 4.27). Infection with PA103 ΔpcrV does not result in relocation of LAMP-1 to the cellular surface (Figure 4.28), as expected since this strain lacks a functional T3SS. In contrast PA103 ΔUΔT has a functional T3SS and following infection with this strain LAMP-1 is relocated to the surface of the cell (Figure 4.28). Following infection with PA103 ΔUΔT:exoU, which has a functional T3SS and a functional ExoU effector passing through the T3SS, following infection with this strain LAMP-1 can be detected on the cellular surface (Figure 4.28). There seems to be more LAMP-1 relocated following infection with PA103 ΔUΔT:exoU than PA103 ΔUΔT, which might be due to the cytotoxic effect of the ExoU toxin.
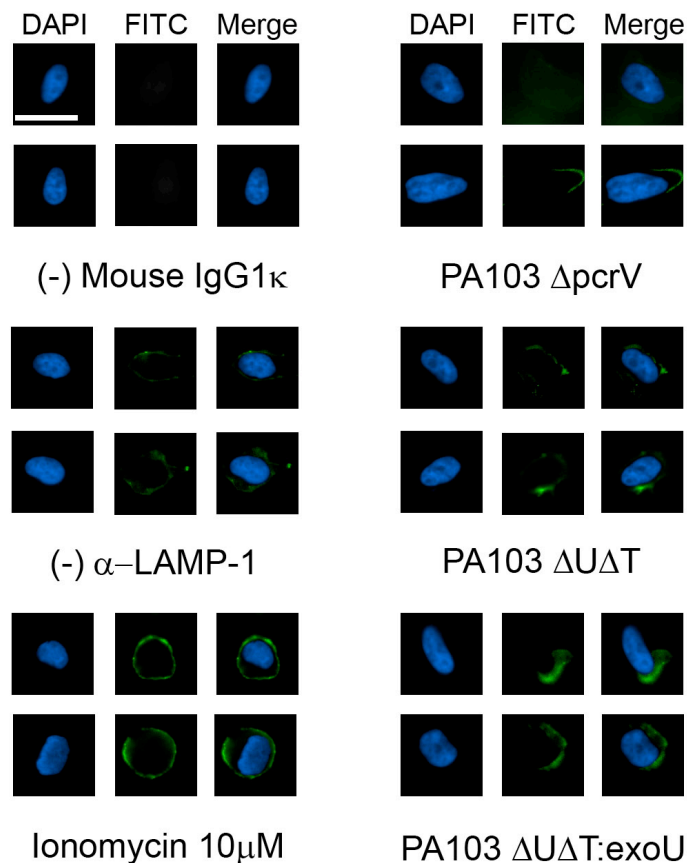
Figure 4.28; Following contact with a functional T3SS LAMP-1 relocates to the cellular surface.

HeLa cells were treated with ionomycin for 10 min or infected with indicated PA103 strains at a MOI of 200 for 90 min, cells were then fixed and immunofluorescence stained with LAMP-1 antibody. Scale bar is 50 µm. Images are representative of three separate experiments.

To quantify the amount of LAMP-1 specific staining on the cellular surface, attempts were made at using FACS. This proved unsuccessful mainly due to technical difficulties and staining problems.

Instead LSC, explained in chapter 2, was used to quantify the LAMP-1 specific staining. This was done in collaboration with Dr. Angela Morton, University of Glasgow. Quantification of the LAMP-1 specific staining following infection with PA103 ΔUΔT results in increased amount of LAMP-1 on the cellular surface compared to uninfected samples as well as unspecific staining (Figure 4.29). Increasing MOI results in more LAMP-1 being relocated to the cellular surface, as expected due to higher bacterial burden and more T3SS. PA103 ΔpcrV has similar amount of LAMP-1 on the cellular surface as cells alone stained with anti-LAMP-1 (results not shown).
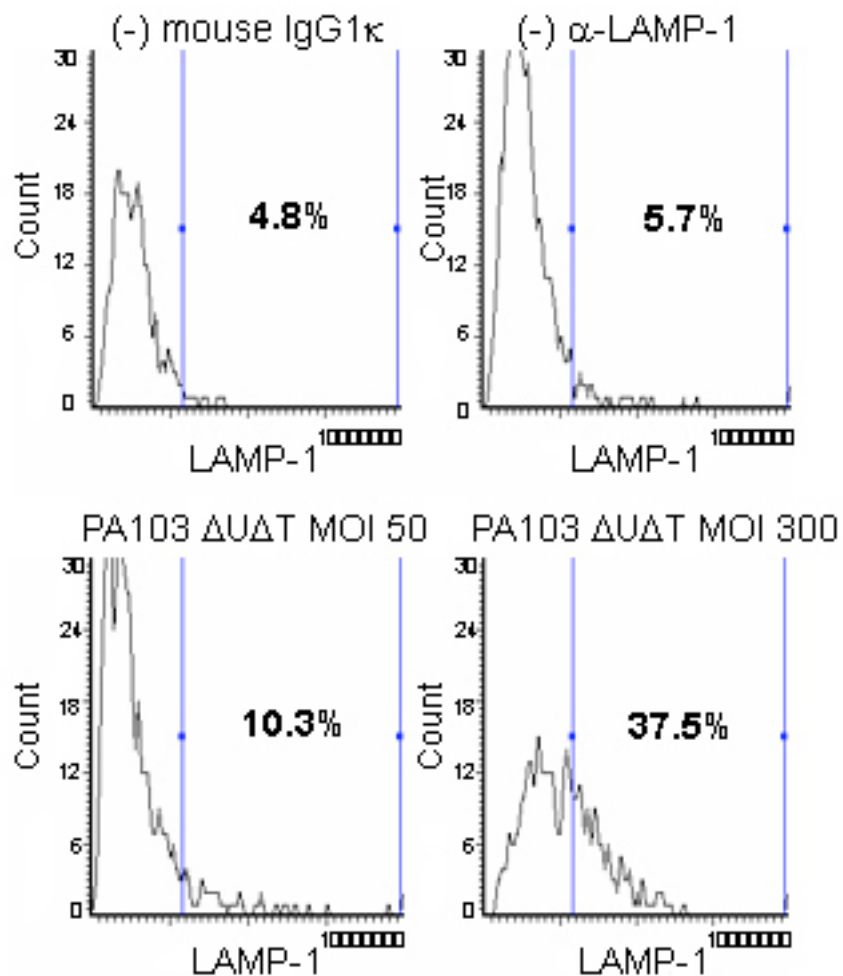
Figure 4.29; LAMP-1 relocates to the cellular surface following contact with a functional T3SS.

HeLa cells were infected with PA103 ΔUΔT at indicated MOIs for 90 min. Cells were immunofluorescence stained with LAMP-1 or mouse IgG1κ antibody and LAMP-1 staining were quantified using LSC.

4.2.5.2 Investigation of β-hexosaminidase release following contact with a functional T3SS

Lysosomal exocytosis results in release of lysosomal contents into the extracellular environment. The enzyme ß-hexosaminidase resides in lysosomes and it is released during lysosomal exocytosis. This enzyme can be used in an assay where 4-methylumbelliferyl *N*-acetyl-ßD-Glucosaminide dehydrate is cleaved by ß-hexosaminidase to 4-methylumbelliferone, which can be measured using a spectrofluorimeter. This method was previously described by [335, 336]. First attempts at this method proved unsuccessful due to incubation in PBS (results not shown). Lysosomal exocytosis is triggered by calcium influx, so if

there is no calcium in the extracellular media the exocytosis will be inhibited. The fluorescence measured from 4-methylumbelliferone is higher in alkaline pH than physiological pH (Sigma): therefore, the samples were measured in the presence of 0.1 M glycine pH 10. Surprisingly, ionomycin did not trigger lysosomal exocytosis as measured by ß-hexosaminidase release (Figure 4.30). Lysosomal exocytosis could only be triggered by PA103 ΔUΔT:ExoU (Figure 4.30), which is due to its cytotoxic effects. Lysosomal exocytosis and ß-hexosaminidase release could never be seen following infection of either PA103 ΔUΔT or PA103 ΔpcrV (Figure 4.30 and results not shown). Similar results were obtained from HeLa cells, CHOs and RAW264.7.
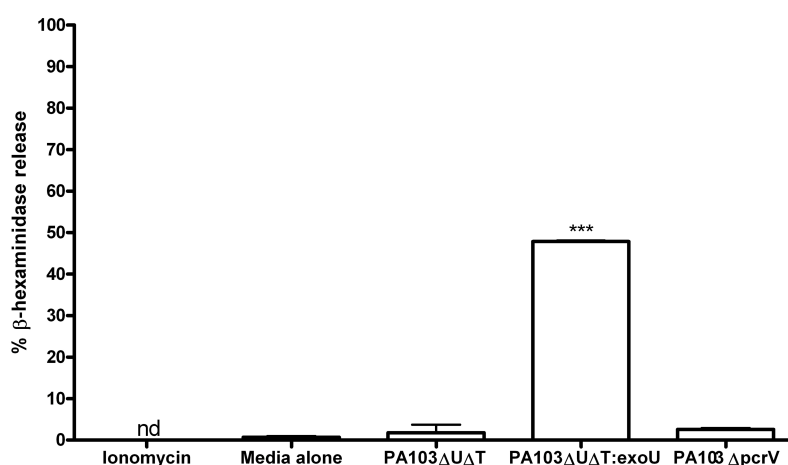
Figure 4.30; Lysosomal exocytosis is not triggered after contact with a functional T3SS.

HeLa cells were infected with PA103 strains at a MOI of 300 or treated with ionomycin. Supernatants were collected and analysed for β-hexosaminidase release. Columns are means of triplicates and error bars are SEM. *** indicate significant increase where p<0.001, unpaired Student's t-test. nd; non detected.

4.2.5.3   Role of Synaptotagmin VII during infection and membrane repair

Synaptotagmin VII is a calcium binding protein located in the lysosomal membranes. When the plasma membrane is damaged this triggers calcium influx, which binds synaptotagmin VII and lysosomal exocytosis is triggered [406]. In order to investigate the role of Syt VII during infection with *P.aeruginosa* siRNA was used to silence the expression of the protein. Syt VII has several isoforms, these have different molecular weights: E (70.6 kDa), D (68 kDa), C (63 kDa) and 45 kDa isoform, as well as a truncated form at much lower molecular weight.

siRNA sequence used were based on results previously published [345]. The gene target was in gene NM_004200 SYT7. There was never any success in silencing Syt VII using purified siRNA. HeLa cells were transfected with Lipofectamine 2000, which was successful for other transfections described in this thesis. Various concentrations of siRNA, as well as other transfection reagents (FuGENE HD and siRNA X-treme GENE transfection reagent, Roche) were tried without any success in silencing the gene. Using the siRNA X-treme GENE transfection reagent resulted in weaker bands for isoform E and also a band at a higher molecular weight (Figure 4.31). However, as these bands disappeared the 45 kDa isoform seemed to be getting stronger (Figure 4.31). This result could not be repeated, using as identical conditions as possible.
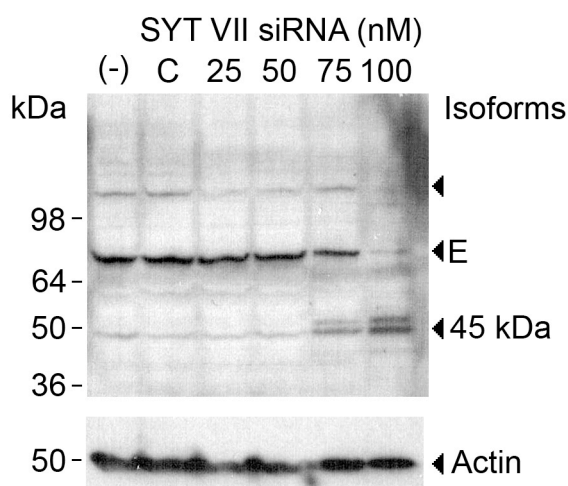
Figure 4.31; Silencing of Syt VII isoform E results in increased amounts of the 45 kDa isoform.

HeLa cells were transfected with Syt VII and control siRNA at indicated concentrations. After 48 h incubation cells were lysed and immunoblotted with Syt VII antibody. Actin was used as a loading control.

As a final attempt to silence Syt VII, hairpin siRNA was used in the vector pSilencer Syt VII. Various amounts of vector were tried using Lipofectamine 2000 without successful silencing of Syt VII. The pSilencer vector with Syt VII targeted the same sequence as previously described, but it was believed to be more stable than purified siRNA. This vector was also used in an attempt to stable transfect HeLas with Syt VII siRNA under selection of G418. This was only tried once, due to time constraints and without success. The silencing of Syt VII was never successful.

Thus, as a more reliable alternative, Syt VII $^{-/-}$ bone marrow was kindly provided by N.W. Andrews (Yale School of Medicine). These cells were used to investigate the role of Syt VII during inflammasome activation during infection with PA103 and PAO1. Following infection with PA103 ΔUΔT, there was no significant difference between IL-1ß secretion from KO compared to WT cells (Figure 4.32A). This is also true for cell death where there is no difference in percent cytotoxicity in WT compared to KO after infection with PA103 ΔUΔT (Figure 4.32B). This is also true for LPS primed BMDM stimulated with ATP, no differences can be detected in IL-1ß secretion, percent cytotoxicity or caspase-1 activation in WT compared to KO cells (Figure 4.32). In contrast, infection with PAO1 results in significantly more IL-1ß secretion and cell death in Syt VII KO cells compared to WT (Figure 4.32A & B). However, no differences can be seen in caspase-1 activation for this strain in WT compared to KO cells (Figure 4.32C).
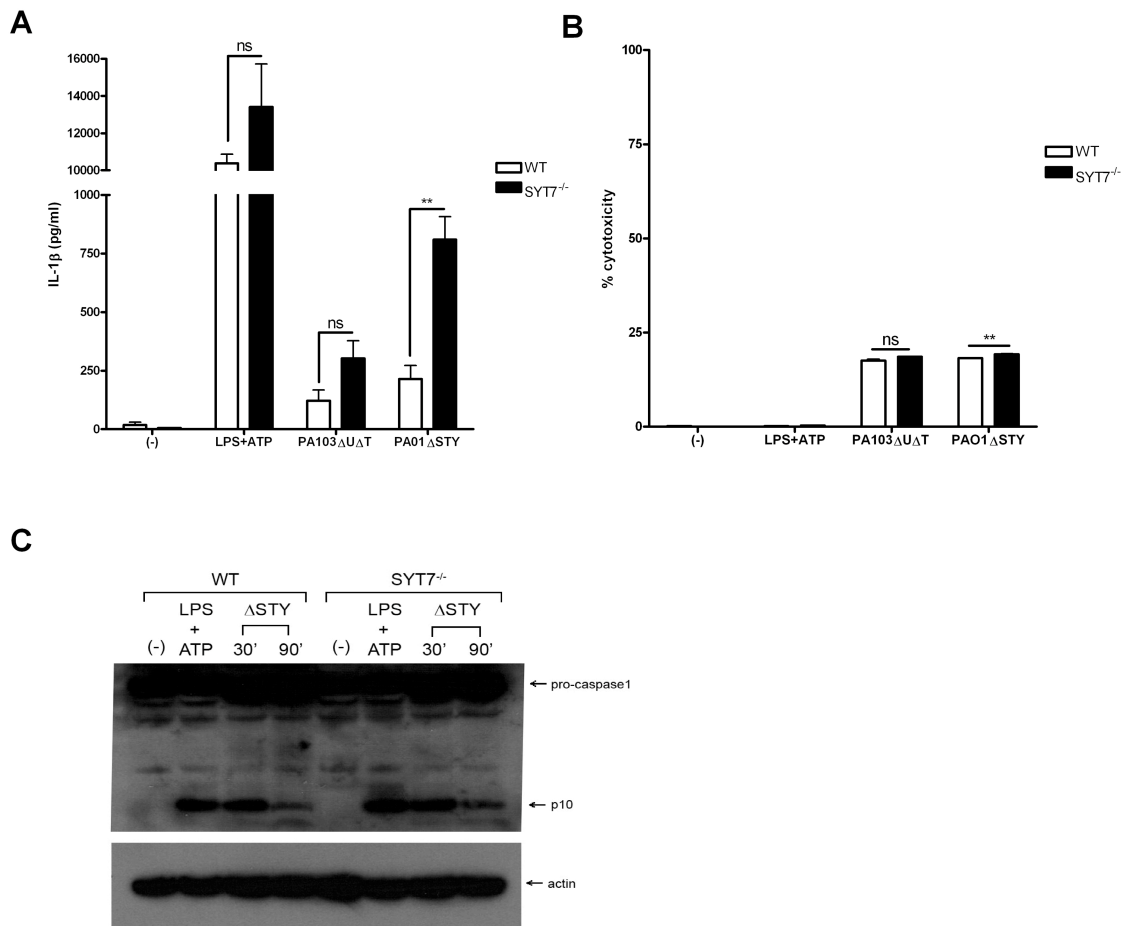
Figure 4.32; Syt VII is not involved in inflammasome activation by PA103 or PAO1.

A; BMDM WT and SYT7^{-/-} were infected with PA103 ΔUΔT or PAO1 ΔSTY at a MOI of 20 for 90 min or primed with LPS followed by ATP stimulation at 5 mM for 20 min. Supernatants were analysed for IL-1β secretion by ELISA. B; Supernatants from A were analysed for percent cytotoxicity by LDH release. Columns are means of triplicates and error bars are SEM. ** indicate significant difference where p<0.01, ns is non-significant difference, unpaired Student's t-test. C; BMDM WT and SYT7-/- were infected with PAO1 ΔSTY at a MOI of 20 for 30 and 90 min or primed with LPS followed by ATP stimulation. Cell lysates were immunoblotted with caspase-1 antibody.

4.3 Discussion

4.3.1 Potassium-dependent inflammasome activation

As previously described in chapter 3, *P.aeruginosa* activates the NLRC4 inflammasome during infection. This has also been reported by Sutterwala et al. [249], Franchi et al. [253] and Miao et al. [354]. Potassium-dependent activation of the NLRC4 inflammasome has not been shown previously. Thus, these results demonstrate a novel potassium-dependent pathway for activation of the NLRC4 inflammasome. Inflammasomes are activated by danger signals and pathogen products [161]. These results imply that the same danger signal, such as potassium efflux, can activate different inflammasome complexes, for example the NLRP3 and NLRC4. There are more than 23 members of the NLR-protein family in humans and mice. Only a few have a described function. Due to this the field is likely to get more complicated and more inflammasome complexes are likely to exist. It is therefore not unlikely that the same danger signal could trigger different inflammasome complexes. The triggering is therefore probably dependent on the sensing of DAMPs, as well as PAMPs. Certain combinations of these stimuli are likely to trigger different inflammasome complexes.

The NLRC4 has been shown to respond to bacterial products delivered by bacterial secretion systems [161]. In contrast, NLRP3 responds to a wide variety of products and danger signals, such as potassium-efflux triggered by pore-forming toxins, large foreign particles, UV etc. [161]. Considering the T3SS- and potassium-dependent activation of the inflammasome by *P.aeruginosa* this implies potassium efflux being made possible by the T3SS. Four potential explanations exist; i) where potassium can pass through the pore formed by the T3SS, ii) an indirect triggering of a potassium channel in the plasma membrane as a result of an effect by the T3SS, iii) the depolarization of the plasma membrane as a trigger of the inflammasome complex, and iv) involvement of intracellular potassium stored in intracellular compartments. During this study no ions or molecules could be detected entering or exiting the host cell following contact with a T3SS. Furthermore, no changes in intracellular potassium could be detected following infection. This favours the model where the plasma membrane is depolarized followed by inflammasome activation. The

fact that no changes can be seen in intracellular potassium concentration, as well as other ions and molecules, indicate that only a very small amount of potassium is needed to change in order to depolarize the membrane. Another possibility is that potassium flux out of critical intracellular compartments is responsible for the changes seen. Presumably these changes are below detection level for the methods used.

The potassium-dependent triggering of the NLRC4 inflammasome demonstrates that potassium-dependence can not be used as the sole determinant for NLRP3-dependence. Instead other methods should be used to determine what inflammasome is triggered by a certain stimuli. These could include the use of KO animals, as well as shRNAs. In addition, it has been shown that Anthrax toxin triggers potassium efflux, which is dependent on NLRP1 [240-242], further strengthening that potassium-dependence can not be used as a sole determinant for NLRP3-dependence.

Potassium efflux might trigger inflammasome activation by altering the ionic composition or the ionic strength around the inflammasome complex [374]. Changes in ionic strength have been shown to trigger isolated pro-caspase-1 [436]. The apoptosome is inactive in the presence of physiological concentrations of potassium, which indicate that this prevents APAF-1 oligomerization and thus apoptosome formation. Cytochrome C is the mediator which overcomes potassium inhibition and drives the apoptosome into an active state [437].

The resting membrane potential of a cell is -70 mV. The equilibrium potential is when the influx and efflux of ions are equal over the plasma membrane. The concentration gradient for potassium is outward from the cell, whereas the electrical is inward. This results in an equilibrium potential of -90 mV for potassium, which is different from the resting membrane potential. Sodium, on the other hand, has inward directed concentration and electrical gradient. This implies that the cell gradually gains sodium and lose potassium ions in order to maintain their resting membrane potential. However, due to the Na^+-K^+ ATPase there is an active transport of sodium out of the cell against its electrical gradient and this is coupled to an active transport of potassium into the cell. As discussed in the introduction, low intracellular potassium act as a danger signal

and activates the inflammasome complexes. When an ion on one side of the plasma membrane is inhibited in diffusion other ions will be affected in order to maintain the membrane potential [438]. At equilibrium there is an excess of cations on the outside of the cell and as a consequence an excess of anions on the inside, this is maintained by Na^+-K^+ ATPase [438]. This ATPase is electrogenic since it pumps out three sodium ions per two potassium ions, which contributes to the membrane potential. The number of ions required to maintain the membrane potential is a minute number of the total ion number present. Furthermore the concentrations of positive and negative ions are equal except along the cellular membrane. The cell membrane is more permeable to potassium due to potassium channels, due to this sodium does not compensate for the potassium efflux. A change in membrane potential could possibly trigger inflammasome activation, it has previously been shown to be involved in apoptosis [439]. Since the change in membrane potential is triggered by a minute number of the total ion concentration this would be impossible to measure using flame photometry and fluorescent microscopy imaging methods. In this study no change in intracellular potassium concentration could be seen with these methods, but when potassium efflux was inhibited so was the inflammasome activation. To further investigate this, a patch-clamp experiment could be performed where the membrane potential is changed and inflammasome activation following this treatment is investigated. Interestingly, infection with PAO1 leads to decreased intracellular potassium concentration in the host cell. The reason for this is unknown but might involve an additional lytic toxin.

The amount of IL-1β secreted was found in this study to be dependent on extracellular potassium concentration, both for *P.aeruginosa* and *Salmonella*. Increasing amounts of extracellular potassium resulted in decreasing amounts of IL-1β secretion. This has been shown previously following stimulation with α-toxin, where a clear dose-response was observed [367]. Interestingly the potassium-dependent inhibition decreased with the duration of LPS stimulation [367]. In this study cells were primed with LPS for 3 h before infection, furthermore LPS was present throughout the infection, which means the total time in LPS was 4.5 h. This was shown in a previously published study [367] to

result in some IL-1ß secretion, which was also detected in this study, presumably due to the decreased potassium-dependent inhibition described.

It was shown by Franchi et al. that inflammasome activation by extracellular bacteria such as *E.coli* and *S.aureus* requires ATP stimulation [236]. Furthermore, inflammasome activation by intracellular bacteria, such as *Salmonella* and *Listeria*, was shown to be independent of ATP and potassium efflux via the P2X7-receptor [236].

The results in this chapter describe potassium-dependent inflammasome activation by *Salmonella*, SL1344. This is in contrast to previously published results [236, 238]. *Salmonella* was originally intended to be used as a positive control. The differences from previous publications might be due to different conditions used. In the study by Petrilli et al. the high extracellular potassium media was added after 1 h of infection, which might give different results from this study where the potassium media was present throughout the infection. The inflammasome independent activation by *Salmonella* seen by Petrilli et al. might be due to activation of the inflammasome before addition of the high extracellular potassium, which is then detected upon analysis. The study by Franchi et al. used 20 mM KCl as their high potassium media, whereas all other conditions were identical to the results presented in this thesis. However, 20 mM KCl does not inhibit inflammasome activation for *Salmonella* or *Pseudomonas*, as seen in this study. Therefore, the results obtained in this thesis are similar to previously published data by Franchi et al. The potassium-dependent inflammasome activation by *Salmonella* has thus never been investigated in a similar manner to the results presented here.

Addition of extracellular potassium to the media will have an effect on other ions as well, since the cell will try to maintain the membrane potential. Muruve et al. [440], used Glybenclamide to investigate the effects of inhibited potassium efflux on inflammasome activation by DNA. Glybenclamide is a blocker of ATP-dependent potassium channels in the plasma membrane. It will possibly still have an effect on the membrane potential, but not on the total ion concentration in the extracellular media. In this chapter, it was shown that inhibition by Glybenclamide resulted in inhibited inflammasome activation by *P.aeruginosa* as well as *Salmonella*. This further strengthens the theory that

inflammasome activation by these bacteria involves a crucial change in ionic environment.

Pannexin-1 was identified as the protein responsible for the large pore formed upon activation of the P2X7R, as discussed in section 4.1.2. In the study by Pelegrin et al. pannexin-1-mimetic inhibitory peptide were used and this was shown to block ethidium bromide uptake as well as caspase-1 cleavage and IL-1β processing [346]. In this study pannexin-1 peptide was shown to block uptake of ethidium bromide. However, no effect could be detected on caspase-1 activation and IL-1β release in any of the samples studied. The experiments were performed as described by Pelegrin et al. The pannexin-1 peptide was able to block ethidium bromide uptake in the experiments shown in this chapter, section 4.2.1.3. This means it is a fully functional reagent and the cell type used (BMDM) has P2X7R. However, no changes in IL-1β secretion were seen, which contradicts previously published results. In this study BMDM were used, whereas in the previously published results human THP1 macrophages, mouse J774 macrophages and human alveolar macrophages were used. This indicates a difference depending on what cell type is being used. This suggests that there is not a role for IL-1β secretion by the pannexin-1 channel. Furthermore, there have not been any other publications describing the effect of a pannexin-1 inhibitory peptide in IL-1β secretion, which suggests that the reagent is not very effective.

In this study there was no effect of CBX treatment on IL-1β secretion from BMDM. This correlates with the lack of effect seen with the pannexin-1 inhibitory peptide. It is likely that there is no effect following CBX treatment when there is also a lack of effect following pannexin-1 treatment. In previously published results [346], a greater effect was seen following pannexin-1 treatment compared to CBX treatment. No conclusions can be drawn for the role of CBX in ethidium bromide uptake in this study as this was never investigated.

A further study by Pelegrin et al. [333], showed that the dye-uptake via pannexin-1 following P2X7R activation is not necessary for inflammasome activation. It was found that the inflammasome activation by nigericin and maitotoxin is dependent on pannexin-1. Only noncytolytic pathways were investigated by using time periods where no LDH release could be observed.

Noncytolytic conditions for ATP stimulation following LPS priming has been shown to be 5 mM ATP for 20 min in J774 macrophages [333]. This also worked well in this study using BMDM. During the study presented in this thesis the LDH release following LPS-priming and ATP stimulation never resulted in significantly increased cytotoxicity. It has been known for some time that extracellular ATP triggers IL-1ß secretion from macrophages in a potassium-dependent manner [379]. Previously published result also showed that the IL-1ß secretion is not necessarily associated with cell death, since IL-1ß was released before other cytoplasmic markers [379]. However, the bacteria do result in cell death following infection but for PA103 ΔUΔT it is rarely above 20 %. As previously discussed, the ethidium bromide uptake could be blocked by the pannexin-1 inhibitory peptide in this study, whereas there was no effect on IL-1ß secretion and thus inflammasome activation. The study by Pelegrin et al. shows that dye uptake is separate from inflammasome activation, but there is a role for pannexin-1 in the inflammasome activation. The previously published results used J774 macrophages, whereas in this study primary BMDM were used. This might explain the differences seen. Furthermore, the pannexin-1 inhibitory peptide has not been shown to block potassium-efflux, which has been shown to be a trigger for inflammasome activation. In the study by Pelegrin et al. it is discussed that the slow dye uptake seen might be due to incomplete block by the pannexin-1 peptide, which they believe is highly unlikely as the hemichannel function can be completely blocked in HEK cells stably expressing P2X7R. This further strengthens the possibility that different experimental set-ups might be responsible for the differences seen between previously published results and results presented in this study. The published study had the conditions optimized for J774 macrophages and the conditions needed to block the pannexin-1 in BMDM might be slightly different.

The ethidium bromide uptake was not altered in high extracellular potassium in the investigation by Pelegrin et al. This is not something that was investigated in this study.

Both *Salmonella* and *P.aeruginosa* have a T3SS, and both bacteria have been shown to activate the NLRC4 inflammasome dependent on ASC. In this study potassium-dependent inflammasome activation is seen during infection with both *Salmonella* and *P.aeruginosa*. This suggests a model where NLRC4 is

triggered by a functional T3SS as well as depolarization of the membrane via potassium efflux. In contrast NLRP3 has also been shown to be activated by potassium efflux triggered by bacterial toxins and other danger signals but not bacterial secretion systems or products delivered by these. Thus, the triggering of the different inflammasome complexes is dependent on the method by which the triggering signal is delivered.

4.3.2 Pore formation by the T3SS and membrane repair

As discussed in the introduction of this chapter, it was previously shown for *Yersinia* strains lacking effectors that this would allow dye uptake and release from infected cells through the pore formed by the T3SS. This was investigated in this study, but no leaky pore could be detected. *Yersinia* and *Pseudomonas* have homologous T3SS and these can complement each other [71]. We therefore hypothesized that the T3SS pore formed by *Pseudomonas* would behave similar to *Yersinia*. PA103 ΔUΔT used in this study lacks functional effectors passing through the T3SS and is therefore similar to the *Yersinia* used in previously published results [332]. The results shown in this study indicate that there are differences between the two different T3SS. Similar results to previously published data were obtained when SLO was used as a pore-forming toxin.

Neyt et al. showed that the pore formed by the *Yersinia* T3SS allows passage of extra- or intracellular dyes when there are no effectors passing through the system. Under normal conditions where there are effectors being translocated, these block any T3SS leak. This study therefore shows a difference between the T3SS of *P.aeruginosa* compared to *Yersinia*, which was not previously known. Furthermore, it was shown by Roy et al. [392], that the T3SS of *Yersinia* and *Salmonella* allows passage of ethidium bromide into the host cell, a process which was shown to be dependent on a functional T3SS. This was shown for strains with and without effectors passing through the T3SS. The results presented in this chapter indicate that the T3SS of *P.aeruginosa* forms a tight association with the host cell and does not allow entry or exit of other molecules or ions. It has previously been shown by Sundin et al. that less than 0.1% of secreted effectors escape to the extracellular milieu, strengthening the theory of a tight association with the host cell [89]. However, the ethidium uptake was

never investigated during infection with *P.aeruginosa*, but results with the other experiments suggest that no uptake would be detected.

It has been shown that the T3SS of *Salmonella* allows passage of calcium [391, 392]. The ability of the T3SS formed by *P.aeruginosa* to allow passage of ions was investigated in this study. No passage of ions could be detected during infection with *P.aeruginosa*. Other work in the laboratory showed that calcium entered the cells following infection with *P.aeruginosa*, which has a functional ExoU toxin, which is a result of its cytolytic activity. The microscopic methods for measuring changes in ion concentrations following infection described in this chapter, have not been described previously.

Membrane repair can be analysed by detection of LAMP-1 on the cellular surface, as well as release of lysosomal contents such as β-hexosaminidase. Both of these methods were used to investigate membrane repair following infection by *P.aeruginosa*. LAMP-1 was detected on the cellular surface following infection in a T3SS-dependent manner similar to results previously published for *Salmonella* and *Yersinia* [392], using fluorescent microscopy method. This staining was quantified using LSC. It was previously described that LAMP-1 relocation can be detected by LAMP-1 specific FACS-staining [413, 441]. During this study the LAMP-1 FACS-staining was unsuccessful.

In contrast to LAMP-1 staining however, no release of β-hexosaminidase could be detected, not even for the positive control with ionomycin, which is in contrast to previous publication [413]. This method would need further optimisation, but due to the time constraints for this project this has not been done.

As discussed in the introduction, it has been shown that Syt VII is involved in the cellular response to *Salmonella,* as well as *Yersinia* [392]. One of the aims of this study was to investigate the role of Syt VII during infection with *P.aeruginosa*. Attempts were made to silence Syt VII using siRNA and then investigate the effects following infection. However, no success was made in the attempts to silence the Syt VII expression. There are several different isoforms and splice variants of Syt VII [424] and all of them were never silenced at once. Due to this unsuccessful result, attempts were made to investigate the role of Syt VII in inflammasome activation by *P.aeruginosa* using KO BMDM provided by N.W

Andrews at Yale University. This has not been investigated previously. However, no role for Syt VII in inflammasome activation by *P.aeruginosa* could be determined. The trends in IL-1ß secretion in Syt VII KO mice suggest a role for Syt VII in the release of IL-1ß, since more IL-1ß is secreted in these cells in response to ATP and infection. Further studies are needed in order to determine a role for Syt VII in IL-1ß secretion. It has recently been proposed that Syt VII has a role in translocation of MHC to the cell surface during DC maturation [442].

In conclusion, the results presented in this chapter show a novel potassium-dependent inflammasome activation by *P.aeruginosa*, as well as a not previously described potassium-dependent inflammasome activation by *Salmonella*. Furthermore, it is shown that the T3SS of *P.aeruginosa* forms a tight association upon contact with the host cell, which does not allow entry or exit of other molecules and ions. These results are in contrast to previously published results. Finally, it is shown that membrane repair from lysosomes is triggered following infection, but no conclusions can be drawn considering the involvement of Syt VII.

5 Inflammasome activation by *Pseudomonas aeruginosa* – Role of flagellin and pilin

5.1 Introduction

5.1.1 NLRC4-dependent inflammasome activation

Activation of the NLRC4 inflammasome has been shown to be important in host defence for a number of pathogens. The first bacterium described to activate the inflammasome in a NLRC4-dependent manner was *Salmonella typhimurium* [234]. Despite this NLRC4-deficient mice did not have enhanced susceptibility to infection with *S.typhimurium* but caspase-1-deficient mice did [350]. This indicates that additional pathways are involved in the caspase-1 activation by *Salmonella*. *L.pneumophila* also activates the inflammasome in a NLRC4-dependent manner [352]. In addition, NLRC4 plays a role in *L.pneumophila* mediated phagosome maturation, NLRC4- and caspase-1 deficient mice allowed bacterial phagosomal replication due to a deficient phagosome-lysosome fusion [443]. *S.flexneri* is another example of a pathogen which activates caspase-1 dependent on NLRC4 [254]. As previously discussed, *P.aeruginosa* has also been shown to activate the inflammasome in a NLRC4-dependent manner [249, 253, 354]. Additionally it has been shown that NLRC4-deficient mice are more susceptible to infection by *P.aeruginosa* in a pulmonary and peritoneal *in vivo* infection model [249, 253].

NLRC4 can interact directly with pro-caspase-1 through a CARD-CARD interaction. Therefore the role of the adaptor molecule ASC is unclear. It might have a role in stabilizing the complex or facilitating caspase-1 recruitment [161]. Despite this, a number of publications have detected a role for ASC in NLRC4-dependent caspase-1 activation. Infection with *S.typhimurium*, *S.flexneri* and *P.aeruginosa* are all dependent on ASC [234, 249, 254]. In addition it has been shown, as previously discussed in chapter 3.1.2., that NAIP5 plays a role in NLRC4-dependent inflammasome activation by *L.pneumophila* [251, 352, 357]. In contrast, it has been shown that A/J mice (NAIP5-deficient) were unaffected by the NAIP5-deficiency following infection by *S.typhimurium*, *P.aeruginosa* and *L.monocytogenes* [354].

So far a critical component to activate the NLRC4-inflammasome is a functional type III or type IV secretion system. This has been shown for *S.typhimurium*, *P.aeruginosa*, *L.pneumophila* and *S.flexneri* (Figure 5.1) [246, 248, 249, 352].

5.1.2 Flagellin-dependent inflammasome activation

Flagellin-deficient mutants from *S.typhimurium* and *L.pneumophila* are defective in their ability to activate the inflammasome complex [251, 337, 351, 352, 390]. Furthermore, following transfection of flagellin it was shown that the NLRC4-inflammasome was activated [337, 390]. This led to the hypothesis that flagellin monomers gain entry into the cytosol of infected cells through a T3SS or T4SS (Figure 5.1) [337, 390]. It has been shown that the T3SS can act as a conduit for flagellin, strengthening this hypothesis further [365]. In addition, flagellin monomers are assembled into a flagellum by passage through a flagellar T3SS [444]. The direct binding of flagellin to the LRR-region of NLRC4 has not been demonstrated. The molecular basis of inflammasome activation in response to flagellin from *L.pneumophila* was recently described [312]. It was shown that the C-terminal portion of flagellin is enough to trigger a NLRC4- and NAIP5-dependent inflammasome response.

However, flagellin cannot be the only NLRC4 activator since the non-flagellated bacterium *S.flexneri*, as well as *P.aeruginosa*, previously described in chapter 3, can still activate the NLRC4-inflammasome (Figure 5.1) [227, 249]. Furthermore, at high MOIs it was shown that flagellin-deficient *S.typhimurium* were still able to induce IL-1β secretion [337].
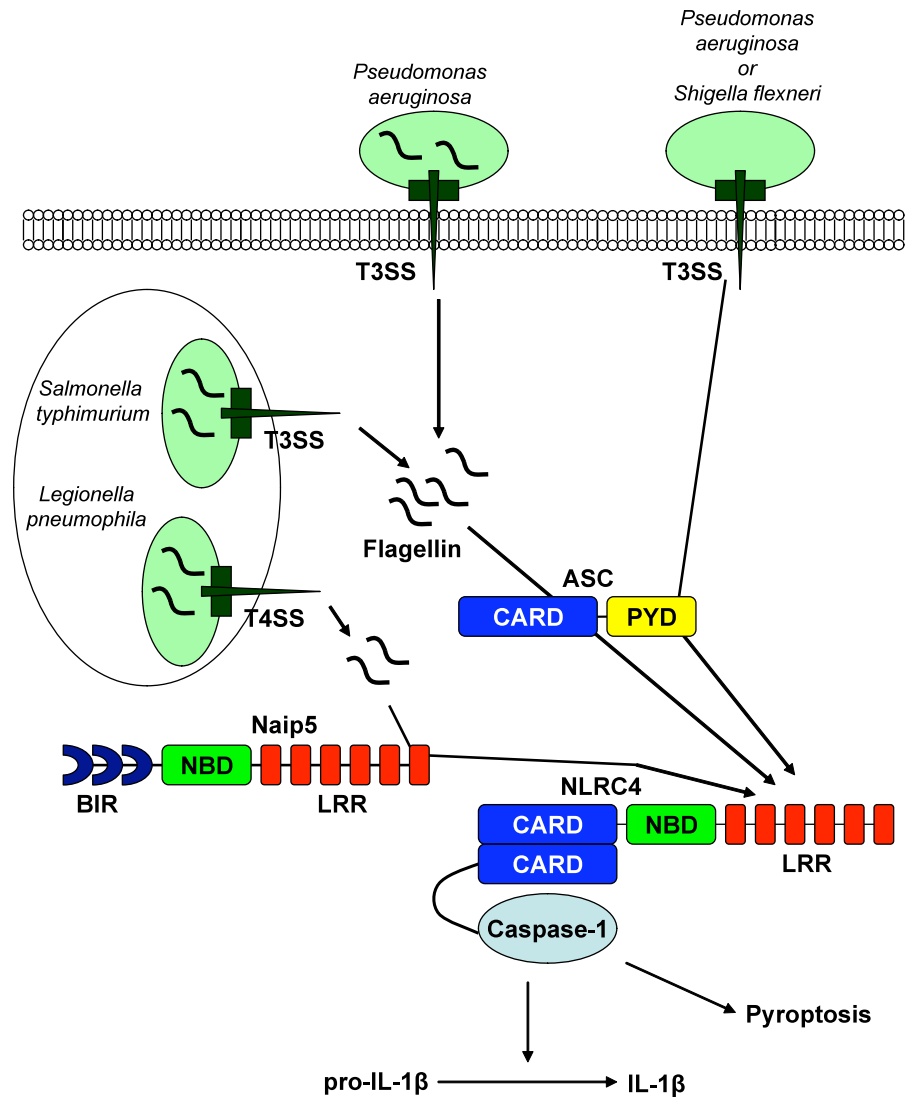
Figure 5.1; Flagellin-dependent inflammasome activation

Activation of caspase-1 following infection of *S.typhimurium*, *P.aeruginosa*, *S.flexneri* or *L.pneumophila* requires a functional type III or type IV secretion system. Caspase-1 binds NLRC4 via homophilic CARD-CARD interactions, which leads to activation of caspase-1. ASC is required for NLRC4-mediated caspase-1 activation by *S.typhimurium*, *P.aeruginosa* and *S.flexneri*, whereas *L.pneumophila* requires NAIP5. *P.aeruginosa*, *S.typhimurium* and *L.pneumophila* activates the NLRC4 in a flagellin-dependent manner. NLRC4-activation can also occur independently of flagellin following infection by *P.aeruginosa* and *S.flexneri*.

5.1.3 Pilin

Pili are located at the bacterial surface as protruding hair-like organelles. Type

IV pili are expressed by many Gram-negative bacteria such as EPEC, EHEC,

Salmonella enterica serovar Typhi, *Pseudomonas aeruginosa*, *Legionella*

pneumophila, *Neisseria gonorrhoeae*, *Neisseria miningitidis* and *Vibrio cholerae*

[26], as previously described in chapter 1.2.2.2. The type IV pili are composed of a homopolymer of a single pilin subunit, such as PilA in *P.aeruginosa*. The pili are formed at the cytoplasmic membrane and the intact organelle is extruded across the outer membrane [50]. Type IV pili are able to retract through the bacterial cell wall while the tip remains adhered to the target surface, resulting in bacterial cell movement known as twitching motility. Pilin monomers in the bacterial cell are used to retract and rebuild the pili structure [48-50].

The work in this chapter investigates the role of pilin, as well as flagellin as inflammasome activators. This is investigated by transfection experiments and infection models. The results reveal pilin as a novel inflammasome activator, thus providing an explanation to how flagellin-deficient bacteria can activate the NLRC4-inflammasome.

5.2 Results

5.2.1 Flagellin-dependent inflammasome activation

Flagellin have been shown to activate the inflammasome in a number of publications [251, 253, 337, 351, 354, 390, 443]. Here recombinant flagellin from *Salmonella muenchen* was used to confirm that flagellin was able to activate the inflammasome. Following transfection into BMDM IL-1ß was released into the supernatant in a flagellin-dependent manner (Figure 5.2). As a control, cells treated with ATP were used, which also triggers IL-1ß release (Figure 5.2). In addition, transfection with flagellin results in some cytotoxicity of the cells, whereas ATP-dependent inflammasome activation does not (Figure 5.2), as previously described in chapter 4.
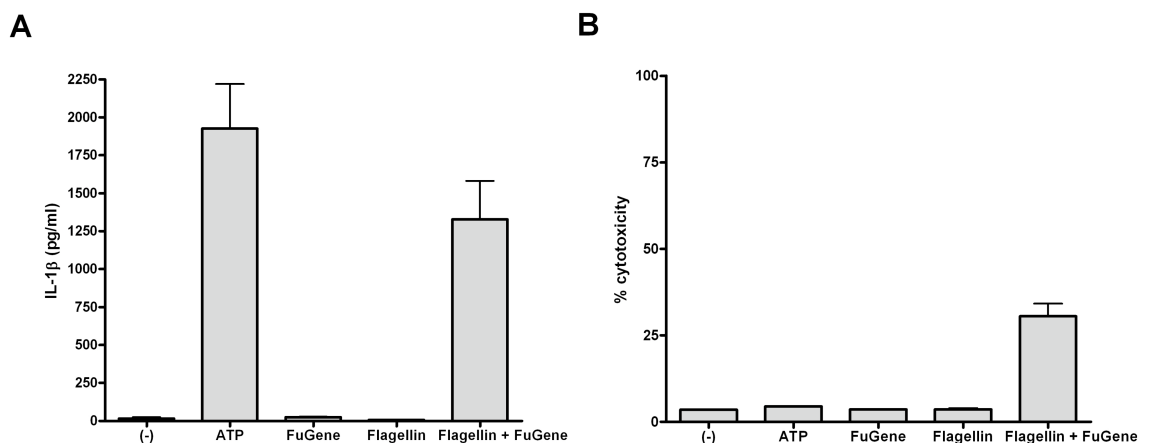
Figure 5.2; Flagellin-dependent inflammasome activation

LPS-primed BMDM were transfected with Flagellin (630 ng / 2.5×10^5 cells) together with FuGene or treated with ATP. Supernatants were analysed by ELISA for IL-1β release (A) and by LDH release for percent cytotoxicity (B). Columns are means for triplicates and error bars are SEM.

Transfected flagellin results in caspase-1 activation, which could be detected by immunoblotting of the p10 fragment (Figure 5.3). The transfection reagent or flagellin alone did not result in caspase-1 activation, as no p10 band could be detected for these samples (Figure 5.3). This corresponds to the IL-1ß secretion seen from these samples (Figure 5.2).
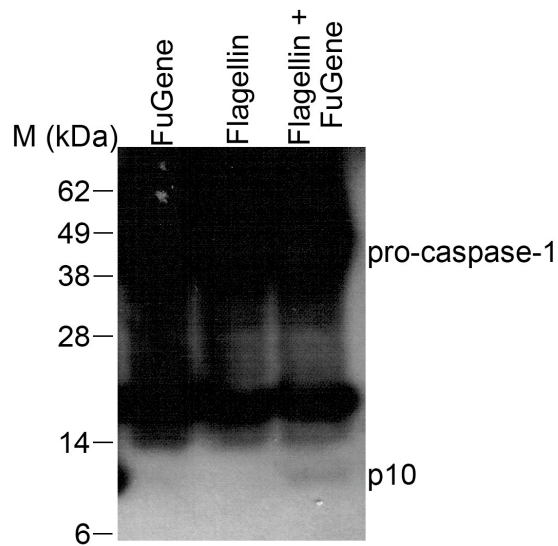
Figure 5.3; Flagellin transfection results in caspase-1 activation

Cell lysates from LPS-primed BMDM transfected with Flagellin together with FuGene were immunoblotted with caspase-1 antibody. Activated caspase-1 (p10) can be detected when cells are treated with flagellin together with FuGene.

It has previously been shown that *P.aeruginosa* can activate the inflammasome in a flagellin-dependent manner [253, 354]. This was shown for the strains PAK and PAO1. Following infection with a flagellin-deficient mutant of PAO1 significantly less IL-1β is released compared to the WT strain (Figure 5.4). Furthermore, if a strain which lacks flagellin (PAOC) is complemented with flagellin from PAO1 the inflammasome activation is restored (Figure 5.4). Infection with the complemented strain results in significant higher levels of IL-1β release compared to the WT strain. This can possibly be explained by a higher level of expression from the complementing plasmid compared to wildtype levels.
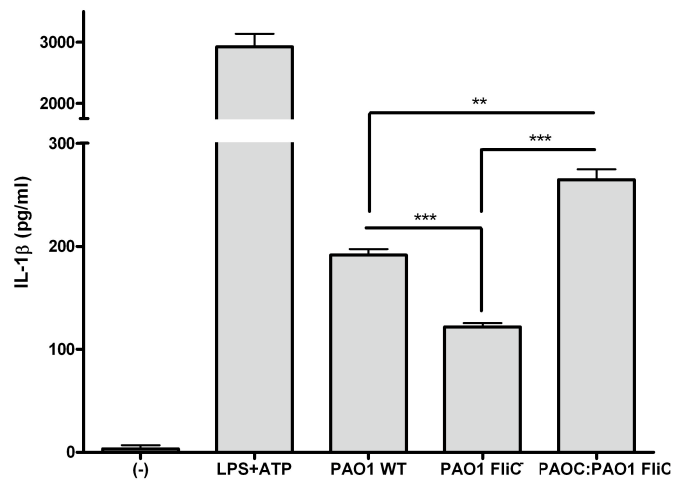
Figure 5.4; PAO1 activates the inflammasome in a flagellin-dependent manner

BMDM were primed with LPS and treated with ATP or left unprimed and were infected with PAO1 WT, PAO1 FliC⁻ and PAOC:PAO1 FliC for 90 min at a MOI of 50. Columns are mean of triplicates and error bars are SEM. ** and *** indicate significant difference where ** is $p<0.01$ and *** is $p<0.001$, unpaired Student's t-test.

The caspase-1 activation was also investigated following infection with PAO1 WT, FliC⁻ and complemented PAOC; PAOC:PAO1 FliC. The caspase-1 activation corresponds to the IL-1ß release detected, where the strains with flagellin are able to activate caspase-1, whereas the flagellin deficient strain does not (Figure 5.5 Top panel). Pro-caspase-1 levels were similar in all samples (Figure 5.5 Lower panel).
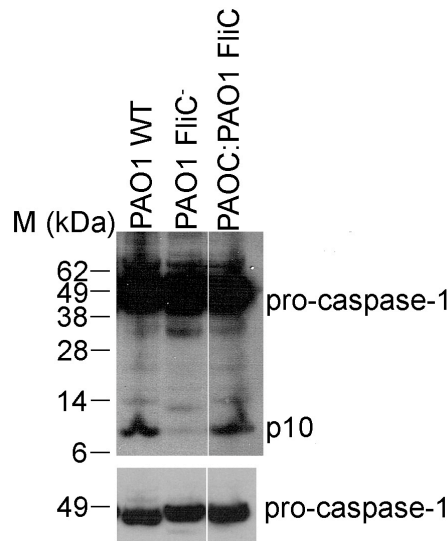
Figure 5.5; PAO1 activates caspase-1 in a flagellin-dependent manner

Cell lysates from Figure 5.4 were immunoblotted with caspase-1 antibody. Top panel shows pro-caspase-1 and activated caspase-1 (p10), whereas bottom panel shows a shorter exposure of pro-caspase-1.

Flagellin can be purified from bacteria by simply vortexing the culture, as described in chapter 2. It is previously known that PAO1 express flagellin whereas PA103 does not [23, 445]. Flagellin was purified from PAO1 WT and proteins were stained with colloidal Coomassie blue after resolving on a SDS-PAGE gel (Figure 5.6). At the same time proteins that were shed from PA103 ΔUΔT during the purification was resolved and stained. As expected, no flagellin could be detected from PA103 ΔUΔT. However, there was another protein of ~16 kDa detected in the cell-free supernatant (Figure 5.6).
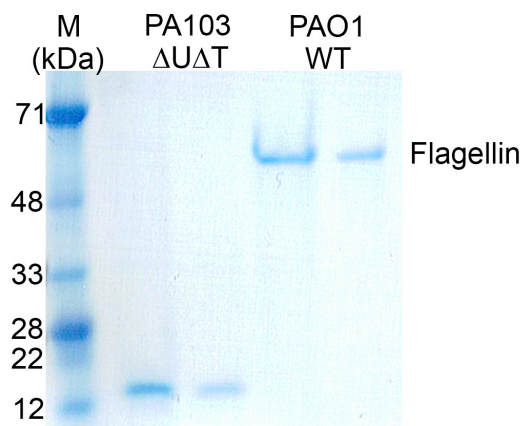
Figure 5.6; PA103 ΔUΔT lacks flagellin, whereas PAO1 WT express flagellin

Surface proteins were purified from PA103 ΔUΔT and PAO1 WT, two concentrations of these proteins were resolved by SDS-PAGE and stained with Colloidal Coomassie blue.

Attempts were made to detect flagellin from whole cell cultures of PA103 ΔUΔT and PAO1 by immunoblotting. This was never successful, possibly due to the high concentration of protein. Instead, surface proteins were purified from these strains and resolved using SDS-PAGE, as above (Figure 5.6). Following immunoblotting with a flagellin antibody, flagellin could be detected from PAO1 WT but not from PA103 ΔUΔT, as expected (Figure 5.7). Flagellin from PAO1 has a molecular mass of approximately 53 kDa [446].
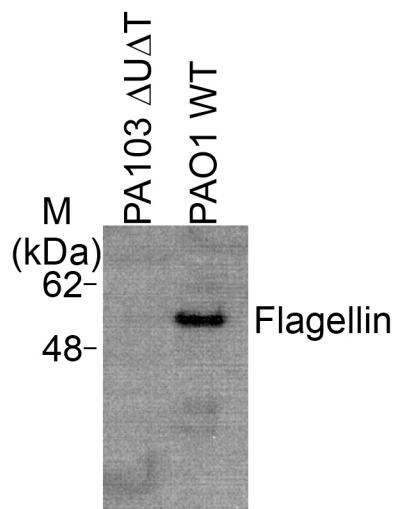
Figure 5.7; PAO1 WT express flagellin

Purified surface proteins from PA103 ΔUΔT and PAO1 WT were immunoblotted with flagellin antibody.

Flagellin expression allows the bacteria to swim on an agar plate with low percentage agar (0.5%) [447]. PAO1 WT and PA103 ΔUΔT were inoculated onto swimming plates, following incubation, a distinct swimming pattern could be seen for PAO1 WT, whereas PA103 ΔUΔT did not swim (Figure 5.8).

PAO1 WT   **PA103 ΔUΔT**
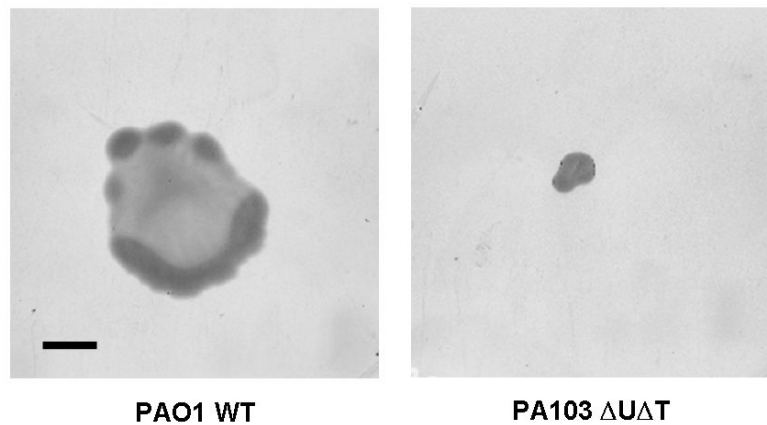
Figure 5.8; PAO1 WT can swim whereas PA103 ΔUΔT cannot

PAO1 WT and PA103 ΔUΔT were inoculated onto a swimming plate (LB with 0.5% agar) and incubated overnight at 37°C. Black scale bar is 10 mm.

Together these results show that flagellin can activate the inflammasome and that PAO1 activates the inflammasome in a flagellin-dependent manner. However, PA103 ΔUΔT can activate the inflammasome, described in chapter 3, independent of flagellin. The results here confirm that PA103 ΔUΔT lacks flagellin.

5.2.2 Pilin-dependent inflammasome activation

When PA103 ΔUΔT is exposed to a flagellin purification method no flagellin can be detected, instead a protein of roughly 16 kDa was found (Figure 5.6). Since PA103 ΔUΔT can activate the NLRC4 inflammasome dependent on ASC but independent of flagellin, this detected protein could be a candidate for the inflammasome activation. The 16 kDa protein was isolated by SDS-PAGE and blotting and digested with trypsin. Peptides were separated by liquid chromatography and individual peptides isolated and sequenced by mass spectroscopy at the University of Dundee by K. Beattie. Matches to the peptide sequences were obtained using the programme MASCOT (Matrix science). The sequencing revealed that the protein purified was pilin from PA103 with a mass of 15.8 kDa (Table 5.1). The other proteins which were identified correspond to contaminants, such as keratin and trypsin at low abundance (Table 5.1). The entire MASCOT result is presented in appendix 1.

Table 5.1; Results obtained after Mass-spec sequencing of purified PA103 ΔUΔT surface protein

Protein	gi #	Mass (Da)	Score	Queries matched	emPAI
Pilin strain PA103	120436	15789	830	24	17.27
Cytokeratin-1	1346343	65978	174	2	0.13
PilE strain PAO1	15599752	15270	85	1	0.28
Keratin 9	453155	61950	66	1	0.07
Trypsin precursor bovine	67549	23978	65	1	0.18

gi #; gene info identifier, emPAI; exponentially modified protein abundance index

To confirm this result, pilin was purified from PA103ΔUΔT using published protocols. Again, a significant release of IL-1ß following transfection with PA103 pilin compared to the transfection reagent alone were found (Figure 5.9A), similar to levels obtained using transfected flagellin. Furthermore, no effect was detected from PA103 pilin alone (Figure 5.9A). In this experiment the cytotoxicity resulting from transfections was relatively high (Figure 5.9B). This is most likely to be due to an effect of the transfection reagent DOTAP rather than a specific effect of pilin, discussed below.
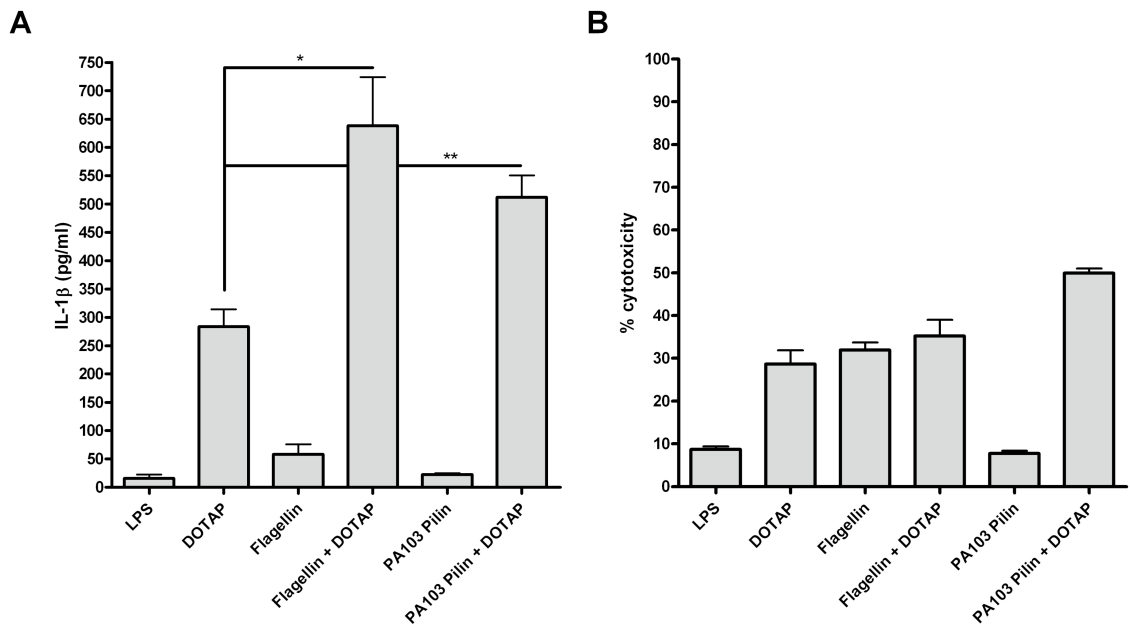
Figure 5.9; PA103 pilin-dependent inflammasome activation

LPS-primed BMDM were treated with DOTAP, Flagellin or PA103 pilin as indicated for 3h. Supernatants were analysed for IL-1β release by ELISA (A) and percent cytotoxicity by LDH release assay (B). Columns are means of triplicates and error bars are SEM. * and ** indicate significant difference where * is p<0.05 and ** is p<0.01, unpaired Student's t-test.

Both flagellin and pilin are able to trigger inflammasome activation. PA103 pilin was transfected into cells and compared to the response seen following OVA transfection. Significantly more IL-1ß is released from cells after transfection with PA103 pilin compared to transfected OVA (Figure 5.10). OVA transfection does not result in IL-1ß release compared to the transfection reagent alone (Figure 5.10).
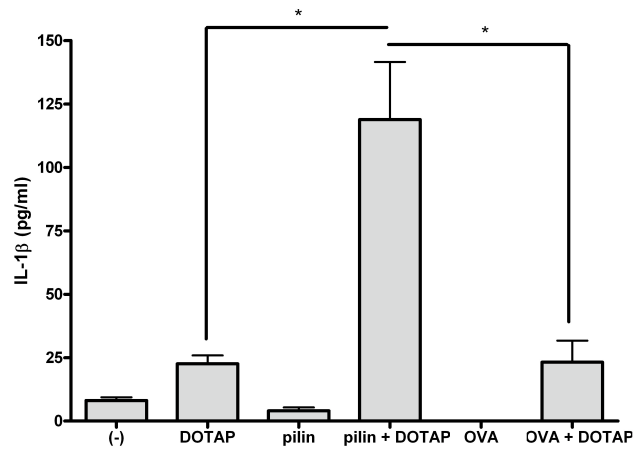
Figure 5.10; Pilin-dependent inflammasome activation

LPS-primed BMDM were treated with DOTAP, pilin and OVA, as indicated. Supernatants were analysed for IL-1β release by ELISA. Columns are means of triplicates and error bars are SEM. * indicate significant difference where * is p<0.05, unpaired Student's t-test.

Previous publications have investigated the response following protein transfection after 2 and 3 h, respectively [337, 390]. The response to PA103 pilin was investigated at different time-points, up to 3 h. It was found that the amount of IL-1ß secreted increased with increasing transfection time (Figure 5.11A). The cytotoxicity caused remains below 10% for the transfected protein over the entire time period tested (Figure 5.11B). In this experiment the cell death caused by DOTAP alone is low (Figure 5.11B).
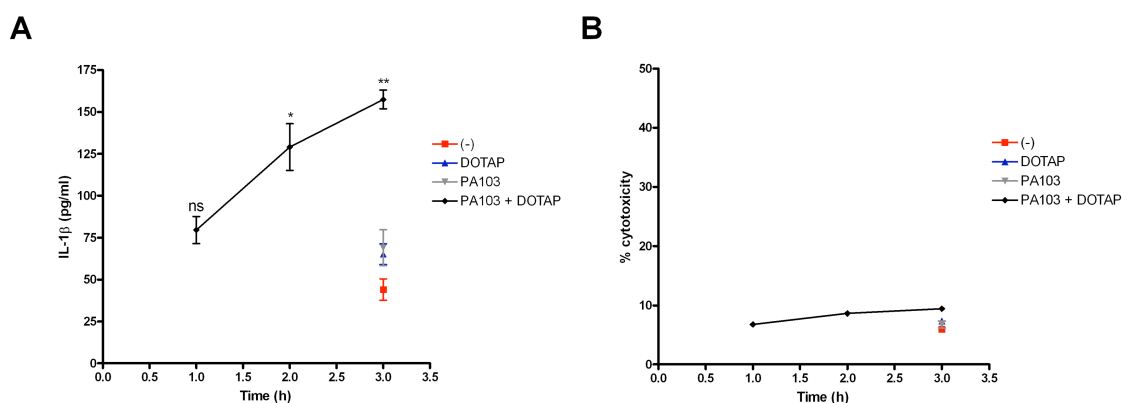
Figure 5.11; Increasing transfection time results in increasing inflammasome activation by PA103 pilin

LPS-primed BMDM were treated with DOTAP and PA103 pilin for indicated times. Supernatants were analysed for IL-1β release by ELISA (A) and percent cytotoxicity by LDH release assay (B). Means of triplicates are plotted, error bars are SEM. * and ** indicate significant difference where * is p<0.05 and ** is p<0.01, ns is non significant difference p>0.05, unpaired Student's t-test.

The inflammasome activation by transfected flagellin could be completely abrogated after overnight treatment with Proteinase K [337]. To investigate whether the same was true for transfected pilin, PA103 pilin was treated with Proteinase K for 60 min according to manufacturer's instructions. In addition, the pilin preparation was boiled in order to investigate whether this has an effect on the inflammasome activation observed following pilin transfection. Both transfected Proteinase K treated and boiled pilin results in less, but not significantly less, IL-1β secretion compared to pilin alone (Figure 5.12A). The transfected Proteinase K and boiled pilin are not significantly different from DOTAP alone, but the trend suggests that they are not completely without effect (Figure 5.12A). The cytotoxicity remains low and constant for all samples (Figure 5.12B).
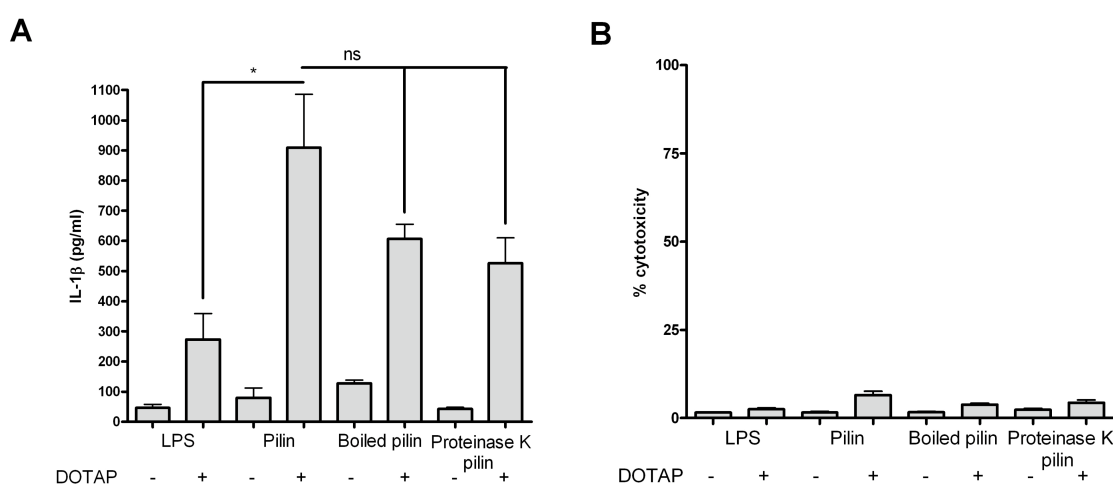
Figure 5.12; Less IL-1β is released following boiling or Proteinase K treatment of pilin

Pilin were boiled, treated with Proteinase K or left untreated and transfected into LPS-primed BMDM for 3.5 h. Supernatants were analysed for IL-1β release by ELISA (A) and percent cytotoxicity by LDH release assay (B). Columns are means of triplicates and error bars are SEM. * indicate significant difference where * is p<0.05, ns is non-significant difference p>0.05, unpaired Student's t-test.

The Proteinase K treated and boiled pilin were also visualised using SDS-PAGE and colloidal Coomassie blue staining. Following Proteinase K treatment, an undigested core of pilin could be observed at approximately 7 kDa (Figure 5.13). Not surprisingly, the boiled pilin has the same molecular weight as the purified pilin, since they are both boiled prior to loading onto the gel (Figure 5.13).
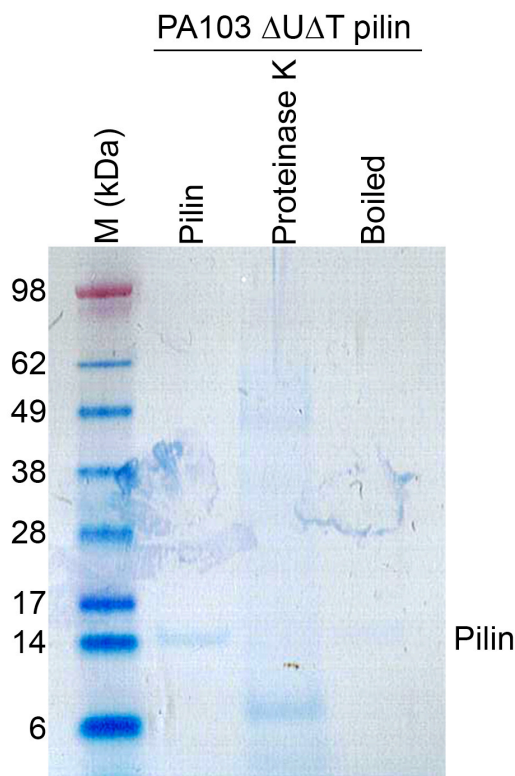
Figure 5.13; PA103 pilin has a core which is unaffected by Proteinase K treatment

PA103 pilin was left untreated, boiled or treated with Proteinase K. These samples were then resolved by SDS-PAGE and stained by Colloidal Coomassie blue.

The results presented in this section shows that PA103 pilin can activate the inflammasome, comparable to inflammasome activation seen by flagellin.

5.2.3 PA103 and PAO1 pilin-dependent inflammasome activation

PA103 pilin was shown, in the previous section, to be able to activate the inflammasome response. To investigate whether PAO1 pilin activates the inflammasome in a similar manner, attempts were made to purify pilin from the PAO1 strain. When pilin is purified from PAO1 WT, using the protocol described in section 2.2.18, the same protocol which is used to purify pilin from PA103, the resulting proteins are flagellin (Figure 5.6). In order to obtain pilin from PAO1 using this purification protocol it is necessary to use flagellin-deficient PAO1; PAO1 FliC⁻. Pilin purification from this strain results in a band comparable to that of PA103 pilin (Figure 5.14).
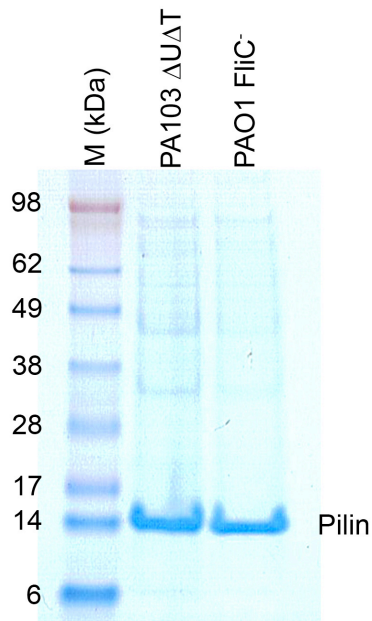
Figure 5.14; Pilin purified from PA103 ΔUΔT and PAO1 FliC⁻

Pilin was purified from PA103 ΔUΔT and PAO1, resolved by SDS-PAGE and stained with Colloidal Coomassie blue.

The ability of PAO1 pilin to activate the inflammasome complex was compared to that of PA103 pilin. Cells were transfected with increasing amounts of pilin (Figure 5.15). As a control OVA was used, as well as DOTAP alone. Increasing amounts of PA103 pilin being transfected into the BMDM results in increasing amounts of IL-1ß secretion (Figure 5.15A). Transfection with PAO1 pilin does result in significantly more IL-1ß secretion compared to transfection reagent alone (Figure 5.15A), but not to the same degree as PA103 pilin. The cytotoxicity mediated by the two different pilins are not significantly different from the cytotoxicity observed following treatment with DOTAP alone (Figure 5.15B).
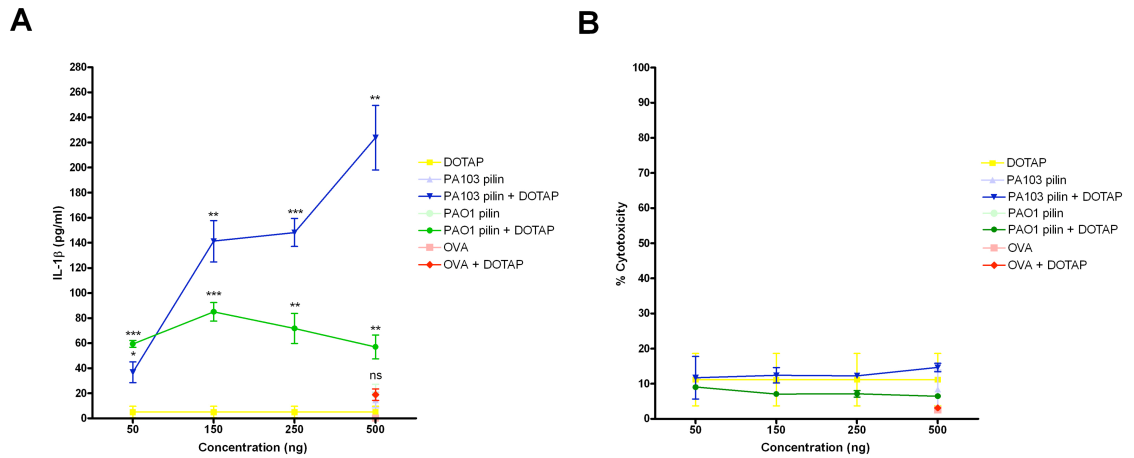
Figure 5.15; Pilin-dependent inflammasome activation by PA103 and PAO1 pilin

LPS-primed BMDM were transfected with indicated conditions for 3.5 h. Supernatants were analysed for IL-1β release by ELISA (A) and percent cytotoxicity by LDH release assay (B). Means of triplicates are plotted with error bars (SEM). Asterixes indicate significant difference where * is $p<0.05$, ** is $p<0.01$ and *** is $p<0.001$, ns is non-significant difference $p>0.05$, unpaired Student's t-test.

Transfected PA103 pilin can activate caspase-1, since a p10 band can be detected following pilin transfection (Figure 5.16). Neither pilin alone, DOTAP alone, nor OVA, with or without DOTAP, activates caspase-1 (Figure 5.16).
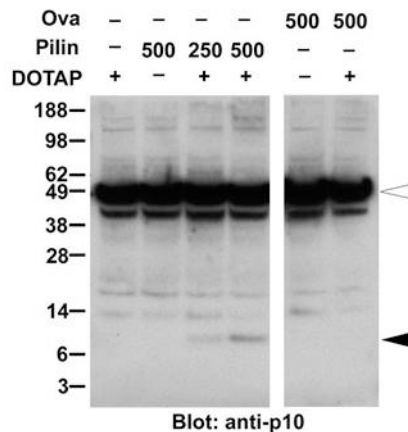
Figure 5.16; PA103 pilin-dependent caspase-1 activation

Cell lysates from indicated samples from Figure 5.15 were immunoblotted with caspase-1 antibody. Only pilin together with DOTAP results in caspase-1 activation (p10 band, black arrow head). Pro-casapse-1 can be detected in all samples (white arrow head).

Increasing transfected amounts of both PA103 pilin and PAO1 pilin results in increasing caspase-1 activation (Figure 5.17). The PAO1 pilin does not seem as

potent as the PA103 pilin, since PAO1 pilin transfection results in less caspase-1 activation. This is comparable to the IL-1ß secretion seen (Figure 5.15A).
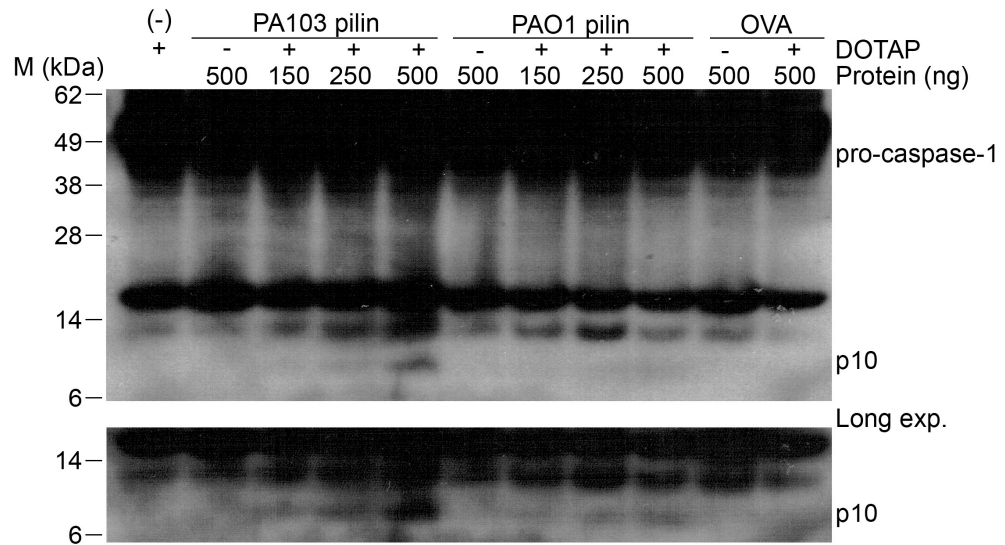
Figure 5.17; PA103 pilin activates more caspase-1 than PAO1 pilin

Cell lysates from Figure 5.15 were immunoblotted with caspase-1 antibody. Top panel shows caspase-1 activation in these samples. Bottom panel is a longer exposure of the same film.

Pilin transfection does not result in increased secretion of IL-6 or TNF-α compared to cells alone (Figure 5.18).
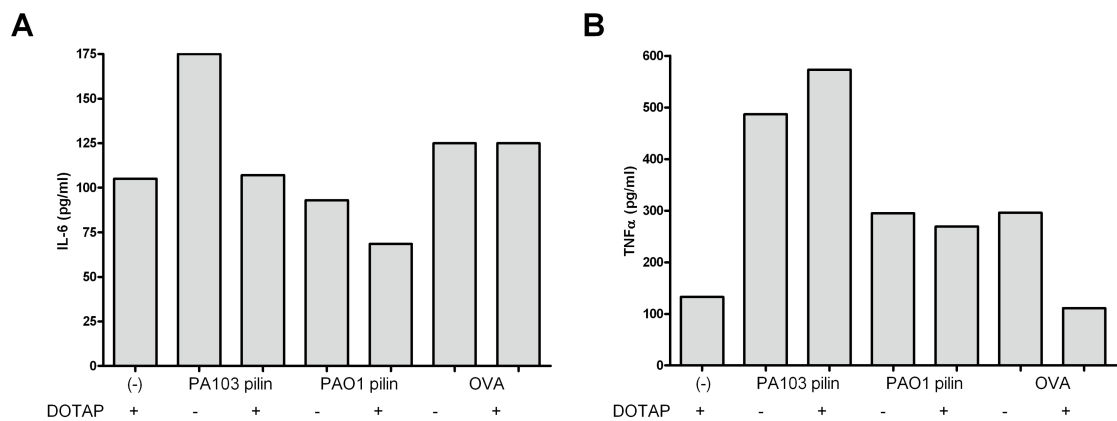
Figure 5.18; IL-6 and TNF-α release are not dependent on pilin transfection

Supernatants from Figure 5.15 were analysed for IL-6 release (A) and TNF-α release (B) by ELISA. Columns are pooled triplicate samples.

The results presented in this section show that both pilin from PA103 and PAO1 can activate the inflammasome complex. PA103 pilin seems to be more potent than PAO1 pilin, discussed in more detail below.

5.2.4 Recombinant pilin-dependent inflammasome activation

Purification of recombinant pilin and crystallisation is impossible unless the expressed protein lacks the N-terminal hydrophobic α-helix [40], as this produces aggregation and renders the recombinant protein insoluble. A truncated version of the PA103 pilin coding DNA was constructed, lacking the N-terminal hydrophobic helix. This was engineered to contain a His-tag by cloning into the pET41c vector, which produces the pilin fused to the Glutathione S-transferase (GST) protein which increases expression levels and solubility. The recombinant truncated form of PA103 pilin fused to GST was then expressed by *E.coli* and purified from bacterial lysates on a Ni-NTA His-Bind column, as described in chapter 2.2.22. The eluted His-tagged pilin-GST was then cleaved with recombinant Enterokinase and the His-tagged GST protein was removed on a second Ni-NTA His-Bind column (Figure 5.19).
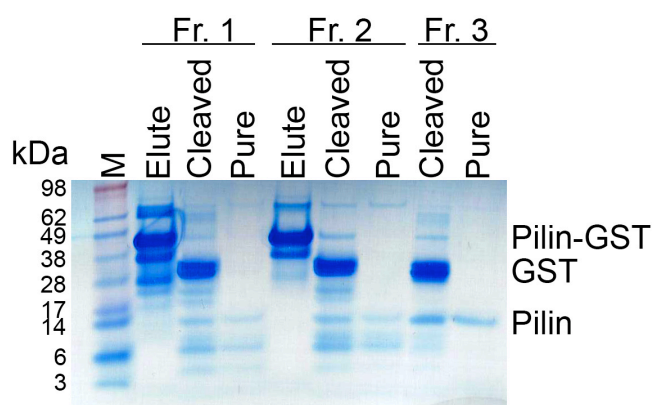
Figure 5.19; Purification of recombinant PA103 pilin

Following expression of PA103 pilin in *E.coli* the proteins were eluted from the NiNTA agarose column in indicated fractions. This was then cleaved by recombinant Enterokinase and cleaned on NiNTA agarose again. The elutes, cleaved and pure proteins were resolved on a SDS-PAGE gel and stained by Colloidal Coomassie blue. Pure pilin from fraction 3 was used in subsequent experiments.

The purified recombinant pilin was transfected into BMDM to investigate whether it could activate the inflammasome complex. Following transfection

with recombinant pilin, IL-1β is secreted from BMDM (Figure 5.20A). The cytotoxicity remains low for all samples (Figure 5.20B).
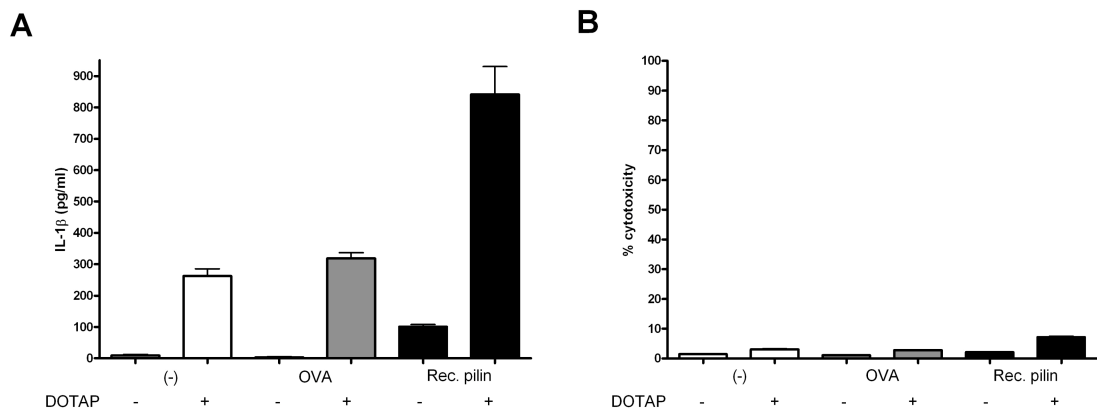
Figure 5.20; Recombinant PA103 pilin can activate the inflammasome

LPS-primed BMDM were transfected with 500 ng OVA or recombinant PA103 pilin for 3.5 h. Supernatants were analysed for IL-1β release by ELISA (A) and percent cytotoxicity by LDH release assay (B). Columns are means for triplicates and error bars are SEM.

So far, it has been shown that PA103, PAO1 and recombinant pilin can activate the inflammasome complex. The three different pilin preparations were compared in their ability to induce secretion of IL-1β. All of the pilin preparations result in significantly more IL-1β secretion than the transfection reagent alone (Figure 5.21A). As previously seen, OVA transfection does not result in IL-1β secretion (Figure 5.21A). Furthermore, PA103 pilin transfection results in significantly more IL-1β secretion than PAO1 and recombinant pilin (Figure 5.21A). This further strengthens the theory that PA103 pilin is more potent than PAO1 pilin. It also suggests a role for the N-terminal α-helix, which is lacking in the recombinant pilin.
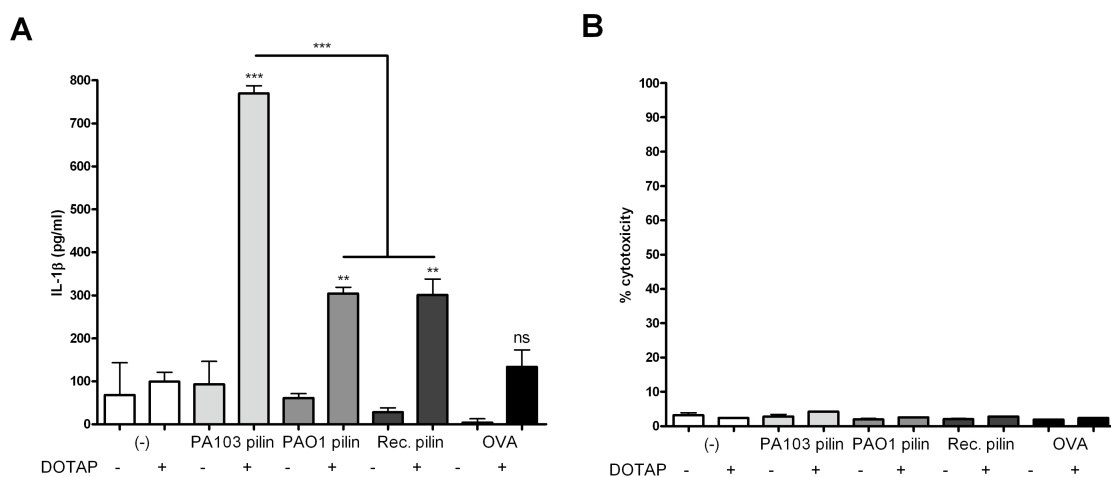
Figure 5.21; Comparison between PA103, PAO1 and recombinant pilin

LPS-primed BMDM were transfected with 500 ng of indicated proteins for 3.5 h. Supernatants were analysed for IL-1β release by ELISA (A) and percent cytotoxicity by LDH release assay (B). Columns are means of triplicates and error bars are SEM. ** and *** indicates significant difference where ** is $p<0.01$ and *** is $p<0.001$, ns is non-significant difference $p>0.05$, unpaired Student's t-test.

It was recently shown that DNA can activate the inflammasome complex and result in IL-1β secretion, as well as caspase-1 activation [440]. Following digest of the DNA by DNase I this activation was completely abrogated. In order to determine if the pilin preparations were contaminated by DNA, which would then be responsible for the inflammasome activation, the DNA content in the preparations were investigated by agarose gel-dependent determination of DNA concentration and following DNase I treatment. The DNA concentration found in the pilin preparations was less than 2 µg/ml for both PA103 and PAO1, the limit of detectability of the ethidium binding assay. This means that for a 20 ng/µl pilin preparation, when this is transfected into cells at an amount of 300 ng, a maximum of 30 ng of DNA is transfected with the pilin. It was therefore investigated whether 50 ng DNA (plasmid) was able to activate the inflammasome, as well as whether DNase I treatment of PA103 and recombinant pilin had any effect on the inflammasome activation seen. Transfection of DNase I treated pilin had no effect on the inflammasome activation (Figure 5.22). Significantly more IL-1β was secreted following transfection with all the pilin preparations, independent of DNase I treatment, compared to the transfection reagent alone (Figure 5.22). If anything there was an increase in IL-1β secretion following transfection with DNase I treated samples. In contrast, the DNA was

able to induce IL-1ß secretion, but this was completely abrogated following treatment with DNase I (Figure 5.22).
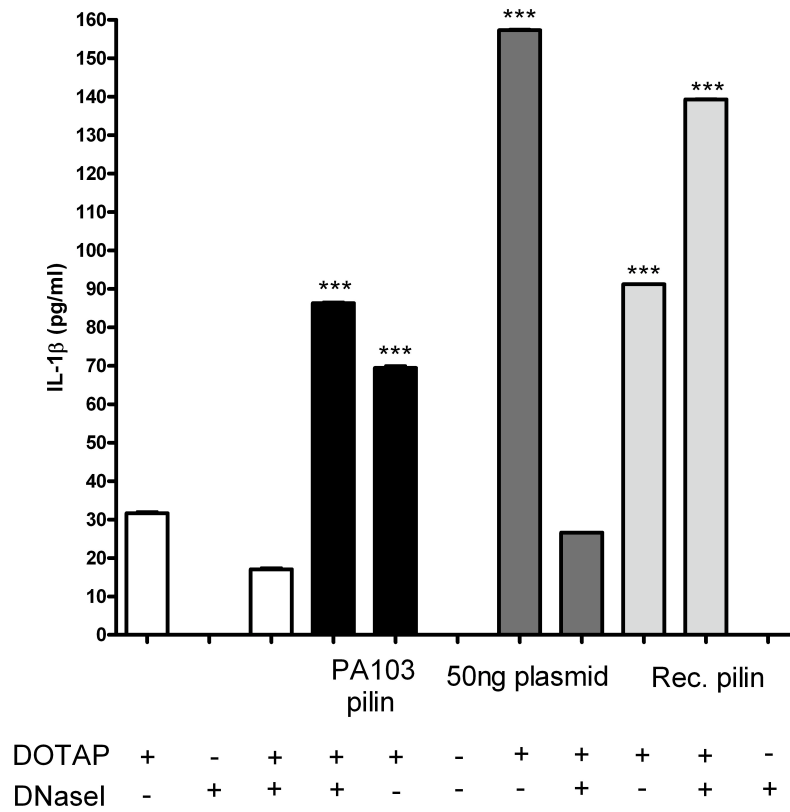
Figure 5.22; DNA contamination of pilin preparations are not responsible for the inflammasome activation seen

PA103 pilin, pCDNA3 plasmid and recombinant pilin were treated with DNase I. LPS-primed BMDM were then transfected with indicated samples for 3.5 h. Supernatants were analysed for IL-1β release by ELISA. Columns are means for triplicates and error bars are SEM. *** indicate significant difference compared to DOTAP alone where *** is p<0.001, unpaired Student's t-test.

5.2.5 The inflammasome component dependence of pilin

Inflammasome activation by *P.aeruginosa* PA103 is dependent on a functional T3SS, NLRC4 and ASC, as described in section 3.2.2. BMDM with deletions for specific inflammasome components were transfected with PA103 pilin. Surprisingly, inflammasome activation by PA103 pilin was dependent on caspase-1 but independent of NLRC4, NLRP3 and ASC (Figure 5.23A). Slightly higher cytotoxicity was seen in the samples transfected with pilin (Figure 5.23B). The caspase-1 activation corresponds to the IL-1ß secretion seen, both for cell lysates and precipitated proteins (results not shown).
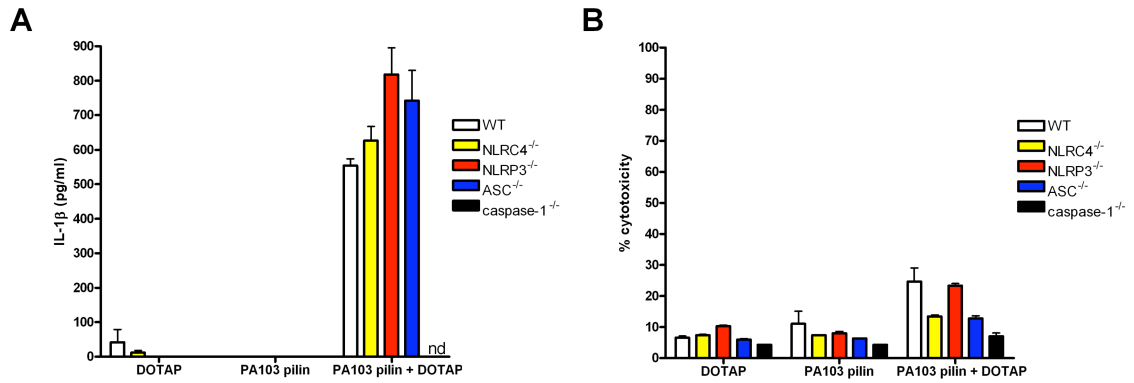
Figure 5.23; PA103 pilin-dependent inflammasome activation is dependent on caspase-1

LPS-primed BMDM from mice with KO:s for specific inflammasome components were transfected with DOTAP (2 μg/well), PA103 pilin (300 ng) or DOTAP together with PA103 pilin. Supernatants were analysed for IL-1β release by ELISA (A) and percent cytotoxicity by LDH release assay (B). Columns are means of triplicates and error bars are SEM. Nd is non-detected.

Similar to PA103 pilin, the inflammasome component dependence of recombinant pilin transfection was also investigated. Unexpectedly, it was found that inflammasome activation by transfected recombinant pilin is dependent on NLRP3, ASC and caspase-1 (Figure 5.24A). The cytotoxicity is equivalent and low in all samples (Figure 5.24B).
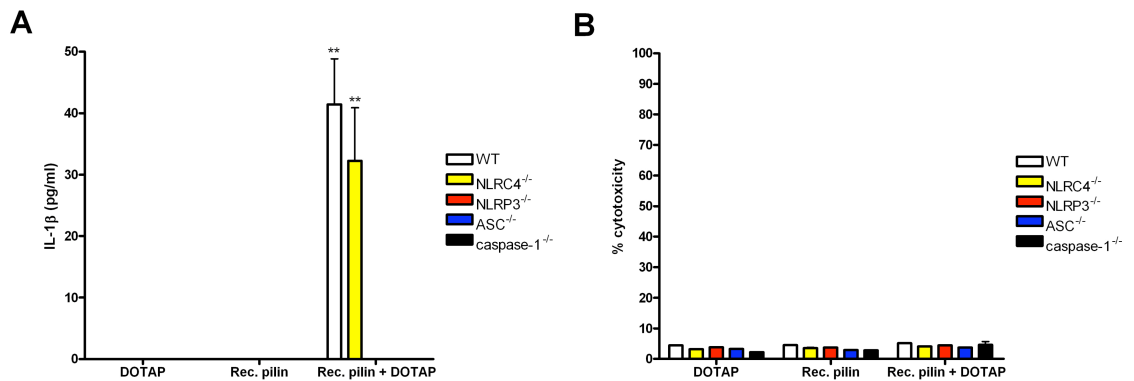
Figure 5.24; Recombinant pilin activates the inflammasomes dependent on NLRP3, ASC and caspase-1

LPS-primed BMDM from mice with KO:s for specific inflammasome components were transfected with DOTAP (2 μg/well), recombinant pilin (300 ng) or DOTAP together with recombinant pilin. Supernatants were analysed for IL-1β release by ELISA (A) and percent cytotoxicity by LDH release assay (B). Columns are means of triplicates and error bars are SEM. ** indicate significant difference compared to DOTAP alone where ** is $p<0.01$, unpaired Student's t-test.

The caspase-1 activation detected by immunoblotting in cell lysates following transfection with recombinant pilin corresponds to the IL-1ß secretion seen. Caspase-1 is activated in a NLRP3, ASC and caspase-1 dependent manner (Figure 5.25).
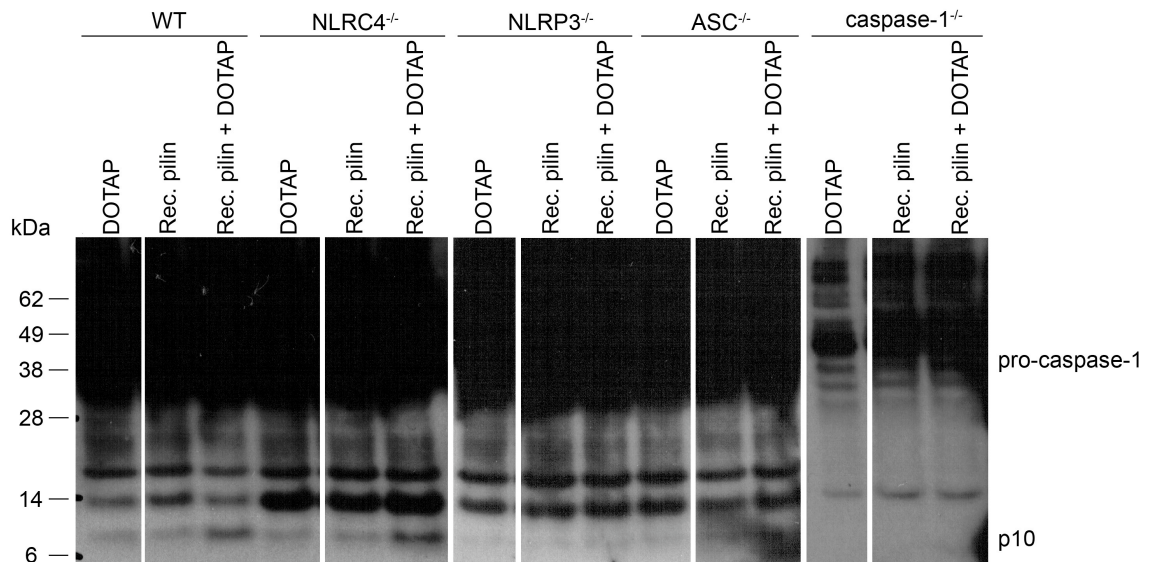
Figure 5.25; Caspase-1 activation by recombinant pilin is dependent on NLRP3, ASC and caspase-1

Cell lysates from Figure 5.24 were immunoblotted with caspase-1 antibody.

No difference could be detected in IL-1 release between A/J mice and C57Bl/6 mice following infection with *P.aeruginosa*, which implies that NAIP5 is not involved in the inflammasome activation by this bacterium, described in chapter 3.2.3. No difference in IL-1ß secretion following transfection with PA103 pilin could be seen in A/J mice compared to C57/BL6 (Figure 5.26A). Similar to effects seen during infection, a slightly higher cytotoxicity could be detected in the C57/BL6 cells compared to A/J cells for all samples tested (Figure 5.26B). The reason for this remains unknown.

A

IL-1β (pg/ml)

70 — 60 — 50 — 40 — 30 — 20 — 10 — 0

□ C57/BL6
■ A/J

(-)   DOTAP   Pilin   Pilin + DOTAP   OVA   OVA + DOTAP

B

% cytotoxicity

10 — 9 — 8 — 7 — 6 — 5 — 4 — 3 — 2 — 1 — 0

□ C57/BL6
■ A/J

(-)   DOTAP   Pilin   Pilin + DOTAP   OVA   OVA + DOTAP
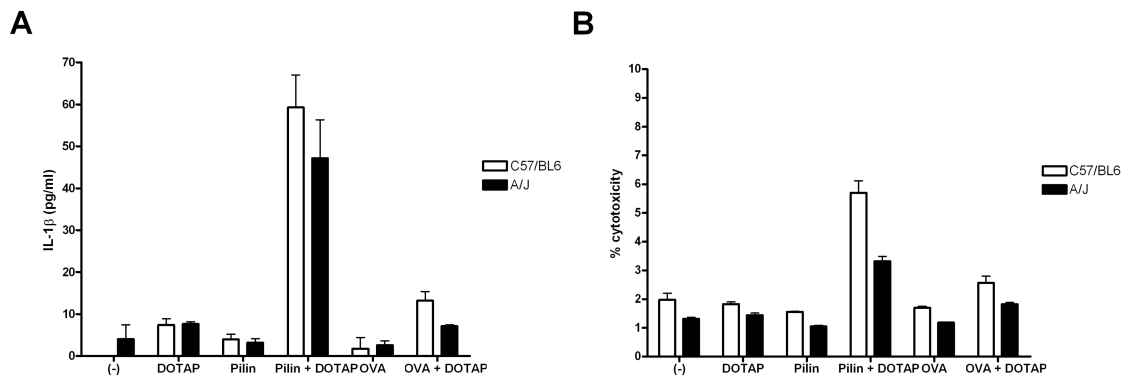
Figure 5.26; Inflammasome activation by PA103 pilin is not affected in A/J mice

LPS-primed BMDM from C57/BL6 and A/J mice were transfected with indicated samples (500 ng protein and 2 µg/well DOTAP). Supernatants were analysed for IL-1β release by ELISA (A) and percent cytotoxicity by LDH release assay (B). Columns are means of triplicates and error bars are SEM.

5.2.6 Retroviral transduction of pilin

A recently published method investigated the effect of retrovirally transduced flagellin on inflammasome activation, using inflammasome-dependent cell death, pyroptosis, as the marker of inflammasome activation [312]. It is argued that this eliminates the possibility that bacterial secretion systems, transfection reagents and/or bacterial contaminants that might contribute to the activation of caspase-1 [312]. So far the results presented in this chapter have investigated a pilin-dependent inflammasome activation following transfection of the protein. To investigate whether pilin can activate caspase-1 after retroviral transduction similar to flagellin, PA103 pilin was cloned into the retroviral MigR1 vector. This vector will express cloned DNA, as well as GFP, via an internal ribosomal entry site (IRES). Thus, GFP expression can serve as a surrogate for expression of the cloned DNA. Retroviruses were generated from the retroviral packaging cell line GP+E.86 and BMDM were transduced with these viruses. Following incubation, the BMDM were analysed using FACS to detect GFP-expression. Untransduced BMDM were used as a control. Cells analysed on FACS were gated based on their side-scatter and forward-scatter properties (Figure 5.27). The cells were stained with 7AAD (a marker of cell viability) and the cells gated based on their FSC and SSC were further gated based on their 7AAD staining (Figure 5.27). 7AAD negative cells were then gated based on their GFP-expression into a high and total GFP-expressing population (Figure 5.27).

Untransduced cells do not express any GFP, as expected (Figure 5.27). Of the BMDM transduced with retroviral expression vector alone 6.21% expressed GFP and 1.69% of these were GFP high (Figure 5.27). In contrast BMDM transduced with MigR1 pilin had a lower level of GFP expression, 3.96%, and virtually no cells had high GFP expression (Figure 5.27). These results indicated that the cells could tolerate a low level of GFP expression following transfection with MigR1 pilin, but GFP high cells would die due to cytotoxicity caused by inflammasome activation by pilin.
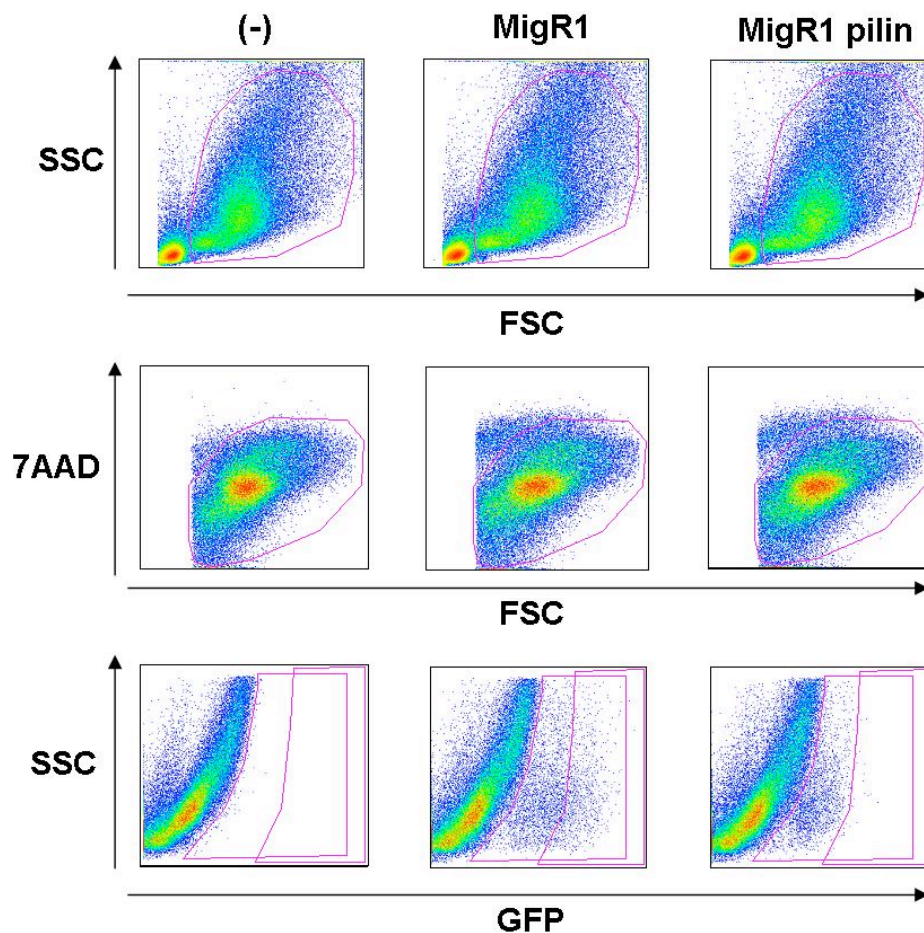
Figure 5.27; Gating during FACS analysis of retroviral transduced BMDM

Transduced or untransduced BMDM were first gated based on their forward and side scatter (SSC vs FSC where the gate is for 59.7% (-), 61.7% MigR1 and 63.1% MigR1 pilin, top panel). These were then gated based on 7AAD staining (Percent 7AAD⁻ 97.4% (-), 94.1% MigR1 and 94.3% MigR1 pilin, middle panel). 7AAD- cells were finally gated based on GFP expression (bottom panel). Two populations were indentified, GFP low (0.2% (-), 6.21% MigR1 and 3.96% MigR1 pilin) and GFP high (0% (-), 1.69% MigR1 and 0.048% MigR1 pilin).

Previously, it was shown that the GFP-expression following transduction with flagellin initially increased, but as the cells died the expression then decreased [312]. Therefore, BMDM were transduced with MigR1 or MigR1 pilin and analysed at set time points following this transduction. There was more GFP-expression at a higher level after transduction with MigR1 compared to MigR1 pilin at all time points (Figure 5.28). Again this indicates that there is a selective loss of cells transfected with MigR1 pilin that have high pilin expression levels.
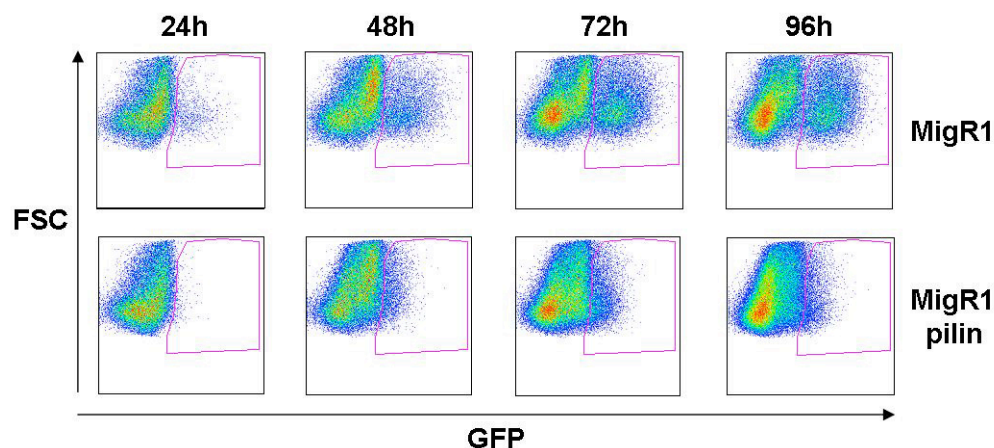
Figure 5.28; There are more GFP$^+$ cells following transduction with MigR1 compared to MigR1 pilin

BMDM were transduced with MigR1 or MigR1 pilin and incubated for indicated time points. 7AAD$^-$ cells were gated based on GFP expression. GFP$^+$ cells were after 24 h 4.44% for MigR1 compared to 0.79% for MigR1 pilin, after 48 h 14.3% MigR1 and 6.68% MigR1 pilin, after 72 h 25.4% MigR1 and 10.2% MigR1 pilin and after 96 h 25.9% MigR1 and 4.84% MigR1 pilin.

There were less GFP-positive cells expressed by the MigR1 pilin transduced BMDM compared to MigR1 transduced cells after 24 h. Due to this, earlier time points were investigated following transduction. Untransduced BMDM do not express any GFP (Figure 5.29A). The GFP-expression for both MigR1 and MigR1 pilin transduced cells increase over a 24 h time period (Figure 5.29A). However, the GFP-expression for MigR1 pilin remains lower than that for MigR1 for all time points. The GFP-expression for the samples shown in Figure 5.28 was also plotted against time for easier comparison (Figure 5.29B). Again, this shows a lower and steadier GFP-expression for MigR1 pilin transduced cells compared to MigR1 transduced cells. Finally the mean fluorescent intensity of the GFP-expression was plotted against time from the samples in Figure 5.28. This clearly

shows that the GFP-expression is at a higher level for cells transduced with MigR1 compared to cells transduced with MigR1 pilin (Figure 5.29C).
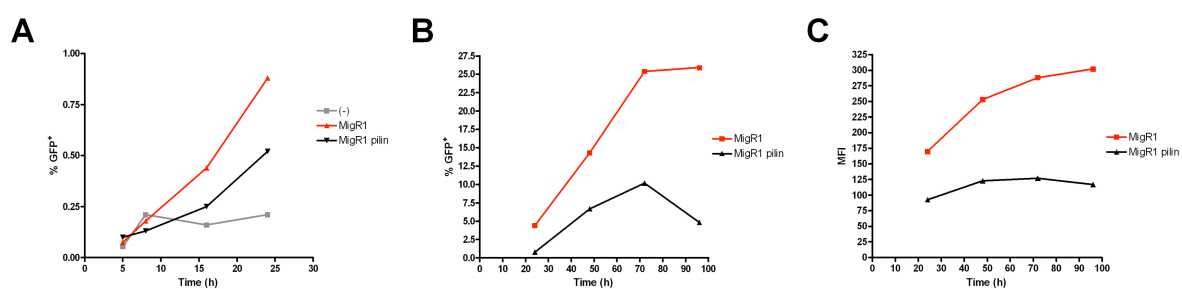
Figure 5.29; There are more GFP$^+$ cells for MigR1 transduced cells compared to MigR1 pilin

BMDM were transduced with MigR1 or MigR1 pilin and left for indicated time points. Cells were then analysed by FACS for GFP-expression. A, GFP-expression increase over 24 h for both MigR1 and MigR1 pilin, untransduced cells remains unaltered. % GFP$^+$ cells against time are plotted for each sample. B, GFP-expression increase over 96 h for MigR1 whereas MigR1 pilin has a much slower increase. % GFP$^+$ cells against time were plotted from Figure 5.28. C, MFI increase over 96 h for MigR1 whereas MigR1 pilin remains constant. Mean fluorescence intensity (MFI) for GFP$^+$ cells from B were plotted against time.

To investigate whether expression of pilin following transduction of BMDM is dependent on any known inflammasome components, cells from inflammasome KO mice were transduced with MigR1 and MigR1 pilin. More cells are 7AAD-positive when caspase-1 KO cells are transduced with MigR1 pilin compared to MigR1 (Figure 5.30A). All the other inflammasome KO cells have similar levels of cytotoxicity following transduction with MigR1 compared to MigR1 pilin (Figure 5.30A). The 7AAD-negative cells were further investigated for their GFP-expression. Similar levels of GFP-expression were observed for MigR1 and MigR1 pilin transduced cells in all KOs (Figure 5.30B). Thus, no inflammasome dependence could be observed for cells transduced with MigR1 pilin. This implies another reason to why the level of GFP-expression is lower in these cells, which will be discussed further in the discussion of this chapter.
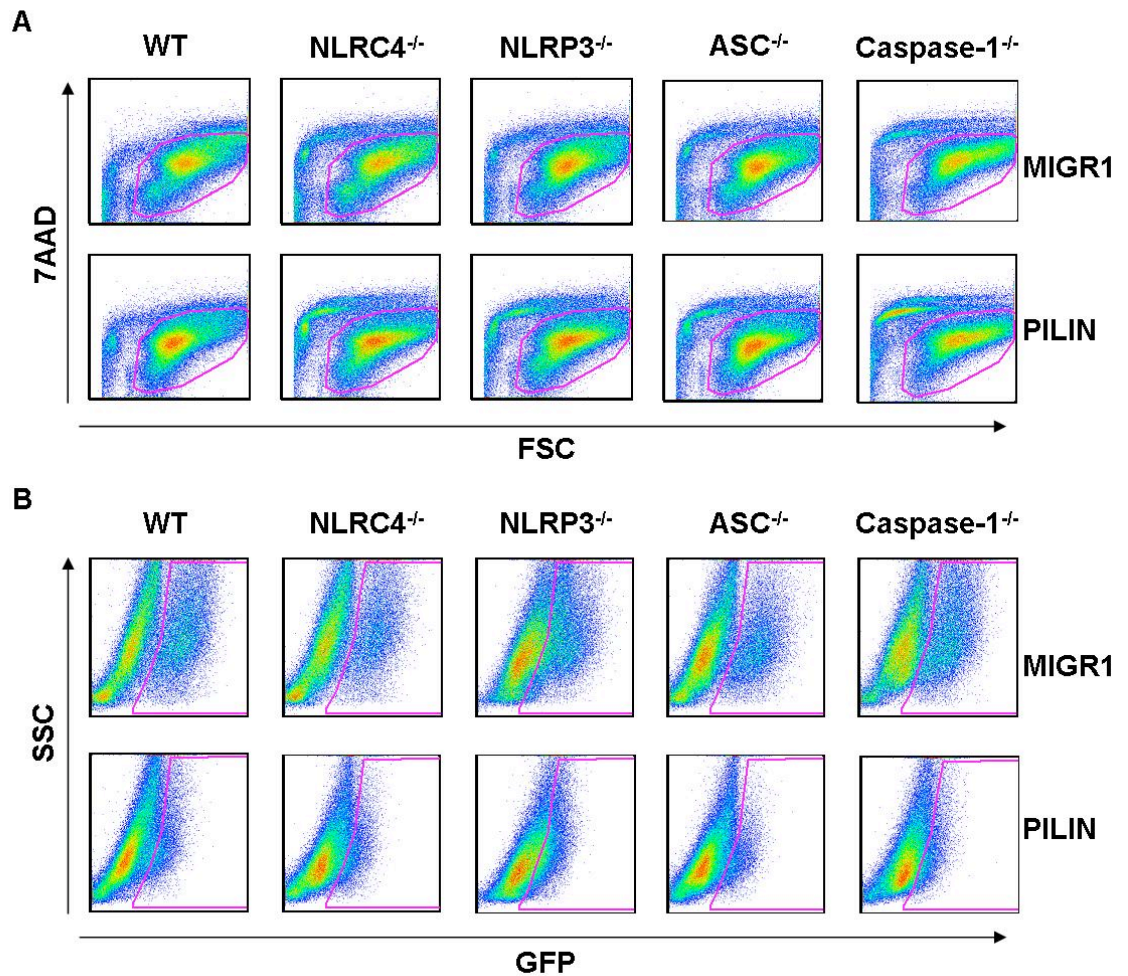
Figure 5.30; Retroviral transduction of inflammasome KO BMDM

BMDM from inflammasome KO mice were transduced with MigR1 or MigR1 pilin (PILIN) and analysed for GFP expression after 3 days. A, Cells were gated based on 7AAD-staining. % 7AAD⁻ cells for each condition; WT 74.6% MigR1 and 83.1% MigR1 pilin, NLRC4 71.3% MigR1 and 72.5% MigR1 pilin, NLRP3 78.6% MigR1 and 74.1% MigR1 pilin, ASC 77.3% MigR1 and 78.2% MigR1 pilin and caspase-1 74.9% MigR1 and 66.6% MigR1 pilin. B, 7AAD⁻ cells were gated based on GFP expression. GFP⁺ cells; WT 25.5% MigR1 and 9.62% MigR1 pilin, NLRC4 16.7% MigR1 and 10.6% MigR1 pilin, NLRP3 34.1% MigR1 and 23.5% MigR1 pilin, ASC 18.7% MigR1 and 8.08% MigR1 pilin and caspase-1 26.2% MigR1 and 10.2% MigR1 pilin.

The GFP-expression is consistently lower when BMDM are transduced with MigR1 pilin compared to MigR1 alone. To investigate whether mutations of the pilin gene would result in increasing GFP-expression the MigR1 pilin was mutated by site-directed mutagenesis. This was performed by Prof. Tom Evans in the lab. The mutations chosen were based on the pilin structure [40]. The pilin gene in the MigR1 vector was truncated by insertion of a stop codon immediately upstream of the disulfide bond, MigR1 pilin T133*. The second mutation introduced replaced the cysteine, which is important in disulphide bonded loop

formation [40, 448], MigR1 pilin C134A. BMDM were then transduced with these constructs. No difference could be seen in GFP-expression comparing the different MigR1 pilin constructs (Figure 5.31). In addition cells were treated with LPS 12 h before analysis on the FACS, in order to investigate whether any IL-1ß secretion or caspase-1 activation could be detected from these cells. The LPS treatment resulted in a lot of cell death and even less GFP-expression, but the levels were similar between samples, as seen before (Figure 5.31). No IL-1ß secretion could be detected in any of the samples (results not shown). Transduced cells were also sorted based on their GFP-expression. GFP-positive cells were lysed and immunoblotted with caspase-1 antibody to investigate whether pilin transduction results in caspase-1 activation, but no active caspase-1 could be detected (results not shown).
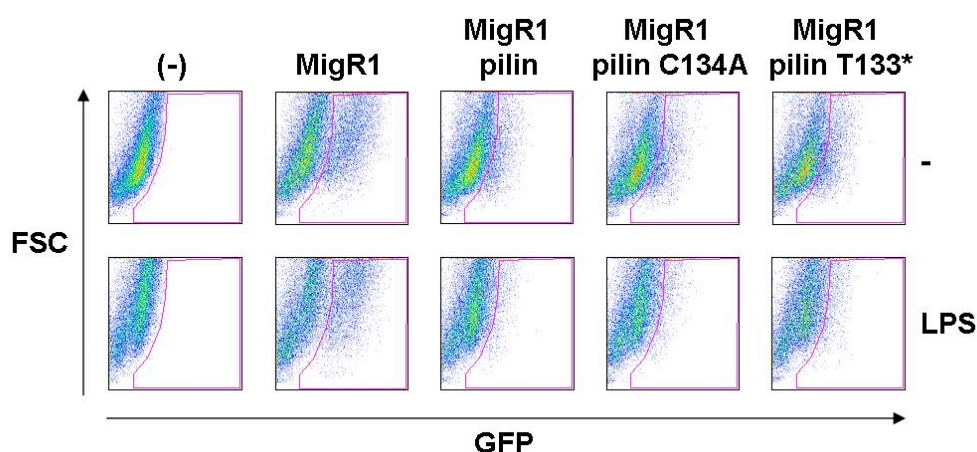
Figure 5.31; Mutation of pilin does not alter its ability for GFP expression following transduction

BMDM were transduced with indicated MigR1 constructs, after 3 days cells were treated with 50 ng/ml LPS for 12 h and then analysed using FASC for GFP expression. Percent GFP^{+} cells without LPS; 0.076% (-), 21.9% MigR1, 4.85% MigR1 pilin, 5.93% MigR1 pilin C134A and 7.07% MigR1 pilin T133*. Percent GFP+ cells following treatment with LPS; 0.077% (-), 31.3% MigR1, 3.43% MigR1 pilin, 3.97% MigR1 pilin C134A and 5.7% MigR1 pilin T133*.

5.2.7 Role of pilin in infection; PA103 pilA[-]

Pilin transfection activates the inflammasome in a caspase-1 dependent manner, as shown in section 5.2.5 of this chapter. Furthermore, it was shown in chapter 3 that a non-flagellated strain of *P.aeruginosa* can activate the NLRC4 inflammasome, dependent on ASC. This has also been shown previously [249]. Therefore, the effect of pilin in infection was investigated next. Pilin is

important for attachment to the cells [44-46], therefore a deletion of pilin might influence the ability of the bacteria to cause infection. PA103 pilA⁻ was available in the lab and the effect of this strain on inflammasome activation was investigated. Following infection with PA103 pilA⁻ significantly less IL-1ß was secreted compared to cells infected with PA103 ΔUΔT (Figure 5.32A). The lack of IL-1ß secretion was present in all strains exhibiting a functional ExoU effector i.e. PA103 WT, pilA⁻ and ΔUΔT:ExoU (Figure 5.32A). In contrast IL-1ß was secreted from PA103 strains lacking ExoU, i.e. ΔUΔT and ΔUΔT:ExoUS142A (Figure 5.32A). Even though no IL-1ß was secreted from strains with a functional ExoU effector these strains still caused cytotoxicity (Figure 5.32B). This indicates that all strains tested with a functional ExoU can translocate the toxin, which results in ExoU-dependent cytotoxicity.
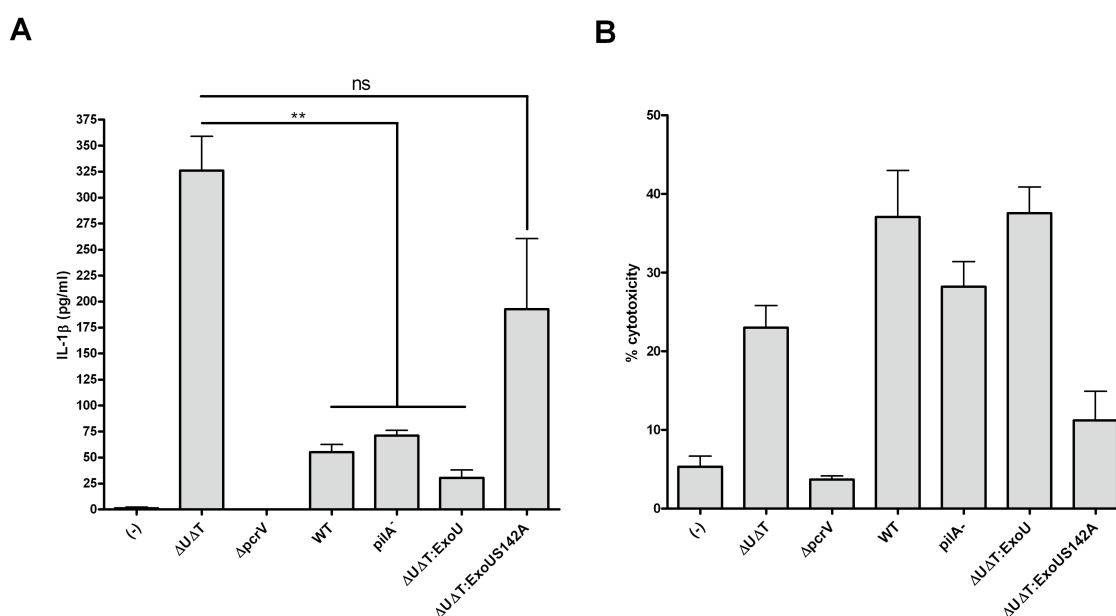
Figure 5.32; PA103 pilA⁻ can translocate ExoU

BMDM were infected with indicated PA103 strains at a MOI of 30 for 90 min. Supernatants were analysed for IL-1β release by ELISA (A) and percent cytotoxicity by LDH release assay (B). Columns are means of triplicates and error bars are SEM. ** indicate significant difference where ** is $p<0.01$, ns is non-significant difference $p>0.05$, unpaired Student's t-test.

The IL-6 and TNF-α released following infection with the PA103 strains were also measured. A similar level of IL-6 was released following infection with all these strains (Figure 5.33A) and the same was true for TNF-α (Figure 5.33B).
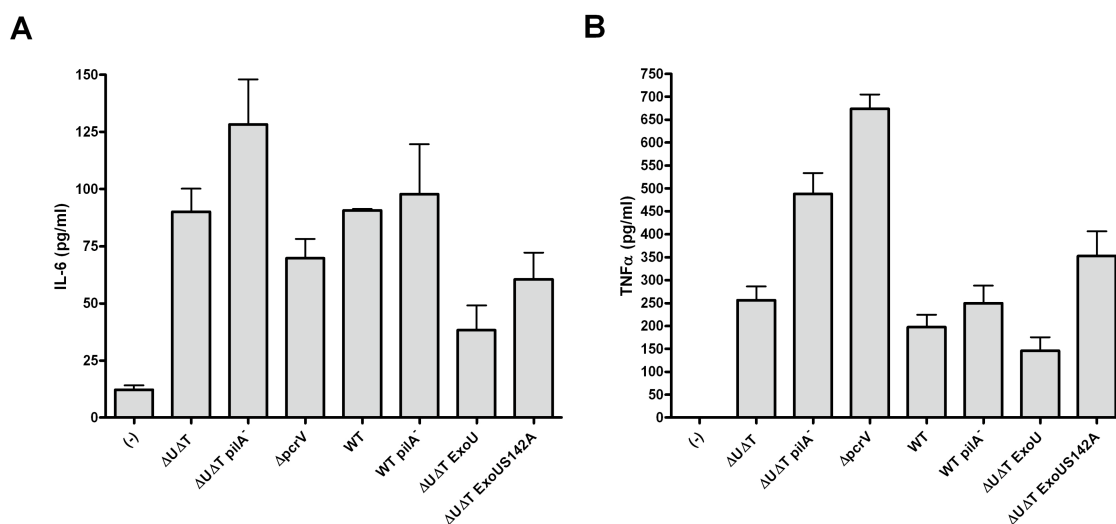
Figure 5.33; The same amount of IL-6 and TNF-α is released following infection with PA103 mutants

BMDM were infected with indicated PA103 strains at a MOI of 50 for 90 min. Supernatants were analysed for IL-6 release (A) and TNF-α release (B) by ELISA. Columns are means of triplicates and error bars are SEM.

The strains with a functional ExoU, PA103 WT and pilA-, fail to activate IL-1β secretion following infection (Figure 5.32). These strains also fail to activate caspase-1, as expected from the IL-1β secretion results (Figure 5.34). In contrast, the strains lacking a functional ExoU, PA103 ΔUΔT and ΔUΔT:ExoUS142A, activate caspase-1 and a p10 band can be detected by immunoblotting (Figure 5.34). This is dependent on a functional T3SS, as described in chapter 3 and shown here, since PA103 ΔpcrV does not result in caspase-1 activation (Figure 5.34).
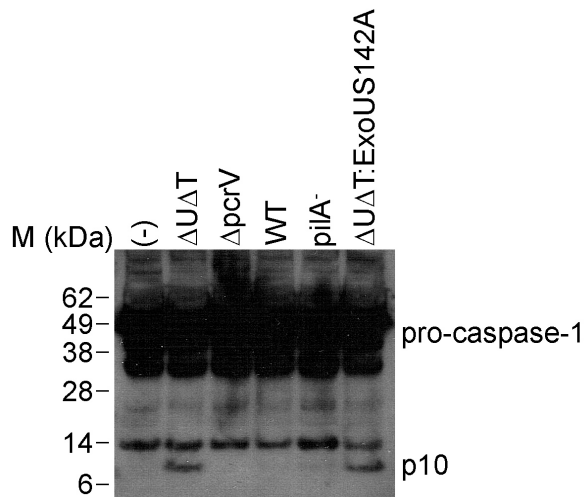
Figure 5.34; ExoU inhibits caspase-1 activation

BMDM were infected with indicated PA103 strains for 90 min at a MOI of 30. Cell lysates were immunoblotted with caspase-1 antibody. Activated caspase-1 (p10) and pro-caspase-1 is detected.

MAFP is an irreversible phospholipase A inhibitor, which has been shown to specifically inhibit ExoU-dependent cytotoxicity [142, 143]. MAFP is able to inhibit the ExoU cytotoxicity since ExoU is a potent intracellular phospholipase [143]. Previous results indicate that PA103 pilA⁻ can translocate ExoU into the cell leading to ExoU dependent cytotoxicity (Figure 5.32B). If the cytotoxicity is caused by ExoU translocation it should be possible to inhibit it with MAFP treatment. BMDM were treated with MAFP and then infected with a range of PA103 strains. All strains with a functional ExoU, PA103 WT, pilA⁻ and ΔUΔT:ExoU, caused significantly less cytotoxicity in MAFP treated cells (Figure 5.35A). In contrast, the cytotoxicity caused by PA103 ΔUΔT and PA103 ΔUΔT:ExoUS142A was not inhibited by MAFP since these strains lack a functional ExoU (Figure 5.35A). The amount of cytotoxicity caused by PA103 pilA⁻ was similar to the cytotoxicity caused by PA103 WT (Figure 5.35A), indicating that PA103 pilA⁻, despite lacking pilin is able to translocate toxins at a similar level to PA103 WT. Unexpectedly, MAFP had a significant effect on the IL-1β secretion from all PA103 strains independent of ExoU expression (Figure 5.35B).
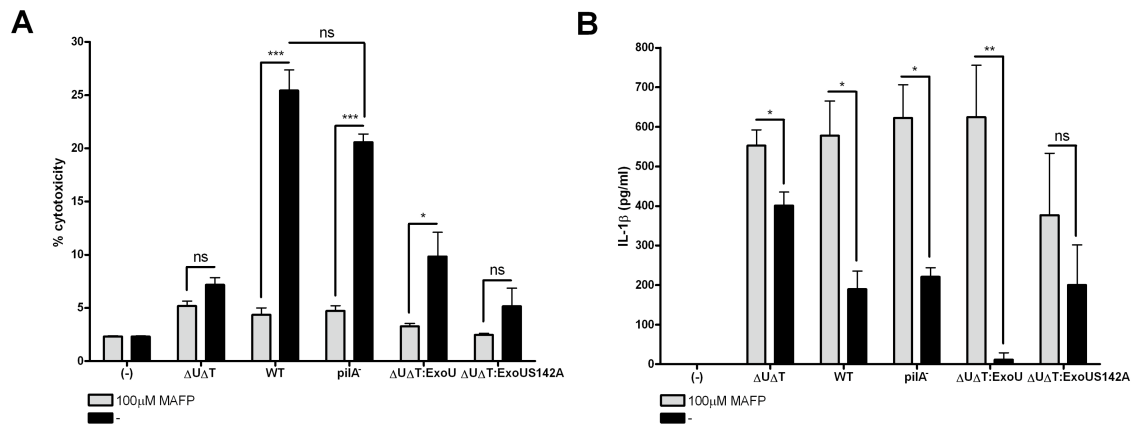
Figure 5.35; MAFP can inhibit cell death caused by PA103 pilA⁻

LPS-primed BMDM pretreated with 100 µM MAFP 60 min before or left untreated were infected with indicated PA103 strains at a MOI of 30 for 90 min. Supernatants were analysed for percent cytotoxicity by LDH release assay (A) and IL-1β release by ELISA (B). Columns are means of triplicates and error bars are SEM. Asterixes indicate significant difference where * is p<0.05, ** is p<0.01 and *** is p<0.001, ns is non-significant difference p>0.05, unpaired Student's t-test.

In addition to an effect on IL-1ß secretion by MAFP treatment the caspase-1 activation was increased following treatment with MAFP in all PA103 strains (Figure 5.36). The reasons for this effect are unknown and require further investigation.
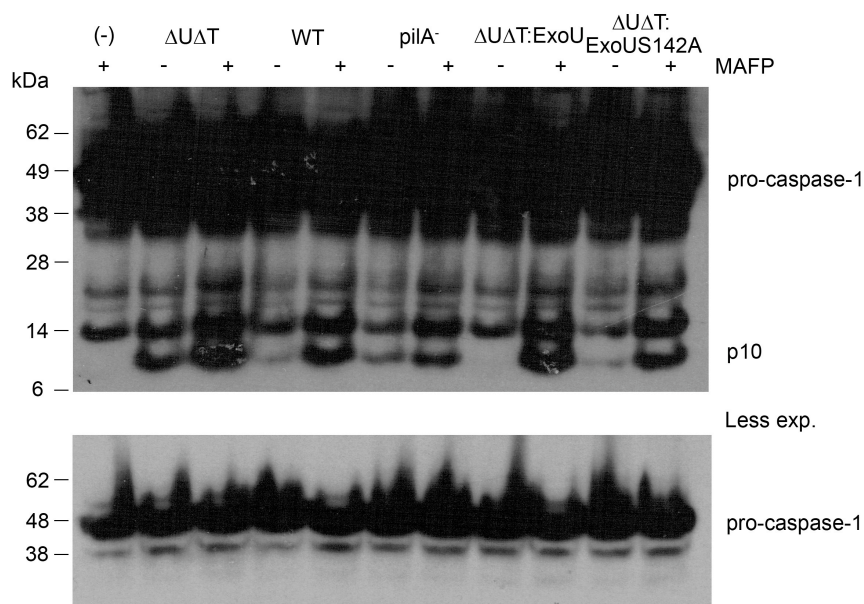
Figure 5.36; MAFP causes caspase-1 activation

Cell lysates from Figure 5.35 were immunoblotted with caspase-1 antibody. Top panel shows activated caspase-1 (p10). Bottom panel shows pro-caspase-1 on a less exposed film.

The results presented here show that PA103 pilA⁻ is able to translocate ExoU to the same extent as PA103 WT. However, due to the effect of ExoU on inflammasome activation this strain is not suitable for inflammasome activation studies for the role of pilin in infection.

5.2.8 Role of pilin in infection, PA103 ΔUΔT:pilA⁻

In order to investigate the role of pilin in an infection model, PA103 ΔUΔT:pilA⁻ was constructed. DNA from PA103 pilA⁻ was transformed into PA103 ΔUΔT and following recombination the mutants were selected. As previously described, in the introduction, type IV pili mediate attachment, as well as twitching motility [55, 449]. Therefore the ability of PA103 ΔUΔT and PA103 ΔUΔT:pilA⁻ to twitch was investigated on twitch agar. After incubation a pilin-dependent twitch zone was observed for PA103 ΔUΔT (Figure 5.37). In contrast no twitch zone could be observed for PA103 ΔUΔT:pilA⁻, which confirms that this strain lacks pilin expression (Figure 5.37).
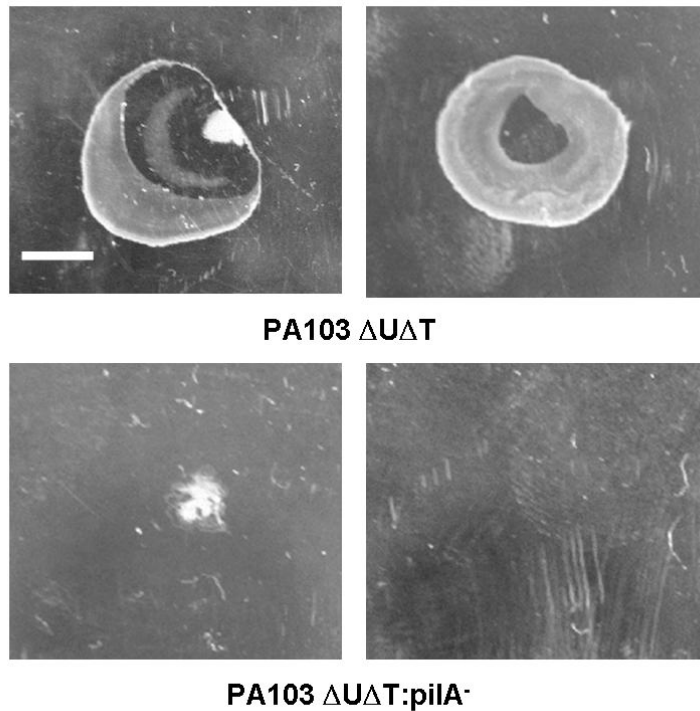
Figure 5.37; PA103 ΔUΔT:pilA⁻ does not twitch

PA103 ΔUΔT and PA103 ΔUΔT:pilA⁻ were inoculated beneath twitch agar. After two days the agar was peeled off and the twitch zone was photographed. White scale bar is 10 mm.

Since PA103 pilA⁻ were able to translocate effectors during infection, it was presumed that PA103 ΔUΔT:pilA⁻ was fully functional despite its pilin deletion. The effect of this strain on inflammasome activation was therefore investigated. No IL-1ß secretion can be detected following infection with PA103 ΔUΔT:pilA⁻ at varied MOIs (Figure 5.38A). In contrast to PA103 ΔUΔT, which results in significantly more IL-1ß secretion at all conditions tested compared to cells alone (Figure 5.38A). No difference could be detected between PA103 ΔUΔT and PA103 ΔUΔT:pilA⁻ in cytotoxicity caused or in IL-6 and TNF-α secretion (Figure 5.38B,C,D).
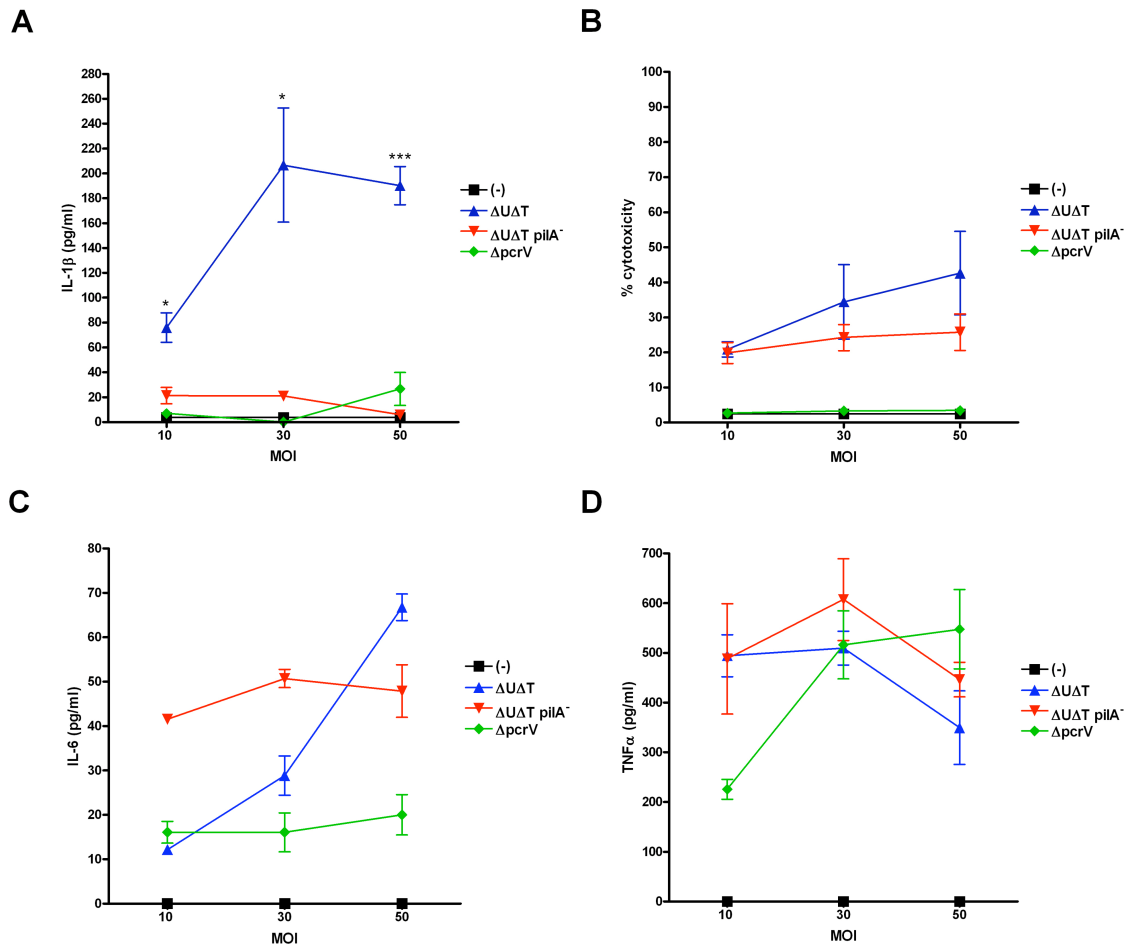
Figure 5.38; PA103 ΔUΔT:pilA⁻ fail to activate the inflammasome

BMDM were infected with indicated PA103 strains for 90 min at indicated MOIs. Supernatants were analysed for IL-1β (A), IL-6 (C) and TNF-α (D) release by ELISA and for percent cytotoxicity by LDH release assay (D). Means for triplicates are plotted and error bars are SEM. * and *** indicate significant difference compared to cells alone where * is p<0.05 and *** is p<0.001, unpaired Student's t-test.

Caspase-1 activation is also impaired in PA103 ΔUΔT:pilA⁻ compared to PA103 ΔUΔT. A very weak p10 band could be detected in all PA103 ΔUΔT:pilA⁻ samples compared to a stronger band in PA103 ΔUΔT samples by immunoblotting (Figure 5.39).
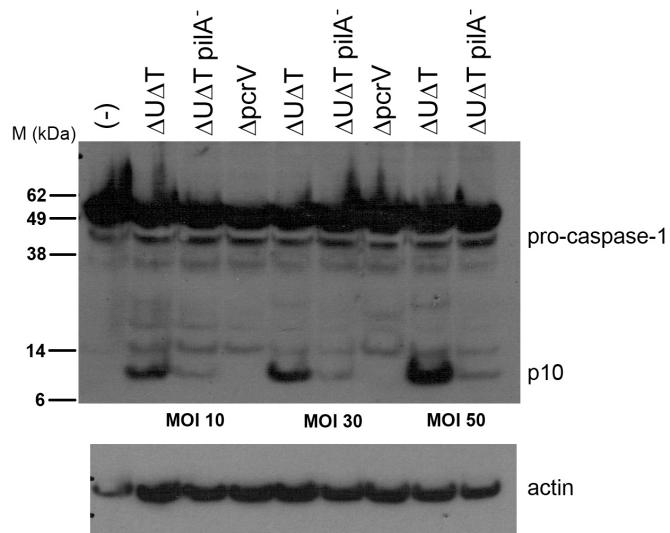
Figure 5.39; PA103 ΔUΔT:pilA⁻ does not activate caspase-1 to the same extent as PA103 ΔUΔT.

Cell lysates from Figure 5.38 were immunoblotted with caspase-1 antibody. Activated caspase-1 (p10) and pro-caspase-1 is shown on top panel. The blot was reprobed with actin antibody to show even loading (bottom panel).

Attempts were then made to complement the PA103 ΔUΔT:pilA- strain with a plasmid containing pilin from PA103 to restore its ability to activate the inflammasome complex. Unfortunately this was never successful; any double resistant mutants obtained could not be further propagated either in liquid broth or following restreaking onto a new agar plate. The reason for this is unknown. However, we were successful in complementing PAO1 pilin mutants with an expression vector encoding pilin from PAO1, described below in section 5.2.9.

The results presented in this section show that PA103 ΔUΔT activates the inflammasome in a T3SS- and pilin-dependent manner.

5.2.9 Role of pilin in infection by PAO1

PAO1 was previously shown to activate the inflammasome in a flagellin-dependent manner, section 5.2.1. To investigate whether pilin has a role in the inflammasome activation by this strain pilin mutants was studied. PAO1 WT express pilin and form twitch zones after incubation under twitch agar (Figure 5.40). As expected, no twitch zone could be detected for PAO1 FliC-pilA⁻, but this could be restored by transforming this strain with a PA1O3 pilin expressing plasmid (Figure 5.40).
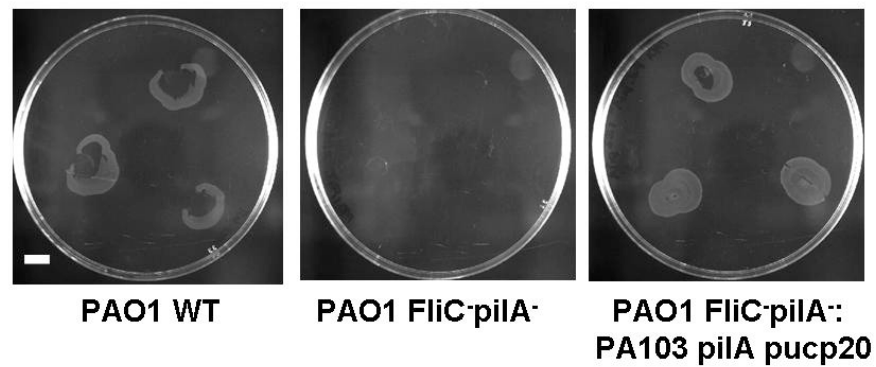
Figure 5.40; PAO1 WT PAO1 FliC⁻pilA⁻:PA103 pilA pucp20 twitch, whereas PAO1 FliC⁻pilA⁻ does not

PAO1 strains were inoculated beneath twitch agar. After two days the agar was peeled off and the twitch zone was photographed. White scale bar is 10 mm.

The IL-1ß secretion following infection with PAO1 pilA⁻ is similar to the secretion seen after infection with PAO1 WT (Figure 5.41A). In contrast, strains lacking flagellin, PAO1 FliC⁻ and FliC⁻pilA⁻ do not induce IL-1ß secretion after infection (Figure 5.41A). Note that the activation of the inflammasome by PAO1 pilA⁻ is additional evidence that pili are not required for effective type III secretion into macrophages, since inflammasome activation by this strain is entirely dependent on the T3SS.

The IL-1ß secretion by FliC⁻pilA⁻ could be restored by transforming the strain with a PAO1 pilin expression plasmid (Figure 5.41A). Following transformation with a PA103 expression plasmid (Figure 5.41A), IL-1 ß secretion was also increased, but this did not achieve statistical significance, which will be discussed further below. The PA103 strains are included as reference and the effects seen are similar to those described in section 5.2.8. The cytotoxicity resulting from PAO1 infection is also dependent on flagellin with a pattern similar to the IL-1ß secretion seen (Figure 5.41B).

A   **B**
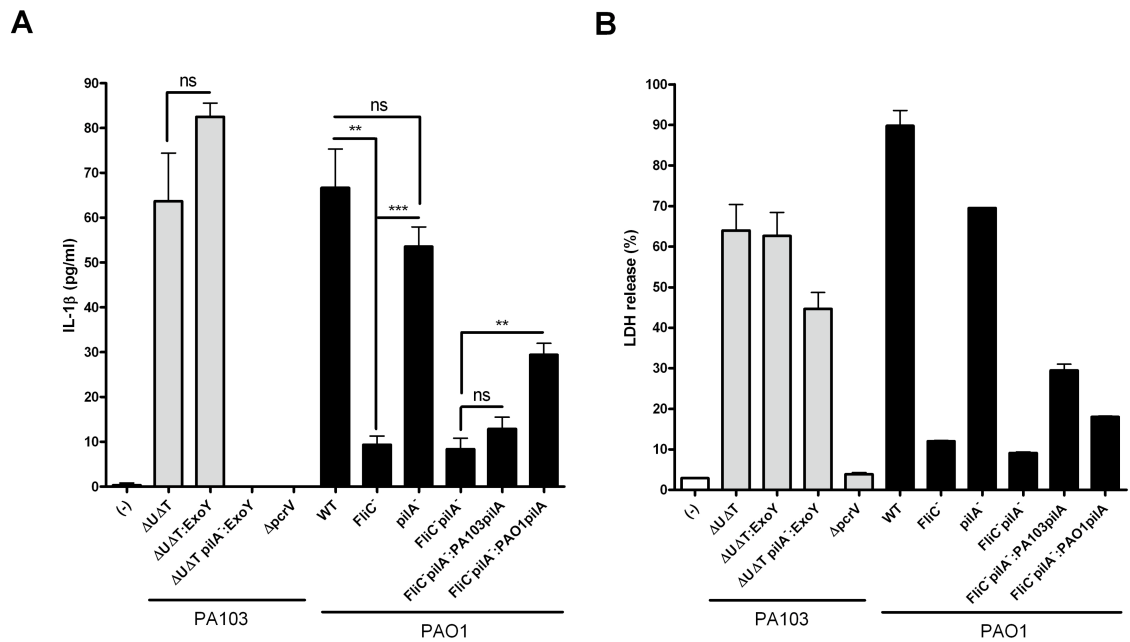
Figure 5.41; Flagellin-dependent inflammasome activation by PAO1

BMDM were infected with indicated PA103 and PAO1 strains at a MOI of 20 for 90 min. Supernatants were analysed for IL-1β release by ELISA (A) and percent cytotoxicity by LDH release assay (B). Columns are means of triplicates and error bars are SEM. Asterixes indicate significant difference where ** is p<0.01 and *** is p<0.001, ns is non-significant difference p>0.05, unpaired Student's t-test.

The IL-1β secretion following infection with PAO1 strains are dependent on flagellin. The caspase-1 activation also corresponds to these results, where strains that lack flagellin fail to activate caspase-1 (Figure 5.42). In contrast the caspase-1 activation in a flagellin and pilin deficient strain can be restored by the expression of PAO1 pilin (Figure 5.42). There is some p10 detected following infection of BMDMs with PAO1 FliC⁻pilA⁻: pUCP20 PA103 pilin, which can be detected after a longer exposure (Figure 5.42). There is a small non-significant increase in IL-1β secretion following infection with this strain compared to PAO1 FliC⁻pilA⁻, which could be explained by the caspase-1 activation seen (Figure 5.41 & 1.44).
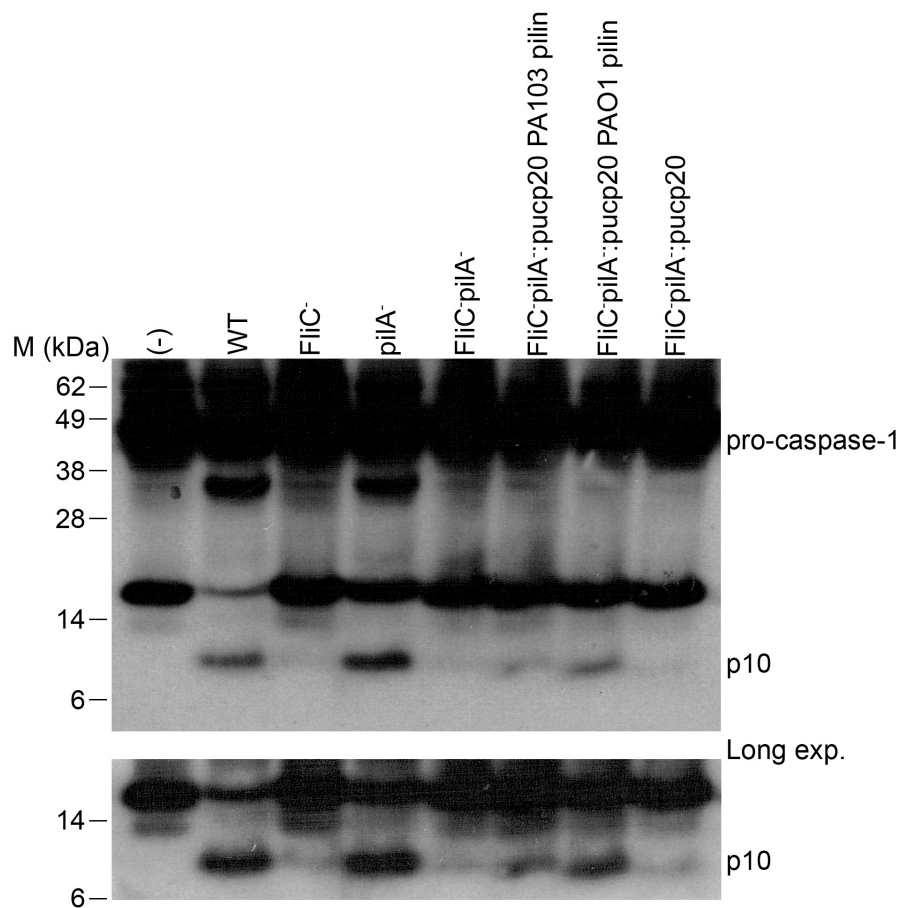
Figure 5.42; Flagellin-dependent caspase-1 activation by PAO1

BMDM were infected with indicated PAO1 strains at a MOI of 30 for 90 min. Cell lysates were immunoblotted with caspase-1 antibody. Top panel shows pro-caspase-1 and activated caspase-1 (p10). Bottom panel shows a longer exposure of activated caspase-1.

In previous publications, infections by strains lacking flagellin and pilin have been centrifuged immediately after bacterial addition to the cell culture [249, 390]. It is argued that this will help the non-motile bacteria to reach the cells and cause infection. In order to investigate this in the infection model used in this study, cultures centrifuged immediately following infection were compared to cultures which were left unspun. The IL-1β secretion following centrifuged cultures is similar in all samples tested (Figure 5.43A). In contrast, when cultures are left uncentrifuged the IL-1β secretion corresponds to results described in previous figures where IL-1β secretion by PAO1 is dependent on flagellin and the secretion can be restored by introducing PAO1 pilin (Figure 5.43A). Furthermore, centrifugation of the cultures result in increased cytotoxicity for most of the samples (Figure 5.43B), which indicate an added stress for the cells introduced by the centrifugation step.
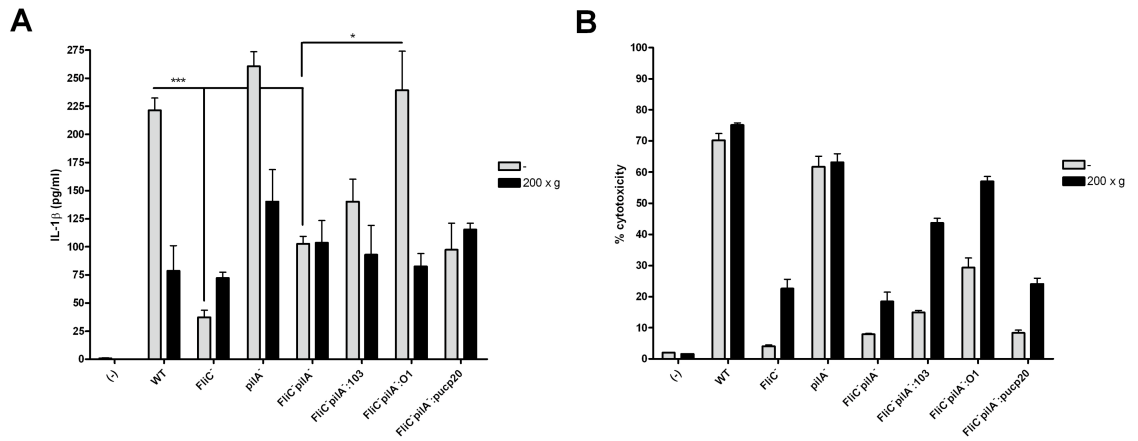
Figure 5.43; Inflammasome activation by PAO1 is flagellin-dependent but pilin-indpendent

BMDM were infected with indicated PAO1 strains at a MOI of 30 for 90 min. Immediately following addition of the bacteria half of the samples were centrifuged at 200 x g for 5 min. Supernatants were analysed for IL-1β release by ELISA (A) and percent cytotoxicity by LDH release assay (B). * and *** indicate significant difference where * is $p < 0.05$ and *** is $p < 0.001$, unpaired Student's t-test.

These results show a minor role for pilin-dependent inflammasome activation by PAO1 in the presence of flagellin expression. This will be discussed further below.

5.3 Discussion

P.aeruginosa activates the inflammasome in a NLRC4- and ASC-dependent manner during infection, as described in chapter 3. This has also been described in the literature [249, 253, 354]. The results in this chapter show that PA103 ΔUΔT can activate the inflammasome complex independent of flagellin, since this strain does not express flagellin. Flagellin-independent activation of the NLRC4-inflammasome has also been described by Sutterwala et al. [249]. In addition flagellin-independent but T3SS-dependent inflammasome activation by *Salmonella* at higher MOIs was described by Miao et al. [337]. The mediator of this inflammasome activation has not yet been identified, but results presented in this chapter indicate that type IV pilin can activate the inflammasome and it is responsible for the activation produced by PA103 ΔUΔT.

The amount of IL-1β detected following transfection with pilin, as well as flagellin, presented in this chapter is similar to the amount seen for flagellin in previous publications [337]. There is a variation between different experiments in the amount of IL-1β secretion. Possible explanations include variations between batches of primary BMDM, different pilin preparations and, as discussed below, differences between batches of DOTAP and transfection efficiency.

A range of transfection reagents was tried for the protein transfection during the time of this project. Following optimisation it was found that DOTAP gave the most reproducible results. FuGene (Roche), Proteojuice (Novagen) and TransPass P (NEB) were found to cause a high amount of cytotoxicity following transfection of the cells. However, DOTAP transfection efficiency and cytotoxicity varies from batch to batch. This is the reason to why some experiments have a relatively high IL-1β secretion following DOTAP treatment alone. It should be noted that the levels for pilin together with DOTAP were always higher than DOTAP alone. This also poses a problem for the detection of caspase-1 activation by immunoblotting.

The results presented here show that pilin, as well as flagellin, has to be transfected into the cells in order to promote inflammasome activation. No effect can be detected following treatment of cells with flagellin, pilin or DOTAP

alone. This is in agreement with previously published results [236, 390]. BMDM does not express TLR5, which means there will not be an effect of flagellin alone via TLR5 signalling [450]. It was found in previous publications that the inflammasome activation by flagellin is independent of potassium efflux when transfected into the cells [236]. Due to time constraints the role of potassium following pilin transfection was not investigated in this study. However, as previously discussed in chapter 4, the inflammasome activation following infection with PA103 is highly dependent on potassium. This implies that the inflammasome activation by pilin is indeed dependent on potassium but studies are needed to confirm this hypothesis. However, there is a possibility that the method of delivery affects the dependence of potassium. Again, no conclusions can be drawn until the experiments have been performed.

When attempts were made to purify pilin from PAO1 it was found that PAO1 FliC$^-$ had to be used in order to obtain pilin. Following the pilin purification method used in this chapter on PAO1 WT, only purified flagellin with no band for pilin were obtained. The reason for this is unknown. Possibly, PAO1 WT does not express a lot of pilin when flagellin is expressed, or that pilin is not readily released from cells in the presence of flagellin.

Pilin has been shown to bind DNA [451] and DNA has been shown to activate caspase-1 and IL-1ß secretion [440]. Therefore, the purified pilin preparations might be contaminated by DNA. However, the inflammasome activation following DNase I treatment of pilin was unaltered. This further strengthens the theory that pilin is able to activate the inflammasome complex and that the inflammasome activation seen is not due to DNA contamination of the purified pilin. Additionally, DNA activation of the inflammasome is NLRP3 dependent in contrast to the activation produced by pilin, discussed below.

Proteinase K treatment of pilin results in less inflammasome activity, as described in section 5.2.2. Previous published results showed a complete abrogation of inflammasome activation by Proteinase K treated flagellin [337]. The differences might be due to the different properties of flagellin compared to pilin, or due to different digest times by Proteinase K. Miao et al. digested the flagellin overnight whereas the pilin in this study was digested for 60 min, according to manufacturer's instructions. There was an undigested portion left

following Proteinase K treatment of pilin, which might account for the remaining inflammasome activation seen. There is a possibility that this undigested core would be digested following longer incubation with Proteinase K. Alternatively, there is a portion of pilin which is resistant to Proteinase K treatment. Further investigation is needed in order to prove these hypotheses.

Caspase-1 activation by pilin was investigated by immunoblotting of cell lysates in this study. This proved successful when the inflammasome activation by *P.aeruginosa* was investigated, described in chapter 3. It proved more difficult to detect caspase-1 activation following pilin transfection. There are a lot of parameters which affect the detection, such as transfection efficiency, time and antibody batch, as well as the streptavidin being used. Several other studies have investigated caspase-1 activation in the supernatants [238, 452], however this did not provide any better results when tried in this study. Other studies have used another antibody for the detection of activated caspase-1 but this antibody is not available commercially and thus could not be used in this study. However, the IL-1ß secretion and the immunoblots that worked clearly demonstrate a role for pilin in inflammasome activation.

IL-6 secretion is not dependent on pilin transfection. In addition, IL-6 secretion is unaltered for the PA103 ΔUΔT:pilA⁻ strain. The same results were observed for TNF-α. This has previously been reported for flagellin-dependent inflammasome activation by *Salmonella* [390].

Individual pilin subunits have been found to be insoluble, full-length pili from *P.aeruginosa* strain PAK could only be crystallised in the presence of detergent [42]. This is a useful approach for crystallisation studies but not very useful during transfection studies. However, if the hydrophobic N-terminal region of 28 amino acids is removed this makes it possible to purify soluble pili subunits [40, 41]. This approach was therefore used in order to purify recombinant PA103 pilin from *E.coli*.

Transfection with PA103 pilin results in a caspase-1 dependent inflammasome response. Any other NLR-proteins involved are yet to be determined. This could be initially investigated by shRNA silencing of NLR-proteins or by the use of other KO cells. Due to the time constraints of this project it has not yet been

investigated. In contrast, infection with PA103 ΔUΔT results in NLRC4- and ASC-dependent inflammasome activation, which is clearly different from the transfected pilin. This has previously been described for DNA-dependent inflammasome activation [440]. Internalised adenoviral DNA induce NLRP3- and ASC-dependent inflammasome response, whereas transfected DNA results in ASC-dependent but NLRP3-independent inflammasome activation. The difference seen for pilin-dependent inflammasome activation might be due to the different methods of delivery. During transfection pilin is delivered using a liposomal transfection reagent, DOTAP, whereas during infection pilin is believed to be delivered via the bacterial T3SS. This might therefore influence the inflammasome activation by triggering of different cellular responses. DOTAP has previously been described to be used for endosomal translocation of DNA [453, 454]. This further strengthens the possibility that transfected pilin and pilin entering the cell via infection results in a different cellular response and thus a different inflammasome response.

Transfection with purified pilin from PA103 is dependent on caspase-1 but not any of the other inflammasome components tested. This is different from the results following transfection with recombinant pilin. Recombinant pilin is dependent on ASC, caspase-1 and NLRP3. The different inflammasome dependence is an unexpected result since the recombinant pilin is homologous to PA103 except for the lack of the N-terminal hydrophobic domain. The lack of the hydrophobic domain prevents polymerisation of the recombinant pilin, thus the recombinant pilin remains as monomers upon transfection. It is unknown if this influences the ability to trigger various inflammasome complexes. In addition, the recombinant pilin is expressed by *E.coli* and purified by lysing the bacteria rather than from the bacterial surface. This might influence the pilin and produce pilin which is slightly different from the pilin expressed on the surface of *P.aeruginosa*. *P.aeruginosa* might provide modifications of the expressed pilin that the *E.coli* is not able to provide. Further studies are needed to evaluate the reason for the different dependence between purified PA103 pilin and recombinant pilin.

A method for introducing an inflammasome activating molecule into the host cell cytoplasm was recently described [312]. This method use retroviral transduction of flagellin, which eliminates the need for bacterial secretion systems,

transfection reagents and limits the potential bacterial contaminants. Following transduction the ability of the transduced protein to cause cytotoxicity was measured. Flagellin have been shown to cause pyroptosis [248], which makes the transduction method ideal. However, transfection with pilin does not result in a high amount of cytotoxicity. This is therefore a possibility to why the retroviral transduction method with pilin was unsuccessful. In addition, it seems the expression of pilin influence the expression of GFP from the MigR1 plasmid. Transduction with the MigR1 plasmid alone produces a higher GFP expression than transduction with MigR1 pilin. A control plasmid, which expresses a control protein instead of pilin would provide a better control than the empty expression plasmid alone, as previously described [312]. Furthermore, mutations of the pilin gene did not influence the GFP expression. This might reflect the inability of pilin to cause cytotoxicity and therefore no difference is detected. Instead it would be interesting to investigate caspase-1 activation and IL-1ß secretion following transduction of pilin expressing retroviruses. This was attempted in this investigation, but due to time constraints it was not successful. Following optimization of the amount and time of LPS-treatment, transduction efficiency and incubation times it might be possible to detect active caspase-1 and IL-1ß secretion. This would provide further evidence for the ability of pilin to trigger inflammasome activation, independent of bacterial secretion systems and transfection reagents. If this would be successful, the ability of the mutated pilin-expressing retroviral plasmids to trigger inflammasome activation could be further investigated.

The results presented in this chapter indicate that the effector ExoU inhibits inflammasome activation, since any bacterial strain expressing this toxin fail to activate caspase-1 and secrete IL-1ß. This has previously been shown by Sutterwala et al. [249]. It was shown that ExoU was able to inhibit caspase-1 through ExoU phospholipase activity [249]. Furthermore, it has been shown for *Yersinia enterocolitica* that it can induce inflammasome activation dependent on a functional T3SS, however, this is inhibited by the effectors being translocated [455]. The effector responsible for this effect has not been determined [455]. Due to the ability of ExoU to inhibit inflammasome activation the PA103 pilA⁻ strain was unsuitable for the study of the effect of pilin and inflammasome activation in an infection model. What the studies presented in

this chapter show however, is that even though PA103 pilA⁻ lacks pilin it is able to translocate ExoU into the cells. This is proved by the lack of inflammasome activation, as well as the cytotoxicity caused, which are both similar to PA103 WT. *P.aeruginosa* type IV pili are the main adhesive organelles and type IV pili mediated attachment has been implicated in efficient delivery of effectors via the T3SS into epithelial cells [44-46]. Despite this the results in this chapter clearly demonstrate that pilA-deficient strains are able to translocate toxins through the T3SS into macrophages. Type IV pili is not the only surface structure that mediates attachment of *P.aeruginosa* to cells: other examples are porin F [456], lectins [457] alginate [458, 459] and outer membrane proteins [34].

The translocation ability of PA103 pilA⁻ is also strengthened by the results following treatment with MAFP. MAFP is an irreversible inhibitor of the intracellular lipase cPLA$_2$ [460]. MAFP is clearly able to inhibit the ExoU-dependent cell death caused by the ExoU-dependent phospholipase A$_2$ activity for all strains expressing ExoU. The cytotoxicity caused by the strains lacking ExoU is unaffected. This has also been seen in previously published results [142, 143]. Interestingly, MAFP treatment has a positive effect on the caspase-1 activation and IL-1β secretion following infection with all strains, independent of ExoU-expression. As expected, the IL-1β secretion and caspase-1 activation for the ExoU-expressing strains are restored to levels similar to that of ExoU-defective strains following MAFP treatment. However, the ExoU-defective strains are also affected. Further experiments are needed to evaluate these results. It implies a role for MAFP in inflammasome activation via a yet unexplored pathway. Similar results were previously published by Sutterwala et al. using another inhibitor of A$_2$ phospholipases, AACOCF$_3$ (Arachidonyl trifluoromethyl ketone) [249].

PA103 pilA⁻ was shown to translocate effectors in this study. Therefore it is also believed that PA103 ΔUΔT:pilA⁻ is able to translocate effectors. A system using β-lactamase reporter gene constructs could also be used to prove translocation. Examples of this system have previously been used in the study by Sun et al. [365]. In addition, fluorescent imaging based methods could be used for the detection of translocation; however, described methods all involve fusion of the translocated protein with another gene to facilitate detection in the host cell [461].

Attempts were made to recomplement PA103 ΔUΔT:pilA⁻ with pilin expressing plasmid encoding PA103 and PAO1 pilin respectively. However, this was never successful. There is nothing wrong with the pilin expressing plasmids as the complementation of PAO1 FliC⁻pilA⁻ was successful, discussed further below. Instead there seems to be a specific problem preventing transformation of PA103 with a pilin-expressing plasmid, since other plasmids (e.g. pucp20 ExoY) were successfully transformed into this strain. Several attempts were made but each time a double resistant colony grew, it eventually stopped growing after restreaking or growth in liquid media. This suggests that the plasmid is lost by the strain for reasons that are currently unexplainable. This is also surprising due to the fact that it has been shown that pili can be artificially transferred between bacterial species, where they assemble and function in twitching motility [462-464]. The differences might be due to different use of expression plasmids and experimental conditions.

Inflammasome activation by PAO1 does not seem to be dependent on pilin; rather it is very strongly dependent on flagellin expression. The PAO1 pilA⁻ strain still expresses flagellin, which can activate the inflammasome. This further strengthens the conclusion that the T3SS is able to function in a pilin-deficient strain, since the flagellin is believed to pass through the T3SS and this is unaffected in the PAO1 pilA⁻ strain. In addition, the inflammasome activation by the PAO1 FliC⁻pilA⁻ strain is not further affected by the pilin-deficiency compared to PAO1 FliC⁻. In some experiments the IL-1β secretion by the flagellin- and pilin-deficient strain is increased compared to the flagellin-deficient strain. This indicates the involvement of another bacterial product, separate from flagellin and pilin, involved in the inflammasome activation. It is possible that this yet unidentified product is upregulated as a response to the flagellin- and pilin-deficiency. In addition, the expression level of pilin might be different in PAO1 compared to PA103, which is indicated by the fact pilin can only be purified from flagellin-deficient PAO1, as previously discussed.

Interestingly, the IL-1β secretion can be restored in PAO1 FliC⁻pilA⁻ with the expression of a PAO1 pilin expressing plasmid. This shows that PAO1 pilin is able to activate the inflammasome in an infection model. Complementation with PA103 pilin also increased IL-1β secretion but not to a statistically significant degree. This may reflect different levels of protein expression.

The results presented in this chapter indicate that pilin is necessary for inflammasome activation by PA103, but not PAO1. As previously discussed, the expression levels of pilin in these strains might not be at the same level. It has been shown that strains lacking flagellin express higher levels of the T3SS genes [6]. In addition, there are sequence differences between the strains which might influence the inflammasome activation [28]. The amino acid sequence for PA103 is 80% identical to that of PAO1 and 65% to that of PAK [28]. Furthermore, PA103 does not express flagellin whereas PAO1 does, which can also influence the inflammasome activation. Further studies are needed to determine whether the sequence differences seen between PA103 and PAO1 account for the differences in inflammasome activation. Variability in the sequence might allow the bacterium to evade immune responses. It has previously been shown that sequence variation in flagellin between species results in evasion of the TLR5 response [178]. Therefore, it would also be interesting to investigate the ability of pilins from other bacterial strains to activate the inflammasome complex. First of all, pilin from strains belonging to the same type IV pilin class as *P.aeruginosa*, such as pilin from *Neisseria gonorrhoeae*. However, this was not possible within the time frame of this project.

Several previous publications have introduced a centrifugation step immediately following infection with flagellin-deficient strains [249, 253, 390]. However, as described in this study, PA103 lacks flagellin but is still able to infect cells without the need for a centrifugation step. Furthermore, following centrifugation of the flagellin-deficient PAO1 strains it was found that it caused increased cell death, which possibly alters the inflammasome response due to increased stress of the cells. In addition, although cells can be pelleted at these centrifugal speeds, bacteria cannot. Instead they require much higher speeds, thus, a centrifugation step at this low speed would not increase infection efficiency only provide an unnecessary step.

Studies for both *L.pneumophila* and *Salmonella* have shown that the flagellum secretion apparatus is not needed for caspase-1 activation [337, 351, 390]. The flagellum secretion apparatus is required specifically for transport of flagellin to the bacterial cell surface and assembly of the flagellum [444]. This suggests that other specialized secretion systems in the bacteria may be delivering flagellin directly into the cytosol of the host cell. This has been shown for flagellin

passing through the SPI-1 T3SS of *Salmonella* [365]. The flagellar assembly apparatus is similar to the T3SS of bacteria [18, 19]. It has been shown that flagella can secrete, but not translocate, some T3SS effectors under specific circumstances [465]. It is therefore not surprising that the T3SS can accidentally translocate flagellin into the host cell cytosol. In contrast the type IV pili are related to bacterial T2SS. Homologs of all proteins involved in type VI pili synthesis can be found as components of the T2SS [466]. Pili formation is believed to occur when the growing type IV pilus structure is translocated to the cell surface via the secretin PilQ [50]. This allows machinery at the inner membrane-periplasm interface to mediate retraction, fibre formation mediated by PilF and depolymerisation by PilT [50].

Due to the nature of bacterial secretion system it is believed that in order for flagellin to pass through the system it needs to be in monomeric form. The results published in this study do not investigate whether it is pilin monomers or polymers that activate the inflammasome complex. Furthermore, it might be different for the transfection model compared to the infection model. In addition, if monomers pass through the T3SS they could possibly reassemble in the cytosol of the host cell. The recombinant pilin used in this study lacks the N-terminal hydrophobic domain and can thus not form polymeric structures. It was shown in this chapter that recombinant pilin is not as potent as purified PA103 pilin in inflammasome activation. These results imply that in order for maximum inflammasome activation the structure of pilin is polymeric. The results presented in this chapter further suggest that pilin can pass through the T3SS, since a functional T3SS is required for the inflammasome activation by *P.aeruginosa*. Type IV pili constantly retract and extend from the bacterium. This results in available pilin monomers inside the bacterial cell, which are available for pili synthesis [48-50]. Similar to flagellin, pilin might accidentally be engaged by a bacterial secretion system and thus 'mistakenly' delivered into the host cell cytosol. However, the inflammasome activation by *P.aeruginosa* might be detrimental for the host. This will be discussed further in chapter 7. It would be interesting to investigate whether pilin could be detected in the host cell following infection, however due to lack of suitable antibodies this has not been tested in this study. Furthermore, the amount of pilin needed to activate the inflammasome complex might be below detection level of for example

immunoblot methods. Pilin has previously been detected by immunoblotting of proteins from a growing colony [55]; however the concentration of pilin in this case will presumably be a lot higher than the concentration inside the host cell. Another potential detection system would be to tag pilin with glycogen synthase kinase (GSK) and track the host cell kinase-dependent phosphorylation of this tag [467]. However, the amount of translocated material might influence the detection via this method as well.

The direct binding of flagellin to NLRC4 has not yet been demonstrated. Thus, flagellin, as well as pilin, during infection, might trigger NLRC4-dependent inflammasome activation via another molecule or sensor. In the study by Lightfield et al. [312] it was shown that point mutations of the flagellin C-terminal abolished its ability to activate the inflammasome. This suggests a direct interaction between flagellin and NLRC4. Another possibility is that the flagellin peptide indirectly triggers the inflammasome via interference with a cellular process. Considering the possibility that flagellin, as well as pilin, trigger NLRC4 activation and the differences between these molecules the second explanation seems more likely. There might also be additional, yet unidentified, bacterial molecules which trigger NLRC4 activation. Furthermore, transfected pilin is not dependent on NLRC4 activation, which indicates an involvement of an additional host sensor in the response to pilin. However, a wide variety of molecules can activate, for example, the innate immune receptor TLR2, which suggests that other innate immune sensors might also have evolved to detect several danger signals. Further studies are needed to be able to draw any final conclusions.

Flagellin-dependent inflammasome activation by *L.pneumophila* was shown to be dependent on NLRC4 and NAIP5 [251, 352, 357]. However, NAIP5-independent but NLRC4-dependent inflammasome activation has also been described [312]. NLRC4 might therefore provide a scaffold for the assembly of many distinct inflammasomes, some which require NAIP5 and others which require yet unidentified proteins.

The results presented in this chapter identify pilin as a novel inflammasome activator. The activation is dependent on a functional T3SS. Previous published results have shown NLRC4-dependent but flagellin-independent inflammasome

activation, but have failed to identify a potential activating protein [227, 249, 337]. Recent data presented by E. Miao at Keystone Symposia, Banff April 2009, identified the rod protein of the T3SS as a potential candidate for the flagellin-independent inflammasome activation. This was shown by retroviral transduction. There are still several problems with this model. For instance, how does the rod protein enter the host cell, since upon T3SS-assembly the rod protein is incorporated before the needle proteins and the needle length is determined by the molecular ruler, as described in chapter 1.3.1.1. The retroviral transduction eliminates the need for a bacterial secretion system, but makes it hard to prove the biological significance. If the rod protein were to be mutated this would render the T3SS non-functional and thus the relevance in an infection model is difficult to prove.

In conclusion, the results presented in this chapter identify pilin as a novel inflammasome activator. This is the first demonstration of recognition of type IV pili by pathogen recognition receptors. Pilin from both PAO1 and PA103 is able to trigger caspase-1 activation and IL-1β secretion following transfection. The role of pilin in an infection model was also investigated, which identifies pilin-dependent inflammasome activation by PA103. Pilin is therefore proposed as the bacterial molecule which mediates inflammasome activation in flagellin-deficient bacteria, thus adding to the understanding of the complex process of inflammasome activation by various bacterial molecules.

6 Nod1 activation by *Pseudomonas aeruginosa*

6.1 Introduction

6.1.1 NF-κB activation by Pseudomonas aeruginosa

NF-κB is a transcription factor expressed in virtually all cell types. It is involved in the expression of numerous cytokines and adhesion molecules [468, 469]. Thus, NF-κB has an essential role in the host response to infections, stress and injury [468]. The name NF-κB originates from its first identification as a nuclear factor necessary for immunoglobulin kappa light chain transcription in B-cells [470]. NF-κB is located in the cytoplasm as an inactive form bound to the inhibitor IκB. This masks the nuclear localization signal of NF-κB and thus retains it in the cytoplasm [471]. Following activation, NF-κB translocates to the nucleus and upregulates transcription of specific genes of a common purpose; enhancing the immune response [468].

There have been several reports concerning NF-κB activation by *P.aeruginosa*. Several publications have investigated the role of NF-κB activation in cystic fibrosis sufferers. A wide variety of mechanisms have been reported and a select few will be described here. As previously described, TLR-signalling leads to NF-κB activation and *P.aeruginosa* possess a wide range of TLR activating factors, such as LPS, flagellin and CpG DNA [472-474].

The NF-κB activation by *P.aeruginosa* has been shown to be dependent on pilin attachment to epithelial cells [475]. In addition, it has also been shown that NF-κB activation in airway epithelial cells is dependent on flagellin [476]. This was shown for the pseudomonal strains PAK, PAO-1 and PA14. Furthermore, it was shown by Travassos et al. that the pseudomonal strain PAK, as well as PAO-1, can activate NF-κB [17]. This was shown to be dependent on peptidoglycan and Nod1 activation, which will be discussed below.

6.1.2 Nod protein activation

Nod1 was the first NLR-protein identified in mammals. It is homologous to CED-4, which regulates apoptosis in *C.elegans* [197, 217]. Nod1 has similar structure to other NLR-proteins, with a central nucleotide-binding and oligomerization

domain, an N-terminal CARD domain and C-terminal leucine-rich repeats. When Nod1 is overexpressed it activates NF-κB. Nod1 is ubiquitously expressed [197], whereas Nod2 is mainly found within monocytes and macrophages [477].

The first Nod1 activator was thought to be LPS [478]. However, it was later shown that the activation by LPS was due to contaminating material. Both Nod1 and Nod2 sense bacterial peptidoglycan through their carboxy-terminal LRRs [343, 478-481]. Peptidoglycan is one of the major components of Gram-positive bacterial cell wall [482]. In Gram-negative bacteria it is found as a thin layer in the periplasmic space. Peptidoglycan provides shape and mechanical rigidity to bacteria [482]. Nod1 responds to γ-D-glutamyl-meso-diaminopimelic acid (iE-DAP) (Figure 6.1) [343, 479, 483]. This acid is found in all Gram-negative bacteria, as well as in certain Gram-positive species, such as *Bacillus* and *Listeria* spp. In contrast, Nod2 responds to muramyl dipeptide (MDP), which is found in both Gram-positive and –negative bacteria (Figure 6.1) [480, 481, 484]. Muramyl dipeptide is the minimal motif in all peptidoglycans [485]. Peptidoglycan is a complex structure of carbohydrate chains of β (1-4)-linked, alternating N-acetylglucosamine (GlcNAc) and N-acetylmuramic acid (MurNAc) sugars cross-linked by short peptide bridges (Figure 6.1) [486]. Gram-negative bacteria and some Gram-positive have diaminopimelic acid (DAP) in the third position of the peptide chain, in contrast most Gram-positive bacteria have a lysine at this position [484, 485]. Bacteria can generate small molecules containing iE-DAP or MDP structures, which are generated as intermediates of PGN biosynthesis [487, 488]. Furthermore, PGN is remodelled by bacteria for cell division and growth and this process generates small PGN fragments containing these motifs [489]. In the host, lysozyme can cleave the glycan chain of PGN generating small muropeptides, which contain the iE-DAP and MDP structures [490, 491].
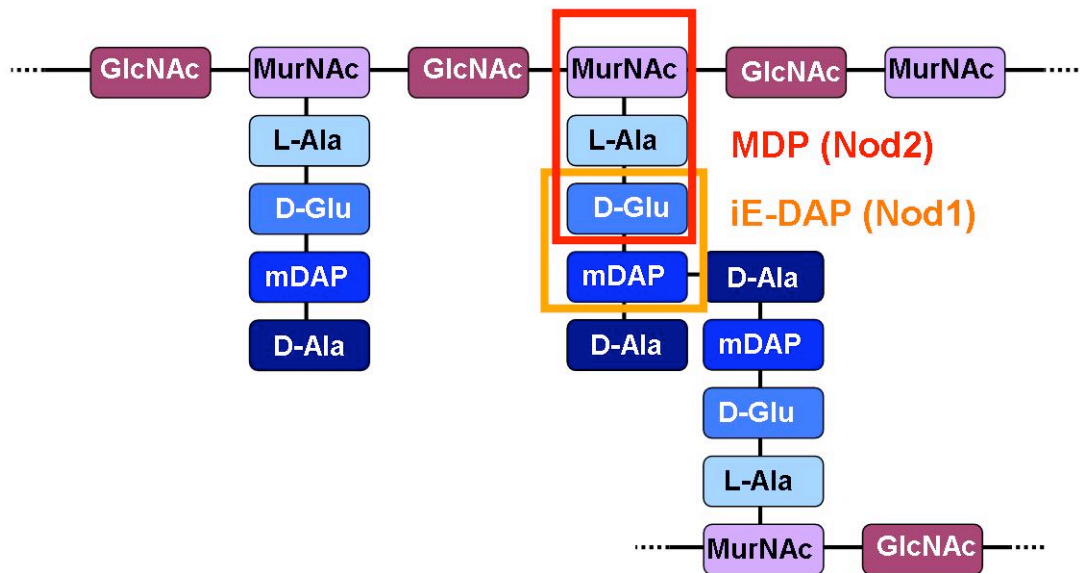
Figure 6.1; Peptidoglycan motifs recognised by Nod1 and Nod2

Structure of peptidoglycan. MDP (red box) and iE-DAP (orange box) is the minimal peptidoglycan motif required for recognition by Nod2 and Nod1 respectively. Adapted from [486].

Experiments on Nod1 knock-out mice demonstrated an important role for Nod1 as a sensor of intracellular peptidoglycan in epithelial cells [343]. Nod proteins are the only known receptors for peptidoglycan in mammalian cells [492]. TLR2 was previously identified as a receptor for peptidoglycan [493, 494] but it was later shown, similar to LPS and Nod1 activation, that the activation was mediated by contaminants in the peptidoglycan preparations. These contaminants are believed to be lipoteicoic acid or lipoproteins [492]. However, there is still a debate whether PGN activates TLR2 or not, as it was subsequently shown that PGN from *S.aureus* activates TLR2 [495].

Nod1 plays an important role in the epithelium in the NF-κB activation following infection with Gram-negative bacteria that do not activate NF-κB through TLR signalling pathways [197]. The Nod1 pathway provides an additional signalling pathway for activation of NF-κB following infection, which favours host survival when bacteria bypass TLR recognition [496]. Both pathways have a common kinase (RIP2 or RICK), described in more detail below [497], even if this is controversial and has been challenged [498].

Activation and oligomerization of Nod1 and Nod2 leads to activation of kinase receptor-interacting protein2 kinase (RIP2 also known as RICK) eventually

leading to activation of NF-κB and MAFP [197, 217, 477] (Figure 6.2). RICK contains an N-terminal domain which is homologous to serine/threonine kinases and a C-terminal CARD domain [499]. The CARD of RICK interacts with the CARDs of Nod1 and Nod2 [477, 500]. Following interaction RICK directly activates the NF-κB pathway through activation of the IKK complex via ubiquitinylation [501-505]. This leads to the phosphorylation and subsequently degradation of IκBα and release of NF-κB, which translocates to the nucleus where it drives the transcription of pro-inflammatory target genes [485, 505]. The ultimate result of Nod1 and Nod2 activation is an inflammatory response which aids host defence (Figure 6.2). NF-κB responsive genes include acute phase response proteins such as C3 complement, adhesion molecules such as VCAM-1 and ICAM-1 and cytokines such as IL-1, IL-2, IL-6, IL-8 and TNF-α [468].
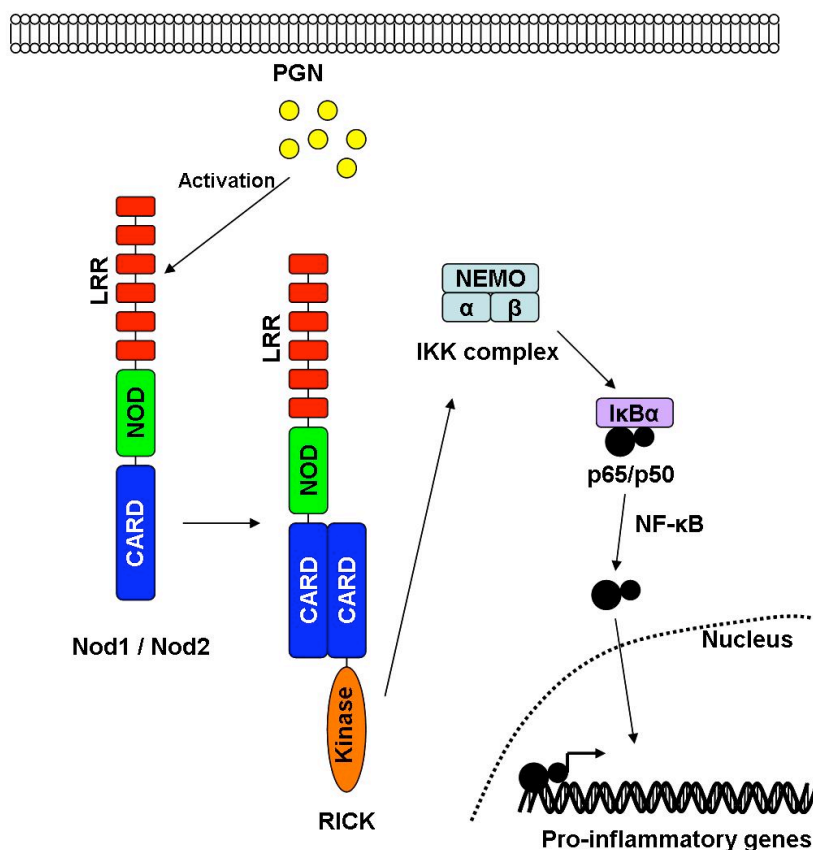
Figure 6.2; Nod1 and Nod2 NF-κB signalling pathway

Peptidoglycan activates Nod1 and Nod2. Upon activation the serine/threonine kinase RICK is recruited. RICK then directly activates the IKK complex which leads to degradation of IκBα. NF-κB is released and translocated into the nucleus where it binds to the promoter of pro-inflammatory genes. The expressed factors are then involved in the host response. Figure adapted from [485].

6.1.3 Nod1 activation by bacteria

Many bacteria remain extracellular and thus limit the need for an intracellular pathogen detection system. The commensal bacteria within the gut have the same molecular motifs as pathogenic bacteria, which limits the use of an extracellular detection system. An intracellular system could be used to detect invasion by bacteria, which indicates a threat to the host.

The extracellular pathogen *Helicobacter pylori* was shown to activate the intracellular Nod1 [222]. It was shown that the host response to *H.pylori* is mediated by intracellular peptidoglycan recognition by Nod1. Nod1 knock-out mice had higher susceptibility to *H.pylori*. The activation was shown to be dependent on a functional T4SS [222]. Peptidoglycan is believed to pass through this T4SS into the host cell where it activates Nod1. Commensal bacteria do not have a secretion system, thus the host has developed a system which can discriminate between commensal and pathogenic bacteria. It is not known how peptidoglycan enters the T4SS.

Following *Shigella flexneri* infection NF-κB is activated in a Nod1-dependent manner [506, 507]. *S.flexneri* is a Gram-negative bacterium responsible for shigellosis (bloody diarrhoea). It was subsequently shown that Nod1 localise at the plasma membrane [508]. This maximises the interaction possibilities between the intracellular sensor and invading pathogens. Nod1 was shown to localise to the site of bacterial entry during *S.flexneri* infection, which was shown to be dependent on membrane binding [508]. Thus, Nod1 is activated very rapidly after bacterial invasion and association with the plasma membrane is essential for the host response. Other bacteria which have been identified as Nod1-dependent NF-κB activators include enteroinvasive *E.coli* [496], *Chlamydia* spp. [509, 510], *Campylobacter jejuni* [511], *Salmonella* [512], *L.monocytogenes* [498, 513-515], *Bacillus* spp. [516] and *P.aeruginosa* (as mentioned above) [17].

Nod2 has also been shown to relocate to the plasma membrane together with RIP2 (also known as RICK) [517, 518]. Specific localisation of the sensor increases the efficiency by which the cell recognises invading pathogens, as previously mentioned. Membrane recruitment of Nod2 was shown to increase binding to erbin which leads to the inhibition of signalling. Thus, as well as increasing

efficiency, membrane recruitment might also be important in terminating proinflammatory signalling events [519].

It is not just bacterial secretion systems which can mediate delivery of peptidoglycan to the intracellular space. This can also be mediated by bacterial pore-forming toxins such as pneumolysin [520]. Furthermore, it has been shown that the intestinal apical di/tripeptide transporter (hPepT1) can transport muramyl dipeptide into the cytoplasm [521, 522]. These can then activate Nod2, whereas the peptidoglycan derived activator of Nod1 cannot be transported by this transporter [521].

The work presented in this chapter investigates whether NF-κB activation by *P.aeruginosa* is dependent on a functional T3SS and peptidoglycan activation of Nod1. The cell line HEK293 was used since these cells have been shown to respond to intracellular stimulation with Gram-negative bacteria, or peptidoglycan via a Nod-1 dependent pathway [17, 222, 343, 507]. The results show that *P.aeruginosa* is able to activate NF-κB in a T3SS-dependent manner, independent of translocated effectors. Furthermore, it is shown that the NF-κB activation by *P.aeruginosa* is independent of Nod1 activation.

6.2 Results

6.2.1 Pseudomonas aeruginosa activates NF-κB during infection

NF-κB activation during *P.aeruginosa* infection has previously been described, as discussed above. In order to investigate whether this activation is dependent on a functional T3SS, a NF-κB reporter gene system was used. HEK293 cells were transfected with a NF-κB-luciferase reporter plasmid together with a β-galactosidase reporter plasmid, as a control for transfection efficiency. After 24 h of incubation the transfected cells were infected with PA103 ΔUΔT, PA103 ΔpcrV and PA103 ΔUΔT:ExoUS142A. The NF-κB induction was measured following infection, as well as β-galactosidase induction. NF-κB will only be induced in cells where NF-κB activation occurs, whereas the β-galactosidase will be produced in all living transfected cells. This provides a control, which can be used to calculate fold NF-κB activation in living cells. Following infection with *P.aeruginosa*, it was shown that NF-κB is activated in a T3SS-dependent manner (Figure 6.3). Furthermore, this activation was shown to be independent of translocated effectors, as PA103 ΔUΔT:ExoUS142A activates NF-κB to the same extent as PA103 ΔUΔT (Figure 6.3).
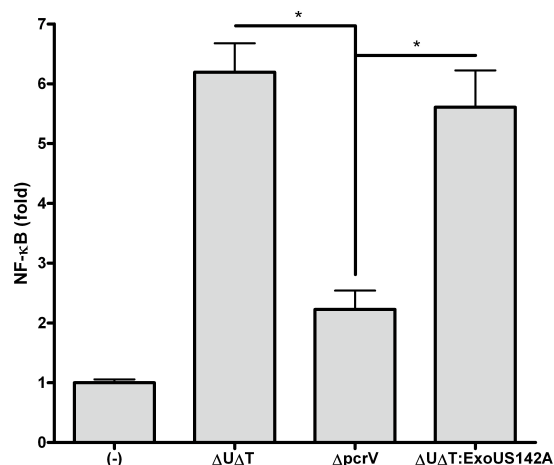
Figure 6.3; *P.aeruginosa* **activates NF-κB during infection, dependent on a functional T3SS but independent of translocated effectors**

HEK293 cells were transfected with pNF-κB-Luc and p-β-gal, after 24 h cells were infected with *P.aeruginosa* strains as indicated at a MOI of 200 for 90 min. Gentamicin were then added for 12 h and then luciferase and β-galactosidase activity in cell lysates were measured. Columns are means of duplicates and error bars are SEM. * indicate significant difference, where $p<0.05$, unpaired Student's t-test.

P.aeruginosa has LPS, but HEK293 cells lack TLR4 and TLR2 and should therefore not respond to LPS stimulation [523, 524]. This was investigated using the NF-κB/ß-gal reporter gene system. Following LPS treatment, with highly purified LPS preparations (ion-exchange chromatography), of HEK293 cells no NF-κB activation could be detected (Figure 6.4). There was a significant increase in NF-κB activation after treatment with LPS from the pseudomonal strain PA10 compared to control and LPS from *E.coli* (Figure 6.4). However, the degree of stimulation was minimal. This might be due to contaminating bacterial products in the LPS preparation, as discussed previously and below.
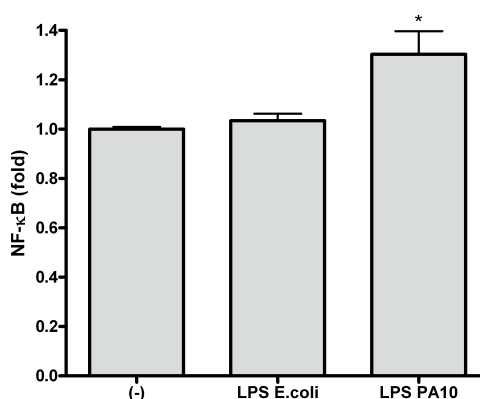
Figure 6.4; HEK293 cells do not have TLR4 and TLR2 and lacks response to LPS

HEK293 cells were tranfected with pNF-κB-Luc and p-β-gal. Together with the transfection mixture LPS were added, cell lysates were analysed for luciferase and β-galactosidase activity 24 h later. Columns are means of triplicates and error bars are SEM. * indicates significant difference compared to control (-) where p<0.05, unpaired Student's t-test.

Peptidoglycan was identified as a molecule which activates NF-κB dependent on Nod1 and Nod2 [343, 479-481]. Peptidoglycan was therefore purified from the *E.coli* SM10 strain. Following stimulation of NF-κB/ß-gal transfected HEK293 cells with PGN, significant activation of NF-κB compared to untreated cells could be detected (Figure 6.5). However, the activation was fairly modest.
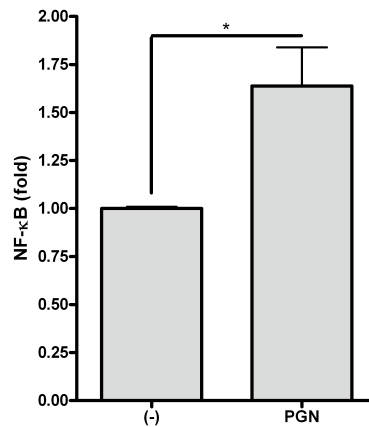
Figure 6.5; NF-κB is activated following treatment of HEK293 cells with peptidoglycan

HEK293 cells were tranfected with pNF-κB-Luc and p-β-gal. Together with the transfection mixture PGN from *E.coli* SM10 were added, cell lysates were analysed for luciferase and β-galactosidase activity 24 h later. Columns are means of triplicates and error bars are SEM. * indicates significant difference where p<0.05, unpaired Student's t-test.

In conclusion, *P.aeruginosa* activates NF-κB during infection in a T3SS-dependent manner. Furthermore, as previously described HEK293 cells do not respond to LPS, due to lack of TLR4 and TLR2. However, PGN is able to activate NF-κB in HEK293 cells.

Previous publications investigating Nod1 dependent NF-κB activation by bacteria have used HEK293 cells transfected with a range of constructs to inhibit Nod1. In order to further investigate the role of Nod1 in NF-κB activation by *P.aeruginosa* a variety of Nod1 constructs were used, described below.

6.2.2 Nod1 is not involved in the NF-κB response to Pseudomonas aeruginosa

As previously described, Nod1 is involved in the triggering of NF-κB as a response to peptidoglycan. Previous section in this chapter described a T3SS-dependent NF-κB activation following infection with *P.aeruginosa*. To investigate whether siRNA silencing of Nod1 had any effect on NF-κB activation by PA103 ΔUΔT, a luciferase reporter gene assay was performed after siRNA transfection. The siRNA sequences used were previously published and validated by Viala et al. [222]. HEK293 cells were transfected with siRNA, two days later they were infected with PA103 ΔUΔT and after another day luciferase activity were

measured. The siRNA transfection had no effect on the NF-κB activation (Figure 6.6).
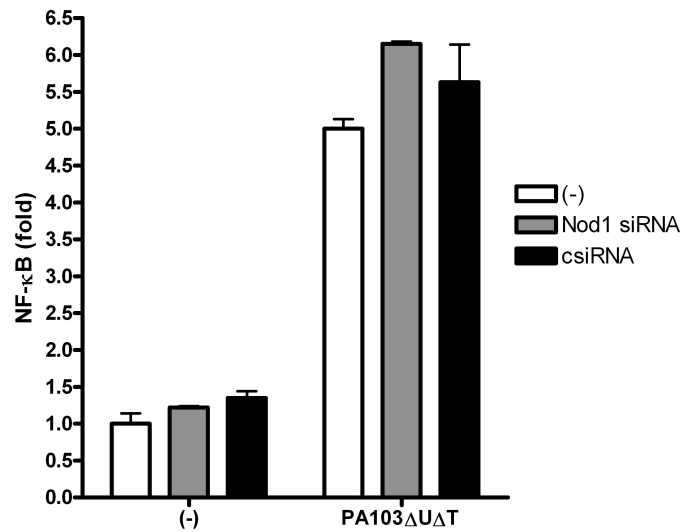
Figure 6.6; siRNA silencing of Nod1 has no effect on NF-κB activation by *P.aeruginosa*

HEK293 cells were transfected with indicated siRNAs and after 24 h cells were transfected again with p-NF-κB-Luc and p-β-gal. After additional 24 h cells were infected with PA103 ΔUΔT at a MOI of 200 for 90 min. Gentamicin was added for 12 h and then luciferase and β-galactosidase activity in cell lysates were measured. Columns are means of duplicates and error bars are SEM.

In addition, the silencing with Nod1 siRNA could not be detected by Western blot. This was not successful and no silencing could be observed (Figure 6.7). The antibody from Abcam detects a band at 32 kDa, which corresponds to Nod1. However, the predicted size of Nod1 is 106 kDa, and a very weak band can be observed at this weight (Figure 6.7).
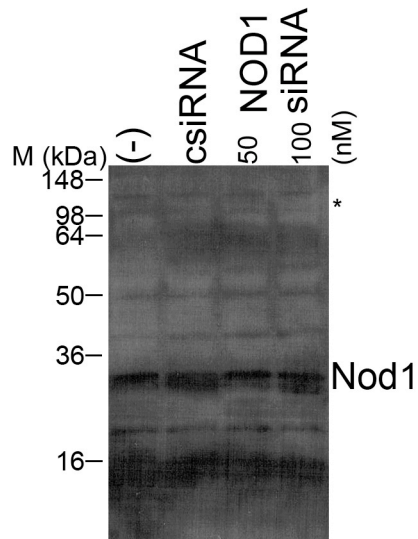
Figure 6.7; Nod1 could not be silenced by siRNA in HEK293 cells

HEK293s were transfected with siRNA against Nod1 and control scrambled siRNA. After 24 h cell lysates were analysed by immunoblotting with Nod1 antibody (Abcam). Band at about 32 kDa is Nod1 even though the predicted size is 106 kDa, indicated with asterix (*).

To try and improve sensitivity, we instead used an antibody against Nod1 from Cell signalling. HEK293 cell lysates were immunoblotted with this antibody. In normal untransfected cells, no Nod1 could be detected (Figure 6.8), indicating a very low expression level of Nod1 in HEK293 cells. However, Nod1 could be detected in HEK293 cells transfected with hNod1 expression plasmid (Figure 6.8). Increasing amounts of Nod1 expression plasmid resulted in increasing Nod1 expression, as expected.
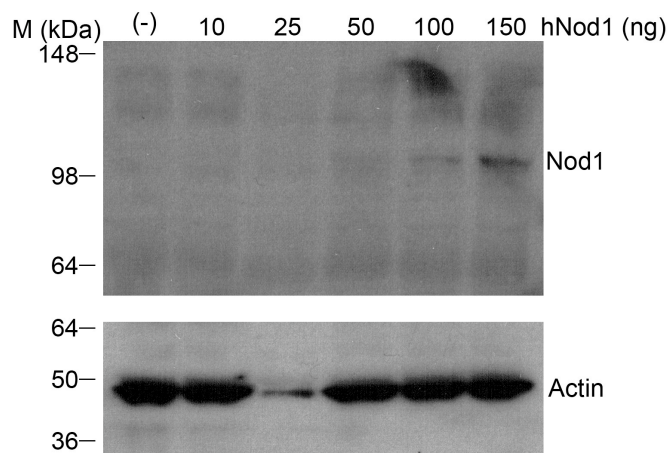
Figure 6.8; Nod1 can be detected in HEK293s following overexpression with pCDNA3 hNod1

HEK293s were transfected with indicated amounts of pCDNA3 hNod1, after 24 h cell lysates were analysed by immunoblotting with Nod1 antibody (Cell signalling). Increasing amounts of hNod1 results in increasing amount of Nod1 detected in the cell lysates (top panel). Lower panel shows actin reprobe to show even loading of the gel, there is less protein loaded in the 25 ng lane.

Expression of exogenous Nod1 resulted in a detectable amount of Nod1 by Western blot, molecular weight of 106 kDa (Figure 6.8). Exogenous Nod1 also had an effect on NF-κB activation by LPS, purified by phenol extraction, and peptidoglycan purified from *E.coli* SM10. Transfection with Nod1 resulted in significant increased NF-κB activation after LPS and PGN treatment compared to control (Figure 6.9). This LPS was purified by phenol extraction and thus contains contaminating peptidoglycan. No effect could be detected after these treatments in cells which were transfected with the expression plasmid alone (Figure 6.9). Previous results showed only minor changes following LPS and PGN treatment in NF-κB activation in HEK293 cells alone (Figure 6.4 and 6.5).
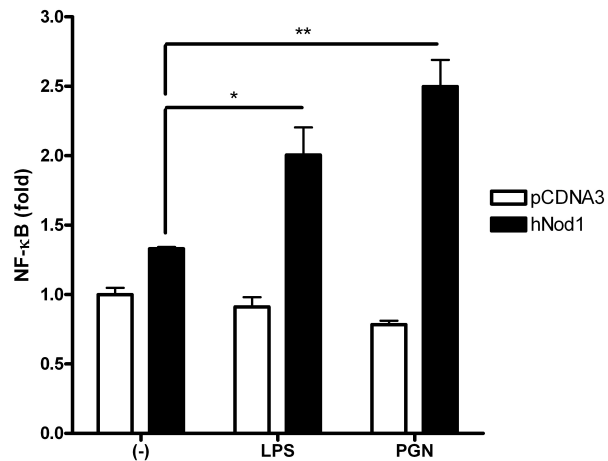
Figure 6.9; NF-κB is activated in HEK293 cells following treatment with LPS purified by phenol extraction and peptidoglycan

HEK293 cells were transfected with pNF-κB-Luc and p-β-gal as well as pCDNA3 hNod1 or pCDNA3. Together with the transfection mixture PGN from *E.coli* SM10 or LPS purified by phenol extraction was added, cell lysates were analysed for luciferase and β-galactosidase activity 24 h later. Columns are means of triplicates and error bars are SEM. * and ** indicates significant difference where * is $p<0.05$ and ** is $p<0.01$, unpaired Student's t-test.

LPS purified by phenol extraction contain contaminating peptidoglycan which can activate Nod1. In contrast, LPS purified by ion-exchange chromatography lacks contaminating material. The effect of these different preparations of LPS was investigated in HEK293 cells transfected with exogenous Nod1 and cotransfected with a dominant-negative construct of Nod1 (ΔCARD), which lacks the CARD necessary for NF-κB activation. No NF-κB activation can be detected in cells treated with ion-exchange LPS compared to control (Figure 6.10). A significant increase was detected following treatment with phenol extraction LPS (Figure 6.10). This effect was inhibited when cells were cotransfected with ΔCARD, bringing the NF-κB activation back to base-line (Figure 6.10). The ΔCARD construct also had an effect on the untreated and ion-exchange LPS treated cells. So even though there is an effect on the phenol extraction LPS treated cells, it also suggests that background levels of expressed hNod1 are activating NF-κB in the transfected cells.
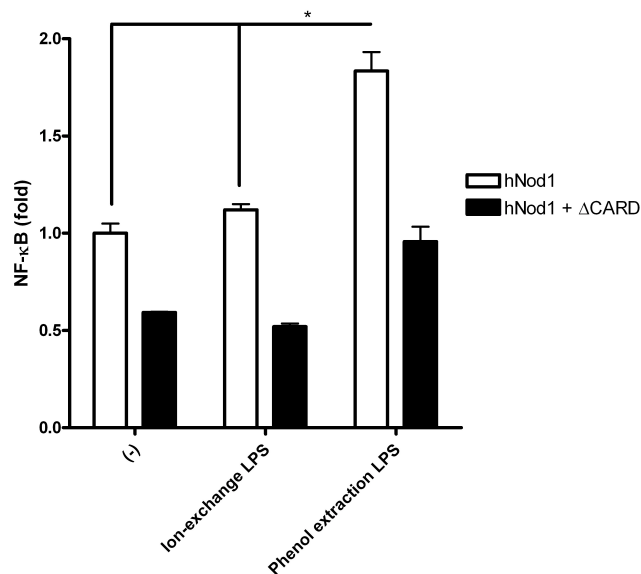
Figure 6.10; NF-κB activation by LPS purified by Phenol extraction is dependent on Nod1

HEK293 cells were transfected with pNF-κB-Luc, p-β-gal and pCDNA3 hNod1 indicated samples were also transfected with pCDNA3 ΔCARD. After 5 h LPS purified by ion-exchange chromatography and phenol extraction was added, cell lysates were analysed for luciferase and β-galactosidase activity 24 h later. Columns are means of duplicates and error bars are SEM. * indicates significant difference where * is p<0.05, unpaired Student's t-test.

siRNA silencing of Nod1 had no effect on the NF-κB activation by *P.aeruginosa*. However, this might be due to unsuccessful silencing of Nod1. As another method, HEK293 cells were transfected with ΔCARD (Figure 6.11). No concentrations of ΔCARD had any effect on the NF-κB activation by PA103 ΔUΔT (Figure 6.11A and B). This further strengthens the conclusion that Nod1 is not involved in the NF-κB activation by *P.aeruginosa*.
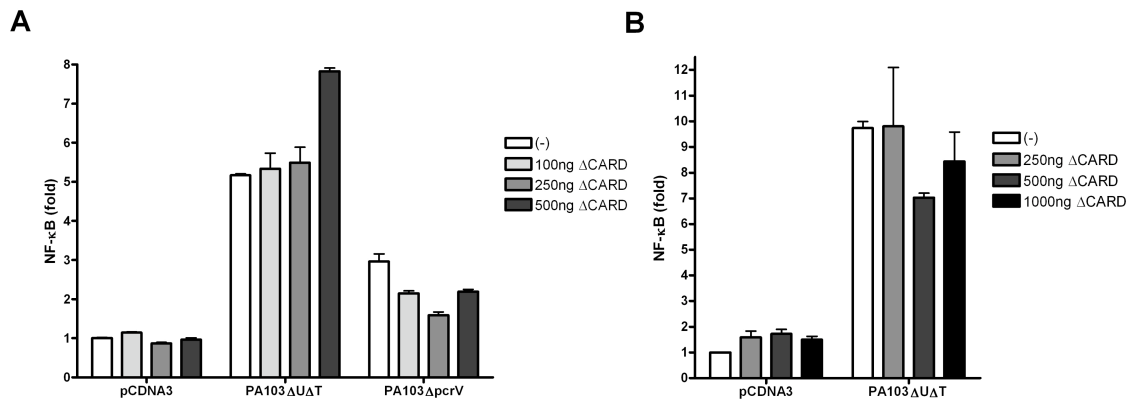
Figure 6.11; NF-κB activation by *P.aeruginosa* is not dependent on Nod1

HEK293 cells were transfected with pNF-κB-Luc and p-β-gal as well as pCDNA3 ΔCARD, at indicated amounts, or pCDNA3 at an amount corresponding to the highest amount of pCDNA3 ΔCARD. After 24 h cells were infected with PA103 ΔUΔT or PA103 ΔpcrV at a MOI of 100 for 90 min. Gentamicin was added for 12 h. Cell lysates were analysed for luciferase and β-galactosidase activity. Columns are means of triplicates and error bars are SEM. A, pCDNA3 ΔCARD at 100 ng, 250 ng and 500 ng. B, pCDNA3 ΔCARD at 250 ng, 500 ng and 1000 ng.

To further investigate the NF-κB activation following expression of exogenous Nod1 and cotransfection with ΔCARD, the effect of phenol extraction LPS was investigated. As previously described, after treatment with phenol extraction LPS the NF-κB activation is abrogated in cells cotransfected with ΔCARD (Figure 6.12). In this experiment, ΔCARD cotransfection had no effect on cells alone (Figure 6.12).
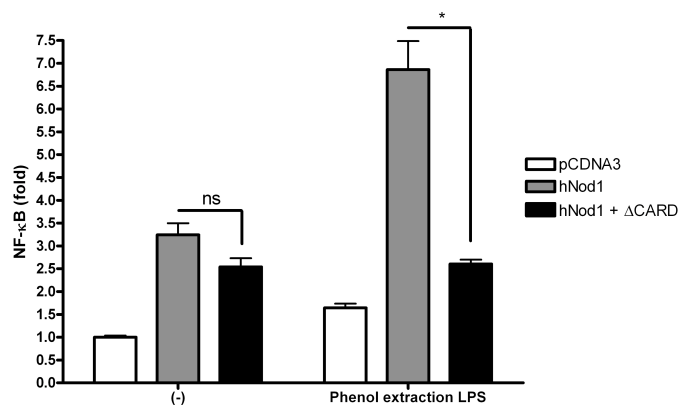
Figure 6.12; NF-κB activation by LPS purified by Phenol extraction is dependent on Nod1

HEK293 cells were transfected with pNF-κB-Luc, p-β-gal and pCDNA3 hNod1 indicated samples were also transfected with pCDNA3 ΔCARD. Together with the transfection mixture LPS purified by phenol extraction was added, cell lysates were analysed for luciferase and β-galactosidase activity 24 h later. Columns are means of triplicates and error bars are SEM. * indicates significant difference where * is $p < 0.05$, ns is non significant difference $p > 0.05$, unpaired Student's t-test.

Varied amounts of ΔCARD were used in the cotransfection together with Nod1. In this experiment, there was an increased NF-κB activation in Nod1 transfected PA103 ΔUΔT infected cells, compared to infected cells transfected with the expression plasmid alone (Figure 6.13). This increase might be due to the effect also seen in cells alone, where the NF-κB activation is increased following transfection with hNod1 (Figure 6.13), as previously described. However, infected cells transfected with pCDNA3 alone have an increased NF-κB activation compared to cells alone (Figure 6.13), as previously seen. The NF-κB activation in the infected cells is not altered following cotransfection with ΔCARD (Figure 6.13). Cotransfection resulted in less NF-κB activation in cells alone compared to cells transfected with hNod1 (Figure 6.13), further indicating that there are background levels of NF-κB activated by transfected hNod1 in these cells. This provides additional evidence that Nod1 is not involved in the NF-κB activation by *P.aeruginosa*.
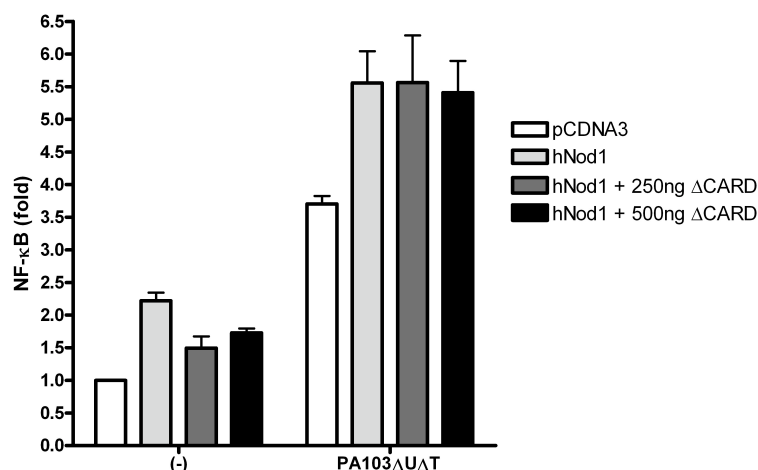
Figure 6.13; *P.aeruginosa* activates NF-κB independent of Nod1

HEK293 cells were transfected with pNF-κB-Luc, p-β-gal and pCDNA3 hNod1 indicated samples were also transfected with pCDNA3 ΔCARD. After 24 h cells were infected with PA103 ΔUΔT at a MOI of 50 for 90 min. Gentamicin was added for 12 h. Cell lysates were then analysed for luciferase and β-galactosidase activity. Columns are means of triplicates and error bars are SEM.

6.3 Discussion

NF-κB is a transcription factor involved in a range of processes. It mediates transcription of proinflammatory chemokines and cytokines. As a result several NF-κB activators have been described, as previously discussed. It has previously been shown that *P.aeruginosa* can activate NF-κB during infection [17, 475, 476].

The silencing of Nod1 by siRNA was never successful in this study. According to a previous publication by Viala et al. the half-life of endogenous Nod1 is relatively long which results in more time required to silence Nod1 (72 h) [222]. The same time periods were used during the experiments presented in this chapter. Further optimization would be needed; perhaps the construction of stably Nod1 siRNA silenced HEK293 cells or the use of cells from a Nod1 KO mouse. The antibody from Abcam, which recognise Nod1 results in several non-specific bands. The predicted size of Nod1 is 106 kDa, but the antibody recognises a band at 32 kDa. Instead of this antibody, an antibody from Cell signalling was used. After overexpression of Nod1 in HEK293 cells, it was possible to detect Nod1 at the correct size of 106 kDa. This indicates that the endogenous level of Nod1 in HEK293 cells is very low. However, it might also reflect the quality of commercial antibodies available directed towards Nod1. Therefore, the reporter gene assay was tested in siRNA transfected cells. No effect on the NF-κB activation by *P.aeruginosa* could be detected. This could be due to the protein not being silenced, but also that Nod1 is not involved in the NF-κB activation by *P.aeruginosa*. In this study it was also attempted to use siRNA to silence Nod1 in Nod1 transfected cells (results not shown). All the attempts resulted in blank blots and this approach was therefore abandoned. The silencing by siRNA of Nod1 in HEK293 cells was successful in the study by Viala et al. [222]. However, the antibody used in that study was in-house and thus not available commercially.

Instead of using siRNA to investigate the effects of Nod1 on NF-κB activation by *P.aeruginosa,* a dominant-negative construct of Nod1, ΔCARD, was used. The results for untreated cells transfected with Nod1 plasmid and cotransfected with ΔCARD vary between the different experiments described in this chapter. The

untreated cells seem to be affected in some of the experiments by ΔCARD. This might be due to an underlying Nod1 effect in the cells, but more likely reflects variations in the experiment due to the cells used, transfection reagent etc. The same transfection reagent and cells are used throughout this chapter but there might be slight differences between the confluency of cells, as well as the batch of transfection reagent. However, the results observed for *P.aeruginosa* is never affected by transfection and thus conclusions from these experiments can still be drawn. The variation seen for the results where cells are treated with LPS might also reflect variations in the batch of LPS used. LPS purified by phenol extraction can be used as a source of peptidoglycan, this will inevitably vary between batches and the exact amount of NF-κB stimulatory molecules added will be unknown.

The results presented in this chapter confirm that HEK293 cells do not respond to pure LPS (purified by ion-exchange chromatography), because these cells lack TLR2 and TLR4 expression [523, 524]. HEK293 cells do express TLR5 however, but this is irrelevant in this study since PA103 lacks flagellin.

Nod1 responds to the iE-DAP part of peptidoglycan from Gram-negative bacteria, as well as some Gram-positives. This reagent is commercially available and attempts were made during this investigation to use it for NF-κB activation. No conclusions could be drawn from these experiments and results are therefore excluded. Further optimisation with concentrations would have to be performed, but due to the time constraints of this project there was no time for these experiments. According to previously published data; high molecular-weight PGN is poorly stimulatory compared to synthetic molecules containing the minimal Nod1 stimulating structure [479, 481]. The molecular basis that accounts for these differences in activity is not understood. This offers some explanation to why the purified PGN is poorly stimulatory in the experiments with untransfected HEK293 cells.

Travassos et al. have described a role for Nod1 in NF-κB activation by *P.aeruginosa* [17]. This publication used the ΔCARD construct used in this study as well as fibroblasts from Nod1 KO mice. The pseudomonal strains used were PAK and PAO-1, which might contribute to the differences seen between this study and previous published results, since results presented here are from the

PA103 strain. The increase in luciferase activity observed by Travassos et al. corresponds to the increase seen in this study. The contradicting results for the Nod1-dependence presented in this chapter might be due to different experimental procedures. It should be mentioned however, that a flagellin deficient strain used by Travassos et al. was still able to activate NF-κB. PA103 does not have flagellin and thus the results presented here are, in this respect, similar to previous published results. Travassos et al. describes the Nod1 signalling pathway as a back-up system to the detection via TLRs. This indicates a more important role for other systems, which indeed agree with the results presented in this chapter. However, it is argued that a flagellin deficient strain will activate NF-κB via Nod1 even though it is able to avoid detection via TLR5. However, additional systems must exist, discussed in more detail below, since the flagellin deficient strain PA103 is able to activate NF-κB independent of both Nod1 and TLR5.

It was shown that Nod1 can respond to peptidoglycan which is delivered by the T4SS of *H.pylori* [222]. Similar to *P.aeruginosa*, *H.pylori* is a non-invasive Gram-negative pathogen. The study by Viala et al. not only investigated Nod1 involvement using the ΔCARD construct, but also used Nod1 KO mice. According to the results published by Viala et al. HEK293 cells express Nod1, which was investigated by mRNA expression. In this study no Nod1 could be detected in HEK293 cells alone, but mRNA expression was never investigated, instead Western blot was used which might not be as sensitive. In the *H.pylori* study the NF-κB activation could be abrogated when cells were cotransfected with the ΔCARD construct. This was not observed during this study, which might simply be due to the fact that different bacterial strains activate different receptors. This activation subsequently results in NF-κB activation.

The results presented in this chapter imply T3SS-dependent NF-κB activation by *P.aeruginosa*. There is an increase in NF-κB activation in cells infected with the PA103 strain which lacks a functional T3SS (PA103 ΔpcrV) compared to untreated cells, but a significantly increased activation when the bacteria has a functional T3SS. The activation seen following infection with PA103 ΔpcrV is probably due to activation of other receptors which lead to NF-κB activation.

P.aeruginosa clearly activates NF-κB during infection of HEK293 cells. This was shown here to be dependent on a functional T3SS, similar to previously published results for T4SS-dependent NF-κB activation by *H.pylori* [222]. In the study by Viala et al. the T4SS-dependent activation was mediated by specific peptidoglycan moieties passing through the secretion system. The mechanism for this however remains unknown. It is likely that the T3SS of *P.aeruginosa* could act as a conduit for NF-κB activating molecules such as peptidoglycan. From results presented in this chapter *P.aeruginosa* does not activate NF-κB in a Nod1-dependent manner. Nod2 is the other receptor which has been identified as a peptidoglycan receptor in mammalian cells [480, 481]. It would therefore be interesting to investigate the role of Nod2 in NF-κB activation by *P.aeruginosa*. There is also the possibility that *P.aeruginosa* activates NF-κB via a yet undiscovered receptor and / or an undiscovered mediator. It would be interesting to investigate the NF-κB activation following infection with *P.aeruginosa* in Nod1 KO mice to confirm the results seen in this study. Other KO mice could potentially also be used to investigate involvement of other receptors in the NF-κB activation seen.

All the results presented in this chapter indicate that Nod1 is not involved in the NF-κB activation following infection with *P.aeruginosa*. The same results have been found for *Yersinia*, which is very similar to *P.aeruginosa* (Presented by V. Auerbuch Stone at ASM, Boston 2008). This, compared to previous published results [17], implies that further studies are needed in order to determine the role of Nod1 in NF-κB activation by *P.aeruginosa*.

In conclusion, the results presented in this chapter describe a novel NF-κB activation by *P.aeruginosa* independent of Nod1 and TLR signalling. Furthermore, the NF-κB activation is increased when the bacteria has a functional T3SS, but is unaltered by the presence of translocated effectors. This implies a role for the T3SS as a conduit for a molecule, which is capable of activating NF-κB, via a hitherto unknown receptor.

7 General discussion and conclusions

P.aeruginosa is a Gram-negative, extracellular pathogen. It mainly causes infection in immuno-compromized individuals and treatment is difficult due to high levels of antibiotic resistance. This and the ability of *P.aeruginosa* to survive in a wide range of environments results in 10.1 % of all hospital acquired infections being caused by this pathogen. Among these infections only 50 % are treatable. Several vaccines and monoclonal antibodies against *P.aeruginosa* have been developed, but none of them has obtained market authorization [525]. The antigens that have been explored for vaccine development include LPS, extracellular proteins, flagella, pcrV of the T3SS, pili as well as whole killed bacteria and attenuated bacteria [525]. Due to the high antibiotic resistance of *P.aeruginosa* there is a need for other treatment options. New potential targets and options can be developed if the understanding of this pathogen is increased, for example the mechanism by which infection is caused and the host-response to this infection.

Innate immunity is the first response against infection. Even though it has been extensively studied over the years new PRRs and PAMPs are still being identified. NLRs were recently discovered as intracellular PRRs, as discussed in section 1.5.4. The aim of this thesis was to investigate whether and by which mechanism the extracellular *P.aeruginosa* can trigger intracellular PRR. To achieve this, the ability of *P.aeruginosa* to trigger inflammasome activation was investigated by the detection of mature IL-1ß secretion and active caspase-1, as well as the ability to trigger Nod1 activation by detection of activated NF-κB. These studies resulted in a number of novel findings, which will be discussed below.

The results in chapter 3 show that *P.aeruginosa* is able to activate the inflammasome complex dependent on NLRC4 and ASC. This was shown to be dependent on a functional T3SS. Similar results have been published, confirming the results presented in this thesis. Further studies revealed that this activation is dependent on extracellular potassium (chapter 4) and pilin (chapter 5), both identifying novel ways to trigger the NLRC4 inflammasome complex.

In the context of an infection bacteria are likely activate the innate immune response through several PRRs. This study, as well as previously published results, have identified several receptors being activated upon infection with *P.aeruginosa*; LPS via TLR4 [474], flagellin via TLR5 [472] and CpG DNA via TLR9

[473], as well as the activation of the NLRC4 inflammasome [249, 253, 354]. The results presented in this thesis shows that Nod1 activation is not involved in the innate immune response to *P.aeruginosa,* at least not under the conditions used in this study, chapter 6. Only a few of the 23 NLR-proteins identified in humans have had the activating PAMP or DAMP identified [172]. In addition, new stimuli, activating already described NLR-proteins, are constantly being presented, for example in this study for NLRC4. It is therefore likely that other receptors and PAMPs involved in the immune response against *P.aeruginosa* will be identified in the future, adding to our knowledge of this pathogen further. Furthermore, it is highly likely that several more NLR-protein complexes and collaborations between receptors will be identified. This will add to our understanding of the innate immune response, as well as the ability of pathogens to trigger inflammation. Costimulation of receptors contributes to a full blown inflammatory response, which the host requires to be specific, rapid and self-limiting [160]. Furthermore, involvement of several receptors has been shown to potentiate their activity through interactions between the receptors. Nod1 have been shown to act synergistically with TLR4 in the induction of proinflammatory cytokines [317, 318]. Dectin-1, involved in antifungal responses, has been shown to act synergistically in the same way with various TLRs [167].

P.aeruginosa has evolved mechanisms to inhibit NLRC4-mediated caspase-1 activation, by ExoU- and ExoS-dependent inhibition of caspase-1 activation and IL-1ß maturation [249, 526]. This suggests that the NLRC4-dependent pathway is important for host defence against Gram-negative bacterial infections. On the other hand, IL-1ß production can be detrimental for the host. Schultz et al. found that IL-1R deficiency had a protective effect in response to pulmonary infection with *P.aeruginosa* [527]. It has also been shown that neutralisation of IL-1ß with antibodies protected acid sphingomyelinase-deficient mice from lethal *P.aeruginosa* infection [528]. In addition, Thakur et al. found in a *P.aeruginosa* keratitis model, that caspase-1 deficiency results in less corneal damage [529, 530]. It should be noted however that it remains unclear from these studies if the adverse effects mediated by IL-1ß and caspase-1 are caused by inflammatory damage or lack of control of bacterial replication. It has also been published, in contrast to these studies, that IL-1R-deficient mice had greater colonization with *P.aeruginosa* compared with WT mice after oral

exposure to the pathogen in drinking water [531]. In the study by Sutterwala et al. it was shown that the NLRC4-inflammasome plays an important role in host defence against *P.aeruginosa* infection [249]. NLRC4-deficiency resulted in increased bacterial burden in the peritoneum and spleen of intraperitoneally infected mice. The mice were infected with PA103 ΔU and the infection correlated with a decrease in serum IL-1ß and IL-18 [249]. Furthermore, IL-1ß has a critical role in gut-derived sepsis caused by *P.aeruginosa*. IL-1ß-deficient mice had a lower survival rate than that of WT mice. *In vitro* phagocytosis and cytokine production by macrophages was impaired in IL-1ß-deficient mice compared to WT mice [532].

Therefore it can be argued that *P.aeruginosa* uses the inflammasome activation as a virulence mechanism. It has been shown, that an absence or reduction in endogenous IL-1ß activity improves host defence against *P.aeruginosa* caused pneumonia while suppressing the inflammatory response [527]. However, the inflammasome activation and IL-1ß secretion is clearly also important for host defence. This implies that the level of activation is important, where too much IL-1ß might aid the bacteria rather than the host. The fact that *P.aeruginosa* has evolved effectors that inhibit IL-1ß secretion suggests that the inflammasome activation is beneficial for the host but not the bacteria. This is further strengthened by the fact that *P.aeruginosa* is able to trigger inflammasome activation independent of effectors passing through the secretion system, indicating that the host has evolved mechanisms to detect PAMPs 'mistakenly' translocated into the host cell. If the level of activation is important a therapeutic model could be to dampen, but not completely abrogate the inflammasome response during, for example, infection. Inappropriate activation of the NLRP3 inflammasome has been linked to gout and silicosis. It was recently shown that Glybenclamide is able to inhibit NLRP3-induced IL-1ß secretion, which was independent of its activity as a potassium-channel inhibitor [533]. Glybenclamide is already approved for the treatment of type 2 diabetes and thus this result provides hope for patients suffering from silicosis. In addition, glybenclamide could potentially be used to dampen, at the correct dose, the inflammasome activation during infection, which would allow the innate immune response to combat infection without the detrimental effects leading to bacterial spread rather than clearance.

Glybenclamide was used in this study as an inhibitor of potassium-channels, to investigate the role of extracellular potassium in the inflammasome activation by *P.aeruginosa*. It was shown that following Glybenclamide treatment the IL-1ß secretion was inhibited, although not completely abrogated. Recently published results indicate that this effect has nothing to do with potassium-channels, rather an effect on the NLRP3 inflammasome [533]. However, it is known from previous publications, as well as from results presented in this thesis, that the inflammasome activation by *P.aeruginosa* is dependent on the NLRC4 inflammasome. Maybe the inhibitory effect of Glybencalmide also affects the NLRC4 inflammasome, as the results presented here would suggest, but further studies are needed to confirm this hypothesis.

It was shown in chapter 4 that both *P.aeruginosa* and *Salmonella* are dependent on extracellular potassium concentration for the activation of the inflammasome. Several potential mechanisms were proposed for this activation. The most likely, based on results in this thesis, include the disruption of membrane potential and / or involvement of intracellular potassium storage compartments. These hypotheses are difficult to examine, since the disruption of membrane potential experimentally most likely involves potassium, and it is already known that changes in extracellular potassium levels will affect the inflammasome activation. Furthermore, not much is known about intracellular potassium compartments, which means investigation of this hypothesis would involve the development of entire new methodology. The other suggestions for the triggering of inflammasome activation by the bacteria involve the formation of a T3SS pore in the host cell membrane, which, as well as effectors, allow passage of other small molecules and ions. The results presented in this thesis indicate that the pore formed by the T3SS of *P.aeruginosa* forms a tight association with the host cell membrane and does not allow other molecules or ions to pass through. Despite the lack of a leaky pore, a membrane repair response could be seen, as LAMP-1 relocates to the cellular surface following infection. It has been shown for *Neisseria meningitidis* that binding of its type IV pili to CD46 on human epithelial cells induces an increase in the concentration of cytosolic free calcium [534]. This pilus-induced calcium flux triggers lysosomal exocytosis, which would lead to relocation of LAMP-1 to the cellular surface. However the consequences of these effects are not yet known [534]. The results

presented in this thesis could not detect a change in intracellular calcium, but that might be explained by the method used.

A wide range of PAMPs and DAMPs have been identified as inflammasome complex activators, as previously described. In addition, the results presented in this thesis have identified a role for extracellular potassium in the activation of the NLRC4 inflammasome complex. Potassium also plays an important role in the activation of the NLRP3 and NLRP1 inflammasome complexes. The NLRC4 inflammasome is activated by PAMPs which pass through a bacterial secretion system, such as flagellin, previously published, and pilin, described in chapter 5 of this thesis. This suggests that the NLRC4 inflammasome is triggered by an effect mediated by the secretion systems, either T3SS or T4SS. In contrast, the NLRP3 inflammasome is triggered by pore-forming toxins and cellular damage caused by various crystals [371].

Pilin is able to activate the inflammasome, as shown in chapter 5. This occurs in a T3SS-dependent manner. In addition, previous studies have identified flagellin as an inflammasome trigger, also dependent on a functional T3SS. This suggests that flagellin and pilin are able to pass through the T3SS, even though it was believed that the translocation through the T3SS is regulated [535]. The finding that flagellin is able to pass through the T3SS of *Salmonella* further strengthens this hypothesis. In addition, it has been shown that PGN is able to pass through the T4SS of *H.pylori*. Together these results suggest that the host has developed mechanisms to detect bacterial mediators that might pass through the bacterial secretion systems by mistake.

Furthermore, this is the first demonstration of recognition of type IV pilin by a PRR. Type IV pili shares features with other PAMPs such as adhesion, which is an important virulence determinant. In addition, there are sequence similarities of the pilin gene between different bacterial species. These and other factors most likely mediate a strong selection pressure for the development of a pilin specific PRR. In addition the Nod-proteins, Nod1 and Nod2 are the only known sensors of PGN [492], although this have been questioned [495]. Furthermore, it has been shown that TLR2 and TLR4 are not the major receptors responding to *P.aeruginosa* infection [536].This clearly demonstrates a very important role for the NLR proteins in innate immunity.

The results presented in this thesis have answered a number of questions regardning the triggering of PRRs by *P.aeruginosa*, but there are still a lot of questions to be answered. However, in conclusion the results provide a deeper understanding for the mechanism by which *P.aeruginosa* triggers the inflammatory response and how the host responds to infection by this pathogen. These are all important points for the discovery and development of new treatment options.

Bibliography

1. Williams, P.A. and M.J. Worsey, *Ubiquity of plasmids in coding for toluene and xylene metabolism in soil bacteria: evidence for the existence of new TOL plasmids.* J Bacteriol, 1976. **125**(3): p. 818-28.

2. Berthelot, P., et al., *Prospective study of nosocomial colonization and infection due to Pseudomonas aeruginosa in mechanically ventilated patients.* Intensive Care Med, 2001. **27**(3): p. 503-12.

3. Lyczak, J.B., C.L. Cannon, and G.B. Pier, *Establishment of Pseudomonas aeruginosa infection: lessons from a versatile opportunist.* Microbes Infect, 2000. **2**(9): p. 1051-60.

4. Sadikot, R.T., et al., *Pathogen-host interactions in Pseudomonas aeruginosa pneumonia.* Am J Respir Crit Care Med, 2005. **171**(11): p. 1209-23.

5. Roy-Burman, A., et al., *Type III Protein Secretion Is Associated with Death in Lower Respiratory and Systemic Pseudomonas aeruginosa Infections.* The Journal of Infectious Diseases, 2001. **183**(12): p. 1767-1774.

6. Soscia, C., et al., *Cross Talk between Type III Secretion and Flagellar Assembly Systems in Pseudomonas aeruginosa.* J Bacteriol, 2007. **189**(8): p. 3124-32.

7. Chitkara, Y.K. and T.C. Feierabend, *Endogenous and exogenous infection with Pseudomonas aeruginosa in a burns unit.* Int Surg, 1981. **66**(3): p. 237-40.

8. Yoshihara, E. and S. Eda, *Diversity in the Oligomeric Channel Structure of the Multidrug Efflux Pumps in Pseudomonas aeruginosa.* Microbiol Immunol, 2007. **51**(1): p. 47-52.

9. Chuanchuen, R., C.T. Narasaki, and H.P. Schweizer, *The MexJK efflux pump of Pseudomonas aeruginosa requires OprM for antibiotic efflux but not for efflux of triclosan.* J Bacteriol, 2002. **184**(18): p. 5036-44.

10. Kohler, T., et al., *Characterization of MexE-MexF-OprN, a positively regulated multidrug efflux system of Pseudomonas aeruginosa.* Mol Microbiol, 1997. **23**(2): p. 345-54.

11. Poole, K., et al., *Overexpression of the mexC-mexD-oprJ efflux operon in nfxB-type multidrug-resistant strains of Pseudomonas aeruginosa.* Mol Microbiol, 1996. **21**(4): p. 713-24.

12. Poole, K., et al., *Multiple antibiotic resistance in Pseudomonas aeruginosa: evidence for involvement of an efflux operon.* J Bacteriol, 1993. **175**(22): p. 7363-72.

13. Stieritz, D.D. and I.A. Holder, *Experimental studies of the pathogenesis of infections due to Pseudomonas aeruginosa: description of a burned mouse model.* J Infect Dis, 1975. **131**(6): p. 688-91.

14. Welsh, M.J., et al., *Cystic fibrosis transmembrane conductance regulator: A chloride channel with novel regulation.* Neuron, 1992. **8**(5): p. 821-829.

15. Davies, J., et al., *Reduction in the adherence of Pseudomonas aeruginosa to native cystic fibrosis epithelium with anti-asialoGM1 antibody and neuraminidase inhibition.* Eur Respir J, 1999. **13**(3): p. 565-570.

16. Govan, J.R. and V. Deretic, *Microbial pathogenesis in cystic fibrosis: mucoid Pseudomonas aeruginosa and Burkholderia cepacia.* Microbiol Rev, 1996. **60**(3): p. 539-74.

17. Travassos, L.H., et al., *Nod1 participates in the innate immune response to Pseudomonas aeruginosa.* J Biol Chem, 2005. **280**(44): p. 36714-8.

18. Gophna, U., E.Z. Ron, and D. Graur, *Bacterial type III secretion systems are ancient and evolved by multiple horizontal-transfer events*. Gene, 2003. **312**: p. 151-63.
19. Saier, M.H., Jr., *Evolution of bacterial type III protein secretion systems*. Trends Microbiol, 2004. **12**(3): p. 113-5.
20. Shapiro, L., *The bacterial flagellum: From genetic network to complex architecture*. Cell, 1995. **80**(4): p. 525-527.
21. Mahenthiralingam, E., M.E. Campbell, and D.P. Speert, *Nonmotility and phagocytic resistance of Pseudomonas aeruginosa isolates from chronically colonized patients with cystic fibrosis*. Infect. Immun., 1994. **62**(2): p. 596-605.
22. Landsperger, W.J., et al., *Inhibition of bacterial motility with human antiflagellar monoclonal antibodies attenuates Pseudomonas aeruginosa-induced pneumonia in the immunocompetent rat*. Infect. Immun., 1994. **62**(11): p. 4825-4830.
23. Montie, T.C., R.C. Craven, and I.A. Holder, *Flagellar preparations from Pseudomonas aeruginosa: isolation and characterization*. Infect. Immun., 1982. **35**(1): p. 281-288.
24. Arora, S.K., et al., *The Pseudomonas aeruginosa Flagellar Cap Protein, FliD, Is Responsible for Mucin Adhesion*. Infect. Immun., 1998. **66**(3): p. 1000-1007.
25. Feldman, M., et al., *Role of Flagella in Pathogenesis of Pseudomonas aeruginosa Pulmonary Infection*. Infect. Immun., 1998. **66**(1): p. 43-51.
26. Craig, L., M.E. Pique, and J.A. Tainer, *Type IV pilus structure and bacterial pathogenicity*. Nat Rev Microbiol, 2004. **2**(5): p. 363-78.
27. Bradley, D.E., *A function of Pseudomonas aeruginosa PAO polar pili: twitching motility*. Can J Microbiol, 1980. **26**(2): p. 146-54.
28. Johnson, K., M.L. Parker, and S. Lory, *Nucleotide sequence and transcriptional initiation site of two Pseudomonas aeruginosa pilin genes*. J. Biol. Chem., 1986. **261**(33): p. 15703-15708.
29. Woods, D.E., et al., *Role of pili in adherence of Pseudomonas aeruginosa to mammalian buccal epithelial cells*. Infect. Immun., 1980. **29**(3): p. 1146-1151.
30. Frost, L.S. and W. Paranchych, *Composition and molecular weight of pili purified from Pseudomonas aeruginosa K*. J. Bacteriol., 1977. **131**(1): p. 259-269.
31. Hazlett, L.D., et al., *Analysis of adhesion, piliation, protease production and ocular infectivity of several P. aeruginosa strains*. Current Eye Research, 1991. **10**(4): p. 351 - 362.
32. Chi, E., et al., *Interaction of Pseudomonas aeruginosa with A549 pneumocyte cells*. Infect. Immun., 1991. **59**(3): p. 822-828.
33. Sheth, H.B., et al., *The pili of Pseudomonas aeruginosa strains PAK and PAO bind specifically to the carbohydrate sequence beta GalNAc(1-4)beta Gal found in glycosphingolipids asialo-GM1 and asialo-GM2*. Mol Microbiol, 1994. **11**(4): p. 715-23.
34. Ramphal, R., et al., *Adhesion of Pseudomonas aeruginosa pilin-deficient mutants to mucin*. Infect Immun, 1991. **59**(4): p. 1307-11.
35. Comolli, J.C., et al., *Pili Binding to Asialo-GM1 on Epithelial Cells Can Mediate Cytotoxicity or Bacterial Internalization by Pseudomonas aeruginosa*. Infect. Immun., 1999. **67**(7): p. 3207-3214.
36. Schroeder, T.H., T. Zaidi, and G.B. Pier, *Lack of adherence of clinical isolates of Pseudomonas aeruginosa to asialo-GM(1) on epithelial cells*. Infect Immun, 2001. **69**(2): p. 719-29.

37.   Harvey, H., et al., *Single-residue changes in the C-terminal disulfide-bonded loop of the Pseudomonas aeruginosa type IV pilin influence pilus assembly and twitching motility.* J Bacteriol, 2009. **191**(21): p. 6513-24.

38.   Doig, P., et al., *Role of pili in adhesion of Pseudomonas aeruginosa to human respiratory epithelial cells.* Infect. Immun., 1988. **56**(6): p. 1641-1646.

39.   Farinha, M.A., et al., *Alteration of the pilin adhesin of Pseudomonas aeruginosa PAO results in normal pilus biogenesis but a loss of adherence to human pneumocyte cells and decreased virulence in mice.* Infect. Immun., 1994. **62**(10): p. 4118-4123.

40.   Hazes, B., et al., *Crystal structure of Pseudomonas aeruginosa PAK pilin suggests a main-chain-dominated mode of receptor binding.* Journal of Molecular Biology, 2000. **299**(4): p. 1005-1017.

41.   Keizer, D.W., et al., *Structure of a Pilin Monomer from Pseudomonas aeruginosa. IMPLICATIONS FOR THE ASSEMBLY OF PILI.* J. Biol. Chem., 2001. **276**(26): p. 24186-24193.

42.   Craig, L., et al., *Type IV pilin structure and assembly: X-ray and EM analyses of Vibrio cholerae toxin-coregulated pilus and Pseudomonas aeruginosa PAK pilin.* Mol Cell, 2003. **11**(5): p. 1139-50.

43.   Zhang, H.Z. and M.S. Donnenberg, *DsbA is required for stability of the type IV pilin of enteropathogenic escherichia coli.* Mol Microbiol, 1996. **21**(4): p. 787-97.

44.   Suh, J.Y., et al., *Backbone dynamics of receptor binding and antigenic regions of a Pseudomonas aeruginosa pilin monomer.* Biochemistry, 2001. **40**(13): p. 3985-95.

45.   Comolli, J.C., et al., *Pseudomonas aeruginosa Gene Products PilT and PilU Are Required for Cytotoxicity In Vitro and Virulence in a Mouse Model of Acute Pneumonia.* Infect. Immun., 1999. **67**(7): p. 3625-3630.

46.   Kang, P.J., et al., *Identification of Pseudomonas aeruginosa genes required for epithelial cell injury.* Mol Microbiol, 1997. **24**(6): p. 1249-62.

47.   Merz, A.J., M. So, and M.P. Sheetz, *Pilus retraction powers bacterial twitching motility.* Nature, 2000. **407**(6800): p. 98-102.

48.   Skerker, J.M. and H.C. Berg, *Direct observation of extension and retraction of type IV pili.* Proceedings of the National Academy of Sciences of the United States of America, 2001. **98**(12): p. 6901-6904.

49.   Fussenegger, M., et al., *Transformation competence and type-4 pilus biogenesis in Neisseria gonorrhoeae - a review.* Gene, 1997. **192**(1): p. 125-134.

50.   Wolfgang, M., et al., *Components and dynamics of fiber formation define a ubiquitous biogenesis pathway for bacterial pili.* EMBO J, 2000. **19**(23): p. 6408-18.

51.   Whitchurch, C.B., et al., *Characterisation of a Pseudomonas aeruginosa twitching motility gene and evidence for a specialised protein export system widespread in eubacteria.* Gene, 1991. **101**(1): p. 33-44.

52.   Zolfaghar, I., D.J. Evans, and S.M.J. Fleiszig, *Twitching Motility Contributes to the Role of Pili in Corneal Infection Caused by Pseudomonas aeruginosa.* Infect. Immun., 2003. **71**(9): p. 5389-5393.

53.   Martin, P.R., et al., *Characterization of pilQ, a new gene required for the biogenesis of type 4 fimbriae in Pseudomonas aeruginosa.* Mol Microbiol, 1993. **9**(4): p. 857-68.

54.   Bitter, W., et al., *Formation of oligomeric rings by XcpQ and PilQ, which are involved in protein transport across the outer membrane of Pseudomonas aeruginosa.* Mol Microbiol, 1998. **27**(1): p. 209-19.

55. Semmler, A.B.T., C.B. Whitchurch, and J.S. Mattick, *A re-examination of twitching motility in Pseudomonas aeruginosa.* Microbiology, 1999. **145**(10): p. 2863-2873.

56. Tang, H., M. Kays, and A. Prince, *Role of Pseudomonas aeruginosa pili in acute pulmonary infection.* Infect Immun, 1995. **63**(4): p. 1278-85.

57. Pier, G.B. and P. Ames, *Mediation of the killing of rough, mucoid isolates of Pseudomonas aeruginosa from patients with cystic fibrosis by the alternative pathway of complement.* J Infect Dis, 1984. **150**(2): p. 223-8.

58. Folschweiller, N., et al., *The pyoverdin receptor FpvA, a TonB-dependent receptor involved in iron uptake by Pseudomonas aeruginosa (review).* Mol Membr Biol, 2000. **17**(3): p. 123-33.

59. Poole, K. and G.A. McKay, *Iron acquisition and its control in Pseudomonas aeruginosa: many roads lead to Rome.* Front Biosci, 2003. **8**: p. d661-86.

60. Bejarano, P.A., et al., *Degradation of basement membranes by Pseudomonas aeruginosa elastase.* Infect Immun, 1989. **57**(12): p. 3783-7.

61. Pavlovskis, O.R. and B. Wretlind, *Assessment of protease (elastase) as a Pseudomonas aeruginosa virulence factor in experimental mouse burn infection.* Infect Immun, 1979. **24**(1): p. 181-7.

62. Kharazmi, A. and H. Nielsen, *Inhibition of human monocyte chemotaxis and chemiluminescence by Pseudomonas aeruginosa elastase.* APMIS, 1991. **99**(1): p. 93-5.

63. Iglewski, B.H. and D. Kabat, *NAD-dependent inhibition of protein synthesis by Pseudomonas aeruginosa toxin.* Proc Natl Acad Sci U S A, 1975. **72**(6): p. 2284-8.

64. Allured, V.S., et al., *Structure of exotoxin A of Pseudomonas aeruginosa at 3.0-Angstrom resolution.* Proc Natl Acad Sci U S A, 1986. **83**(5): p. 1320-4.

65. McClure, C.D. and N.L. Schiller, *Effects of Pseudomonas aeruginosa rhamnolipids on human monocyte-derived macrophages.* J Leukoc Biol, 1992. **51**(2): p. 97-102.

66. Terada, L.S., et al., *Pseudomonas aeruginosa hemolytic phospholipase C suppresses neutrophil respiratory burst activity.* Infect Immun, 1999. **67**(5): p. 2371-6.

67. Lau, G.W., et al., *The role of pyocyanin in Pseudomonas aeruginosa infection.* Trends Mol Med, 2004. **10**(12): p. 599-606.

68. Tseng, T.T., B.M. Tyler, and J.C. Setubal, *Protein secretion systems in bacterial-host associations, and their description in the Gene Ontology.* BMC Microbiol, 2009. **9 Suppl 1**: p. S2.

69. Desvaux, M., et al., *Type III secretion: what's in a name?* Trends In Microbiology, 2006. **14**(4): p. 157-160.

70. Frank, D.W., *The exoenzyme S regulon of Pseudomonas aeruginosa.* Molecular Microbiology, 1997. **26**(4): p. 621-629.

71. Hauser, A.R., *The type III secretion system of Pseudomonas aeruginosa: infection by injection.* Nat Rev Micro, 2009. **7**(9): p. 654-665.

72. Hauser, A.R., et al., *Type III protein secretion is associated with poor clinical outcomes in patients with ventilator-associated pneumonia caused by Pseudomonas aeruginosa.* Crit Care Med, 2002. **30**(3): p. 521-8.

73. FinckBarbancon, V., et al., *ExoU expression by Pseudomonas aeruginosa correlates with acute cytotoxicity and epithelial injury.* Molecular Microbiology, 1997. **25**(3): p. 547-557.

74. Hauser, A.R., P.J. Kang, and J.N. Engel, *PepA, a secreted protein of Pseudomonas aeruginosa, is necessary for cytotoxicity and virulence.* Molecular Microbiology, 1998. **27**(4): p. 807-818.

75. Lee, V.T., et al., *Activities of pseudomonas aeruginosa effectors secreted by the type III secretion system in vitro and during infection.* Infection And Immunity, 2005. **73**(3): p. 1695-1705.

76. Sawa, T., et al., *In vitro cellular toxicity predicts Pseudomonas aeruginosa virulence in lung infections.* Infect Immun, 1998. **66**(7): p. 3242-9.

77. Lee, E.J., D.J. Evans, and S.M. Fleiszig, *Role of Pseudomonas aeruginosa ExsA in penetration through corneal epithelium in a novel in vivo model.* Invest Ophthalmol Vis Sci, 2003. **44**(12): p. 5220-7.

78. Vance, R.E., A. Rietsch, and J.J. Mekalanos, *Role of the type III secreted exoenzymes S, T, and Y in systemic spread of Pseudomonas aeruginosa PAO1 in vivo.* Infect Immun, 2005. **73**(3): p. 1706-13.

79. Holder, I.A., A.N. Neely, and D.W. Frank, *Type III secretion/intoxication system important in virulence of Pseudomonas aeruginosa infections in burns.* Burns, 2001. **27**(2): p. 129-30.

80. Pastor, A., et al., *PscF is a major component of the Pseudomonas aeruginosa type III secretion needle.* FEMS Microbiol Lett, 2005. **253**(1): p. 95-101.

81. Hoiczyk, E. and G. Blobel, *Polymerization of a single protein of the pathogen Yersinia enterocolitica into needles punctures eukaryotic cells.* Proc Natl Acad Sci U S A, 2001. **98**(8): p. 4669-74.

82. Kubori, T., et al., *Supramolecular structure of the Salmonella typhimurium type III protein secretion system.* Science, 1998. **280**(5363): p. 602-605.

83. Woestyn, S., et al., *YscN, the putative energizer of the Yersinia Yop secretion machinery.* J Bacteriol, 1994. **176**(6): p. 1561-9.

84. Blaylock, B., et al., *Characterization of the Yersinia enterocolitica type III secretion ATPase YscN and its regulator, YscL.* J Bacteriol, 2006. **188**(10): p. 3525-34.

85. Burghout, P., et al., *Role of the pilot protein YscW in the biogenesis of the YscC secretin in Yersinia enterocolitica.* J Bacteriol, 2004. **186**(16): p. 5366-75.

86. Koster, M., et al., *The outer membrane component, YscC, of the Yop secretion machinery of Yersinia enterocolitica forms a ring-shaped multimeric complex.* Mol Microbiol, 1997. **26**(4): p. 789-97.

87. Journet, L., et al., *The needle length of bacterial injectisomes is determined by a molecular ruler.* Science, 2003. **302**(5651): p. 1757-1760.

88. Burns, R.E., A. McDaniel-Craig, and A. Sukhan, *Site-directed mutagenesis of the Pseudomonas aeruginosa type III secretion system protein PscJ reveals an essential role for surface-localized residues in needle complex function.* Microb Pathog, 2008. **45**(3): p. 225-30.

89. Sundin, C., et al., *Polarisation of type III translocation by Pseudomonas aeruginosa requires PcrG, PcrV and PopN.* Microbial Pathogenesis, 2004. **37**(6): p. 313-322.

90. Hakansson, S., et al., *The YopB protein of Yersinia pseudotuberculosis is essential for the translocation of Yop effector proteins across the target cell plasma membrane and displays a contact-dependent membrane disrupting activity.* Embo Journal, 1996. **15**(21): p. 5812-5823.

91. Cornelis, G.R., *The Yersinia Ysc-Yop 'type III' weaponry.* Nat Rev Mol Cell Biol, 2002. **3**(10): p. 742-52.

92. Dacheux, D., et al., *Pore-forming activity of type III system-secreted proteins leads to oncosis of Pseudomonas aeruginosa-infected macrophages.* Molecular Microbiology, 2001. **40**(1): p. 76-85.

93. Sawa, T., et al., *Active and passive immunization with the Pseudomonas V antigen protects against type III intoxication and lung injury.* Nature Medicine, 1999. **5**(4): p. 392-398.

94. Sundin, C., et al., *Type IV pili are not specifically required for contact dependent translocation of exoenzymes by Pseudomonas aeruginosa.* Microbial Pathogenesis, 2002. **33**(6): p. 265-277.

95. Faudry, E., et al., *Synergistic pore formation by type III toxin translocators of Pseudomonas aeruginosa.* Biochemistry, 2006. **45**(26): p. 8117-8123.

96. Schoehn, G., et al., *Oligomerization of type III secretion proteins PopB and PopD precedes pore formation in Pseudomonas.* Embo Journal, 2003. **22**(19): p. 4957-4967.

97. Goure, J., et al., *Protective Anti–€ V Antibodies Inhibit Pseudomonas and Yersinia Translocon Assembly within Host Membranes.* The Journal of Infectious Diseases, 2005. **192**(2): p. 218-225.

98. Goure, J., et al., *The V antigen of Pseudomonas aeruginosa is required for assembly of the functional PopB/PopD translocation pore in host cell membranes.* Infect Immun, 2004. **72**(8): p. 4741-50.

99. Holmstrom, A., et al., *LcrV is a channel size-determining component of the Yop effector translocon of Yersinia.* Molecular Microbiology, 2001. **39**(3): p. 620-632.

100. Frank, D., et al., *Generation and Characterization of a Protective Monoclonal Antibody to Pseudomonas aeruginosa PcrV.* The Journal of Infectious Diseases, 2002. **186**(1): p. 64-73.

101. Holder, I.A., A.N. Neely, and D.W. Frank, *PcrV immunization enhances survival of burned Pseudomonas aeruginosa-infected mice.* Infect Immun, 2001. **69**(9): p. 5908-10.

102. Mueller, C.A., et al., *The V-antigen of Yersinia forms a distinct structure at the tip of injectisome needles.* Science, 2005. **310**(5748): p. 674-676.

103. Mota, L.J., *Type III secretion gets an LcrV tip.* Trends Microbiol, 2006. **14**(5): p. 197-200.

104. Frithz-Lindsten, E., et al., *Functional conservation of the effector protein translocators PopB/YopB and PopD/YopD of Pseudomonas aeruginosa and Yersinia pseudotuberculosis.* Mol Microbiol, 1998. **29**(5): p. 1155-65.

105. Rosqvist, R., K.E. Magnusson, and H. Wolf-Watz, *Target cell contact triggers expression and polarized transfer of Yersinia YopE cytotoxin into mammalian cells.* Embo J, 1994. **13**(4): p. 964-72.

106. Pettersson, J., et al., *Modulation of virulence factor expression by pathogen target cell contact.* Science, 1996. **273**(5279): p. 1231-3.

107. Vallis, A.J., et al., *Regulation of ExoS production and secretion by Pseudomonas aeruginosa in response to tissue culture conditions.* Infection And Immunity, 1999. **67**(2): p. 914-920.

108. Hornef, M.W., et al., *Triggering the ExoS regulon of Pseudomonas aeruginosa: A GFP-reporter analysis of exoenzyme (Exo) S, ExoT and ExoU synthesis.* Microb Pathog, 2000. **29**(6): p. 329-43.

109. Yahr, T.L., J. Goranson, and D.W. Frank, *Exoenzyme S of Pseudomonas aeruginosa is secreted by a type III pathway.* Mol Microbiol, 1996. **22**(5): p. 991-1003.

110. Hovey, A.K. and D.W. Frank, *Analyses of the DNA-binding and transcriptional activation properties of ExsA, the transcriptional*

activator of the Pseudomonas aeruginosa exoenzyme S regulon. J Bacteriol, 1995. **177**(15): p. 4427-36.

111. Dasgupta, N., et al., *A novel anti-anti-activator mechanism regulates expression of the Pseudomonas aeruginosa type III secretion system.* Mol Microbiol, 2004. **53**(1): p. 297-308.

112. McCaw, M.L., et al., *ExsD is a negative regulator of the Pseudomonas aeruginosa type III secretion regulon.* Mol Microbiol, 2002. **46**(4): p. 1123-33.

113. Urbanowski, M.L., G.L. Lykken, and T.L. Yahr, *A secreted regulatory protein couples transcription to the secretory activity of the Pseudomonas aeruginosa type III secretion system.* Proc Natl Acad Sci U S A, 2005. **102**(28): p. 9930-5.

114. Zheng, Z., et al., *Biochemical characterization of a regulatory cascade controlling transcription of the Pseudomonas aeruginosa type III secretion system.* J Biol Chem, 2007. **282**(9): p. 6136-42.

115. Rietsch, A., et al., *ExsE, a secreted regulator of type III secretion genes in Pseudomonas aeruginosa.* Proc Natl Acad Sci U S A, 2005. **102**(22): p. 8006-11.

116. Urbanowski, M.L., E.D. Brutinel, and T.L. Yahr, *Translocation of ExsE into Chinese hamster ovary cells is required for transcriptional induction of the Pseudomonas aeruginosa type III secretion system.* Infect Immun, 2007. **75**(9): p. 4432-9.

117. Yahr, T.L., et al., *ExoY, an adenylate cyclase secreted by the Pseudomonas aeruginosa type III system.* Proc Natl Acad Sci U S A, 1998. **95**(23): p. 13899-904.

118. Frithz-Lindsten, E., et al., *Intracellular targeting of exoenzyme S of Pseudomonas aeruginosa via type III-dependent translocation induces phagocytosis resistance, cytotoxicity and disruption of actin microfilaments.* Mol Microbiol, 1997. **25**(6): p. 1125-39.

119. Feltman, H., et al., *Prevalence of type III secretion genes in clinical and environmental isolates of Pseudomonas aeruginosa.* Microbiology, 2001. **147**(10): p. 2659-2669.

120. Fleiszig, S.M., et al., *Pseudomonas aeruginosa-mediated cytotoxicity and invasion correlate with distinct genotypes at the loci encoding exoenzyme S.* Infect Immun, 1997. **65**(2): p. 579-86.

121. Engel, J. and P. Balachandran, *Role of Pseudomonas aeruginosa type III effectors in disease.* Curr Opin Microbiol, 2009. **12**(1): p. 61-6.

122. Parsot, C., C. Hamiaux, and A.L. Page, *The various and varying roles of specific chaperones in type III secretion systems.* Curr Opin Microbiol, 2003. **6**(1): p. 7-14.

123. Goehring, U.M., et al., *The N-terminal domain of Pseudomonas aeruginosa exoenzyme S is a GTPase-activating protein for Rho GTPases.* J Biol Chem, 1999. **274**(51): p. 36369-72.

124. Ganesan, A.K., et al., *Pseudomonas aeruginosa exoenzyme S ADP-ribosylates Ras at multiple sites.* J Biol Chem, 1998. **273**(13): p. 7332-7.

125. Henriksson, M.L., et al., *Ras effector pathway activation by epidermal growth factor is inhibited in vivo by exoenzyme S ADP-ribosylation of Ras.* Biochem J, 2000. **347 Pt 1**: p. 217-22.

126. Liu, S., S.M. Kulich, and J.T. Barbieri, *Identification of glutamic acid 381 as a candidate active site residue of Pseudomonas aeruginosa exoenzyme S.* Biochemistry, 1996. **35**(8): p. 2754-8.

127. Pederson, K.J. and J.T. Barbieri, *Intracellular expression of the ADP-ribosyltransferase domain of Pseudomonas exoenzyme S is cytotoxic to eukaryotic cells*. Mol Microbiol, 1998. **30**(4): p. 751-9.

128. Vincent, T.S., et al., *ADP-ribosylation of oncogenic Ras proteins by pseudomonas aeruginosa exoenzyme S in vivo*. Mol Microbiol, 1999. **32**(5): p. 1054-64.

129. Coburn, J., et al., *Pseudomonas aeruginosa exoenzyme S requires a eukaryotic protein for ADP-ribosyltransferase activity*. J Biol Chem, 1991. **266**(10): p. 6438-46.

130. Garrity-Ryan, L., et al., *The arginine finger domain of ExoT contributes to actin cytoskeleton disruption and inhibition of internalization of Pseudomonas aeruginosa by epithelial cells and macrophages*. Infect Immun, 2000. **68**(12): p. 7100-13.

131. Kaufman, M.R., et al., *Pseudomonas aeruginosa mediated apoptosis requires the ADP-ribosylating activity of exoS*. Microbiology, 2000. **146 (Pt 10)**: p. 2531-41.

132. Cisz, M., P.C. Lee, and A. Rietsch, *ExoS controls the cell contact-mediated switch to effector secretion in Pseudomonas aeruginosa*. J Bacteriol, 2008. **190**(8): p. 2726-38.

133. Yahr, T.L., et al., *Transcriptional analysis of the Pseudomonas aeruginosa exoenzyme S structural gene*. J Bacteriol, 1995. **177**(5): p. 1169-78.

134. Zhang, Y. and J.T. Barbieri, *A leucine-rich motif targets Pseudomonas aeruginosa ExoS within mammalian cells*. Infect Immun, 2005. **73**(12): p. 7938-45.

135. Zhang, Y., Q. Deng, and J.T. Barbieri, *Intracellular localization of type III-delivered Pseudomonas ExoS with endosome vesicles*. J Biol Chem, 2007. **282**(17): p. 13022-32.

136. Deng, Q. and J.T. Barbieri, *Molecular mechanisms of the cytotoxicity of ADP-ribosylating toxins*. Annu Rev Microbiol, 2008. **62**: p. 271-88.

137. Kazmierczak, B.I. and J.N. Engel, *Pseudomonas aeruginosa ExoT acts in vivo as a GTPase-activating protein for RhoA, Rac1, and Cdc42*. Infect Immun, 2002. **70**(4): p. 2198-205.

138. Shafikhani, S.H. and J. Engel, *Pseudomonas aeruginosa type III-secreted toxin ExoT inhibits host-cell division by targeting cytokinesis at multiple steps*. Proc Natl Acad Sci U S A, 2006. **103**(42): p. 15605-10.

139. Liu, S., et al., *Biochemical relationships between the 53-kilodalton (Exo53) and 49-kilodalton (ExoS) forms of exoenzyme S of Pseudomonas aeruginosa*. J Bacteriol, 1997. **179**(5): p. 1609-13.

140. Allewelt, M., et al., *Acquisition of expression of the Pseudomonas aeruginosa ExoU cytotoxin leads to increased bacterial virulence in a murine model of acute pneumonia and systemic spread*. Infection And Immunity, 2000. **68**(7): p. 3998-4004.

141. Kurahashi, K., et al., *Pathogenesis of septic shock in Pseudomonas aeruginosa pneumonia*. J Clin Invest, 1999. **104**(6): p. 743-50.

142. Phillips, R.M., et al., *In Vivo Phospholipase Activity of the Pseudomonas aeruginosa Cytotoxin ExoU and Protection of Mammalian Cells with Phospholipase A2 Inhibitors*. J. Biol. Chem., 2003. **278**(42): p. 41326-41332.

143. Sato, H., et al., *The mechanism of action of the Pseudomonas aeruginosa-encoded type III cytotoxin, ExoU*. Embo Journal, 2003. **22**(12): p. 2959-2969.

144. Rabin, S.D.P. and A.R. Hauser, *Functional regions of the Pseudomonas aeruginosa cytotoxin ExoU*. Infection And Immunity, 2005. **73**(1): p. 573-582.

145. Sato, H., J.B. Feix, and D.W. Frank, *Identification of superoxide dismutase as a cofactor for the Pseudomonas type III toxin, ExoU*. Biochemistry, 2006. **45**(34): p. 10368-10375.

146. Finck-Barbancon, V., T.L. Yahr, and D.W. Frank, *Identification and characterization of SpcU, a chaperone required for efficient secretion of the ExoU cytotoxin*. J Bacteriol, 1998. **180**(23): p. 6224-31.

147. Rabin, S.D.P., et al., *A C-terminal domain targets the Pseudomonas aeruginosa cytotoxin ExoU to the plasma membrane of host cells*. Infection And Immunity, 2006. **74**(5): p. 2552-2561.

148. Stirling, F.R., et al., *Eukaryotic localization, activation and ubiquitinylation of a bacterial type III secreted toxin*. Cellular Microbiology, 2006. **8**(8): p. 1294-1309.

149. Ichikawa, J.K., et al., *Genome-wide analysis of host responses to the Pseudomonas aeruginosa type III secretion system yields synergistic effects*. Cellular Microbiology, 2005. **7**(11): p. 1635-1646.

150. Vallis, A.J., et al., *Biological effects of Pseudomonas aeruginosa type III-secreted proteins on CHO cells*. Infection And Immunity, 1999. **67**(4): p. 2040-2044.

151. Cowell, B.A., D.J. Evans, and S.M. Fleiszig, *Actin cytoskeleton disruption by ExoY and its effects on Pseudomonas aeruginosa invasion*. FEMS Microbiol Lett, 2005. **250**(1): p. 71-6.

152. Sayner, S.L., et al., *Paradoxical cAMP-induced lung endothelial hyperpermeability revealed by Pseudomonas aeruginosa ExoY*. Circ Res, 2004. **95**(2): p. 196-203.

153. Cao, T.B. and M.H. Saier, Jr., *The general protein secretory pathway: phylogenetic analyses leading to evolutionary conclusions*. Biochim Biophys Acta, 2003. **1609**(1): p. 115-25.

154. Cianciotto, N.P., *Type II secretion: a protein secretion system for all seasons*. Trends Microbiol, 2005. **13**(12): p. 581-8.

155. Christie, P.J. and E. Cascales, *Structural and dynamic properties of bacterial type IV secretion systems (review)*. Mol Membr Biol, 2005. **22**(1-2): p. 51-61.

156. Cascales, E. and P.J. Christie, *The versatile bacterial type IV secretion systems*. Nat Rev Microbiol, 2003. **1**(2): p. 137-49.

157. Censini, S., et al., *cag, a pathogenicity island of Helicobacter pylori, encodes type I-specific and disease-associated virulence factors*. Proc Natl Acad Sci U S A, 1996. **93**(25): p. 14648-53.

158. Vogel, J.P., et al., *Conjugative transfer by the virulence system of Legionella pneumophila*. Science, 1998. **279**(5352): p. 873-6.

159. Ferrero-Miliani, L., et al., *Chronic inflammation: importance of NOD2 and NALP3 in interleukin-1beta generation*. Clin Exp Immunol, 2007. **147**(2): p. 227-35.

160. Barton, G.M., *A calculated response: control of inflammation by the innate immune system*. J Clin Invest, 2008. **118**(2): p. 413-20.

161. Martinon, F., A. Mayor, and J.r. Tschopp, *The Inflammasomes: Guardians of the Body*. Annual Review of Immunology, 2009. **27**(1): p. 229-265.

162. Matzinger, P., *The danger model: a renewed sense of self*. Science, 2002. **296**(5566): p. 301-5.

163. Janeway, C.A., Jr., *The immune system evolved to discriminate infectious nonself from noninfectious self*. Immunol Today, 1992. **13**(1): p. 11-6.

164. Martinon, F., et al., *Gout-associated uric acid crystals activate the NALP3 inflammasome*. Nature, 2006. **440**(7081): p. 237-41.

165. Medzhitov, R. and C.A. Janeway, *Innate immunity: impact on the adaptive immune response*. 1997. **9**(1): p. 4-9.

166. Akira, S., S. Uematsu, and O. Takeuchi, *Pathogen recognition and innate immunity*. Cell, 2006. **124**(4): p. 783-801.

167. Brown, G.D., *Dectin-1: a signalling non-TLR pattern-recognition receptor*. Nat Rev Immunol, 2006. **6**(1): p. 33-43.

168. Nakhaei, P., et al., *RIG-I-like receptors: Sensing and responding to RNA virus infection*. Seminars in Immunology, 2009. **21**(4): p. 215-222.

169. Burckstummer, T., et al., *An orthogonal proteomic-genomic screen identifies AIM2 as a cytoplasmic DNA sensor for the inflammasome*. Nat Immunol, 2009. **10**(3): p. 266-72.

170. Fernandes-Alnemri, T., et al., *AIM2 activates the inflammasome and cell death in response to cytoplasmic DNA*. Nature, 2009. **458**(7237): p. 509-13.

171. Hornung, V., et al., *AIM2 recognizes cytosolic dsDNA and forms a caspase-1-activating inflammasome with ASC*. Nature, 2009. **458**(7237): p. 514-8.

172. Bryant, C. and K.A. Fitzgerald, *Molecular mechanisms involved in inflammasome activation*. Trends Cell Biol, 2009. **19**(9): p. 455-64.

173. Medzhitov, R., P. Preston-Hurlburt, and C.A. Janeway, Jr., *A human homologue of the Drosophila Toll protein signals activation of adaptive immunity*. Nature, 1997. **388**(6640): p. 394-7.

174. Lemaitre, B., et al., *The Dorsoventral Regulatory Gene Cassette spätzle/Toll/cactus Controls the Potent Antifungal Response in Drosophila Adults*. Cell, 1996. **86**(6): p. 973-983.

175. Akira, S. and K. Takeda, *Toll-like receptor signalling*. Nat Rev Immunol, 2004. **4**(7): p. 499-511.

176. Ishii, K.J., et al., *Host innate immune receptors and beyond: making sense of microbial infections*. Cell Host Microbe, 2008. **3**(6): p. 352-63.

177. Kawai, T. and S. Akira, *TLR signaling*. Cell Death Differ, 2006. **13**(5): p. 816-825.

178. Andersen-Nissen, E., et al., *Evasion of Toll-like receptor 5 by flagellated bacteria*. Proceedings of the National Academy of Sciences of the United States of America, 2005. **102**(26): p. 9247-9252.

179. Hayashi, F., et al., *The innate immune response to bacterial flagellin is mediated by Toll-like receptor 5*. Nature, 2001. **410**(6832): p. 1099-103.

180. Kumar, H., T. Kawai, and S. Akira, *Pathogen recognition in the innate immune response*. Biochemical Journal, 2009. **420**(1): p. 1-16.

181. Liu, L., et al., *Structural basis of toll-like receptor 3 signaling with double-stranded RNA*. Science, 2008. **320**(5874): p. 379-81.

182. Brodsky, I. and R. Medzhitov, *Two modes of ligand recognition by TLRs*. Cell, 2007. **130**(6): p. 979-81.

183. Beutler, B., *Microbe sensing, positive feedback loops, and the pathogenesis of inflammatory diseases*. Immunol Rev, 2009. **227**(1): p. 248-63.

184. Andrejeva, J., et al., *The V proteins of paramyxoviruses bind the IFN-inducible RNA helicase, mda-5, and inhibit its activation of the IFN-beta promoter*. Proc Natl Acad Sci U S A, 2004. **101**(49): p. 17264-9.

185. Sumpter, R., Jr., et al., *Regulating intracellular antiviral defense and permissiveness to hepatitis C virus RNA replication through a cellular RNA helicase, RIG-I.* J Virol, 2005. **79**(5): p. 2689-99.

186. Yoneyama, M., et al., *The RNA helicase RIG-I has an essential function in double-stranded RNA-induced innate antiviral responses.* Nat Immunol, 2004. **5**(7): p. 730-7.

187. Gitlin, L., et al., *Essential role of mda-5 in type I IFN responses to polyriboinosinic:polyribocytidylic acid and encephalomyocarditis picornavirus.* Proc Natl Acad Sci U S A, 2006. **103**(22): p. 8459-64.

188. Kato, H., et al., *Differential roles of MDA5 and RIG-I helicases in the recognition of RNA viruses.* Nature, 2006. **441**(7089): p. 101-5.

189. Loo, Y.M., et al., *Distinct RIG-I and MDA5 signaling by RNA viruses in innate immunity.* J Virol, 2008. **82**(1): p. 335-45.

190. Hornung, V., et al., *5'-Triphosphate RNA is the ligand for RIG-I.* Science, 2006. **314**(5801): p. 994-7.

191. Willment, J.A. and G.D. Brown, *C-type lectin receptors in antifungal immunity.* Trends in Microbiology, 2008. **16**(1): p. 27-32.

192. Klis, F.M., P. de Groot, and K. Hellingwerf, *Molecular organization of the cell wall of Candida albicans.* Med Mycol, 2001. **39 Suppl 1**: p. 1-8.

193. Taylor, P.R., S. Gordon, and L. Martinez-Pomares, *The mannose receptor: linking homeostasis and immunity through sugar recognition.* Trends Immunol, 2005. **26**(2): p. 104-10.

194. McGreal, E.P., et al., *The carbohydrate-recognition domain of Dectin-2 is a C-type lectin with specificity for high mannose.* Glycobiology, 2006. **16**(5): p. 422-30.

195. Sato, K., et al., *Dectin-2 is a pattern recognition receptor for fungi that couples with the Fc receptor gamma chain to induce innate immune responses.* J Biol Chem, 2006. **281**(50): p. 38854-66.

196. Jones, D.A. and D. Takemoto, *Plant innate immunity - direct and indirect recognition of general and specific pathogen-associated molecules.* 2004. **16**(1): p. 48.

197. Inohara, N., et al., *Nod1, an Apaf-1-like activator of caspase-9 and nuclear factor-kappaB.* J Biol Chem, 1999. **274**(21): p. 14560-7.

198. Ting, J.P., et al., *The NLR gene family: a standard nomenclature.* Immunity, 2008. **28**(3): p. 285-7.

199. Bella, J., et al., *The leucine-rich repeat structure.* Cell Mol Life Sci, 2008. **65**(15): p. 2307-33.

200. Faustin, B., et al., *Reconstituted NALP1 inflammasome reveals two-step mechanism of caspase-1 activation.* Mol Cell, 2007. **25**(5): p. 713-24.

201. Martinon, F. and J. Tschopp, *Inflammatory caspases: linking an intracellular innate immune system to autoinflammatory diseases.* Cell, 2004. **117**(5): p. 561-74.

202. Park, H.H., et al., *The death domain superfamily in intracellular signaling of apoptosis and inflammation.* Annu Rev Immunol, 2007. **25**: p. 561-86.

203. Proell, M., et al., *The Nod-Like Receptor (NLR) Family: A Tale of Similarities and Differences.* PLoS ONE, 2008. **3**(4): p. e2119.

204. Tschopp, J., F. Martinon, and K. Burns, *NALPs: a novel protein family involved in inflammation.* Nat Rev Mol Cell Biol, 2003. **4**(2): p. 95-104.

205. Martinon, F. and J. Tschopp, *NLRs join TLRs as innate sensors of pathogens.* Trends Immunol, 2005. **26**(8): p. 447-54.

206. Reith, W. and B. Mach, *The bare lymphocyte syndrome and the regulation of MHC expression.* Annu Rev Immunol, 2001. **19**: p. 331-73.

207. Meylan, E. and J. Tschopp, *NLRX1: friend or foe?* EMBO Rep, 2008. **9**(3): p. 243-5.
208. Moore, C.B., et al., *NLRX1 is a regulator of mitochondrial antiviral immunity.* Nature, 2008. **451**(7178): p. 573-7.
209. Tattoli, I., et al., *NLRX1 is a mitochondrial NOD-like receptor that amplifies NF-kappaB and JNK pathways by inducing reactive oxygen species production.* EMBO Rep, 2008. **9**(3): p. 293-300.
210. Kufer, T.A., J.H. Fritz, and D.J. Philpott, *NACHT-LRR proteins (NLRs) in bacterial infection and immunity.* Trends Microbiol, 2005. **13**(8): p. 381-8.
211. Kummer, J.A., et al., *Inflammasome Components NALP 1 and 3 Show Distinct but Separate Expression Profiles in Human Tissues Suggesting a Site-specific Role in the Inflammatory Response.* J. Histochem. Cytochem. , 2007. **55**(5): p. 443-452.
212. Vinzing, M., et al., *NAIP and Ipaf Control Legionella pneumophila Replication in Human Cells.* J Immunol, 2008. **180**(10): p. 6808-6815.
213. McCall, S.H., et al., *Osteoblasts express NLRP3, a nucleotide-binding domain and leucine-rich repeat region containing receptor implicated in bacterially induced cell death.* J Bone Miner Res, 2008. **23**(1): p. 30-40.
214. Diez, E., et al., *The neuronal apoptosis inhibitory protein (Naip) is expressed in macrophages and is modulated after phagocytosis and during intracellular infection with Legionella pneumophila.* J Immunol, 2000. **164**(3): p. 1470-7.
215. Poyet, J.L., et al., *Identification of Ipaf, a human caspase-1-activating protein related to Apaf-1.* J Biol Chem, 2001. **276**(30): p. 28309-13.
216. Becker, C.E. and L.A. O'Neill, *Inflammasomes in inflammatory disorders: the role of TLRs and their interactions with NLRs.* Semin Immunopathol, 2007. **29**(3): p. 239-48.
217. Bertin, J., et al., *Human CARD4 protein is a novel CED-4/Apaf-1 cell death family member that activates NF-kappaB.* J Biol Chem, 1999. **274**(19): p. 12955-8.
218. Tattoli, I., et al., *The Nodosome: Nod1 and Nod2 control bacterial infections and inflammation.* Semin Immunopathol, 2007. **29**(3): p. 289-301.
219. Girardin, S.E. and D.J. Philpott, *Mini-review: the role of peptidoglycan recognition in innate immunity.* Eur J Immunol, 2004. **34**(7): p. 1777-82.
220. McDonald, C., N. Inohara, and G. Nunez, *Peptidoglycan Signaling in Innate Immunity and Inflammatory Disease.* J. Biol. Chem. , 2005. **280**(21): p. 20177-20180.
221. Kobayashi, K.S., et al., *Nod2-dependent regulation of innate and adaptive immunity in the intestinal tract.* Science, 2005. **307**(5710): p. 731-4.
222. Viala, J., et al., *Nod1 responds to peptidoglycan delivered by the Helicobacter pylori cag pathogenicity island.* Nat Immunol, 2004. **5**(11): p. 1166-74.
223. Vignal, C., et al., *How NOD2 mutations predispose to Crohn's disease?* Microbes Infect, 2007. **9**(5): p. 658-63.
224. Tanabe, T., et al., *Regulatory regions and critical residues of NOD2 involved in muramyl dipeptide recognition.* EMBO J, 2004. **23**(7): p. 1587-97.
225. Hsu, L.-C., et al., *A NOD2-NALP1 complex mediates caspase-1-dependent IL-1{beta} secretion in response to Bacillus anthracis infection and*

muramyl dipeptide. Proceedings of the National Academy of Sciences, 2008. **105**(22): p. 7803-7808.

226. Pan, Q., et al., *MDP-induced interleukin-1{beta} processing requires Nod2 and CIAS1/NALP3.* J Leukoc Biol 2007. **82**(1): p. 177-183.

227. Martinon, F., K. Burns, and J. Tschopp, *The inflammasome: a molecular platform triggering activation of inflammatory caspases and processing of proIL-beta.* Mol Cell, 2002. **10**(2): p. 417-26.

228. Zou, H., et al., *An APAF-1.cytochrome c multimeric complex is a functional apoptosome that activates procaspase-9.* J Biol Chem, 1999. **274**(17): p. 11549-56.

229. Martinon, F., et al., *NALP inflammasomes: a central role in innate immunity.* Semin Immunopathol, 2007. **29**(3): p. 213-29.

230. Franchi, L., et al., *Intracellular NOD-like receptors in innate immunity, infection and disease.* Cell Microbiol, 2008. **10**(1): p. 1-8.

231. Miao, E.A., et al., *TLR5 and Ipaf: dual sensors of bacterial flagellin in the innate immune system.* Semin Immunopathol, 2007. **29**(3): p. 275-88.

232. Martinon, F., *Orchestration of pathogen recognition by inflammasome diversity: Variations on a common theme.* Eur J Immunol, 2007. **37**(11): p. 3003-6.

233. Srinivasula, S.M., et al., *The PYRIN-CARD protein ASC is an activating adaptor for caspase-1.* J Biol Chem, 2002. **277**(24): p. 21119-22.

234. Mariathasan, S., et al., *Differential activation of the inflammasome by caspase-1 adaptors ASC and Ipaf.* Nature, 2004. **430**(6996): p. 213-8.

235. Bryan, N.B., et al., *Activation of Inflammasomes Requires Intracellular Redistribution of the Apoptotic Speck-Like Protein Containing a Caspase Recruitment Domain.* J Immunol, 2009. **182**(5): p. 3173-3182.

236. Franchi, L., et al., *Differential Requirement of P2X7 Receptor and Intracellular K+ for Caspase-1 Activation Induced by Intracellular and Extracellular Bacteria.* J Biol Chem, 2007. **282**(26): p. 18810-8.

237. Kahlenberg, J.M. and G.R. Dubyak, *Mechanisms of caspase-1 activation by P2X7 receptor-mediated K+ release.* Am J Physiol Cell Physiol, 2004. **286**(5): p. C1100-8.

238. Petrilli, V., et al., *Activation of the NALP3 inflammasome is triggered by low intracellular potassium concentration.* Cell Death Differ, 2007. **14**(9): p. 1583-9.

239. Boyden, E.D. and W.F. Dietrich, *Nalp1b controls mouse macrophage susceptibility to anthrax lethal toxin.* Nat Genet, 2006. **38**(2): p. 240-4.

240. Fink, S.L., T. Bergsbaken, and B.T. Cookson, *Anthrax lethal toxin and Salmonella elicit the common cell death pathway of caspase-1-dependent pyroptosis via distinct mechanisms.* Proc Natl Acad Sci U S A, 2008. **105**(11): p. 4312-7.

241. Squires, R.C., S.M. Muehlbauer, and J. Brojatsch, *Proteasomes control caspase-1 activation in anthrax lethal toxin-mediated cell killing.* J Biol Chem, 2007. **282**(47): p. 34260-7.

242. Wickliffe, K.E., S.H. Leppla, and M. Moayeri, *Anthrax lethal toxin-induced inflammasome formation and caspase-1 activation are late events dependent on ion fluxes and the proteasome.* Cell Microbiol, 2008. **10**(2): p. 332-43.

243. Duncan, J.A., et al., *Cryopyrin/NALP3 binds ATP/dATP, is an ATPase, and requires ATP binding to mediate inflammatory signaling.* Proc Natl Acad Sci U S A, 2007. **104**(19): p. 8041-6.

244. Fink, S.L. and B.T. Cookson, *Apoptosis, Pyroptosis, and Necrosis: Mechanistic Description of Dead and Dying Eukaryotic Cells.* Infect. Immun. , 2005. **73**(4): p. 1907-1916.
245. Chen, Y., et al., *A bacterial invasin induces macrophage apoptosis by binding directly to ICE.* Embo J, 1996. **15**(15): p. 3853-60.
246. Hilbi, H., et al., *Shigella-induced apoptosis is dependent on caspase-1 which binds to IpaB.* J Biol Chem, 1998. **273**(49): p. 32895-900.
247. Bergsbaken, T. and B.T. Cookson, *Macrophage Activation Redirects Yersinia-Infected Host Cell Death from Apoptosis to Caspase-1-Dependent Pyroptosis.* PLoS Pathogens, 2007. **3**(11): p. e161.
248. Hersh, D., et al., *The Salmonella invasin SipB induces macrophage apoptosis by binding to caspase-1.* Proc Natl Acad Sci U S A, 1999. **96**(5): p. 2396-401.
249. Sutterwala, F.S., et al., *Immune recognition of Pseudomonas aeruginosa mediated by the IPAF/NLRC4 inflammasome.* J Exp Med, 2007. **204**(13): p. 3235-45.
250. Mariathasan, S., et al., *Innate immunity against Francisella tularensis is dependent on the ASC/caspase-1 axis.* J. Exp. Med. , 2005. **202**(8): p. 1043-1049.
251. Molofsky, A.B., et al., *Cytosolic recognition of flagellin by mouse macrophages restricts Legionella pneumophila infection.* J Exp Med, 2006. **203**(4): p. 1093-104.
252. Cervantes, J., et al., *Intracytosolic Listeria monocytogenes induces cell death through caspase-1 activation in murine macrophages.* Cell Microbiol, 2008. **10**(1): p. 41-52.
253. Franchi, L., et al., *Critical role for Ipaf in Pseudomonas aeruginosa-induced caspase-1 activation.* Eur J Immunol, 2007. **37**(11): p. 3030-9.
254. Suzuki, T., et al., *Differential Regulation of Caspase-1 Activation, Pyroptosis, and Autophagy via Ipaf and ASC in Shigella-Infected Macrophages.* PLoS Pathog, 2007. **3**(8): p. e111.
255. Fernandes-Alnemri, T., et al., *The pyroptosome: a supramolecular assembly of ASC dimers mediating inflammatory cell death via caspase-1 activation.* Cell Death Differ, 2007. **14**(9): p. 1590-604.
256. Evans, T.J., *Bacterial triggering of inflammation by intracellular sensors.* Future Microbiology, 2009. **4**(1): p. 65-75.
257. Greten, F.R., et al., *NF-kappaB Is a Negative Regulator of IL-1beta Secretion as Revealed by Genetic and Pharmacological Inhibition of IKKbeta.* Cell, 2007. **130**(5): p. 918-31.
258. Stehlik, C. and A. Dorfleutner, *COPs and POPs: Modulators of Inflammasome Activity.* J Immunol, 2007. **179**(12): p. 7993-8.
259. Chae, J.J., et al., *Targeted disruption of pyrin, the FMF protein, causes heightened sensitivity to endotoxin and a defect in macrophage apoptosis.* Mol Cell, 2003. **11**(3): p. 591-604.
260. Martinon, F. and J. Tschopp, *Inflammatory caspases and inflammasomes: master switches of inflammation.* Cell Death Differ, 2007. **14**(1): p. 10-22.
261. Saleh, M., et al., *Enhanced bacterial clearance and sepsis resistance in caspase-12-deficient mice.* Nature, 2006. **440**(7087): p. 1064-8.
262. da Silva Correia, J., et al., *SGT1 is essential for Nod1 activation.* Proceedings of the National Academy of Sciences 2007. **104**(16): p. 6764-6769.

263. Mayor, A., et al., *A crucial function of SGT1 and HSP90 in inflammasome activity links mammalian and plant innate immune responses*. Nat Immunol, 2007. **8**(5): p. 497-503.

264. McGonagle, D., S. Savic, and M.F. McDermott, *The NLR network and the immunological disease continuum of adaptive and innate immune-mediated inflammation against self*. Semin Immunopathol, 2007. **29**(3): p. 303-13.

265. Agostini, L., et al., *NALP3 forms an IL-1beta-processing inflammasome with increased activity in Muckle-Wells autoinflammatory disorder*. Immunity, 2004. **20**(3): p. 319-25.

266. Shinkai, K., T.H. McCalmont, and K.S. Leslie, *Cryopyrin-associated periodic syndromes and autoinflammation*. Clin Exp Dermatol, 2008. **33**(1): p. 1-9.

267. Masters, S.L., et al., *Recent advances in the molecular pathogenesis of hereditary recurrent fevers*. Curr Opin Allergy Clin Immunol, 2006. **6**(6): p. 428-33.

268. McDermott, M.F. and J. Tschopp, *From inflammasomes to fevers, crystals and hypertension: how basic research explains inflammatory diseases*. Trends Mol Med, 2007. **13**(9): p. 381-8.

269. Chedid, L., *Adjuvants of immunity*. Ann Inst Pasteur Immunol, 1985. **136D**(3): p. 283-91.

270. Lindblad, E.B., *Aluminium compounds for use in vaccines*. Immunol Cell Biol, 2004. **82**(5): p. 497-505.

271. Shi, Y., J.E. Evans, and K.L. Rock, *Molecular identification of a danger signal that alerts the immune system to dying cells*. Nature, 2003. **425**(6957): p. 516-21.

272. Eisenbarth, S.C., et al., *Crucial role for the Nalp3 inflammasome in the immunostimulatory properties of aluminium adjuvants*. Nature, 2008. **453**(7198): p. 1122-6.

273. Kool, M., et al., *Cutting Edge: Alum Adjuvant Stimulates Inflammatory Dendritic Cells through Activation of the NALP3 Inflammasome*. J Immunol, 2008. **181**(6): p. 3755-3759.

274. Li, H., et al., *Cutting edge: inflammasome activation by alum and alum's adjuvant effect are mediated by NLRP3*. J Immunol, 2008. **181**(1): p. 17-21.

275. Cohen, G.M., *Caspases: the executioners of apoptosis*. Biochem J, 1997. **326 (Pt 1)**: p. 1-16.

276. Nadiri, A., M.K. Wolinski, and M. Saleh, *The inflammatory caspases: key players in the host response to pathogenic invasion and sepsis*. J Immunol, 2006. **177**(7): p. 4239-45.

277. Black, R.A., et al., *A pre-aspartate-specific protease from human leukocytes that cleaves pro-interleukin-1 beta*. J. Biol. Chem., 1989. **264**(10): p. 5323-5326.

278. Lüthi, A.U., et al., *Suppression of Interleukin-33 Bioactivity through Proteolysis by Apoptotic Caspases*. 2009. **31**(1): p. 84-98.

279. Talabot-Ayer, D., et al., *Interleukin-33 is biologically active independently of caspase-1 cleavage*. J Biol Chem, 2009. **284**(29): p. 19420-6.

280. Gurcel, L., et al., *Caspase-1 activation of lipid metabolic pathways in response to bacterial pore-forming toxins promotes cell survival*. Cell, 2006. **126**(6): p. 1135-45.

281. Keller, M., et al., *Active caspase-1 is a regulator of unconventional protein secretion*. Cell, 2008. **132**(5): p. 818-31.

282. Miggin, S.M., et al., *NF-kappaB activation by the Toll-IL-1 receptor domain protein MyD88 adapter-like is regulated by caspase-1.* Proc Natl Acad Sci U S A, 2007. **104**(9): p. 3372-7.

283. Shao, W., et al., *The Caspase-1 Digestome Identifies the Glycolysis Pathway as a Target during Infection and Septic Shock.* J. Biol. Chem., 2007. **282**(50): p. 36321-36329.

284. Kostura, M.J., et al., *Identification of a Monocyte Specific Pre-Interleukin 1{beta} Convertase Activity.* Proceedings of the National Academy of Sciences 1989. **86**(14): p. 5227-5231.

285. Dinarello, C.A., *Immunological and Inflammatory Functions of the Interleukin-1 Family.* Annual Review of Immunology, 2009. **27**(1): p. 519-550.

286. Dinarello, C.A., *Biologic basis for interleukin-1 in disease.* Blood, 1996. **87**(6): p. 2095-147.

287. Heitmeier, M.R., A.L. Scarim, and J.A. Corbett, *Double-stranded RNA-induced inducible nitric-oxide synthase expression and interleukin-1 release by murine macrophages requires NF-kappaB activation.* J Biol Chem, 1998. **273**(24): p. 15301-7.

288. Hiscott, J., et al., *Characterization of a functional NF-kappa B site in the human interleukin 1 beta promoter: evidence for a positive autoregulatory loop.* Mol Cell Biol, 1993. **13**(10): p. 6231-40.

289. Eder, C., *Mechanisms of interleukin-1beta release.* Immunobiology, 2009.

290. Rubartelli, A., et al., *A novel secretory pathway for interleukin-1 beta, a protein lacking a signal sequence.* Embo J, 1990. **9**(5): p. 1503-10.

291. Andrei, C., et al., *The Secretory Route of the Leaderless Protein Interleukin 1beta Involves Exocytosis of Endolysosome-related Vesicles.* Mol. Biol. Cell, 1999. **10**(5): p. 1463-1475.

292. Andrei, C., et al., *Phospholipases C and A2 control lysosome-mediated IL-1 beta secretion: Implications for inflammatory processes.* Proc Natl Acad Sci U S A, 2004. **101**(26): p. 9745-50.

293. MacKenzie, A., et al., *Rapid Secretion of Interleukin-1[beta] by Microvesicle Shedding.* Immunity, 2001. **15**(5): p. 825-835.

294. Brough, D. and N.J. Rothwell, *Caspase-1-dependent processing of pro-interleukin-1beta is cytosolic and precedes cell death.* J Cell Sci, 2007. **120**(Pt 5): p. 772-81.

295. Qu, Y., et al., *Nonclassical IL-1beta Secretion Stimulated by P2X7 Receptors Is Dependent on Inflammasome Activation and Correlated with Exosome Release in Murine Macrophages.* J Immunol, 2007. **179**(3): p. 1913-25.

296. Hogquist, K.A., et al., *Interleukin 1 is processed and released during apoptosis.* Proc Natl Acad Sci U S A, 1991. **88**(19): p. 8485-9.

297. Laliberte, R.E., J. Eggler, and C.A. Gabel, *ATP Treatment of Human Monocytes Promotes Caspase-1 Maturation and Externalization.* J. Biol. Chem., 1999. **274**(52): p. 36944-36951.

298. Coeshott, C., et al., *Converting enzyme-independent release of tumor necrosis factor alpha and IL-1beta from a stimulated human monocytic cell line in the presence of activated neutrophils or purified proteinase 3.* Proc Natl Acad Sci U S A, 1999. **96**(11): p. 6261-6.

299. Hawkins, P.N., H.J. Lachmann, and M.F. McDermott, *Interleukin-1-receptor antagonist in the Muckle-Wells syndrome.* N Engl J Med, 2003. **348**(25): p. 2583-4.

300. Hoffman, H.M., et al., *Prevention of cold-associated acute inflammation in familial cold autoinflammatory syndrome by interleukin-1 receptor antagonist*. Lancet, 2004. **364**(9447): p. 1779-85.

301. Chisholm, S.T., et al., *Host-Microbe Interactions: Shaping the Evolution of the Plant Immune Response*. 2006. **124**(4): p. 803.

302. Schneider, D.S., *Plant immunity and film Noir: what gumshoe detectives can teach us about plant-pathogen interactions*. Cell, 2002. **109**(5): p. 537-40.

303. Staskawicz, B.J., *Genetics of plant-pathogen interactions specifying plant disease resistance*. Plant Physiol, 2001. **125**(1): p. 73-6.

304. Dangl, J.L. and J.D. Jones, *Plant pathogens and integrated defence responses to infection*. Nature, 2001. **411**(6839): p. 826-33.

305. Jones, J.D. and J.L. Dangl, *The plant immune system*. Nature, 2006. **444**(7117): p. 323-9.

306. Caplan, J., M. Padmanabhan, and S.P. Dinesh-Kumar, *Plant NB-LRR immune receptors: from recognition to transcriptional reprogramming*. Cell Host Microbe, 2008. **3**(3): p. 126-35.

307. Bent, A.F. and D. Mackey, *Elicitors, effectors, and R genes: the new paradigm and a lifetime supply of questions*. Annu Rev Phytopathol, 2007. **45**: p. 399-436.

308. Ausubel, F.M., *Are innate immune signaling pathways in plants and animals conserved?* Nat Immunol, 2005. **6**(10): p. 973-9.

309. Napolitani, G., et al., *Selected Toll-like receptor agonist combinations synergistically trigger a T helper type 1-polarizing program in dendritic cells*. Nat Immunol, 2005. **6**(8): p. 769-76.

310. Underhill, D.M., *Collaboration between the innate immune receptors dectin-1, TLRs, and Nods*. Immunol Rev, 2007. **219**: p. 75-87.

311. Bagchi, A., et al., *MyD88-dependent and MyD88-independent pathways in synergy, priming, and tolerance between TLR agonists*. J Immunol, 2007. **178**(2): p. 1164-71.

312. Lightfield, K.L., et al., *Critical function for Naip5 in inflammasome activation by a conserved carboxy-terminal domain of flagellin*. Nat Immunol, 2008. **9**(10): p. 1171-1178.

313. Hise, A.G., et al., *An Essential Role for the NLRP3 Inflammasome in Host Defense against the Human Fungal Pathogen Candida albicans*. Cell Host & Microbe, 2009. **5**(5): p. 487-497.

314. Bauernfeind, F.G., et al., *Cutting edge: NF-kappaB activating pattern recognition and cytokine receptors license NLRP3 inflammasome activation by regulating NLRP3 expression*. J Immunol, 2009. **183**(2): p. 787-91.

315. Franchi, L., T. Eigenbrod, and G. Nunez, *Cutting edge: TNF-alpha mediates sensitization to ATP and silica via the NLRP3 inflammasome in the absence of microbial stimulation*. J Immunol, 2009. **183**(2): p. 792-6.

316. Carneiro, L.A.M., L.H. Travassos, and S.E. Girardin, *Nod-like receptors in innate immunity and inflammatory diseases*. Annals of Medicine, 2007. **39**(8): p. 581 - 593.

317. Fritz, J.H., et al., *Synergistic stimulation of human monocytes and dendritic cells by Toll-like receptor 4 and NOD1- and NOD2-activating agonists*. Eur J Immunol, 2005. **35**(8): p. 2459-70.

318. van Heel, D.A., et al., *Synergistic enhancement of Toll-like receptor responses by NOD1 activation*. Eur J Immunol, 2005. **35**(8): p. 2471-6.

319. Palm, N.W. and R. Medzhitov, *Pattern recognition receptors and control of adaptive immunity*. Immunol Rev, 2009. **227**(1): p. 221-33.

320. Misson, P., et al., *Type 2 immune response associated with silicosis is not instrumental in the development of the disease.* Am J Physiol Lung Cell Mol Physiol, 2007. **292**(1): p. L107-13.
321. Helmby, H. and R.K. Grencis, *Interleukin 1 plays a major role in the development of Th2-mediated immunity.* Eur J Immunol, 2004. **34**(12): p. 3674-81.
322. Schmitz, J., et al., *IL-33, an interleukin-1-like cytokine that signals via the IL-1 receptor-related protein ST2 and induces T helper type 2-associated cytokines.* Immunity, 2005. **23**(5): p. 479-90.
323. LeibundGut-Landmann, S., et al., *Syk- and CARD9-dependent coupling of innate immunity to the induction of T helper cells that produce interleukin 17.* Nat Immunol, 2007. **8**(6): p. 630-8.
324. Guarda, G., et al., *T cells dampen innate immune responses through inhibition of NLRP1 and NLRP3 inflammasomes.* Nature, 2009. **460**(7252): p. 269-73.
325. Shaw, G., et al., *Preferential transformation of human neuronal cells by human adenoviruses and the origin of HEK 293 cells.* FASEB J, 2002. **16**(8): p. 869-71.
326. Miller, A.D. and F. Chen, *Retrovirus packaging cells based on 10A1 murine leukemia virus for production of vectors that use multiple receptors for cell entry.* J. Virol., 1996. **70**(8): p. 5564-5571.
327. Grady, G.C., et al., *Cyclic Adenosine 5'-Monophosphate Response Element Binding Protein Plays a Central Role in Mediating Proliferation and Differentiation Downstream of the Pre-TCR Complex in Developing Thymocytes.* J Immunol, 2004. **173**(3): p. 1802-1810.
328. Markowitz, D., S. Goff, and A. Bank, *A safe packaging line for gene transfer: separating viral genes on two different plasmids.* J. Virol., 1988. **62**(4): p. 1120-1124.
329. Miller, D.G., M.A. Adam, and A.D. Miller, *Gene transfer by retrovirus vectors occurs only in cells that are actively replicating at the time of infection.* Mol. Cell. Biol., 1990. **10**(8): p. 4239-4242.
330. Celada, A., et al., *Evidence for a gamma-interferon receptor that regulates macrophage tumoricidal activity.* J Exp Med, 1984. **160**(1): p. 55-74.
331. Grierson, A.M., et al., *Direct quantitation of T cell signaling by laser scanning cytometry.* Journal Of Immunological Methods, 2005. **301**(1-2): p. 140-153.
332. Neyt, C. and G.R. Cornelis, *Insertion of a Yop translocation pore into the macrophage plasma membrane by Yersinia enterocolitica: requirement for translocators YopB and YopD, but not LcrG.* Molecular Microbiology, 1999. **33**(5): p. 971-981.
333. Pelegrin, P. and A. Surprenant, *Pannexin-1 couples to maitotoxin- and nigericin-induced interleukin-1beta release through a dye uptake-independent pathway.* J Biol Chem, 2007. **282**(4): p. 2386-94.
334. Bhakdi, S., et al., *Potent Leukocidal Action Of Escherichia-Coli Hemolysin Mediated By Permeabilization Of Target-Cell Membranes.* Journal Of Experimental Medicine, 1989. **169**(3): p. 737-754.
335. Cerny, J., *The small chemical vacuolin-1 inhibits Ca2+-dependent lysosomal exocytosis but not cell resealing (vol 5, pg 883, 2004).* Embo Reports, 2005. **6**(9): p. 898-898.
336. Veldman, R.J., et al., *A neutral sphingomyelinase resides in sphingolipid-enriched microdomains and is inhibited by the caveolin-scaffolding*

domain: potential implications in tumour necrosis factor signalling. Biochemical Journal, 2001. **355**: p. 859-868.

337.   Miao, E.A., et al., *Cytoplasmic flagellin activates caspase-1 and secretion of interleukin 1beta via Ipaf.* Nat Immunol, 2006. **7**(6): p. 569-75.

338.   Harris, D.C. Quantitative Chemical Analysis 4th edition 1995, New York: W. H. Freeman and Company.

339.   Pfeifer, C.G., et al., *Salmonella typhimurium virulence genes are induced upon bacterial invasion into phagocytic and nonphagocytic cells.* Infect Immun, 1999. **67**(11): p. 5690-8.

340.   Choi, K.H., A. Kumar, and H.P. Schweizer, *A 10-min method for preparation of highly electrocompetent Pseudomonas aeruginosa cells: Application for DNA fragment transfer between chromosomes and plasmid transformation.* Journal Of Microbiological Methods, 2006. **64**(3): p. 391-397.

341.   Smedley, J.G., III, et al., *Influence of Pilin Glycosylation on Pseudomonas aeruginosa 1244 Pilus Function.* Infect. Immun. , 2005. **73**(12): p. 7922-7931.

342.   Huang, B., C.B. Whitchurch, and J.S. Mattick, *FimX, a Multidomain Protein Connecting Environmental Signals to Twitching Motility in Pseudomonas aeruginosa.* J. Bacteriol., 2003. **185**(24): p. 7068-7076.

343.   Girardin, S.E., et al., *Nod1 detects a unique muropeptide from gram-negative bacterial peptidoglycan.* Science, 2003. **300**(5625): p. 1584-7.

344.   Pear, W.S., et al., *Efficient and rapid induction of a chronic myelogenous leukemia-like myeloproliferative disease in mice receiving P210 bcr/abl-transduced bone marrow.* Blood, 1998. **92**(10): p. 3780-92.

345.   Fukuda, M., et al., *Synaptotagmin VII is targeted to dense-core vesicles and regulates their Ca2+ -dependent exocytosis in PC12 cells.* J Biol Chem, 2004. **279**(50): p. 52677-84.

346.   Pelegrin, P. and A. Surprenant, *Pannexin-1 mediates large pore formation and interleukin-1beta release by the ATP-gated P2X7 receptor.* Embo J, 2006. **25**(21): p. 5071-82.

347.   Liu, P.V., *The roles of various fractions of Pseudomonas aeruginosa in its pathogenesis. 3. Identity of the lethal toxins produced in vitro and in vivo.* J Infect Dis, 1966. **116**(4): p. 481-9.

348.   Murray, T.S. and B.I. Kazmierczak, *Pseudomonas aeruginosa exhibits sliding motility in the absence of type IV pili and flagella.* J Bacteriol, 2008. **190**(8): p. 2700-8.

349.   Arora, S.K., et al., *Role of Motility and Flagellin Glycosylation in the Pathogenesis of Pseudomonas aeruginosa Burn Wound Infections.* Infect. Immun., 2005. **73**(7): p. 4395-4398.

350.   Lara-Tejero, M., et al., *Role of the caspase-1 inflammasome in Salmonella typhimurium pathogenesis.* J Exp Med, 2006. **203**(6): p. 1407-12.

351.   Ren, T., et al., *Flagellin-deficient Legionella mutants evade caspase-1- and Naip5-mediated macrophage immunity.* PLoS Pathog, 2006. **2**(3): p. e18.

352.   Zamboni, D.S., et al., *The Birc1e cytosolic pattern-recognition receptor contributes to the detection and control of Legionella pneumophila infection.* Nat Immunol, 2006. **7**(3): p. 318-25.

353.   Case, C.L., S. Shin, and C.R. Roy, *Asc and Ipaf Inflammasomes direct distinct pathways for caspase-1 activation in response to Legionella pneumophila.* Infect Immun, 2009. **77**(5): p. 1981-91.

354. Miao, E.A., et al., *Pseudomonas aeruginosa activates caspase 1 through Ipaf*. Proc Natl Acad Sci U S A, 2008. **105**(7): p. 2562-7.
355. Mariathasan, S., et al., *Cryopyrin activates the inflammasome in response to toxins and ATP*. Nature, 2006. **440**(7081): p. 228-32.
356. Henry, T., et al., *Type I interferon signaling is required for activation of the inflammasome during Francisella infection*. J. Exp. Med., 2007. **204**(5): p. 987-994.
357. Lamkanfi, M., et al., *The Nod-Like Receptor Family Member Naip5/Birc1e Restricts Legionella pneumophila Growth Independently of Caspase-1 Activation*. J Immunol, 2007. **178**(12): p. 8022-7.
358. Wright, E.K., et al., *Naip5 Affects Host Susceptibility to the Intracellular Pathogen Legionella pneumophila*. Current Biology, 2003. **13**(1): p. 27-36.
359. Cookson, B.T. and M.A. Brennan, *Pro-inflammatory programmed cell death*. Trends in Microbiology, 2001. **9**(3): p. 113-114.
360. Petrilli, V., et al., *The inflammasome: a danger sensing complex triggering innate immunity*. Curr Opin Immunol, 2007. **19**(6): p. 615-22.
361. Poltorak, A., et al., *Defective LPS signaling in C3H/HeJ and C57BL/10ScCr mice: mutations in Tlr4 gene*. Science, 1998. **282**(5396): p. 2085-8.
362. Hoshino, K., et al., *Cutting Edge: Toll-Like Receptor 4 (TLR4)-Deficient Mice Are Hyporesponsive to Lipopolysaccharide: Evidence for TLR4 as the Lps Gene Product*. J Immunol, 1999. **162**(7): p. 3749-3752.
363. Kanneganti, T.D., et al., *Bacterial RNA and small antiviral compounds activate caspase-1 through cryopyrin/Nalp3*. Nature, 2006. **440**(7081): p. 233-6.
364. Sutterwala, F.S., et al., *Critical role for NALP3/CIAS1/Cryopyrin in innate and adaptive immunity through its regulation of caspase-1*. Immunity, 2006. **24**(3): p. 317-27.
365. Sun, Y.H., H.G. Rolan, and R.M. Tsolis, *Injection of flagellin into the host cell cytosol by Salmonella enterica serotype Typhimurium*. J Biol Chem, 2007. **282**(47): p. 33897-901.
366. Fleiszig, S.M., et al., *Relationship between cytotoxicity and corneal epithelial cell invasion by clinical isolates of Pseudomonas aeruginosa*. Infect Immun, 1996. **64**(6): p. 2288-94.
367. Walev, I., et al., *Potassium-inhibited processing of IL-1 beta in human monocytes*. Embo J, 1995. **14**(8): p. 1607-14.
368. Cassel, S.L., et al., *The Nalp3 inflammasome is essential for the development of silicosis*. Proceedings of the National Academy of Sciences, 2008. **105**(26): p. 9035-9040.
369. Hornung, V., et al., *Silica crystals and aluminum salts activate the NALP3 inflammasome through phagosomal destabilization*. Nat Immunol, 2008. **9**(8): p. 847-856.
370. Dostert, C., et al., *Innate immune activation through Nalp3 inflammasome sensing of asbestos and silica*. Science, 2008. **320**(5876): p. 674-7.
371. Freche, B., N. Reig, and F.G. van der Goot, *The role of the inflammasome in cellular responses to toxins and bacterial effectors*. Semin Immunopathol, 2007. **29**(3): p. 249-60.
372. Cassel, S.L., S. Joly, and F.S. Sutterwala, *The NLRP3 inflammasome: A sensor of immune danger signals*. Seminars in Immunology, 2009. **21**(4): p. 194-198.
373. Perregaux, D. and C.A. Gabel, *Interleukin-1 beta maturation and release in response to ATP and nigericin. Evidence that potassium depletion*

mediated by these agents is a necessary and common feature of their activity. J Biol Chem, 1994. **269**(21): p. 15195-203.

374. Di Virgilio, F., *Liaisons dangereuses: P2X7 and the inflammasome.* Trends in Pharmacological Sciences, 2007. **28**(9): p. 465-472.

375. Eckle, T., et al., *Identification of Ectonucleotidases CD39 and CD73 in Innate Protection during Acute Lung Injury.* J Immunol, 2007. **178**(12): p. 8127-8137.

376. Haag, F., et al., *Extracellular NAD and ATP: Partners in immune cell modulation.* Purinergic Signalling, 2007. **3**(1): p. 71-81.

377. Li, P., et al., *Cytochrome c and dATP-Dependent Formation of Apaf-1/Caspase-9 Complex Initiates an Apoptotic Protease Cascade.* Cell, 1997. **91**(4): p. 479-489.

378. Ferrari, D., et al., *The P2X7 receptor: a key player in IL-1 processing and release.* J Immunol, 2006. **176**(7): p. 3877-83.

379. Ferrari, D., et al., *Extracellular ATP triggers IL-1 beta release by activating the purinergic P2Z receptor of human macrophages.* J Immunol, 1997. **159**(3): p. 1451-8.

380. Solle, M., et al., *Altered cytokine production in mice lacking P2X(7) receptors.* J Biol Chem, 2001. **276**(1): p. 125-32.

381. North, R.A., *Molecular Physiology of P2X Receptors.* Physiol. Rev., 2002. **82**(4): p. 1013-1067.

382. Colomar, A., et al., *Maturation and Release of Interleukin-1{beta} by Lipopolysaccharide-primed Mouse Schwann Cells Require the Stimulation of P2X7 Receptors.* J. Biol. Chem. , 2003. **278**(33): p. 30732-30740.

383. Locovei, S., et al., *Pannexin1 is part of the pore forming unit of the P2X(7) receptor death complex.* FEBS Lett, 2007. **581**(3): p. 483-8.

384. Bruzzone, R., et al., *Pannexins, a family of gap junction proteins expressed in brain.* Proceedings of the National Academy of Sciences of the United States of America, 2003. **100**(23): p. 13644-13649.

385. Huang, Y.-J., et al., *The role of pannexin 1 hemichannels in ATP release and cell–cell communication in mouse taste buds.* Proceedings of the National Academy of Sciences, 2007. **104**(15): p. 6436-6441.

386. Piccini, A., et al., *ATP is released by monocytes stimulated with pathogen-sensing receptor ligands and induces IL-1β and IL-18 secretion in an autocrine way.* Proceedings of the National Academy of Sciences, 2008. **105**(23): p. 8067-8072.

387. Pelegrin, P. and A. Surprenant, *The P2X(7) receptor-pannexin connection to dye uptake and IL-1beta release.* Purinergic Signal, 2009. **5**(2): p. 129-37.

388. Marina-Garcia, N., et al., *Pannexin-1-Mediated Intracellular Delivery of Muramyl Dipeptide Induces Caspase-1 Activation via Cryopyrin/NLRP3 Independently of Nod2.* J Immunol, 2008. **180**(6): p. 4050-4057.

389. Martinon, F., et al., *Identification of bacterial muramyl dipeptide as activator of the NALP3/cryopyrin inflammasome.* Curr Biol, 2004. **14**(21): p. 1929-34.

390. Franchi, L., et al., *Cytosolic flagellin requires Ipaf for activation of caspase-1 and interleukin 1beta in salmonella-infected macrophages.* Nat Immunol, 2006. **7**(6): p. 576-82.

391. Pace, J., M.J. Hayman, and J.E. Galán, *Signal transduction and invasion of epithelial cells by S. typhimurium.* Cell, 1993. **72**(4): p. 505-514.

392. Roy, D., et al., *A process for controlling intracellular bacterial infections induced by membrane injury.* Science, 2004. **304**(5676): p. 1515-1518.

393. Walev, I., et al., *Delivery of proteins into living cells by reversible membrane permeabilization with streptolysin-O.* Proc Natl Acad Sci U S A, 2001. **98**(6): p. 3185-90.
394. McNeil, P.L. and R.A. Steinhardt, *Plasma membrane disruption: Repair, prevention, adaptation.* Annual Review Of Cell And Developmental Biology, 2003. **19**: p. 697-731.
395. Chambers, R. and E.L. Chambers, *Explorations into the Nature of the Living Cell.* 1961, Cambridge, MA: Harvard University Press.
396. Heilbrunn, L.V., *The Dynamics of Living Protoplasm.* 1958, New York: Academic. 634 pp.
397. Bi, G.Q., J.M. Alderton, and R.A. Steinhardt, *Calcium-regulated exocytosis is required for cell membrane resealing.* Journal Of Cell Biology, 1995. **131**(6): p. 1747-1758.
398. Miyake, K. and P.L. McNeil, *Vesicle accumulation and exocytosis at sites of plasma membrane disruption.* Journal Of Cell Biology, 1995. **131**(6): p. 1737-1745.
399. Steinhardt, R.A., G.Q. Bi, and J.M. Alderton, *Cell-Membrane Resealing By A Vesicular Mechanism Similar To Neurotransmitter Release.* Science, 1994. **263**(5145): p. 390-393.
400. Togo, T., et al., *The mechanism of facilitated cell membrane resealing.* Journal Of Cell Science, 1999. **112**(5): p. 719-731.
401. McNeil, P.L., et al., *Patching plasma membrane disruptions with cytoplasmic membrane.* Journal Of Cell Science, 2000. **113**(11): p. 1891-1902.
402. Terasaki, M., K. Miyake, and P.L. McNeil, *Large plasma membrane disruptions are rapidly resealed by Ca2+-dependent vesicle-vesicle fusion events.* Journal Of Cell Biology, 1997. **139**(1): p. 63-74.
403. McNeil, P.L. and M.M. Baker, *Cell surface events during resealing visualized by scanning-electron microscopy.* Cell And Tissue Research, 2001. **304**(1): p. 141-146.
404. Andrews, N.W., *Regulated secretion of conventional lysosomes.* Trends In Cell Biology, 2000. **10**(8): p. 316-321.
405. Jaiswal, J.K., N.W. Andrews, and S.M. Simon, *Membrane proximal lysosomes are the major vesicles responsible for calcium-dependent exocytosis in nonsecretory cells.* Journal Of Cell Biology, 2002. **159**(4): p. 625-635.
406. Martinez, I., et al., *Synaptotagmin VII regulates Ca2+-dependent exocytosis of lysosomes in fibroblasts.* Journal Of Cell Biology, 2000. **148**(6): p. 1141-1149.
407. Ninomiya, Y., et al., *Ca2+-dependent exocytotic pathways in Chinese hamster ovary fibroblasts revealed by a caged-Ca2+ compound.* Journal Of Biological Chemistry, 1996. **271**(30): p. 17751-17754.
408. Reddy, A., E.V. Caler, and N.W. Andrews, *Plasma membrane repair is mediated by Ca2+-regulated exocytosis of lysosomes.* Cell, 2001. **106**(2): p. 157-169.
409. Rodriguez, A., et al., *Lysosomes behave as Ca2+-regulated exocytic vesicles in fibroblasts and epithelial cells.* Journal Of Cell Biology, 1997. **137**(1): p. 93-104.
410. Borgonovo, B., et al., *Regulated exocytosis: a novel, widely expressed system.* Nature Cell Biology, 2002. **4**(12): p. 955-962.
411. Coorssen, J.R., H. Schmitt, and W. Almers, *Ca2+-triggers massive exocytosis in Chinese hamster ovary cells.* Embo Journal, 1996. **15**(15): p. 3787-3791.

412. Kasai, H., et al., *Multiple and diverse forms of regulated exocytosis in wild-type and defective PC12 cells.* Proceedings Of The National Academy Of Sciences Of The United States Of America, 1999. **96**(3): p. 945-949.

413. Huynh, C. and N.W. Andrews, *The small chemical vacuolin-1 alters the morphology of lysosomes without inhibiting Ca2+-regulated exocytosis.* Embo Reports, 2005. **6**(9): p. 843-847.

414. Matthew, W.D., L. Tsavaler, and L.F. Reichardt, *Identification of a synaptic vesicle-specific membrane protein with a wide distribution in neuronal and neurosecretory tissue.* J. Cell Biol., 1981. **91**(1): p. 257-269.

415. Perin, M.S., et al., *Phospholipid binding by a synaptic vesicle protein homologous to the regulatory region of protein kinase C.* Nature, 1990. **345**(6272): p. 260-263.

416. Perin, M.S., et al., *Structural and functional conservation of synaptotagmin (p65) in Drosophila and humans.* J. Biol. Chem., 1991. **266**(1): p. 615-622.

417. Chapman, E.R., *Synaptotagmin: A Ca2+ sensor that triggers exocytosis?* Nature Reviews Molecular Cell Biology, 2002. **3**(7): p. 498-508.

418. Sudhof, T.C. and J. Rizo, *Synaptotagmins: C-2-domain proteins that regulate membrane traffic.* Neuron, 1996. **17**(3): p. 379-388.

419. Littleton, J.T., et al., *synaptotagmin Mutants Reveal Essential Functions for the C2B Domain in Ca2+-Triggered Fusion and Recycling of Synaptic Vesicles In Vivo.* J. Neurosci., 2001. **21**(5): p. 1421-1433.

420. Osborne, S.L., et al., *Calcium-dependent oligomerization of synaptotagmins I and II. Synaptotagmins I and II are localized on the same synaptic vesicle and heterodimerize in the presence of calcium.* J Biol Chem, 1999. **274**(1): p. 59-66.

421. Craxton, M. and M. Goedert, *Alternative splicing of synaptotagmins involving transmembrane exon skipping.* FEBS Lett, 1999. **460**(3): p. 417-22.

422. Li, P., et al., *Mice deficient in IL-1 beta-converting enzyme are defective in production of mature IL-1 beta and resistant to endotoxic shock.* Cell, 1995. **80**(3): p. 401-11.

423. Ullrich, B. and T.C. Sudhof, *Differential Distributions Of Novel Synaptotagmins - Comparison To Synapsins.* Neuropharmacology, 1995. **34**(11): p. 1371-1377.

424. Sugita, S., et al., *Synaptotagmin VII as a plasma membrane Ca(2+) sensor in exocytosis.* Neuron, 2001. **30**(2): p. 459-73.

425. Czibener, C., et al., *Ca^{2+} and synaptotagmin VII-dependent delivery of lysosomal membrane to nascent phagosomes.* Journal of Cell Biology, 2006. **174**: p. 997-1007.

426. Jaconi, M.E.E., et al., *Cytosolic Free Calcium Elevation Mediates The Phagosome-Lysosome Fusion During Phagocytosis In Human Neutrophils.* Journal Of Cell Biology, 1990. **110**(5): p. 1555-1564.

427. Malik, Z.A., G.M. Denning, and D.J. Kusner, *Inhibition of Ca2+ signaling by Mycobacterium tuberculosis is associated with reduced phagosome-lysosome fusion and increased survival within human macrophages.* Journal Of Experimental Medicine, 2000. **191**(2): p. 287-302.

428. Caler, E.V., et al., *The exocytosis-regulatory protein synaptotagminVII mediates cell invasion by Trypanosoma cruzi.* Journal Of Experimental Medicine, 2001. **193**(9): p. 1097-1104.

429. Jaiswal, J.K., et al., *Synaptotagmin VII restricts fusion pore expansion during lysosomal exocytosis.* Plos Biology, 2004. **2**(8): p. 1224-1232.

430. Chakrabarti, S., et al., *Impaired membrane resealing and autoimmune myositis in synaptotagmin VII-deficient mice.* Journal Of Cell Biology, 2003. **162**(4): p. 543-549.

431. Fukuda, M., *RNA interference-mediated silencing of synaptotagmin IX, but not synaptotagmin I, inhibits dense-core vesicle exocytosis in PC12 cells.* Biochem J, 2004. **380**(Pt 3): p. 875-9.

432. Shen, S.S., et al., *Molecular regulation of membrane resealing in 3T3 fibroblasts.* Journal Of Biological Chemistry, 2005. **280**(2): p. 1652-1660.

433. Steinhardt, R.A., *The mechanisms of cell membrane repair - A tutorial guide to key experiments.* Cell Injury: Mechanisms, Responses, And Repair Annals of the New York Academy of Sciences, 2005. **1066**: p. 152-165.

434. Idone, V., et al., *Repair of injured plasma membrane by rapid Ca2+-dependent endocytosis.* J Cell Biol, 2008. **180**(5): p. 905-14.

435. Nichols, C.G., *KATP channels as molecular sensors of cellular metabolism.* Nature, 2006. **440**(7083): p. 470-6.

436. Cheneval, D., et al., *Increased Mature Interleukin-1beta (IL-1beta) Secretion from THP-1 Cells Induced by Nigericin Is a Result of Activation of p45 IL-1beta -converting Enzyme Processing.* J. Biol. Chem., 1998. **273**(28): p. 17846-17851.

437. Cain, K., et al., *Physiological Concentrations of K+ Inhibit Cytochrome c-dependent Formation of the Apoptosome.* J. Biol. Chem., 2001. **276**(45): p. 41985-41990.

438. Ganong, W.F.M.D., *Review of Medical Physiology.* 22 ed. 2005: McGraw-Hill Medical.

439. Franco, R., C.D. Bortner, and J.A. Cidlowski, *Potential Roles of Electrogenic Ion Transport and Plasma Membrane Depolarization in Apoptosis.* Journal of Membrane Biology, 2006. **209**(1): p. 43-58.

440. Muruve, D.A., et al., *The inflammasome recognizes cytosolic microbial and host DNA and triggers an innate immune response.* Nature, 2008. **452**(7183): p. 103-7.

441. Huynh, C., et al., *Defective lysosomal exocytosis and plasma membrane repair in Chediak-Higashi/beige cells.* Proceedings Of The National Academy Of Sciences Of The United States Of America, 2004. **101**(48): p. 16795-16800.

442. Becker, S.M., et al., *Differential role of the Ca(2+) sensor synaptotagmin VII in macrophages and dendritic cells.* Immunobiology, 2009.

443. Amer, A., et al., *Regulation of Legionella phagosome maturation and infection through flagellin and host Ipaf.* J Biol Chem, 2006. **281**(46): p. 35217-23.

444. Aldridge, P. and K.T. Hughes, *Regulation of flagellar assembly.* Curr Opin Microbiol, 2002. **5**(2): p. 160-5.

445. Stover, C.K., et al., *Complete genome sequence of Pseudomonas aeruginosa PA01, an opportunistic pathogen.* Nature, 2000. **406**(6799): p. 959-64.

446. Arora, S.K., et al., *Identification of Two Distinct Types of Flagellar Cap Proteins, FliD, in Pseudomonas aeruginosa.* Infect. Immun., 2000. **68**(3): p. 1474-1479.

447. Kazmierczak, B.I., M.B. Lebron, and T.S. Murray, *Analysis of FimX, a phosphodiesterase that governs twitching motility in Pseudomonas aeruginosa.* Mol Microbiol, 2006. **60**(4): p. 1026-43.

448. Harvey, H., et al., *Single residue changes in the C terminal disulfide-bonded loop of the Pseudomonas aeruginosa type IV pilin influence pilus assembly and twitching motility.* J. Bacteriol., 2009: p. JB.00943-09.

449. Mattick, J.S., *Type IV pili and twitching motility.* Annu Rev Microbiol, 2002. **56**: p. 289-314.

450. Means, T.K., et al., *The Toll-Like Receptor 5 Stimulus Bacterial Flagellin Induces Maturation and Chemokine Production in Human Dendritic Cells.* J Immunol, 2003. **170**(10): p. 5165-5175.

451. van Schaik, E.J., et al., *DNA Binding: a Novel Function of Pseudomonas aeruginosa Type IV Pili.* J. Bacteriol., 2005. **187**(4): p. 1455-1464.

452. Kahlenberg, J.M., et al., *Potentiation of Caspase-1 Activation by the P2X7 Receptor Is Dependent on TLR Signals and Requires NF-{kappa}B-Driven Protein Synthesis.* J Immunol, 2005. **175**(11): p. 7611-7622.

453. Diebold, S.S., et al., *Innate antiviral responses by means of TLR7-mediated recognition of single-stranded RNA.* Science, 2004. **303**(5663): p. 1529-31.

454. Heil, F., et al., *Species-specific recognition of single-stranded RNA via toll-like receptor 7 and 8.* Science, 2004. **303**(5663): p. 1526-9.

455. Shin, H. and G.R. Cornelis, *Type III secretion translocation pores of Yersinia enterocolitica trigger maturation and release of pro-inflammatory IL-1b.* Cellular Microbiology, 2007. **9**(12): p. 2893.

456. Azghani, A.O., et al., *Pseudomonas aeruginosa outer membrane protein F is an adhesin in bacterial binding to lung epithelial cells in culture.* Microb Pathog, 2002. **33**(3): p. 109-14.

457. Kirkeby, S., et al., *The mink as an animal model for Pseudomonas aeruginosa adhesion: binding of the bacterial lectins (PA-IL and PA-IIL) to neoglycoproteins and to sections of pancreas and lung tissues from healthy mink.* Microbes Infect, 2007. **9**(5): p. 566-73.

458. Doig, P., et al., *Characterization of the binding of Pseudomonas aeruginosa alginate to human epithelial cells.* Infect Immun, 1987. **55**(6): p. 1517-22.

459. Ramphal, R. and G.B. Pier, *Role of Pseudomonas aeruginosa mucoid exopolysaccharide in adherence to tracheal cells.* Infect Immun, 1985. **47**(1): p. 1-4.

460. Cummings, B.S., J. McHowat, and R.G. Schnellmann, *Phospholipase A(2)s in cell injury and death.* J Pharmacol Exp Ther, 2000. **294**(3): p. 793-9.

461. Ehsani, S., C.D. Rodrigues, and J. Enninga, *Turning on the spotlight--using light to monitor and characterize bacterial effector secretion and translocation.* Curr Opin Microbiol, 2009. **12**(1): p. 24-30.

462. Beard, M.K., et al., *Morphogenetic expression of Moraxella bovis fimbriae (pili) in Pseudomonas aeruginosa.* J Bacteriol, 1990. **172**(5): p. 2601-7.

463. Mattick, J.S., et al., *Morphogenetic expression of Bacteroides nodosus fimbriae in Pseudomonas aeruginosa.* J Bacteriol, 1987. **169**(1): p. 33-41.

464. Watson, A.A., J.S. Mattick, and R.A. Alm, *Functional expression of heterologous type 4 fimbriae in Pseudomonas aeruginosa.* Gene, 1996. **175**(1-2): p. 143-50.

465. Lee, S.H. and J.E. Galan, *Salmonella type III secretion-associated chaperones confer secretion-pathway specificity.* Mol Microbiol, 2004. **51**(2): p. 483-95.

466. Pugsley, A.P., *The complete general secretory pathway in gram-negative bacteria.* Microbiol Rev, 1993. **57**(1): p. 50-108.

467. Garcia, J.T., Ferracci, F., Jackson, M.W., Joseph, S.S., Pattis, I., Plano, L.R.W., Fischer, W., Plano, G.V., *Measurement of Effector Protein Injection by Type III and Type IV Secretion Systems by Using a 13-Residue Phosphorylatable Glycogen Synthase Kinase Tag.* Infection And Immunity, 2006. **74**(10): p. 5645-5657.

468. Ghosh, S., M.J. May, and E.B. Kopp, *NF-kappa B and Rel proteins: evolutionarily conserved mediators of immune responses.* Annu Rev Immunol, 1998. **16**: p. 225-60.

469. Karin, M. and Y. Ben-Neriah, *Phosphorylation meets ubiquitination: the control of NF-[kappa]B activity.* Annu Rev Immunol, 2000. **18**: p. 621-63.

470. Sen, R. and D. Baltimore, *Multiple nuclear factors interact with the immunoglobulin enhancer sequences.* Cell, 1986. **46**(5): p. 705-16.

471. Verma, I.M., et al., *Rel/NF-kappa B/I kappa B family: intimate tales of association and dissociation.* Genes Dev, 1995. **9**(22): p. 2723-35.

472. Zhang, J., et al., *Toll-like receptor 5-mediated corneal epithelial inflammatory responses to Pseudomonas aeruginosa flagellin.* Invest Ophthalmol Vis Sci, 2003. **44**(10): p. 4247-54.

473. Greene, C.M., et al., *TLR-Induced Inflammation in Cystic Fibrosis and Non-Cystic Fibrosis Airway Epithelial Cells.* J Immunol, 2005. **174**(3): p. 1638-1646.

474. Hajjar, A.M., et al., *Human Toll-like receptor 4 recognizes host-specific LPS modifications.* Nat Immunol, 2002. **3**(4): p. 354-9.

475. DiMango, E., et al., *Activation of NF-kappaB by adherent Pseudomonas aeruginosa in normal and cystic fibrosis respiratory epithelial cells.* J Clin Invest, 1998. **101**(11): p. 2598-605.

476. Pena, J., et al., *Pseudomonas aeruginosa Inhibition of Flagellin-activated NF-kappaB and interleukin-8 by human airway epithelial cells.* Infect Immun, 2009. **77**(7): p. 2857-65.

477. Ogura, Y., et al., *Nod2, a Nod1/Apaf-1 family member that is restricted to monocytes and activates NF-kappaB.* J Biol Chem, 2001. **276**(7): p. 4812-8.

478. Inohara, N., et al., *Human Nod1 confers responsiveness to bacterial lipopolysaccharides.* J Biol Chem, 2001. **276**(4): p. 2551-4.

479. Chamaillard, M., et al., *An essential role for NOD1 in host recognition of bacterial peptidoglycan containing diaminopimelic acid.* Nat Immunol, 2003. **4**(7): p. 702-7.

480. Girardin, S.E., et al., *Nod2 is a general sensor of peptidoglycan through muramyl dipeptide (MDP) detection.* J Biol Chem, 2003. **278**(11): p. 8869-72.

481. Inohara, N., et al., *Host recognition of bacterial muramyl dipeptide mediated through NOD2. Implications for Crohn's disease.* J Biol Chem, 2003. **278**(8): p. 5509-12.

482. Carneiro, L.A.M., J. G. Magalhaes, I. Tattoli, D. J. Philpott, L. H. Travassos, *Nod-like proteins in inflammation and disease.* The Journal of Pathology, 2008. **214**(2): p. 136-148.

483. Girardin, S.E., et al., *Peptidoglycan molecular requirements allowing detection by Nod1 and Nod2.* J Biol Chem, 2003. **278**(43): p. 41702-8.

484. Schleifer, K.H. and O. Kandler, *Peptidoglycan types of bacterial cell walls and their taxonomic implications.* Bacteriol Rev, 1972. **36**(4): p. 407-77.

485. Kufer, T.A., D.J. Banks, and D.J. Philpott, *Innate immune sensing of microbes by Nod proteins.* Ann N Y Acad Sci, 2006. **1072**: p. 19-27.

486. Inohara, et al., *NOD-LRR proteins: role in host-microbial interactions and inflammatory disease.* Annu Rev Biochem, 2005. **74**: p. 355-83.

487. Sinha, R.K. and R.S. Rosenthal, *Release of soluble peptidoglycan from growing conococci: demonstration of anhydro-muramyl-containing fragments.* Infect Immun, 1980. **29**(3): p. 914-25.

488. Cookson, B.T., A.N. Tyler, and W.E. Goldman, *Primary structure of the peptidoglycan-derived tracheal cytotoxin of Bordetella pertussis.* Biochemistry, 1989. **28**(4): p. 1744-9.

489. Holtje, J.V., *Growth of the stress-bearing and shape-maintaining murein sacculus of Escherichia coli.* Microbiol Mol Biol Rev, 1998. **62**(1): p. 181-203.

490. Araki, Y., et al., *Occurrence of non-N-substituted glucosamine residues in lysozyme-resistant peptidoglycan from Bacillus cereus cell walls.* Biochem Biophys Res Commun, 1971. **42**(4): p. 691-7.

491. Gupta, D.K., et al., *Comparison of biosynthesis and subcellular distribution of lysozyme and lysosomal enzymes in U937 monocytes.* Biochim Biophys Acta, 1985. **847**(2): p. 217-22.

492. Travassos, L.H., et al., *Toll-like receptor 2-dependent bacterial sensing does not occur via peptidoglycan recognition.* EMBO Rep, 2004. **5**(10): p. 1000-6.

493. Schwandner, R., et al., *Peptidoglycan- and lipoteichoic acid-induced cell activation is mediated by toll-like receptor 2.* J Biol Chem, 1999. **274**(25): p. 17406-9.

494. Takeuchi, O., et al., *Differential roles of TLR2 and TLR4 in recognition of gram-negative and gram-positive bacterial cell wall components.* Immunity, 1999. **11**(4): p. 443-51.

495. Dziarski, R. and D. Gupta, *Staphylococcus aureus Peptidoglycan Is a Toll-Like Receptor 2 Activator: a Reevaluation.* Infect. Immun. , 2005. **73**(8): p. 5212-5216.

496. Kim, J.G., S.J. Lee, and M.F. Kagnoff, *Nod1 is an essential signal transducer in intestinal epithelial cells infected with bacteria that avoid recognition by toll-like receptors.* Infect Immun, 2004. **72**(3): p. 1487-95.

497. Kobayashi, K., et al., *RICK/Rip2/CARDIAK mediates signalling for receptors of the innate and adaptive immune systems.* Nature, 2002. **416**(6877): p. 194-9.

498. Park, J.-H., et al., *RICK/RIP2 Mediates Innate Immune Responses Induced through Nod1 and Nod2 but Not TLRs.* J Immunol, 2007. **178**(4): p. 2380-2386.

499. McCarthy, J.V., J. Ni, and V.M. Dixit, *RIP2 is a novel NF-kappaB-activating and cell death-inducing kinase.* J Biol Chem, 1998. **273**(27): p. 16968-75.

500. Inohara, N. and G. Nunez, *NODs: intracellular proteins involved in inflammation and apoptosis.* Nat Rev Immunol, 2003. **3**(5): p. 371-82.

501. Abbott, D.W., et al., *The Crohn's Disease Protein, NOD2, Requires RIP2 in Order to Induce Ubiquitinylation of a Novel Site on NEMO.* 2004. **14**(24): p. 2217.

502. Inohara, N., et al., *An induced proximity model for NF-kappa B activation in the Nod1/RICK and RIP signaling pathways.* J Biol Chem, 2000. **275**(36): p. 27823-31.

503. Yang, Y., et al., *NOD2 pathway activation by MDP or Mycobacterium tuberculosis infection involves the stable polyubiquitination of Rip2.* J Biol Chem, 2007. **282**(50): p. 36223-9.

504. Hasegawa, M., et al., *A critical role of RICK/RIP2 polyubiquitination in Nod-induced NF-kappaB activation.* EMBO J, 2008. **27**(2): p. 373-83.

505. Burns, K.A. and F. Martinon, *Inflammatory Diseases: Is Ubiquitinated NEMO at the Hub?* 2004. **14**(24): p. R1040.

506. Philpott, D.J., et al., *Invasive Shigella flexneri activates NF-kappa B through a lipopolysaccharide-dependent innate intracellular response and*

leads to IL-8 expression in epithelial cells. J Immunol, 2000. **165**(2): p. 903-14.

507. Girardin, S.E., et al., *CARD4/Nod1 mediates NF-kappaB and JNK activation by invasive Shigella flexneri.* EMBO Rep, 2001. **2**(8): p. 736-42.

508. Kufer, T.A., et al., *The pattern-recognition molecule Nod1 is localized at the plasma membrane at sites of bacterial interaction.* Cellular Microbiology, 2008. **10**(2): p. 477-486.

509. Opitz, B., et al., *Nod1-mediated endothelial cell activation by Chlamydophila pneumoniae.* Circ Res, 2005. **96**(3): p. 319-26.

510. Welter-Stahl, L., et al., *Stimulation of the cytosolic receptor for peptidoglycan, Nod1, by infection with Chlamydia trachomatis or Chlamydia muridarum.* Cell Microbiol, 2006. **8**(6): p. 1047-57.

511. Zilbauer, M., et al., *A major role for intestinal epithelial nucleotide oligomerization domain 1 (NOD1) in eliciting host bactericidal immune responses to Campylobacter jejuni.* Cell Microbiol, 2007. **9**(10): p. 2404-16.

512. Hisamatsu, T., et al., *CARD15/NOD2 functions as an antibacterial factor in human intestinal epithelial cells.* Gastroenterology, 2003. **124**(4): p. 993-1000.

513. Opitz, B., et al., *Listeria monocytogenes activated p38 MAPK and induced IL-8 secretion in a nucleotide-binding oligomerization domain 1-dependent manner in endothelial cells.* J Immunol, 2006. **176**(1): p. 484-90.

514. Boneca, I.G., et al., *A critical role for peptidoglycan N-deacetylation in Listeria evasion from the host innate immune system.* Proceedings of the National Academy of Sciences, 2007. **104**(3): p. 997-1002.

515. Kim, Y.G., et al., *The cytosolic sensors Nod1 and Nod2 are critical for bacterial recognition and host defense after exposure to Toll-like receptor ligands.* Immunity, 2008. **28**(2): p. 246-57.

516. Hasegawa, M., et al., *Differential release and distribution of Nod1 and Nod2 immunostimulatory molecules among bacterial species and environments.* J Biol Chem, 2006. **281**(39): p. 29054-63.

517. Lecine, P., et al., *The NOD2-RICK Complex Signals from the Plasma Membrane.* J. Biol. Chem., 2007. **282**(20): p. 15197-15207.

518. Barnich, N., et al., *Membrane recruitment of NOD2 in intestinal epithelial cells is essential for nuclear factor-{kappa}B activation in muramyl dipeptide recognition.* J. Cell Biol., 2005. **170**(1): p. 21-26.

519. Eitel, J., et al., *{beta}-PIX and Rac1 GTPase Mediate Trafficking and Negative Regulation of NOD2.* J Immunol, 2008. **181**(4): p. 2664-2671.

520. Ratner, A.J., et al., *Nod1 mediates cytoplasmic sensing of combinations of extracellular bacteria.* Cell Microbiol, 2007. **9**(5): p. 1343-51.

521. Ismair, M.G., et al., *hPepT1 selectively transports muramyl dipeptide but not Nod1-activating muramyl peptides.* Can J Physiol Pharmacol, 2006. **84**(12): p. 1313-9.

522. Vavricka, S.R., et al., *hPepT1 transports muramyl dipeptide, activating NF-kappaB and stimulating IL-8 secretion in human colonic Caco2/bbe cells.* Gastroenterology, 2004. **127**(5): p. 1401-9.

523. Maeda, S., et al., *Distinct mechanism of Helicobacter pylori-mediated NF-kappa B activation between gastric cancer cells and monocytic cells.* J Biol Chem, 2001. **276**(48): p. 44856-64.

524. Medvedev, A.E. and S.N. Vogel, *Overexpression of CD14, TLR4, and MD-2 in HEK 293T cells does not prevent induction of in vitro endotoxin tolerance.* J Endotoxin Res, 2003. **9**(1): p. 60-4.

525. Döring, G. and G.B. Pier, *Vaccines and immunotherapy against Pseudomonas aeruginosa*. Vaccine, 2008. **26**(8): p. 1011-1024.

526. Galle, M., et al., *The Pseudomonas aeruginosa Type III secretion system plays a dual role in the regulation of caspase-1 mediated IL-1beta maturation*. J Cell Mol Med, 2008. **12**(5A): p. 1767-76.

527. Schultz, M.J., et al., *Role of interleukin-1 in the pulmonary immune response during Pseudomonas aeruginosa pneumonia*. Am J Physiol Lung Cell Mol Physiol 2002. **282**(2): p. L285-290.

528. Grassme, H., et al., *Ceramide in bacterial infections and cystic fibrosis*. Biol Chem, 2008. **389**(11): p. 1371-9.

529. Thakur, A., et al., *Regulation of <i>Pseudomonas aeruginosa</i> corneal infection in IL-1ß converting enzyme (ICE, caspase-1) deficient mice*. Current Eye Research, 2004. **29**(4): p. 225 - 233.

530. Thakur, A., et al., *Caspase-1 inhibitor reduces severity of pseudomonas aeruginosa keratitis in mice*. Invest Ophthalmol Vis Sci, 2004. **45**(9): p. 3177-84.

531. Reiniger, N., et al., *Resistance to Pseudomonas aeruginosa Chronic Lung Infection Requires Cystic Fibrosis Transmembrane Conductance Regulator-Modulated Interleukin-1 (IL-1) Release and Signaling through the IL-1 Receptor*. Infect. Immun. , 2007. **75**(4): p. 1598-1608.

532. Horino, T., et al., *Interleukin-1-deficient mice exhibit high sensitivity to gut-derived sepsis caused by Pseudomonas aeruginosa*. Cytokine, 2005. **30**(6): p. 339-46.

533. Lamkanfi, M., et al., *Glyburide inhibits the Cryopyrin/Nalp3 inflammasome*. J Cell Biol, 2009. **187**(1): p. 61-70.

534. Ayala, B.P., et al., *The pilus-induced Ca2+ flux triggers lysosome exocytosis and increases the amount of Lamp1 accessible to Neisseria IgA1 protease*. Cell Microbiol, 2001. **3**(4): p. 265-75.

535. Galan, J.E. and H. Wolf-Watz, *Protein delivery into eukaryotic cells by type III secretion machines*. Nature, 2006. **444**(7119): p. 567-73.

536. Ramphal, R., et al., *TLRs 2 and 4 Are Not Involved in Hypersusceptibility to Acute Pseudomonas aeruginosa Lung Infections*. J Immunol, 2005. **175**(6): p. 3927-3934.

Appendix; MASCOT results

Mascot Search Results

```
User                    : Kenneth Beattie
Email                   : k.a.beattie@dundee.ac.uk
Search title            : Submitted from Cecilia Lindestam NCBIall 230408
by Mascot Daemon on LS17985 (dUFr)
MS data file            : D:\Raw QTrap data\2008_04_23\dUFr.wiff
Database                : NCBInr  (4565699 sequences; 1571958806 residues)
Timestamp               : 24 Apr 2008 at 08:37:15 GMT
Enzyme                  : Trypsin/P
Variable modifications  : Acetyl (N-term),Carbamidomethyl (C),Dioxidation
(M),Gln->pyro-Glu (N-term Q),Oxidation (M)
Mass values             : Monoisotopic
Protein Mass            : Unrestricted
Peptide Mass Tolerance  : ± 1.5 Da (# ¹³C = 2)
Fragment Mass Tolerance : ± 0.5 Da
Max Missed Cleavages    : 2
Instrument type         : ESI-TRAP
Number of queries       : 130
```

Protein hits :	gi|120436	Fimbrial protein precursor (Pilin) (Strain PA103)
	gi|1346343	Keratin, type II cytoskeletal 1 (Cytokeratin-1) (CK-1) (Keratin-1) (K1) (67 kDa cytokeratin) (Hair alpha protein)
	gi|15599752	type 4 fimbrial biogenesis protein PilE [Pseudomonas aeruginosa PAO1]
	gi|453155	keratin 9 [Homo sapiens]
	gi|67549	trypsin (EC 3.4.21.4) precursor - bovine

Select Summary Report

Format As	Select Summary (protein hits) ▼		Help
	Significance threshold p< 0.05	Max. number of hits AUTO	
	Standard scoring ⦿ MudPIT scoring ○	Ions score or expect cut-off 64	Show sub-sets 0
	Show pop-ups ⦿ Suppress pop-ups ○	Sort unassigned Decreasing Score ▼	Require bold red ☑

1. gi\|120436   **Mass:** 15789   **Score:** 830   **Queries matched:** 24   **emPAI:** 17.27

Fimbrial protein precursor (Pilin) (Strain PA103)

Query	Observed	Mr(expt)	Mr(calc)	Delta	Miss	Score	Expect	Rank	Peptide
19	591.643	1181.27	1182.56	-	0	78	0.00	1	K.FNFATGQSSPK.N 20 2

Query	Observed	Mr(expt)	Mr(calc)	Delta	Miss	Score	Expect	Rank	Peptide
	636	2720	6940	1.294220			22		1 23 24 25 26 27
43	686.261429	1370.508306	1370.740509	-0.232203	0	(100)	1.3e-05	1	R.SEGASALATINPLK.T 42 44
53	707.209474	1412.404396	1412.751068	-0.346672	0	108	2.4e-06	1	R.SEGASALATINPLK.T
78	844.954462	1687.894372	1687.935638	-0.041266	1	88	0.0002	1	K.LGTVAVTIKDTGDGTIK.F 74 77
84	657.517027	1969.529253	1969.938156	-0.408903	1	90	0.00015	1	K.DTGDGTIKFNFATGQSSPK.N
92	1035.087207	2068.159862	2068.057587	0.102275	0	137	3.1e-09	1	K.ILIGTTASTADTTYVGIDEK.A 89 90
98	1087.437097	2172.859642	2172.970764	-0.111122	0	90	0.00013	1	R.TAEGVWTCTSTQEEMFIPK.G 97
113	1187.613529	2373.212506	2373.238693	-0.026187	1	130	1.4e-08	1	R.SEGASALATINPLKTTVEESLSR.G 112
115	794.667220	2380.979832	2381.232574	-0.252742	1	110	1.3e-06	1	K.ILIGTTASTADTTYVGIDEKANK.L

---

2. gi|1346343   **Mass:** 65978   **Score:** 174   **Queries matched:** 2   **emPAI:** 0.13

Keratin, type II cytoskeletal 1 (Cytokeratin-1) (CK-1) (Keratin-1) (K1) (67 kDa cytokeratin) (Hair alpha protein)

Query	Observed	Mr(expt)	Mr(calc)	Delta	Miss	Score	Expect	Rank	Peptide
37	633.193333	1264.372114	1264.629913	-0.257799	0	64	0.053	1	R.TNAENEFVTIK.K
116	795.304848	2382.892716	2382.944656	-0.051940	0	110	1.4e-06	1	R.GGGGGYGSGGSSYGSGGGSYGSGGGGGGGR.G

Proteins matching the same set of peptides:

gi|7428712   **Mass:** 65454   **Score:** 174   **Queries matched:** 2
keratin 1, type II, cytoskeletal - human

gi|11935049   **Mass:** 66027   **Score:** 174   **Queries matched:** 2
keratin 1 [Homo sapiens]

gi|119395750   **Mass:** 65999   **Score:** 174   **Queries matched:** 2
keratin 1 [Homo sapiens]

gi|114644564   **Mass:** 64172   **Score:** 171   **Queries matched:** 2
PREDICTED: similar to keratin 1 [Pan troglodytes]

---

3. gi|15599752   **Mass:** 15270   **Score:** 85   **Queries matched:** 1   **emPAI:** 0.28

type 4 fimbrial biogenesis protein PilE [Pseudomonas aeruginosa

PAO1]

Proteins matching the same set of peptides:

gi|84323198 **Mass:** 13809 **Score:** 85 **Queries matched:** 1

COG4968: Tfp pilus assembly protein PilE [Pseudomonas aeruginosa 2192]

---

4. gi|453155 **Mass:** 61950 **Score:** 66 **Queries matched:** 1 **emPAI:** 0.07

keratin 9 [Homo sapiens]

Query	Observed	Mr(expt)	Mr(calc)	Delta	Miss	Score	Expect	Rank	Peptide
129	1075.100490	3222.279642	3222.274384	0.005258	0	66	0.027	1	R.GGSGGSHGGGSGFGGESGGSYGGGEEASGSGGGYGGGSGK.S

Proteins matching the same set of peptides:

gi|55956899 **Mass:** 62027 **Score:** 66 **Queries matched:** 1

keratin 9 [Homo sapiens]

gi|81175178 **Mass:** 62092 **Score:** 66 **Queries matched:** 1

Keratin, type I cytoskeletal 9 (Cytokeratin-9) (CK-9) (Keratin-9) (K9)

gi|113197968 **Mass:** 48057 **Score:** 66 **Queries matched:** 1

KRT9 protein [Homo sapiens]

gi|114667176 **Mass:** 107386 **Score:** 66 **Queries matched:** 1

PREDICTED: similar to Keratin, type I cytoskeletal 14 (Cytokeratin-14) (CK-14) (Keratin-14) (K14) [Pan troglodytes]

---

5. gi|67549 **Mass:** 23978 **Score:** 65 **Queries matched:** 1 **emPAI:** 0.18

trypsin (EC 3.4.21.4) precursor - bovine

Query	Observed	Mr(expt)	Mr(calc)	Delta	Miss	Score	Expect	Rank	Peptide
109	758.271463	2271.792561	2272.152130	-0.359569	0	65	0.045	1	K.SIVHPSYNSNTLNNDIMLIK.L

Proteins matching the same set of peptides:

gi|230338 **Mass:** 23290 **Score:** 65 **Queries matched:** 1

Chain E, Trypsin (E.C.3.4.21.4) Complex With Bowman-Birk Inhibitor (AB-I)

gi|230765 **Mass:** 22871 **Score:** 65 **Queries matched:** 1

Chain E, Bovine Trypsin (E.C.3.4.21.4) Complex With A Modified SSI (Streptomyces Subtilisin Inhibitor) With Met 70 Replaced By Gly And Met 73 Replaced By Lys (SSI(M70G,M73K))

gi|1421532 **Mass:** 23975 **Score:** 65 **Queries matched:** 1

Chain , Trypsinogen-Ca From Peg

[gi|2392548](#)   **Mass:** 23276   **Score:** 65   **Queries matched:** 1
Chain A, Bovine Trypsin Complexed To Appi

[gi|2392803](#)   **Mass:** 23314   **Score:** 65   **Queries matched:** 1
Chain , Structure Of Hydrolase (Serine Proteinase)

[gi|2507249](#)   **Mass:** 25408   **Score:** 65   **Queries matched:** 1
Cationic trypsin precursor (Beta-trypsin) [Contains: Alpha-trypsin chain 1; Alpha-trypsin chain 2]

[gi|5542503](#)   **Mass:** 24704   **Score:** 65   **Queries matched:** 1
Chain A, Trypsin Inhibitors With Rigid Tripeptidyl Aldehydes

[gi|9955040](#)   **Mass:** 23288   **Score:** 65   **Queries matched:** 1
Chain A, Recruiting Zinc To Mediate Potent, Specific Inhibition Of Serine Proteases

[gi|13096612](#)   **Mass:** 23879   **Score:** 65   **Queries matched:** 1
Chain A, Bovine Beta-Trypsin Bound To Meta-Amidino Schiff Base Magnesium(Ii) Chelate

[gi|34810822](#)   **Mass:** 25392   **Score:** 65   **Queries matched:** 1
Chain B, Non-Covalent Complex Between Alpha-1-Pi-Pittsburgh And S195a Trypsin

[gi|49259456](#)   **Mass:** 23288   **Score:** 65   **Queries matched:** 1
Chain T, Benzamidine In Complex With Bovine Trypsin Variant X(Ssri) Bt.C1

[gi|49259463](#)   **Mass:** 23318   **Score:** 65   **Queries matched:** 1
Chain T, Trypsin Inhibitor In Complex With Bovine Trypsin Variant X(Sswi)bt.B4

[gi|49259467](#)   **Mass:** 23203   **Score:** 65   **Queries matched:** 1
Chain T, Benzamidine In Complex With Bovine Trypsin Varinat X(Ssai) Bt.D1

[gi|61873128](#)   **Mass:** 25769   **Score:** 65   **Queries matched:** 1
PREDICTED: similar to pancreas cationic pretrypsinogen isoform 1 [Bos taurus]

[gi|88193016](#)   **Mass:** 23287   **Score:** 65   **Queries matched:** 1
Chain E, Crystal Structure Of A Bpti Variant (Cys14->ser) In Complex With Trypsin

[gi|88193018](#)   **Mass:** 23402   **Score:** 65   **Queries matched:** 1
Chain E, Crystal Structure Of A Bpti Variant (Cys38->ser) In Complex With Trypsin

[gi|49259465](#)   **Mass:** 23321   **Score:** 63   **Queries matched:** 1
Chain T, Benzamidine In Complex With Bovine Trypsin Variant X(Ssfi.Glu)bt.D1

[gi|49259461](#)   **Mass:** 23295   **Score:** 62   **Queries matched:** 1
Chain T, Trypsin Inhibitor In Complex With Bovine Trypsin Variant X(Ssyi)bt.B4

[gi|112490427](#)   **Mass:** 23134   **Score:** 61   **Queries matched:** 1
Chain A, Structure Of Hyper-Vil-Trypsin

Mascot: http://www.matrixscience.com/

Top scoring peptide matches to query 19
File: dUFr.wiff, Sample: dUFr (sample number 1), Elution: 16.43 to
16.51 min, Period: 1, Cycle(s): 405 (Experiment 3), 404 (Experiment 4)
Score greater than 53 indicates homology
Score greater than 64 indicates identity

```
Score greater than 64 indicates identity
Score     Expect       Delta   Hit   Protein       Peptide
 77.8      0.0022    -1.294220    1    gi|120436 K.FNFATGQSSPK.N
 37.5         23     -1.261200                    -.MNFAVVEDSR.S
 37.0         26     -0.266602                    K.NMRRSNMNK.D
 35.6         36     -0.375061                    R.MIYAASKSALK.A
 34.4         47     -0.265931                    R.DNLMPTAFNK.D
 34.4         47     -0.313538                    K.IYQRTAMNK.E
 34.4         47     -0.349945                    -.MSRIVTAFNK.T
 34.0         51     -0.265946                    K.ACSDIVDAFNK.R
 34.0         51     -0.277161                    K.GGMNAEKAFNK.H
 33.8         54     -0.313553                    -.MAKSQQTFNK.S
```

```
Top scoring peptide matches to query 20
File: dUFr.wiff, Sample: dUFr (sample number 1), Elution: 25.51 to
27.95 min, Period: 1, Cycle(s): 527-530, 541, 551 (Experiment 3), 539-
540, 552-553 (Experiment 4)
Score greater than 53 indicates homology
Score greater than 64 indicates identity
Score     Expect       Delta   Hit   Protein       Peptide
 77.1      0.0026    -0.287590    1    gi|120436 K.FNFATGQSSPK.N
 37.1         25     -0.254570                    -.MNFAVVEDSR.S
 34.0         53      0.740699                    R.DNLMPTAFNK.D
 34.0         53      0.693092                    K.IYQRTAMNK.E
 34.0         53      0.656685                    -.MSRIVTAFNK.T
 33.7         56      0.740684                    K.ACSDIVDAFNK.R
 33.7         56      0.729469                    K.GGMNAEKAFNK.H
 31.5         92      0.631569                    R.MIYAASKSALK.A
 30.9      1.1e+02   -0.283074                    M.ESIMKVAMDK.A
 29.3      1.5e+02    0.693077                    -.MAKSQQTFNK.S
```

```
Top scoring peptide matches to query 21
File: dUFr.wiff, Sample: dUFr (sample number 1), Elution: 15.14 to 15.4
min, Period: 1, Cycle(s): 390 (Experiment 3), 391-392 (Experiment 5)
Score greater than 49 indicates homology
Score greater than 64 indicates identity
Score     Expect       Delta   Hit   Protein       Peptide
 65.2      0.039     -0.283554    1    gi|120436 K.FNFATGQSSPK.N
 34.2         50      0.744735                    R.DNLMPTAFNK.D
 34.2         50      0.697128                    K.IYQRTAMNK.E
 34.2         50      0.660721                    -.MSRIVTAFNK.T
 33.9         53      0.744720                    K.ACSDIVDAFNK.R
 33.9         53      0.733505                    K.GGMNAEKAFNK.H
 33.9         53     -0.250534                    -.MNFAVVEDSR.S
 29.9      1.3e+02   -0.224915                    -.MSNMVPVMDK.K
 26.7      2.8e+02   -0.224030                    R.DETKETAMDK.I
 25.1      4.1e+02   -0.290940                    -.MIWISQFDK.F
```

```
Top scoring peptide matches to query 23
File: dUFr.wiff, Sample: dUFr (sample number 1), Elution: 23.11 to
```

```
 28.6   1.8e+02   -0.193663                        -.MSNMVPVMDK.K
 28.5   1.8e+02   -0.192778                        R.DETKETAMDK.I
```

Top scoring peptide matches to query 24
File: dUFr.wiff, Sample: dUFr (sample number 1), Elution: 28.84 to
29.02 min, Period: 1, Cycle(s): 565-567 (Experiment 3)
Score greater than 53 indicates homology
Score greater than 64 indicates identity

Score	Expect	Delta	Hit	Protein	Peptide
68.6	0.018	-0.250120	1	gi|120436	K.FNFATGQSSPK.N
37.3	24	-0.217100			-.MNFAVVEDSR.S
34.1	50	0.778169			R.DNLMPTAFNK.D
34.1	50	0.730562			K.IYQRTAMNK.E
34.1	50	0.694155			-.MSRIVTAFNK.T
33.8	54	0.778154			K.ACSDIVDAFNK.R
33.8	54	0.766939			K.GGMNAEKAFNK.H
30.3	1.2e+02	-0.190596			R.DETKETAMDK.I
30.0	1.3e+02	-0.154219			K.NSSTLDDMDK.F
29.1	1.6e+02	0.785539			K.QDSSTQQFNK.I

Top scoring peptide matches to query 25
File: dUFr.wiff, Sample: dUFr (sample number 1), Elution: 19.6 to 20.15
min, Period: 1, Cycle(s): 456 (Experiment 4), 462 (Experiment 5)
Score greater than 53 indicates homology
Score greater than 64 indicates identity

Score	Expect	Delta	Hit	Protein	Peptide
73.8	0.0054	-0.247228	1	gi|120436	K.FNFATGQSSPK.N
37.4	24	-0.214208			-.MNFAVVEDSR.S
34.3	48	0.781061			R.DNLMPTAFNK.D
34.3	48	0.733454			K.IYQRTAMNK.E
34.3	48	0.697047			-.MSRIVTAFNK.T
34.0	51	0.781046			K.ACSDIVDAFNK.R
34.0	51	0.769831			K.GGMNAEKAFNK.H
32.2	78	-0.187704			R.DETKETAMDK.I
28.8	1.7e+02	0.814082			K.MASLMNAGADK.E
28.6	1.8e+02	0.671931			R.MIYAASKSALK.A

Top scoring peptide matches to query 26
File: dUFr.wiff, Sample: dUFr (sample number 1), Elution: 18.47 to
18.65 min, Period: 1, Cycle(s): 442-443 (Experiment 3), 444 (Experiment
5)
Score greater than 53 indicates homology
Score greater than 64 indicates identity

Score	Expect	Delta	Hit	Protein	Peptide
70.4	0.012	-0.238372	1	gi|120436	K.FNFATGQSSPK.N
37.4	24	-0.205352			-.MNFAVVEDSR.S
34.3	49	0.789917			R.DNLMPTAFNK.D
34.3	49	0.742310			K.IYQRTAMNK.E
34.3	49	0.705903			-.MSRIVTAFNK.T
34.1	51	0.789902			K.ACSDIVDAFNK.R
34.1	51	0.778687			K.GGMNAEKAFNK.H
31.1	1e+02	-0.233856			M.ESIMKVAMDK.A
30.4	1.2e+02	-0.178848			R.DETKETAMDK.I
28.2	2e+02	-0.322357			R.FIERGHLSPK.E

Top scoring peptide matches to query 27
File: dUFr.wiff, Sample: dUFr (sample number 1), Elution: 17.42 to
17.56 min, Period: 1, Cycle(s): 426 (Experiment 3), 425 (Experiment 4),
427 (Experiment 5)
Score greater than 53 indicates homology
Score greater than 64 indicates identity

Score	Expect	Delta	Hit	Protein	Peptide
72.7	0.0071	-0.181452	1	gi|120436	K.FNFATGQSSPK.N

```
 37.0          26   -0.148432                        -.MNFAVVEDSR.S
 33.9          53    0.846837                        R.DNLMPTAFNK.D
 33.9          53    0.799230                        K.IYQRTAMNK.E
 33.9          53    0.762823                        -.MSRIVTAFNK.T
 33.6          56    0.846822                        K.ACSDIVDAFNK.R
 33.6          56    0.835607                        K.GGMNAEKAFNK.H
 29.0     1.7e+02   -0.170207                        K.FQDAIEAFDK.T
 28.7     1.7e+02    0.854207                        K.QDSSTQQFNK.I
 28.6     1.8e+02   -0.170191                        R.YGQAIEAFDK.R
```

Top scoring peptide matches to query 37
File: dUFr.wiff, Sample: dUFr (sample number 1), Elution: 18.36 min,
Period: 1, Cycle(s): 440 (Experiment 4)
Score greater than 64 indicates identity

Score	Expect	Delta	Hit	Protein	Peptide
64.3	0.053	-0.257799	2	gi|1346343	TNAENEFVTIK
64.0	0.055	-1.241823			R.TDAENEFVTLK.K
64.0	0.055	0.701063			R.TIAENEFVTLK.K
59.7	0.15	0.737455			R.TAAENEFVTLK.K
31.8	92	0.747343			K.AITENEFWVR.G
30.1	1.4e+02	2.753095			IVAENFETDPK
29.6	1.5e+02	2.774198			K.WPEADGFVVDK.A
29.5	1.6e+02	1.685057			R.GGGASATLFVTLK.D
28.9	1.8e+02	-1.246523			R.VGRMFENELR.L
27.5	2.5e+02	2.719419			R.GIAERSFERR.F

Top scoring peptide matches to query 42
File: dUFr.wiff, Sample: dUFr (sample number 1), Elution: 23.13 to
26.26 min, Period: 1, Cycle(s): 501, 508, 534 (Experiment 4), 516, 521,
528 (Experiment 5)
Score greater than 56 indicates homology
Score greater than 64 indicates identity

Score	Expect	Delta	Hit	Protein	Peptide
79.2	0.0017	-0.300061	1	gi|120436	R.SEGASALATINPLK.T
39.7	15	-1.306516			R.RAEKAEAAISQAK.T
35.7	38	-0.301404			K.QWRDVALAERK.A
30.9	1.1e+02	-0.265042			R.RGHFESLGATRV.-
28.6	1.9e+02	-0.249783			R.QNGGGREGIAEGVK.G
27.2	2.7e+02	1.693118			R.LQDAEQAIAVRR.R
27.1	2.8e+02	-0.325253			R.VTEILADVGSVVK.K
26.8	2.9e+02	0.607181			R.KIFALAKEALPK.L
26.7	3e+02	-1.258908			K.DAKNLTALEAER.E
26.6	3.1e+02	-0.347714			K.AVRGTVGDLLDKK.D

Top scoring peptide matches to query 43
File: dUFr.wiff, Sample: dUFr (sample number 1), Elution: 28.01 to
28.64 min, Period: 1, Cycle(s): 554, 556 (Experiment 4), 560, 562
(Experiment 5)
Score greater than 55 indicates homology
Score greater than 64 indicates identity

Score	Expect	Delta	Hit	Protein	Peptide
100.2	1.3e-05	-0.232203	1	gi|120436	R.SEGASALATINPLK.T
37.0	28	-1.238658			R.RAEKAEAAISQAK.T
36.0	35	-1.191050			K.DAKNLTALEAER.E
35.5	40	-0.273295			R.SQMRLATLAPRK.A
28.7	1.9e+02	-0.166834			K.SKESAIFDSMIK.T
26.6	3.1e+02	-1.252619			K.EVEVVSAITGAKK.A
26.4	3.2e+02	0.740560			R.VRSGAVDALANIGK.V
26.2	3.4e+02	-1.177149			K.QGEGLAASNARTR.R
25.9	3.6e+02	-0.195841			R.VDEVVTAIADAAR.T
25.4	4.1e+02	-1.282465			K.CNVPLTKIASAKK.I

Top scoring peptide matches to query 44

```
File: dUFr.wiff, Sample: dUFr (sample number 1), Elution: 20.2 to 20.29
min, Period: 1, Cycle(s): 463-464 (Experiment 3)
Score greater than 54 indicates homology
Score greater than 64 indicates identity
Score    Expect      Delta   Hit  Protein    Peptide
 87.3    0.00026   -0.171213   1   gi|120436 R.SEGASALATINPLK.T
 37.1         27   -1.177668             R.RAEKAEAAISQAK.T
 34.2         54   -1.130060             K.DAKNLTALEAER.E
 32.0         88   -0.136194             R.RGHFESLGATRV.-
 25.6    3.9e+02   -0.218805             K.SEKRIAALENLK.P
 24.5    5.1e+02   -0.212305             R.SQMRLATLAPRK.A
 23.5    6.3e+02   -1.127588             K.PLHYATLMNVR.F
 23.2    6.8e+02    2.839682             K.ALDEITALLDPR.L
 23.0    7.1e+02   -1.116175             R.QGRLDDALASGNR.Y
 23.0    7.1e+02   -1.202829             K.RLEELDLASKAK.E


Top scoring peptide matches to query 45
File: dUFr.wiff, Sample: dUFr (sample number 1), Elution: 15.27 to
15.45 min, Period: 1, Cycle(s): 392-393 (Experiment 3), 391 (Experiment
4)
Score greater than 48 indicates homology
Score greater than 64 indicates identity
Score    Expect      Delta   Hit  Protein     Peptide
 84.8    0.00047   -0.258331   3   gi|15599752 R.YYSQNPGVGYTK.D
 30.6    1.2e+02   -0.257675             K.QQDQNMTKPTK.S
 26.6    3.1e+02    1.786987             R.YVMMAVNQSNK.I
 24.9    4.5e+02   -0.319214             K.VKEGAVIPDGMTK.G
 22.7    7.6e+02   -0.311798             K.KSETKENQSPTK.N
 22.5    8.1e+02   -0.265030             K.YMSEKLNCKTK.M
 17.7    2.4e+03   -0.338303             R.QTIAKNFNDAVR.D
 17.6    2.5e+03   -0.305924             R.YYSQIREYVR.S
 17.5    2.5e+03   -0.217438             R.MVSLEPGMSYSK.K
 17.2    2.7e+03    1.702972             K.PMSQLLHTMIR.V


Top scoring peptide matches to query 53
File: dUFr.wiff, Sample: dUFr (sample number 1), Elution: 22 min,
Period: 1, Cycle(s): 488 (Experiment 4)
Score greater than 56 indicates homology
Score greater than 64 indicates identity
Score    Expect      Delta   Hit  Protein    Peptide
107.6    2.4e-06   -0.346672   1   gi|120436 R.SEGASALATINPLK.T
 38.3         21   -1.414696             R.IVEIETADRKIK.R
 37.9         23   -1.341957             R.DQTQLGAIQTGLK.K
 37.5         25   -1.389549             K.VARSKTALDNLGK.E
 27.2    2.6e+02   -0.365318             K.ICGAVAQIAGEIVK.L
 26.4    3.2e+02   -1.357201             R.HDFSPTALSALKK.A
 26.0    3.5e+02   -0.256126             K.EEKSAALSEYMR.K
 26.0    3.5e+02   -1.389565             K.NISVQTVRSQLK.S
 25.9    3.6e+02   -1.341927             R.SPQDGAASLASKLK.D
 25.8    3.7e+02   -0.355431             R.GLWKGTMPNIVR.N


Top scoring peptide matches to query 74
File: dUFr.wiff, Sample: dUFr (sample number 1), Elution: 27.18 to
28.78 min, Period: 1, Cycle(s): 544, 548 (Experiment 4), 558-559, 564
(Experiment 5)
Score greater than 53 indicates homology
```

```
 26.2    3.3e+02    2.885226                        K.IEMMEQMGITVAER.V
 25.0    4.3e+02    2.775592                        R.TAPPGTGRLMLAEAER.R
 23.6      6e+02    2.885226                        K.IEMMEQMGITVAER.V
 23.6      6e+02    2.885226                        K.IEMMEQMGITVAER.V
 23.6      6e+02    2.885226                        K.IEMMEQMGITVAER.V
```

Top scoring peptide matches to query 77
File: dUFr.wiff, Sample: dUFr (sample number 1), Elution: 18.92 to
19.05 min, Period: 1, Cycle(s): 449-450 (Experiment 3), 448 (Experiment
4)
Score greater than 45 indicates homology
Score greater than 64 indicates identity

Score	Expect	Delta	Hit	Protein	Peptide
87.0	0.00028	-0.164122	1	gi|120436	K.LGTVAVTIKDTGDGTIK.F
27.9	2.3e+02	-0.070159			K.KELAEALDQDWKDK.Q
26.9	2.8e+02	-0.103881			R.SHHTVSRSLTEKHK.R
26.8	2.9e+02	-0.201842			R.LGTLGVRGFDRGTVLK.S
24.8	4.6e+02	-0.127715			R.LGGDVLSLGSVDASSIAK.G
22.3	8.2e+02	-0.008162			R.ESMDTIIQIMSNYK.R
22.3	8.2e+02	-0.062301			R.GKITVPADMAEEEIK.R
21.8	9.2e+02	-0.012008			R.AQEAVDAGITCLGENR.D
21.5	9.9e+02	-0.960524			K.YNQAMMDIGATVCTR.S
21.4	1e+03	-0.091338			R.TVSPQTGETPTATASLK.T

Top scoring peptide matches to query 78
File: dUFr.wiff, Sample: dUFr (sample number 1), Elution: 17.62 to
17.83 min, Period: 1, Cycle(s): 430-431 (Experiment 3), 428 (Experiment
4)
Score greater than 47 indicates homology
Score greater than 64 indicates identity

Score	Expect	Delta	Hit	Protein	Peptide
88.3	0.0002	-0.041266	1	gi|120436	K.LGTVAVTIKDTGDGTIK.F
30.1	1.3e+02	-0.078986			R.LGTLGVRGFDRGTVLK.S
25.7	3.7e+02	0.012933			K.QLTALDKDNMLADLK.P
24.1	5.3e+02	0.052697			K.KELAEALDQDWKDK.Q
23.7	5.9e+02	-0.004859			R.LGGDVLSLGSVDASSIAK.G
22.2	8.4e+02	0.012963			K.EQAAEALKLTAKDMK.K
21.3	1e+03	0.001718			R.QMQSDERLLKAEIK.Q
21.2	1e+03	0.006417			K.ASLAAVEVLSTEELEK.A
21.2	1.1e+03	3.147378			K.IEMMEQMGITVAER.V
21.2	1.1e+03	3.147378			K.IEMMEQMGITVAER.V

Top scoring peptide matches to query 84
File: dUFr.wiff, Sample: dUFr (sample number 1), Elution: 19.31 min,
Period: 1, Cycle(s): 453 (Experiment 4)
Score greater than 44 indicates homology
Score greater than 64 indicates identity

Score	Expect	Delta	Hit	Protein	Peptide
89.7	0.00015	-0.408903	1	gi|120436	K.DTGDGTIKFNFATGQSSPK.N
26.4	3.2e+02	3.490831			K.GLYNQGYALGIATGKSRR.G
25.6	3.8e+02	-0.379911			K.TAFDGIGAMGGFDDVALQK.Y
24.5	4.9e+02	1.631716			R.AAMQGMSRSDMVTANSGVR.A
24.0	5.6e+02	-0.398283			R.ACNNTXDRKHADSILEK.Y
20.7	1.2e+03	0.560579			R.ACNNTXDRKHADSILEK.Y
20.7	1.2e+03	0.560579			R.ACNNTXDRKHADSILEK.Y
18.9	1.8e+03	-0.369337			K.RCESISVFECQQDTAVR.S
18.8	1.8e+03	2.565630			M.QAPPPTPNSGYLSLSGSPSK.D
18.8	1.8e+03	-0.390455			R.SSLSSVGDMMSRLNLSGR.G

Top scoring peptide matches to query 89
File: dUFr.wiff, Sample: dUFr (sample number 1), Elution: 20.49 to
20.59 min, Period: 1, Cycle(s): 468-469 (Experiment 3), 467 (Experiment
4)

```
Score greater than 45 indicates homology
Score greater than 64 indicates identity
Score    Expect       Delta   Hit   Protein    Peptide
131.5    9.8e-09   -0.047145    1    gi|120436  K.ILIGTTASTADTTYVGIDEK.A
 25.4       4e+02    0.902333                    R.MARIGMQVRIATSALVFR.K
 19.4     1.6e+03    3.093831                    K.KGPMDCFLTSSLSTTACSGK.R
 18.9     1.8e+03   -0.107493                    K.ILGLTATPYRLGMGWIYK.Y
 17.0     2.8e+03    1.873281                    R.IPAITTATSAATPNTPALTVR.R
 16.9     2.8e+03   -0.055842                    R.PKATYVPNMAPPKLPDGEK.V
 16.2     3.3e+03    0.094182                    R.AMYMTTLLNSPGSATTSMK.W
 15.9     3.5e+03    1.040487                   -.MAYMATSTADIAAMPRGGPR.A
 15.0     4.4e+03    0.954641                    R.LDLTEVKMTDNTLGFGKK.R
 14.9     4.4e+03    0.094197                    R.AMYMTTLLNSPGSATTSMK.W

Top scoring peptide matches to query 90
File: dUFr.wiff, Sample: dUFr (sample number 1), Elution: 21.77 to
29.37 min, Period: 1, Cycle(s): 485-487, 499-500, 510-512, 522-523,
525, 533-534, 536, 545-547, 558-559, 571 (Experiment 3), 498, 560
(Experiment 4)
Score greater than 46 indicates homology
Score greater than 64 indicates identity
Score    Expect       Delta   Hit   Protein    Peptide
 94.8     4.5e-05   -0.022482    1    gi|120436  K.ILIGTTASTADTTYVGIDEK.A
 28.3     2.1e+02    0.926996                    R.MARIGMQVRIATSALVFR.K
 23.2     6.6e+02    1.001093                    R.MQGVEVMTTAIKNLIDTR.S
 18.8     1.8e+03    2.177607                    R.HEDTWICDSDYVADLDK.R
 18.2     2.1e+03    0.931711                    R.YNILMTRTPDTKVIATAK.N
 18.0     2.2e+03    1.050593                    R.FSYYGMRAIFTLYMIK.A
 17.5     2.5e+03    1.008311                    K.LAVIADVDIQTYGMEMLK.A
 17.4     2.5e+03   -0.071447                    R.RFSLGTGQGQVDPLDLPLR.Q
 17.4     2.5e+03    0.956187                    K.INHVPLYVADFPVGIESR.V
 16.9     2.8e+03    2.118723                    R.QDMLGHVTGTSTYFNDHK.L

Top scoring peptide matches to query 92
File: dUFr.wiff, Sample: dUFr (sample number 1), Elution: 21.57 to
29.63 min, Period: 1, Cycle(s): 482, 484, 496-498, 509, 521, 535, 560
(Experiment 3), 485, 512, 522, 533, 545-547, 558-559, 571-572
(Experiment 4), 511, 523, 534, 574 (Experiment 5)
Score greater than 43 indicates homology
Score greater than 64 indicates identity
Score    Expect       Delta   Hit   Protein    Peptide
136.5    3.1e-09    0.102275    1    gi|120436  K.ILIGTTASTADTTYVGIDEK.A
 23.0       7e+02    1.051753                    R.MARIGMQVRIATSALVFR.K
 19.3     1.6e+03    3.243251                    K.KGPMDCFLTSSLSTTACSGK.R
 18.9     1.8e+03    0.093578                    R.PKATYVPNMAPPKLPDGEK.V
 18.0     2.2e+03   -0.858784                    R.GFIDVKTMTWCRTPNIR.V
 17.4     2.5e+03    1.189907                   -.MAYMATSTADIAAMPRGGPR.A
 17.0     2.8e+03    2.022701                    R.IPAITTATSAATPNTPALTVR.R
 15.2     4.2e+03    0.198513                    R.QMWMNVNLPLMKAMGEK.I
 15.2     4.2e+03    0.198513                    R.QMWMNVNLPLMKAMGEK.I
 14.8     4.5e+03    0.057811                    M.TLVTVRKTDMTMVLTATR.N

Top scoring peptide matches to query 97
File: dUFr.wiff, Sample: dUFr (sample number 1), Elution: 22.96 min,
Period: 1, Cycle(s): 499 (Experiment 4)
Score greater than 35 indicates homology
Score greater than 64 indicates identity
```

```
 16.6   2.9e+03  -0.541704                        K.NSDVGVMDFMSTYKRPER.L
 16.4   3.1e+03   2.417555                        R.NMTMWSLHTQNYKFLPK.L
 16.3   3.2e+03  -0.536791                        M.QNDEEPAAAAGTSGLSNGESLR.S
 15.8   3.6e+03  -0.603227                        K.PKMIVCGASAYTREIEFDK.F
 14.9   4.4e+03  -0.733995                        K.RTASTDLKQLNQVNFTLPK.K
```

```
Top scoring peptide matches to query 98
File: dUFr.wiff, Sample: dUFr (sample number 1), Elution: 21.5 to 21.65
min, Period: 1, Cycle(s): 481 (Experiment 4), 483 (Experiment 5)
Score greater than 41 indicates homology
Score greater than 64 indicates identity
Score    Expect      Delta  Hit  Protein    Peptide
 90.2   0.00013  -0.111122    1  gi|120436  R.TAEGVWTCTSTQEEMFIPK.G
 23.7   5.7e+02  -0.133568                        K.NSDVGVMDFMSTYKRPER.L
 19.1   1.7e+03   1.743950                        K.VMAWAAERAPGRVTLTADPK.E
 18.9   1.7e+03  -0.155357                        R.VCRGETYKFVEPQDEFK.A
 15.8   3.6e+03  -1.273445                        R.SNKSQASEYTLNPIAIIQR.G
 14.6   4.7e+03   1.965858                        K.CNCHVSTTTNSNCMCLSLPK.L
 14.6   4.7e+03  -0.267708                        R.NSMLTPSRGVTIGGTGGNIRK.L
 14.2   5.1e+03  -1.099113                        K.NEMMMIPAAAASSSKEMRR.E
 14.2   5.1e+03  -1.099113                        K.NEMMMIPAAAASSSKEMRR.E
 14.0   5.3e+03  -1.175102                        R.KDDAILDNPVPGMEMTAGIR.R
```

```
Top scoring peptide matches to query 109
File: dUFr.wiff, Sample: dUFr (sample number 1), Elution: 20.81 min,
Period: 1, Cycle(s): 471 (Experiment 5)
Score greater than 57 indicates homology
Score greater than 64 indicates identity
Score    Expect      Delta  Hit  Protein    Peptide
 64.8    0.045   -0.359569    5  gi|67549   K.SIVHPSYNSNTLNNDIMLIK.L
 41.7        9   -1.343593                        K.SIVHPSYDSNTLNNDIMLIK.L
 30.2   1.3e+02  -0.505107                        K.STTPLLIPHILNNPKMNIIK.N
 29.2   1.6e+02  -0.144619                        R.CMQAADEHLEQPNEVGNADK.D
 25.4   3.8e+02  -0.326564                        K.GIMSDPRMNGVINPDSSISLK.D
 25.1   4.2e+02  -0.457485                        K.LELTEMARLLPVQENFLLK.F
 22.8   7.1e+02  -1.332347                        K.SMNLDNVLLTNIQSSLYFK.N
 22.6   7.3e+02   0.449727                        R.SLSLSWRILTLVFPIMLLK.E
 22.5   7.5e+02  -0.257808                        K.EAPINWCPSCLTGLANEEVK.D
 22.5   7.5e+02  -0.257808                        K.EAPINWCPSCLTGLANEEVK.D
```

```
Top scoring peptide matches to query 112
File: dUFr.wiff, Sample: dUFr (sample number 1), Elution: 22.07 to
22.31 min, Period: 1, Cycle(s): 489, 491-492 (Experiment 3)
Score greater than 45 indicates homology
Score greater than 64 indicates identity
Score    Expect      Delta  Hit  Protein    Peptide
 88.3   0.00019  -0.310342    1  gi|120436
R.SEGASALATINPLKTTVEESLSR.G
 27.6   2.3e+02  -0.399728                        K.VALLRVDPERLDPHFLAGSLR.A
 26.6   2.9e+02  -0.501016
M.ARVPLLAALVVAMAVLVASSLGPR.A
 26.1   3.2e+02  -0.177606                        R.NTWTLAVGGDYKVTDQWTMR.A
 24.3   4.9e+02  -0.311227                        -
.TVLPVATIQNASTAMLMAASVAR.K
 21.9   8.6e+02  -0.352075                        K.YLKKLQPFLDANNGNLSAAVR.D
 21.4   9.5e+02  -0.322458                        K.IADMSNCTEQVIILTARLAVR.F
 20.7   1.1e+03  -0.311227                        -
.TVLPVATIQNASTAMLMAASVAR.K
 19.9   1.4e+03  -0.322458                        K.DAMNALALLTLQGLLVRSDGMR.A
 18.3      2e+03  -1.201349                        R.QTMRFVAAYLMATIGGNASPTK.D
```

```
Top scoring peptide matches to query 113
File: dUFr.wiff, Sample: dUFr (sample number 1), Elution: 22.16 to
```

```
22.33 min, Period: 1, Cycle(s): 490 (Experiment 3), 491-492 (Experiment
4)
Score greater than 55 indicates homology
Score greater than 64 indicates identity
Score    Expect       Delta  Hit  Protein       Peptide
129.9  1.4e-08   -0.026187    1   gi|120436
R.SEGASALATINPLKTTVEESLSR.G
 35.3       39   -0.027072                     -
.TVLPVATIQNASTAMLMAASVAR.K
 28.0  2.1e+02   -0.027072                     -
.TVLPVATIQNASTAMLMAASVAR.K
 20.6  1.2e+03   -0.005069                     K.ETETLAVPEIHVEQRPATPSK.K
 19.8  1.4e+03    2.972104                     R.ARSFDDLTDQIPGGIVQNLRR.A
 19.1  1.6e+03    2.075955                     K.APGMKALFDRFTTSLEEGEEK.Q
 18.9  1.7e+03    0.099866                     R.DLCIEATLSMLEDRFTRMR.I
 18.8  1.8e+03    1.084729                     K.KKQTSAQVTPESEPNDEGMVR.L
 18.2     2e+03    3.059766
R.DAKKGLATLCIGGGMGIAMCLAR.D
 17.7  2.3e+03    1.144025                     K.PDCGAVVHCHSPRATALSCHR.R
```

```
Top scoring peptide matches to query 115
File: dUFr.wiff, Sample: dUFr (sample number 1), Elution: 19.22 to
19.38 min, Period: 1, Cycle(s): 453-454 (Experiment 3), 452 (Experiment
4)
Score greater than 39 indicates homology
Score greater than 64 indicates identity
Score    Expect       Delta  Hit  Protein       Peptide
110.0  1.3e-06   -0.252742    1   gi|120436
K.ILIGTTASTADTTYVGIDEKANK.L
 20.2  1.3e+03    0.901066
K.QMALEMGGGDGGFVAATPQAGIDR.T
 16.5     3e+03    0.889866                     R.RLNVSTSGVGQSPHMSSEMFR.Q
 15.9  3.5e+03    1.739552
K.VGVVLLAACPGGTTSNLLTHMAR.G
 15.1  4.1e+03    2.815663                     K.KLDASKFEDTSLFTSATFGSGK.K
 15.1  4.1e+03    2.815663                     K.KLDASKFEDTSLFTSATFGXGK.K
 15.0  4.3e+03   -0.225078                     K.PGELYVIRNMGNVIPSQTSYK.E
 14.9  4.4e+03    1.721638                     R.QLLIFDMIFVKNMEAVAASLK.K
 14.8  4.5e+03    2.662953
K.LAAVTQLEAQLGTDAAQAAIILR.L
 14.6  4.6e+03   -1.186474
R.AETGITTELSTTGGTSDGRFIAR.I
```

```
Top scoring peptide matches to query 116
File: dUFr.wiff, Sample: dUFr (sample number 1), Elution: 14.04 to
```

```
 16.9    2.7e+03   -0.320587                          K.DIKMPPKEFELLYYLANNK.N
 16.6    2.9e+03   -0.172653                          R.QCMTVVYERPGGNRVMANMR.S
```

```
Top scoring peptide matches to query 129
File: dUFr.wiff, Sample: dUFr (sample number 1), Elution: 14.55 to
14.68 min, Period: 1, Cycle(s): 382 (Experiment 4), 383 (Experiment 5)
Score greater than 48 indicates homology
Score greater than 63 indicates identity
```

Score	Expect	Delta	Hit	Protein	Peptide
66.4	0.027	0.005258	4	gi|453155	

```
R.GGSGGSHGGGSGFGGESGGSYGGGEEASGSGGGYGGGSGK.S
 32.2       71    1.911493
R.YVQACFGEEAEETAMQAERGMSHLMGSAR.N
 26.4    2.7e+02   -1.212439
K.FFGTLLDAGYVTFCGEESFGTGSNHIREK.D
 25.2    3.6e+02    2.826074
K.YFGNLMDAGRLCLCGEESFGTGSNHIREK.D
 25.1    3.7e+02    1.911493
R.YVQACFGEEAEETAMQAERGMSHLMGSAR.N
 25.1    3.7e+02    1.911478
R.YVQACFGEEAEETAMQAERGMSHLMGSAR.N
 23.6    5.2e+02   -1.310553
K.IEKGCLMCGCGLGSVAGSIGLFGEVAINIWK.P
 23.6    5.2e+02   -1.310553
K.IEKGCLMCGCGLGSVAGSIGLFGEVAINIWK.P
 23.6    5.2e+02   -1.310553
K.IEKGCLMCGCGLGSVAGSIGLFGEVAINIWK.P
 23.5    5.3e+02   -0.100302
K.AMAIMNSFINDISECIAGEASCLMHYNK.H
```